Title	Investigating the efficacy and mechanism of action of mesenchymal stromal cell therapy in burn wound healing
Author(s)	Whelan, Derek S.
Publication date	2017
Original citation	Whelan, D. S. 2017. Investigating the efficacy and mechanism of action of mesenchymal stromal cell therapy in burn wound healing. PhD Thesis, University College Cork.
Type of publication	Doctoral thesis
Rights	© 2017, Derek S. Whelan. http://creativecommons.org/licenses/by-nc-nd/3.0/
Item downloaded from	http://hdl.handle.net/10468/5672

University College Cork, Ireland
Coláiste na hOllscoile Corcaigh

Investigating the Efficacy and Mechanism of Action of Mesenchymal Stromal Cell Therapy in Burn Wound Healing

Submitted to the National University of Ireland in fulfilment of the requirements
for the degree of

Doctor of Philosophy

By

Derek S. Whelan

Centre for Research in Vascular Biology,
Biosciences Institute,
National University of Ireland, Cork,
Ireland

Supervisors: Prof. Noel M. Caplice and Dr. James A. Clover

April 2017

Table of Contents

Table of Figures

Table of Tables

Declaration

This is to certify that the work I am submitting is my own and has not been submitted for another degree, at either University College Cork or elsewhere. All external references and sources are clearly acknowledged and identified within the contents. I have read and understood the regulations of University College Cork concerning plagiarism.

Signed _____

Abstract

Burn injuries represent a significant medical burden and poor healing can lead to loss of function, substantial scarring and morbidity. Several studies suggest that mesenchymal stromal cell (MSC) therapy may be efficacious in accelerating wound healing. For the majority of these studies bone marrow-derived MSC (BM-MSC) have been utilised. However, from a clinical perspective BM-MSC have several drawbacks. Adipose-derived MSC (AD-MSC) on the other hand, present an abundant, readily available source of MSC. Which source of MSC is therapeutically superior has not been well established, especially in large clinically relevant animal models.

Therefore, we investigated the efficacy of BM-MSC and AD-MSC in the treatment of burn wounds in a large porcine model. Donor matched allogeneic AD-MSC and BM-MSC were applied onto partial thickness burns within a fibrin hydrogel. MSC therapy was similarly efficacious in both groups, increasing wound closure, angiogenesis and collagen content, associated with increased wound maturity at two weeks.

To augment this therapeutic response, priming of MSC with inflammatory cytokines was explored. Pre-treatment of MSC with TNFα has been reported to be beneficial in several models but has not been previously established in a burn wound model. Administration of MSC primed with TNFα resulted in a significant acceleration of burn wound closure, re-epithelialisation and increased angiogenesis, AD-MSC and BM-MSC were therapeutically equivalent in their response to TNFα.

To understand the mechanism behind this observation, a mouse model of excisional wound healing was employed. MSC have immunomodulatory effects impacting macrophages, promoting polarisation towards a reparative phenotype. CCL-2 is a potent cytokine involved in the recruitment of macrophages. We hypothesised that MSC derived CCL-2 may be involved in the MSC therapeutic effect by facilitating macrophage repolarisation and may also play a role in TNFα pre-treatment as CCL-2 is greatly induced by TNFα. To further delineate this mechanism, MSC isolated from CCL-2 deficient mice (CCL-2 KO) were applied to excisional wounds in wild-type (WT) mice. Interestingly, CCL-2 deficiency in MSC completely abrogated the therapeutic response compared to WT MSC. CCL-2 KO MSC were unable to repolarise macrophages to the same extent as WT and this was accompanied by a reduced angiogenesis and re-epithelialisation of the wounds at day 10.

TNFα pre-treatment of WT MSC significantly increased therapeutic efficacy, resulting in complete re-epithelisation of all wounds by day 10. CCL-2 KO MSC responded somewhat, with increased CD206+ macrophages and reduced Ly6G+ neutrophils present within the wound, but this biology had no effect on re-epithelialisation.

In summary, this thesis provides new insights into the role of CCL-2 in MSC therapy. Additionally, it was established that AD-MSC are therapeutically equivalent to BM-MSC and are a more optimal source MSC for practical clinical use. Furthermore, TNFα pre-treatment of MSC is beneficial in both a porcine burn model and an excisional mouse model and may be an advantageous method to enhance therapeutic potential of MSC therapy.

Acknowledgments

I would like to express my gratitude to Professor Noel Caplice for seeing the potential in me and for giving me the opportunity to undertake my PhD in the CRVB, for his constant enthusiasm and motivation and honest critiques.

I would also like to thank my co-supervisor Dr. Jim Clover, for his support, guidance and constant encouragement. For always championing my cause, promoting my research and for giving me the opportunity to expand my professional network and collaborate with other research groups.

To all the staff of the CRVB past and present, to Janet, Libby, Gopal for helping me with image analysis, to Ken for his help with the flow cytometer and for reviewing my thesis. I would especially like to thank Vincent for all his help. To Sharon for all her help and support, from organising my swipe access on my first day to organising my viva and everything else in between.

A special thanks to my family, for all their support and kindness; in particular, my parents, who've always been very supportive throughout my many years of education and for the work ethic they have instilled in me.

To Amy, I dedicate this thesis to you. For all of your love and support throughout the years. When the PhD consumed me, you motivated me, took over all the household duties and always had a warm meal waiting for me. Without you, this would not have been possible.

List of publications

Fibrin as a delivery system in wound healing tissue engineering applications.
Whelan D, Caplice NM, Clover AJ.
J Control Release. 2014

Bone Marrow-Derived Mesenchymal Stem Cells Have Innate Procoagulant Activity and Cause Microvascular Obstruction Following Intracoronary Delivery: Amelioration by Antithrombin Therapy.
Gleeson BM, Martin K, Ali MT, Kumar AH, Pillai MG, Kumar SP, O'Sullivan JF, **Whelan D**, Stocca A, Khider W, Barry FP, O'Brien T, Caplice NM.
Stem Cells. 2015

Synthetic chemically modified mRNA-based delivery of cytoprotective factor promotes early cardiomyocyte survival post-acute myocardial infarction.
Huang CL, Leblond AL, Turner EC, Kumar AH, Martin K, **Whelan D**, O'Sullivan DM, Caplice NM.
Mol Pharm. 2015

Mesenchymal Stem Cells and Cutaneous Wound Healing: Current Evidence and Future Potential.
Isakson M, de Blacam C, **Whelan D**, McArdle A, Clover AJ.
Stem Cells Int. 2015

Allogeneic mesenchymal stem cells, but not culture modified monocytes, improve burn wound healing.
Clover AJ, Kumar AH, Isakson M, **Whelan D**, Stocca A, Gleeson BM, Caplice NM.
Burns. 2015

A Novel Selectable Islet 1 Positive Progenitor Cell Reprogrammed to Expandable and Functional Smooth Muscle Cells.
Turner EC, Huang CL, Sawhney N, Govindarajan K, Clover AJ, Martin K, Browne TC, Whelan D, Kumar AH, Mackrill JJ, Wang S, Schmeckpeper J, Stocca A, Pierce WG, Leblond AL, Cai L, O'Sullivan DM, Buneker CK, Choi J, MacSharry J, Ikeda Y, Russell SJ, Caplice NM.
Stem Cells. 2016

Novel methods of local anesthetic delivery in the perioperative and postoperative setting-potential for fibrin hydrogel delivery.

Kearney L, **Whelan D**, O'Donnell BD, Clover AJ.

J Clin Anesth. 2016

Allogeneic MSC persistence may not be necessary for a beneficial effect in burn wound healing.

Whelan D, Caplice NM, Clover AJ.

Burns. 2017.

Selective M2 Macrophage Depletion Leads to Prolonged Inflammation in Surgical Wounds.

Klinkert K, **Whelan D**, Clover AJ, Leblond AL, Kumar AH, Caplice NM.

Eur Surg Res. 2017

Presentations

- **Comparison of allogeneic bone marrow derived mesenchymal stem cell and adipose tissue derived mesenchymal stem cell therapy in porcine burn wound healing**.

  D. Whelan, G. Krishnan, V. Mehigan, NM. Caplice, AJP. Clover

  45th annual European Society for Dermatology Research (ESDR), 9-12th September 2015

- **Rapid re-epithelialisation for accelerated wound healing**

  D. Whelan, L. Turner, NM. Caplice, AJP. Clover

  Irish Association of Plastic Surgeons (IAPS) summer meeting May12-13th 2016

- **Pre-treatment of mesenchymal stem cells with TNF alpha increases efficacy in promoting wound healing**

  D. Whelan, G. Krishnan, V. Mehigan, NM. Caplice, AJP. Clover

  Irish Association of Plastic Surgeons (IAPS) summer meeting May12-13th 2016

Abbreviations

Abbreviation	Meaning	Abbreviation	Meaning
ACKR	Atypical Chemokine Receptor	GVHD	Graft versus host disease
Allo	Allogeneic	h	Hours
ANOVA	Analysis of variance	H&E	Hematoxylin and eosin
BCL-2	B-cell lymphoma 2	HC	Hypoxic conditioning
BM	Bone marrow	HGF	Hepatocyte growth factor
BMP	Bone morphogenetic protein	HIF-1	Hypoxia inducible factor 1
BSA	Bovine serum albumin	HO	Heme oxygenase
CCL	C-C motif chemokine ligand	HPF	High power field
CCR	C-C chemokine receptor	HPRA	Health product regulatory authority
CFU-F	Fibroblast colony forming unit	HSC	Hematopoietic stem cell
CM	Conditioned media	HUVEC	Human umbilical vein endothelial cell
COX	Cyclooxygenase	ICAM-1	Intracellular adhesion molecule 1
CXCL	C-X-C motif chemokine ligand	ID	Intradermally
CXCR4	C-X-C motif chemokine receptor 4	IDO	Indoleamine-pyrrole 2,3-dioxygenase
d	Day	IFN-γ	Interferon-gamma
DAPI	4',6-diamidino-2-phenylindole	IGF	Insulin like growth factor
DC	Dendritic cell	IL	Interleukin
DMEM	Dulbecco's Modified Eagle Medium	IL-1β	Interleukin 1 beta
DSLR	Digital single lens reflex	IM	Intra muscular
EDTA	Ethylenediaminetetraacetic acid	IP	Intraperitoneal
EGF	Endothelial growth factor	IV	Intra venous
ERK	Extracellular signal–regulated kinases	KO	Knock out
FACS	Fluorescence-activated cell sorting	L-NMMA	NG-Monomethyl-L-arginine, monoacetate salt
FAK	Focal adhesion kinase	LPS	Lipopolysaccharides
FBS	Foetal bovine serum	MCPIP	Monocyte chemotactic protein induced protein
FGF	Fibroblast growth factor	MHC	Major histocompatibility complex
FoxP3	Forkhead box P3	MI	Myocardial infarct
GFP	Green fluorescent protein	Min	Minute
GM-CSF	Granulocyte-macrophage colony-stimulating factor	MiR	microRNA
GPCR	G protein-couple receptor	MMP	Matrix metalloproteinase

Abbreviation	Meaning	Abbreviation	Meaning
MNC	Mononuclear cells	rmANOVA	Repeated measures analysis of variance
mRNA	Messenger RNA	ROS	Reactive oxygen species
MSC	Mesenchymal stromal cell	rRNA	Ribosomal RNA
MSC-KO	CCL-2 KO MSC	rt	Room temperature
NF-κB	Nuclear factor kappa-light-chain-enhancer of activated B cells	s	Second
NK	Natural killer cells	SDF-1	Stromal derived factor-1
NO	Nitric oxide	SEM	Standard error mean
NOS	Nitric oxide synthase	SMC	Smooth muscle cell
o/n	Overnight	Src	Sarcoma
OCT	Optimal temperature cutting compound	STAT	Signal transducer and activator of transcription
p	Passage	SVF	Stromal vascular fraction
PB	Peripheral blood	TBSA	Total body surface area
PBMC	Peripheral blood mononuclear cell	TGF-β	Transforming growth factor beta
PBS	Phosphate buffer saline	Th1	Type 1 T helper cells
PBST	PBS + 0.1% Tween	TLR	Toll like receptor
PCR	Polymerase chain reaction	TNFα	Tumour necrosis factor alpha
PDGF	Platelet-derived growth factor	T-reg	T- cell regulator
PFA	Paraformaldehyde	TSG-6	TNF stimulated gene 6
PGE2	Prostaglandin E 2	VCAM-1	Vascular cell adhesion molecule 1
PI-3K	Phosphatidylinositol-4,5-bisphosphate 3-kinase	VEGF	Vascular Endothelial Growth Factor
PKC	Protein kinase C	VSMC	Vascular Smooth muscle cell
PMA	Phorbol 12-myristate 13-acetate	WT	Wild type
PMNL	Polymorphonuclear neutrophil leucocytes	α-MEM	Dulbecco's Modified Eagle Medium alpha modification
qRT-PCR	Real-Time Quantitative Reverse Transcription PCR		

1. Introduction

1.1.   Etiology and pathophysiology of burn wounds

Burn injuries are caused by excessive heat to the skin, which cannot be adequately dissipated, leading to tissue necrosis and disruption of the epidermal barrier, with the temperature and duration of contact of the thermal insult determining the scale of tissue damage. Burn injuries on a global scale affects more people than HIV and Tuberculosis combined, resulting in over 300,000 deaths annually and is a major dilemma for both developed and developing nations [1]. In the United States, 486,000 burn injuries required medical attention with 40,000 requiring further hospitalisation, resulting in an overall mortality rate of 3.2%. Severe burning of over 60% of total body surface area (TBSA) results in systemic shock and significantly increases the mortality rate to 45-85% [2]

Burn injuries arise from a variety of sources and burns due to flame or fire account for the majority of cases (43%) while scald injuries account for 34% [2]. The vast majority of scald burns occur in 1-2 year olds, accounting for 68% of all burn injuries in this age group, the bulk of which occur at home [2].

Burn injuries can result in systemic complications including; pneumonia, cellulitis, septicaemia, wound and urinary tract infections are all increasingly associated with age [2].

The skin consists of three main layers; the epidermis, composed of stratified skin cells called keratinocytes (as shown in **Figure 1.1**), the dermis and hypodermis. Superficial burns are minor and are restricted to the epidermis, typically being induced by UV radiation from exposure to the sun. The skin reddens and is usually painful. In cases of large areas of severely sunburnt skin, medical attention may be required but generally, no treatment is required other than moisturisation of the affected areas.

Partial thickness burns involve the burn extending into the dermis; this layer contains fibroblasts cells and a matrix of collagen fibres that house various skin structures such as hair follicles and sensory nerves (see **Figure 1.1**). In superficial partial thickness burns, tissue damage extends to the hypodermis. These burns are characterised by the formation of a blister and are quite painful due to the proximity of the burn to sensory neurons in the skin. The burnt skin will appear pink due to the intact vasculature and will blanche upon applied pressure. These wounds will heal through re-epithelisation from the surrounding undamaged skin and hair follicles, generally within 10-14 days (d) based on its size and will not result in the formation of a scar [3].
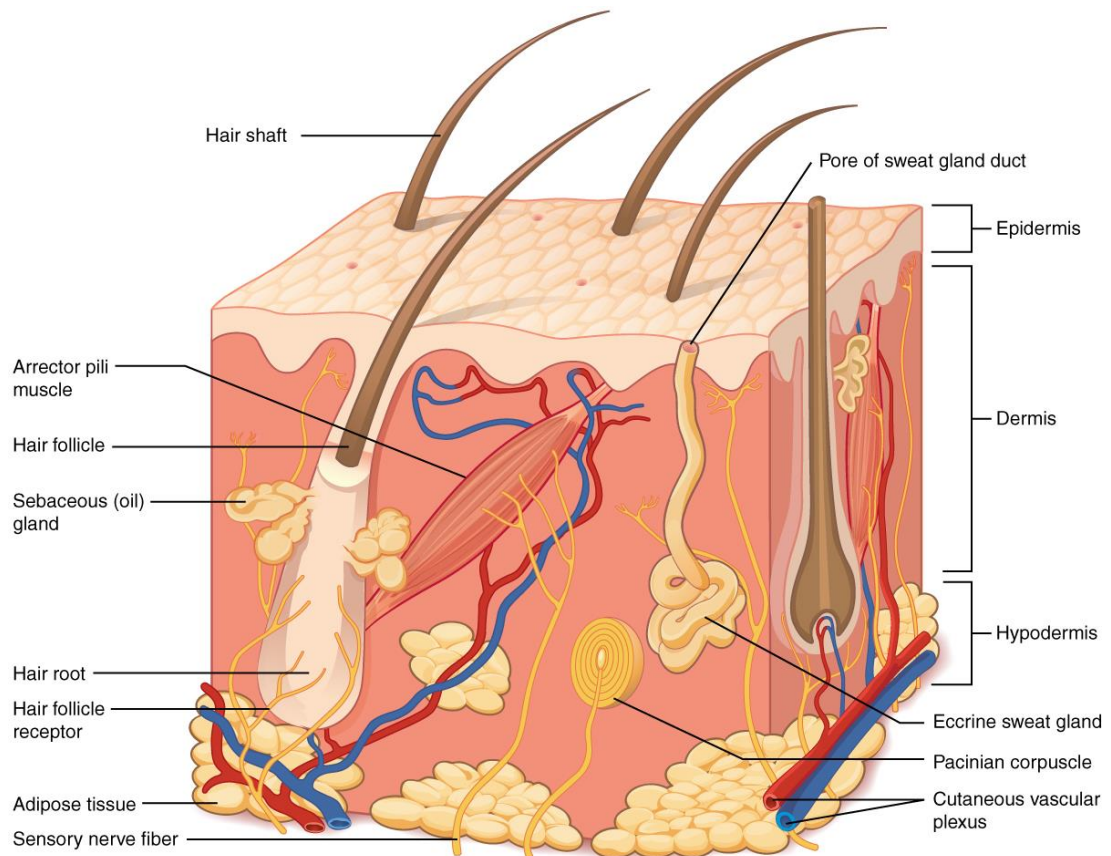
Figure 1.1 The anatomical structure of skin
Figure demonstrating the different layers and organelles contained in skin [4].

Deep partial thickness burns involve the lower parts of the dermis, damaging superficial adnexal structures such as hair follicles, nerve endings and other skin appendages. The wound may appear pale or red due to the extravasation of blood cells from the damaged capillary beds leading to no, or greatly reduced, capillary refill (see **Figure 1.2**). Healing time can be in excess of 21 d and may result in scaring with or without adverse hypertrophic scarring. Surgery is often required to debride necrotic tissue and skin grafts applied to facilitate re-epithelisation and wound closure. Complications of such burns include wound infection, septicaemia and cellulitis.

In a full thickness burn, both the epidermis and dermis are destroyed, in some instances penetrating down into the underlying adipose tissue and bone. Sensation is lost due to the destruction of sensory neurons. Skin may be waxy or charred in appearance with no capillary refill. All skin structures such as hair follicles and sweat glands are destroyed and will not regenerate. The wound will result in scar formation, requiring surgery to excise the dead tissue, relieve contractures and will generally need grafting to restore the epithelial layer promptly. Such burns are very prone to infection and loss of barrier function also induces massive transdermal water loss.

1.1.1. Biology of burns

As postulated by Jackson et al, burns are made up of different zones of damage due to heat transfer through the tissue [5]. The zone of coagulation is a central zone of irreversible skin damage. Surrounding this is the zone of stasis; this is a transitionary zone, which has the potential to be saved or may succumb to inflammatory reaction if the burn is not adequately treated. Adjacent to this is the zone of hyperaemia; this is the zone of least damage and the site of early skin regeneration.

The body usually reacts to gradual heat changes by vasodilation and increased perspiration, which dissipates heat from the dermis through latent heat of evaporation. However, if there is excess heat, for example due to fire or scald, the capacity of the skin to dissipate the heat can be insufficient to prevent tissue damage. If heat is prolonged the damage begins to travel through the deeper

structures. Tissue damage is proportional to the temperature and duration of the thermal insult. For instance, it takes 5-minute (min) exposure to water at 48°C to induce a partial thickness burn, however when the temperature of the water is increased to 70°C a similar degree of injury will result after just 1-2 seconds (s) of exposure [6, 7].

Figure 1.2 Burn victims
Images show patients with various partial thickness, deep partial thickness and full thickness burns.

In response, a large inflammatory reaction (mediated by activation of the kinin system and release of histamine) is incited by widespread necrosis of thermally damaged cells leading to vasodilation of the wound area. Extensive degradation of hyaluronate and collagen fibres promotes extravascular osmotic activity and microvascular permeability also rapidly increases during this time period,

leading to excessive fluid loss proportional to burn surface area [8]. In cases of burn areas involving > 30% TBSA, fluid loss involves all tissues through increased microvascular permeability [7].

Hypercoagulability ensues due to complement activation and inhibition of fibrinolysis [8, 9]. Complement activation induces major polymorphonuclear neutrophil leucocytes (PMNL) recruitment and wound infiltration with the release of multiple factors such as prostaglandins and thromboxanes. At 12-24 hours (h) tissue perfusion deteriorates due to the no reflow phenomenon [10]. Local tissue ischemia sets in leading to further necrosis and cell death. Complement activation and ischemia elicit increased production of oxygen free radicals which further exacerbate the inflammatory response [10].

A late wound healing phase develops as reperfusion increases, PMNL are gradually replaced by macrophages, which secrete an array of wound healing cytokines. Impairment of PMNL function may be a contributory factor to microorganism invasion. Burns not only destroy cells but also eradicate commensal bacteria present on the skin. However, burn wound microbial re-colonization occurs within the first 48 h from gram positive bacteria deep in hair follicles which escaped the initial thermal insult [10]. These initial colonisers are gradually replaced by gram negative bacteria (such as *E. coli*) over the course of a couple of weeks [10].

1.1.2. Systemic effects

Once the burn surface area increases beyond 30%, systemic inflammatory effects become problematic [7]. Thermal injury and the systemic release of inflammatory mediators push the body into a state of shock where tissue perfusion is insufficient to meet the cellular demands. In patients with very high percentage TBSA burnt, large-scale fluid movement initiates hypovolemia, where blood plasma volume is markedly decreased potentially leading to reduced cardiac output. Sympathetic over correction and hypovolemia result in the release of many factors (such as angiotensin II, catecholamines) which cause a contraction of the smooth muscle cells (SMC) lining the arteries, giving rise to increased peripheral vascular resistance. Loss of contractility of myocardial cells has also been observed after thermal injury [6].

Hypovolemia also leads to renal failure due to decreased kidney perfusion and increased free hemoglobin. The gastrointestinal tract is a highly vascularised region, which can also become ischemic after a large burn injury. Thus, increasing permeability and translocation of the endogenous bacteria across the gastrointestinal wall, which may also lead to sepsis and increased morbidity [6]. The end result is acute renal failure, immunosuppression leading to systemic infection, major cardiac dysfunction and eventual death.

1.1.3. Clinical management of burn injuries

Further skin damage can be halted by the application of appropriate first aid to all burns. For minor burns, running cool water over the burn for 15 min, even up

to 3 h after the incident, will reduce the injury [6]. Upon admission into hospital, the TBSA, depth, possible inhalation injury and the cause of the burns are assessed. Burns are then cleaned of debris before applying non-adherent anti-bacterial dressings. Fluid resuscitation through intra venous (IV) administration may be required (in cases with TBSA > 15%) to prevent further burn shock. In burns causing large-scale fluid shifts, fluid resuscitation reduces depth of tissue damage due to hypovolemia and increases perfusion of damaged tissues [3]. In some instances, further pharmacological treatments are administered to suppress inflammatory response and subsequent burn shock, such as steroids and antihistamines [7]. Other drugs may also be administered to promote vasodilation and reperfusion of burn wounds [7].

Wound depth is assessed over several hours as it typically evolves and this will dictate management of the wound. For partial thickness burns, wounds are cleaned followed by application of topical antibiotics such as silver sulfadiazine [7]. A range of dressings may be used to provide hydration as well as absorption of wound exudates. Most partial thickness burns will heal through re-epithelialisation from undamaged dermal appendages. If wounds do not show signs of healing after 1-2 weeks they may require intervention [3]

For deeper partial thickness burns and full thickness burns excision of dead tissue, skin grafting or free flap surgery may be required (as shown in **Figure 1.3**).

Excision of the dead tissue is performed by microtome or Goulian Weck knife (see **Figure 1.3**). Tissue is removed until a healthy bleeding viable wound bed is

established [3]. Early removal of necrotic tissues attenuates systemic inflammatory response and leads to accelerated wound closure and survival [11].

Skin grafting is a process where skin is harvested from an undamaged donor site. This graft is used to restore epithelial layer to the wound. The harvest site will also repair through re-epithelialisation.

In a split thickness graft both the epidermis and a small layer of dermis is harvested. The graft may be meshed to allow it to cover a greater area. Keratinocytes from the graft proliferate and migrate out from the mesh to re-epithelialise the wound. However, mesh grafts are generally not used where a good cosmetic appearance is required such as on the face [3].

Full thickness grafts contain both the epidermal and dermal layers. The donor site may be sown together to close the deficit. However, grafting is problematic in that it only replaces lost dermis and does not provide dermal structures such as sweat glands, sensory nerve endings or hair follicles. For large-scale burns, donor sites may also be limited.
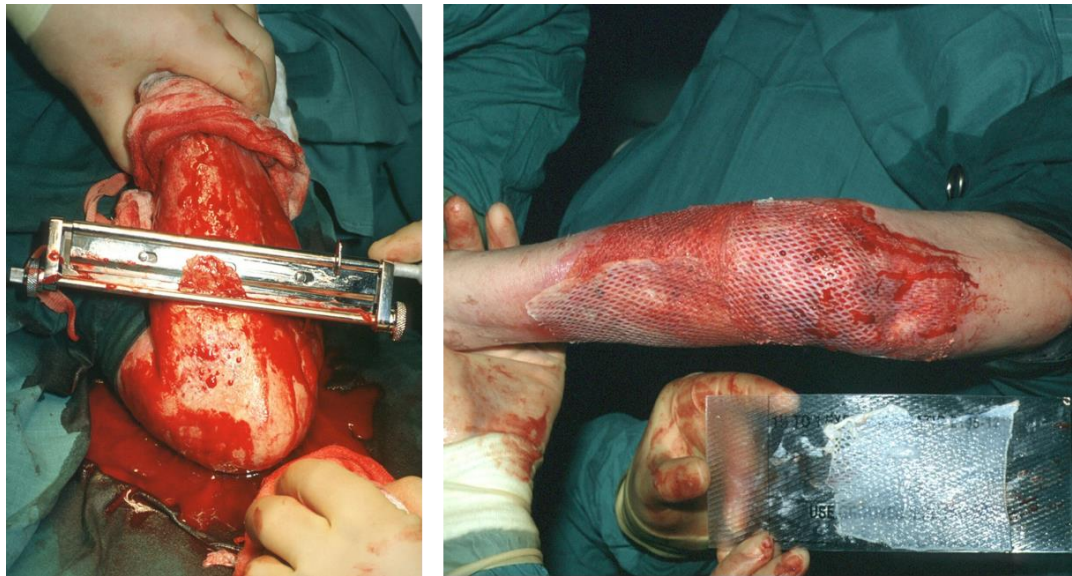
Figure 1.3 Excisional grafting of burn wounds
Patient receiving tangential excision of the wound (left) Meshed graft is then applied to the excised burn (right) [12].

Although much progress has been made in reducing mortality in the case of severe burn wounds, primarily through reduction in sepsis and better management of systemic inflammatory responses, burn injuries remain problematic due to poor wound healing outcomes and extended hospital stays.

The significance of skin grafting cannot be understated, providing an epidermal barrier at an early time point reduces water loss, bacterial infection and consequently, reduces mortality. While grafting solves that problem, it does not prevent scarring. Once the initial excision of the wound is complete, there may be several follow-up surgeries required for skin grafting. As the scars begin to form, the skin in that area will tighten due to myofibroblast contraction. This can lead to loss of function and reduced range of motion of limbs and joints etc.

(**Figure 1.4**). Further revision surgeries will be required along with prolonged physical therapies to manage this.

Figure 1.4 The effects of untreated burns
Images above shows result of burns that did not receive surgery to relieve contractures. Limb mobility and function is greatly reduced.

The current treatment of skin grafting and mesh skin grafting provides a cheap readily available source of epidermis. However, these treatments fall far short in terms of regenerating skin structures (such as sweat glands and hair follicles), retaining cosmetic appearances and have serious shortcomings in large-scale burn injuries.

What is required? An alternative therapy that will accelerate wound closure, reduce the fibrotic response and promote the regeneration of dermal structures.

In this context, the development of cellular therapies may prove to be fruitful alternatives to current treatments. Research is ongoing in developing cellular therapies using a variety of stem cells and engineered skin substitutes. This can be broken into three primary categories; replacement tissue, temporary replacement tissue and augmentation of wound healing therapies.

Replacement tissue

Off the shelf fully functional replacement skin would be ideal; however, there are major technical challenges. Skin is highly immunogenic, therefore, replacement tissue would be quickly rejected if allogeneic. Developing fully functional skin in the laboratory is currently beyond our reach technically due to the multi cellular complexity, but research is ongoing in this area [13, 14]. Finally, the microsurgery required to install the skin would be highly laborious requiring many hours of surgery, and the graft could possibly fail due to ischemia.

Temporary replacement tissue

Tissue engineered skin substitutes, such as Apligraf, consisting of allogeneic fibroblasts and keratinocytes have shown some promise in reducing scarring and promoting wound closure [15]. They provide temporary wound closure; the extra cellular matrix in these skin substitutes may provide directional cues to the

invading recipient cells, while the allogeneic fibroblasts may provide other trophic cues to promote wound healing [16]. Autologous cells would be ideal, however would require the culture of vast amounts of cells from small quantities, which can take time. Research is ongoing in this area to develop novel methods to accelerate epithelial cell culture [17, 18].

Augmentation of wound healing therapies

This rapidly developing paradigm of wound therapy, which holds much potential, harnesses the body's innate ability to heal and regenerate. The progression of wound healing can be controlled using a variety of stem cells, growth factors and biomaterials leading to accelerated and improved wound healing outcomes. Much of this research has been conducted using mesenchymal stromal/stem cells, which is outlined in the next section.

1.2. Mesenchymal stromal cell therapy for cutaneous wound healing

Burns and traumatic injuries by their nature result in the destruction of large amounts of skin tissue and cellular therapies provide a potential way to repair and regenerate this lost tissue by providing the fundamental building blocks. Attempts date back to the 1970's when Rheinwald and Green developed methods to serially culture sheets of keratinocytes which were then transplanted onto burn wounds [19]. Mesenchymal stem cells or stromal cells are a promising candidate as they have unique ability to modulate inflammatory responses and elicit innate healing responses [20]. To date these cells have been applied to

multiple pathologies in both human and animal disease models and are safe and broadly efficacious.

Stem cells have the ability to self-renew and can differentiate into multiple cell types in order to replace and replenish cells lost from tissue damage and general attrition. Mesenchymal stem cells are a population of multi-potent cells with the ability to differentiate into cells of the mesoderm lineage (see **Figure 1.5**). Non hematopoietic cells were first identified in the bone marrow (BM) in 1867 by Conheim [21]. However, it was not until 1966 that a population of fibroblast like non-hematopoietic cells derived from the bone marrow that were plastic adherent and had tri-lineage (osteoblast, adipocyte and chondrocyte) differentiation potential were identified [22]. This cell population has been identified by several names including skeletal stem cells and mesenchymal stromal cells, In 1991 Coplain et al, described these BM derived cells as mesenchymal stem cells [23]. Today however, there is still no clear consensus on the nomenclature for this cell population.

Mesenchymal stem cells were first identified in the BM using single cell colony expansion [24]. These cells could recapitulate a complete heterotrophic bone morrow organ (bone, pericytes, adipocytes and fibroblasts) in vivo. Since then, many similar cell populations have been found to reside in various niches around the body, such as in adipose tissue [25], dental pulp [26], skeletal muscle [27] and numerous other locations. In fact, these cells are believed to reside in the connective tissue surrounding most organs and have been generally termed mesenchymal stem cells [28].

Figure 1.5 Mesenchymal stem cell differentiation potential
Mesenchymal stem cells can be isolated from the bone marrow and differentiated into various cells of the mesoderm lineage [29]

1.2.1. Defining the mesenchymal stem cell population

A widely cited position paper published by International Society for Cellular Therapy (ISCT) in 2006 tried to further define this population of cells by the expression of surface cell receptors, multi-lineage differentiation potential and plastic adherence [30].

Mesenchymal stem cells commonly express a number of cell surface receptors including: CD90, CD73, CD105, CD29, CD44, CD166 and Stro1 while they lack expression of CD45, CD34, CD11b and CD14 and CD19. Due to the general isolation and expansion methods commonly employed, mesenchymal stem cells are a heterogeneous cell population consisting of multi, uni and null potent cells and it is because of this heterogeneity that there is much debate on whether this population should indeed be called stem cells. The ISCT took the position that

15

this cell population should be referred to as mesenchymal stromal cells [30], while there has been some uptake of this, many researchers still refer to them as stem cells. Indeed, several controlled clonal studies of this cell population have demonstrated that they have self-renewal potential and multipotency. Although the majority of these studies were conducted on cells isolated from BM and there is lack of clonal studies of mesenchymal stem cells isolated from other tissue sources. Moreover, no single isolation strategy has been defined as standard in the field, and mesenchymal stem cells are grown under a variety of culture conditions further adding to the heterogeneity. Recognising this, and for the purposes of clarity, this cell population shall be referred to as mesenchymal stromal cells (MSC) throughout this thesis.

1.2.2. MSC biology

The purpose and anatomical locations of native MSC within the body is not well understood. Tracking these cells in vivo is difficult, due to the paucity of unique cell markers. However, there is good evidence to suggest that MSC reside in the BM sinusoids closely associated to endothelial cells and pericytes where they help to maintain the hematopoietic niche [31] and maintain homeostasis by generating multiple types of stromal cells [32]. Nestin+ MSC (about 4% of CD45-stroma) were located in close proximity with hematopoietic stem cell (HSC) and adrenergic nerve fibres and highly expressed HSC maintenance genes such as angiopoietin, C-X-C motif chemokine 12 (CXCL12) and c-kit [31]. Depletion of nestin+ cells reduced BM homing of hematopoietic stem cells. In vitro, this cell population was plastic adherent and quickly differentiated into the various mesenchymal lineages [31].

The classical CD105 marker identifies cells representing 2.5% of total BM fraction. These cells are able to form colony-forming units and can differentiate into the various mesenchymal lineages [33]. A population of BM cells, selected for using the markers D7- FIB+ CD45- and representing 0.01% of BM cells, was found to be CD34- CD90+ CD105+ CD271+ STRO-1+ and have tri-lineage potential [34] . Similarly, CD45- CD271+ lin- BM cells also give rise to standard MSC cultures that are also CD105 CD90 and CD73 positive [35].

The functional significance of these various stromal populations within the BM and their interactions with other cells is still to be delineated, but these cells appear to have major roles in maintenance of the hematopoietic niche, orchestrating the innate immune response and tissue repair.

During infection and wounding, MSC, pericytes and CXCL12 abundant reticular cells (CAR) within the BM detect low levels of circulating toll like receptors (TLR). In response to this, they release Chemokine Ligand 2 (CCL-2) which acts on Chemokine Receptor 2 (CCR-2) of inflammatory monocytes and induces their immobilisation into the circulation [36].

BM resident MSC are involved in maintenance and repair of bone and cartilage. Human CD105+ cells isolated from BM differentiate into osteoblasts in vivo in response to bone morphogenetic protein 2 (BMP-2) [33] while other studies suggest endogenous BM MSC migrate to sites of injury and are incorporated into new bone and BM stroma during fracture repair [35, 37]. Several studies have evaluated the role of endogenous BM derived cells in cutaneous wound healing with differing results [38, 39]. This work has been hampered by the fact that MSC

appear to be resistant to irradiation and do not expand significantly in host BM [40]. BM transplantations using a transgenic mouse that have a promoter sequence of α2(I) collagen gene linked to enhanced green fluorescent protein (GFP) show that BM derived cells did not participate significantly in collagen 1 production during excisional wound healing. However, about 6% of CD45+ transplanted BM derived cells were producing collagen within the wound following bleomycin injection to induce fibrosis [39]. Parabiosis studies, where two animals are surgically joined together, so that their circulatory systems mix, also indicate that BM derived cells do not differentiate into collagen expressing fibroblast cells during wound healing [41]. MSC like cells have also been detected in the peripheral blood and were mobilised from the BM after acute burn injury [42]. Other studies suggest that CD29+ stromal cells capable of multi-lineage differentiation were mobilised into circulation on induction of burn wounds [43]. This mobilisation was mediated through substance P, a highly conserved 11-amino acid neuropeptide. Blockade of substance P inhibited mobilisation of CD29+ stromal cells and increased wound healing time [43].

In summary, it appears that as in vitro, MSC in vivo are a heterogeneous population with varying and distinct functions, with certain populations having roles in maintaining homeostasis and others in responding to trauma. Research is ongoing in this area to establish unique biomarkers for MSC. This will allow for better characterisation of this population for scientific, proprietary and regulatory purposes.

1.2.3. Clinical applications of MSC therapy

To date, multiple clinical trials have been undertaken to assess the safety and efficacy of MSC in the treatment of a wide-range of pathologies. So far, 156 clinical trials have been completed, as registered on clincaltrials.gov [44], a fourfold increase since 2011 [45].

The delivery of MSC to patients appears to be relatively safe and well tolerated in a wide variety of conditions. Primarily, this cell population excels in 3 specific areas, inflammatory driven conditions such as; diabetic wound healing, graft versus host disease (GVHD) [46], in tissue repair; wound healing [47] and non-union bone fractures and bone defects [48] and also, to some degree, in myocardial repair [49].

In the regeneration and repair of cutaneous wounds, MSC therapy holds much promise and several clinical studies have been completed, demonstrating improved wound healing after application of MSC. In a seminal paper by Falanga *et al*, autologous MSC were topically delivered to acute (n=5) and chronic wounds (n=8) in a fibrin spray [50]. No adverse events were observed and the wounds healed well [50]. Large chronic wounds (<1year) in older patients were treated with topically applied MSC (n=3) and healed within 5 weeks after application [51].

Other clinical investigations have used composite grafts consisting of autologous BM MSC cultured on collagen sponges. These grafts were then applied to patients suffering from non-healing wounds. Complete closure of wound was recorded in 13 of the 18 patients [52].

Dash et al conducted the first published controlled and randomised clinical trial to assess the efficacy of MSC in the treatment of chronic wounds [47]. A total of 24 patients with non-healing ulcers were enrolled in the study and were given either autologous BM MSC along with standard wound dressing or standard dressings alone. After 12 weeks the treated wounds had decreased significantly compared to untreated controls. No adverse effects were reported and biopsy of tissue showed development of dermal cells and infiltration of inflammatory cells associated with progression of wound healing [47].

MSC have also been used in several single case studies to treat burn wounds [53] and radiation induced wounds [54] with good healing outcomes and no adverse effects reported.

1.2.4. Mechanism

Initial pre-clinical studies in mice suggested that MSC engrafted into the wound, based on the ability of MSC to differentiate in vitro into cells of the mesoderm lineage and their wound healing properties, differentiating into various skin cell types and helping to rebuild the wound [55, 56].

Sasaki et al injected (IV) 1×10^6 GFP+ allogeneic MSC in mice that were subjected to 10mm full thickness punch wounds. MSC expressed keratinocyte, endothelial and pericyte markers within the wound. They also showed some evidence for MSC transdifferentiation in vitro [55].

In another study, allogeneic GFP+ MSC were intradermally (ID) injected into wounds of normal and diabetic mice [56]. Application of MSC significantly

accelerated wound healing in both compared to neonatal fibroblasts or vehicle alone. Increased angiogenesis was noted as well as co-expression of keratinocyte markers and GFP, indicating potential transdifferentiation of MSC into keratinocytes [56].

Others have reported that regeneration of tissue is not through transdifferentiation of MSC but through cell fusion [57]. In both cases however, the frequency of these events is so low as to have no significant contribution. Furthermore, studies using conditioned media (CM) from cultured MSC have reported similar accelerated wound healing suggesting a paracrine effect [58]. While IV injection of MSC usually become embedded in the lungs or other filter organs such as the liver (as cultured MSC are large cells about 15-19 μm in diameter) and therefore cannot contribute directly to rebuilding of the wound [59]. Therefore, it is unlikely that transdifferentiation or cell fusion explains the reparative effects of MSC.

It is now widely accepted that MSC promote wound healing predominately through paracrine mechanisms. MSC secrete many different cytokines, chemokines and growth factors which have a multitude of effects on cell proliferation, angiogenesis, migration of keratinocytes and fibroblasts, recruitment of inflammatory cells and immunomodulation [60]. Much research has been conducted and is still ongoing; to comprehend which growth factors/chemokines are responsible for this accelerated wound healing.

1.2.4.1. Engraftment and persistence of MSC in the wound

The persistence of MSC in the wound is dependent on several factors, such as allogeneicity and administration route. A study by Chen et al demonstrated that similar amounts of topically applied allogeneic or syngeneic GFP+ MSC persisted in the wounds at d-7, d-14 and d-28, while there was a marked decrease in allogeneic fibroblasts [61]. Both allogeneic and syngeneic MSC persisted until 4 weeks with 75% turnover after 1 week. Other studies have reported a difference in persistence between allogeneic and syngeneic MSC. Zangi et al delivered MSC by intraperitoneal (IP) injection and demonstrated that MSC persisted for 20 d in allogeneic recipients and 40 d in syngeneic recipients, while injected fibroblasts lasted only 10 d in allogeneic animals and 40 d in syngeneic animals [62].

Delivery of MSC by IV injection usually results in much lower persistence of MSC [63]. Whether this is because ID injection may infer some protection from initiating an immune a response, compared to IV injection or whether the tissue provides a source for cell attachment is not known. It may also be a result of MSC becoming entrapped in other organs such as the lungs [59].

1.2.4.2. MSC Angiogenic response

One of the key therapeutic properties of MSC is their ability to induce angiogenesis, that is the sprouting of capillaries from existing blood vessels [64]. MSC have been used to treat both coronary and peripheral vascular ischemia, increasing vascular density and perfusion downstream of the occlusion [65-67]. In one study, digital capillaries were increased in number and size, along with a

reduction in vascular resistance in the affected extremities following the administration of MSC [66].

MSC have been commonly utilised in ischemic hind limb animal models, inducing revascularisation and limb salvation. Transplantation of human MSC 1 to 7 d after ligation of the proximal femoral artery significantly increased laser Doppler perfusion index in a mouse model [68]. Histological examination illustrated increased vessel density as compared to controls [68]. In another study, up to 60% of hind limbs were salvaged with application of human MSC in nude mice [66].

Several other studies support the premise that MSC induce tissue repair and improve cardiac function in the setting of ischemia. After 5 hours of ligation of the coronary artery, 5×10^6 MSC were IV injected into Lewis rats. Capillary density was increased and cardiac infarct size was smaller with associated improved cardiac output [69]. In a model of cerebral artery occlusion, MSC treatment increased Angiopoietin (a factor involved in the production of blood vessels) and its receptor, Tie 2, in the ischemic border. Induced inhibition of either Vascular Endothelial Growth Factor (VEGF) receptor 2 or Tie 2 in mouse brain endothelial cells significantly reduced tube formation in an angiogenic assay with MSC CM [70].

MSC therapy may also have an angiogenic role in cutaneous wound healing. Mice with excisional wounds treated with a topical application of autologous MSC, had increased capillary density after 1 week, as assessed by CD31 immunofluorescent staining, with enhanced vascularity observed in whole section mounts of the

wound [56]. The transplanted MSC were situated in close proximity to blood vessels occupying perivascular locations.

Subsequent studies have confirmed that treatment of wounds with MSC CM increased CD31+ vascular cells and accelerates wound closure [58] further demonstrating that angiogenic potency may also be derived through a paracrine factors. MSC CM contains a variety of growth factors associated with angiogenesis such as VEGF, endothelial growth factor (EGF), CCL-2, Matrix metalloproteinase 9 (MMP-9), angiopoietin 1, 2 and 3, Insulin like growth factor (IGF), CXCL10 and CXCL16 as well as a host of other factors [58, 71].

The microenvironment in which the cell resides also affects cytokine production. Under hypoxic conditions or in reaction to tumour necrosis factor alpha (TNFα), MSC secrete nearly two fold more VEGF mediated through nuclear factor kappa-light-chain-enhancer of activated B cells (NF-κB) activation [72]. In vitro, co-culture and tube formation assays show that MSC interact with endothelial cells and release soluble factors that mediate endothelial cell proliferation, migration and protect these cells from hypoxia induced apoptosis [71, 73, 74]. In particular, Interleukins-6 (IL-6) and IL-8 secretion are increased during TNFα stimulation of MSC and depletion of these factors from MSC CM abrogated MSC induced limb reperfusion effect in a rat ischemic hind limb model [75]. The chemokines IL-6 and IL-8 induced migration and homing of endothelial progenitor cells in vivo.

It is clear that angiogenesis is driven by a variety of growth factors and several knockout (KO) studies have been performed to further delineate this mechanism. Knockout of α6β1 integrin adhesion receptor on MSC was found to reduce

angiogenic sprouting of endothelial cells [76]. Presumably, this integrin is required for interaction and support of developing tube network. In another study, knockdown of VEGF in MSC was found to abolish in vivo protective effects of MSC form hyperoxia induced lung injury [77]. Upstream VEGF is regulated to some extent by microRNA 377 (miR377), knockdown of miR377 increased VEGF while over-expression of mir377 subsequently reduced VEGF protein, which was associated with reduced in vitro tube formation, in vivo vessel density and cardiac function in a myocardial infarct (MI) model. Similar studies have been conducted in ischemic kidney rat models showing that VEGF knockdown in MSC reduces microvessel density [78].

1.2.4.3. MSC Immunomodulatory response

MSC possess a unique ability to modulate immune responses, through a variety of mechanism involving T-cell inhibition, expansion of regulatory T-cell populations, inhibition of natural killer cells (NK) and polarisation of macrophages towards a more reparative phenotype.

The first step in this process involves the activation of MSC. MSC alter their response towards a pro-inflammatory pathogen clearance or an immunosuppressive phenotype based on the inflammatory environment and specific TLR stimulation. In particular pro inflammatory cytokines TNF-α, interferon-gamma (IFN-γ) and interleukin 1 beta (IL-1β) induce immunosuppressive properties [79]. Recent data also suggests that MSC

therapeutic efficacy can be enhanced by pre-stimulation with these factors [75, 80]

T-cell proliferation

Most of the current knowledge about MSC immunosuppressive effects has been garnered from in vitro co-culture studies which show MSC are able to inhibit T-cell proliferation [81]. T-cells are part of the adaptive immune system which is responsible for antigen specific response and development of immunological memory [82]. Several studies demonstrate inhibition of T-cell proliferation of both CD4+ and CD8+ through the release of soluble factors such as hepatocyte growth factor (HGF) heme oxygenase (HO), Indoleamine-pyrrole 2,3-dioxygenase (IDO) Nitric oxide (NO), Prostaglandin E 2 (PGE2) and transforming growth factor beta (TGF-β) in a dose dependent manner [82, 83]. However, important differences exist between species, for instance in human cells IDO is required for inhibition of T-cell proliferation while in mice MSC utilise NO to suppress T-cell proliferation demonstrated by the addition of NO synthase (NOS) inhibitor NG-Monomethyl-L-arginine, monoacetate salt (L-NMMA) [84].

Upon stimulation MSC release chemoattractant cytokines such as CXCL9, CXCL10 and CCL-2 which bring a variety of immune cells into contact with MSC, allowing for direct cell contact and modulation [85].

Another mechanism of T-cell modulation is through Fas induced apoptosis. Akiyama et al elegantly demonstrated that MSC induced apoptosis in T effector cells through Fas ligand-/Fas system which was dependent upon CCL-2 [86].

CD4+ T-cells can either differentiate into Type 1 T helper cells (Th1) with a pro-inflammatory cytokine expression, Th2 that have anti-inflammatory profile or Th17 that secrete IL-17 and are largely associated with autoimmune and allergic responses. A body of evidence now suggests that MSC are also able to shift this balance of helper T-cell subtypes from a Th1 or Th17 driven response to a reparative Th2 profile [85, 87]. Th1 cells secrete TNFα and IFNγ, promoting further inflammatory responses, MSC act like a damper, promoting a Th2 phenotype and increasing the secretion of key anti-inflammatory mediators such as IL-4 and IL-10 [87]. Conversely, in Th2 driven pathologies, MSC can act to skew the balance towards a Th1 response, increasing Th1 associated cytokine release and decreasing Th2 related cytokines [85]. In response to TNFα and other pro-inflammatory molecules, cell contact dependent expression of Cyclooxygenase-2 (COX-2) in MSCs initiates PGE2 synthesis. PGE2 is then secreted and binds to EP4 receptors inhibiting Th17 differentiation [88].

The T-cell population is made up of CD8+ effector cells and CD4+ T helper cells. Among the latter population, are T- cell regulator (T-reg) cells, which function as suppressor cells, damping down the T-cell effector response and regulating the immune response, preventing autoimmune diseases. This population is characterised by the expression of the forkhead box P3 (FoxP3) transcription factor. MSC can induce T-cells towards this regulatory phenotype, the expansion of which requires MSC secretion of PGE2 and TGF-β [85]. This ability to expand the T-reg population may in part explain MSC efficacy in preventing graft versus host diseases and in inflammatory bowel disorders [86].

Inhibition of DC maturation

MSC play a key role in modulating dendritic cells (DC). These cells are responsible for initiating the adaptive immune response. DC, upon engulfing a pathogen migrate to the lymph node where they present the antigen to activate naive T-cells. MSC can interfere with several of these functions. Cultures of DC and MSC show down regulation of key DC maturation markers such as MCHII, CD80 and CD86 [89] which are involved in antigen presentation and co-activation of T-cells. MSC also inhibit the migration of DC to the lymph nodes through down regulation of chemokine receptor CCR-7 [89]. Similarly to macrophages, DC can be directed towards a pro or anti-inflammatory phenotype, the latter having increased secretion of IL-10, reduced levels of pro inflammatory IL-12 along with enhanced phagocytic activity and reduced ability to activate CD4+ T-cells [90].

Cell contact dependent mechanism

MSC employ several cell contact dependent mechanisms to regulate immune responses. Expression of vascular cell adhesion molecule 1 (VCAM-1) and intracellular adhesion molecule 1 (ICAM-1) by MSC are required for interaction with T-cells, both of which are upregulated upon stimulation with inflammatory cytokine such as IFNγ and to some extent TNFα [91]

Inhibition of NK activation

MSC and NK cells interact in vitro and MSC strongly inhibit IL-2 induced cell proliferation through IDO and PGE2 pathways. Furthermore, MSC co-culture reduce NK activation, cytokine release and induce down regulation of NK key activation receptors [92].

Neutrophils

During acute phase of inflammation, Neutrophils infiltrate the wound using oxidative molecules to kill pathogens as well as having a phagocytic role. How MSC modulate neutrophil activation is complex, they can reduce the influx of neutrophils in an endotoxin induced lung injury model [93] and can also protect neutrophils from apoptosis through IL-6 - Signal transducer and activator of transcription 3 (STAT3) mechanism preventing the degranulation and subsequent oxidation burst [94]. MSC may also have secondary inhibitory effects based IL-10, increasing IL-10 from other immune cells, such as macrophages, to inhibit rolling, adhesion and trans-epithelial migration of neutrophils [95] and may prevent neutrophil re-entry into the wound cutting off the negative feedback loop in response to macrophage stimulation.

Macrophage polarisation

In wound healing the main myeloid effector cells are macrophages, an essential component of the immune system. Macrophages can be generally classified into two broad sub types, the classically activated M1 macrophages and the alternately activated M2 type. M1, macrophages are characterised as pro inflammatory, secreting large amount of TNFα, NO and reactive oxygen species (ROS). M2 macrophages are characterised as reparative, with greater phagocytic activity, reduced levels of TNFα and increased secretion of anti-inflammatory cytokines such as IL-10, TGF-β and Arginase 1. Several studies demonstrate that MSC can skew the macrophage phenotype towards a more reparative M2 phenotype [20, 96, 97].

In a seminal paper by Nemth et al (2008), application of MSC isolated from BM (BM-MSC) reduced mortality in a mouse model of sepsis [96]. TNFα was reduced and IL-10 was increased in MSC administered mice compared to control treated mice. Isolation of monocytes from septic lungs showed that MSC treated animals had more monocytes expressing IL-10. Through a series of blocking and knock out studies they determined that PGE2 secreted from MSC bound to EP2 and EP4 receptors on macrophages and monocytes. This subsequently reprogrammed the macrophages, increasing IL-10 secretion. TNFα binds to TLR4 and TNFR1 on MSC resulting in the translocation of NF-κB into the nucleus in a NO dependent fashion. Subsequent binding initiated downstream COX-2 production, which is required for synthesis of PGE2 [96].

Stimulation of MSC by inflammatory mediators such as IFNγ and TNFα, induce human MSC to express IDO. This catalyses the degradation of tryptophan (a key amino acid required for bacteria) into kynurenine. As previously discussed, the metabolites of tryptophan degradation inhibit T-cell proliferation, but also play a role in differentiation of monocytes towards an M2 (reparative) phenotype [98]. Inhibition of IDO enzymatic activity in MSC monocyte co-culture significantly reduced IL-10 compared to control co-cultures [98]. Depletion of monocytes from MSC/ peripheral blood mononuclear cell (PBMC) co-cultures significantly increased T-cell proliferation. Thus, it appears that the increased M2 population also has bystander effects on other cells such as T-cells, amplifying the immunosuppressive effects of MSC [98, 99].

Crucially, in vitro experiments demonstrated that MSC/macrophage cell contact was required for increased IL-10 production [96]. Similar in vitro experiments

show greater polarisation towards M2 phenotype when cells are co-cultured as opposed to using MSC CM, resulting in greater cell surface receptor expression of CD206 and increased gene expression of TGF-β1 and Arginase 1 [97].

However, in some studies of human MSC, cell contact was not required for induction of CD206 in human macrophages [20]. Both co-culture and transwell culture of PBMC and gingiva derived MSC were able to increase CD206 expression in ~30% of CD14+ cells compared to controls. This may well be a function of MSC cell source or inflammatory state as in a study by Hematii et al, where transwell co-culture was able to induce CD206 expression, nevertheless it was not as efficient as co-culture [100]. Induction of CD206 could be blocked by either IL-6 or Granulocyte-macrophage colony-stimulating factor (GM-CSF) neutralising antibodies [20]. Interestingly and in support of MSC activation/licensing (Section 1.2.4.3), addition of MSC to monocytes only modestly increases IL-10, it is not until monocytes are stimulated with Lipopolysaccharides (LPS) that significant increase in IL-10 is induced by MSC [20]. TNF α is significantly reduced in monocyte/MSC co-culture stimulated with Phorbol 12-myristate 13-acetate (PMA). Other soluble factors increased during co-culture are CCL-2, CCL8, IL-6, CXCL1 and GM-CSF [20]. Functionally, phagocytic activity of these macrophages increased after co-culture with MSC [100].

Tumour necrosis stimulating factor 6
In conjunction with the other soluble factors outlined, such as PGE2, IDO and NO, TNF stimulated gene 6 (TSG-6) is another potent Immunomodulatory factor that is secreted by MSC. TSG-6 is a 30kDa hyaluronan binding protein, secreted by

many cells, which has diverse roles in physiological and pathological processes such as inflammation. TSG-6 has a variety of biologic effects such as inhibition of neutrophil migration, modulation of protease network and binding of a variety proteins and glycosaminoglycan such as heparin, aggrecan and hyaluronan [101].

TSG-6 is involved in MSC accelerated cutaneous wound healing [102]. Analysis of wounds showed a significant decrease in macrophage derived TNFα in MSC treated wounds, which was not observed in MSC with TSG-6 knock down. Treatment with MSC reduced TGF-β1 and increased TGF-β3 concentration within the wound, an unbalancing that is thought to result in an anti-fibrogenic effect.
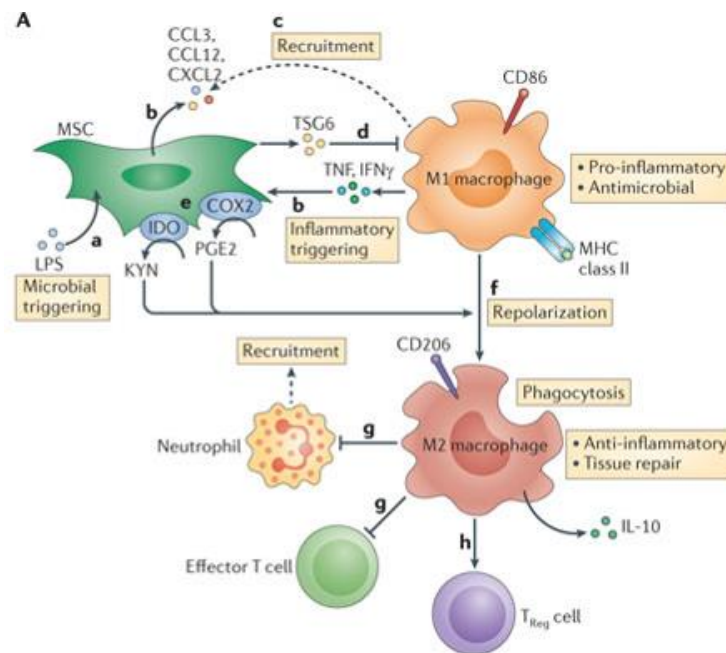
Figure 1.6 The mechanism of MSC immunomodulation
Several mechanisms have been identified that contribute to macrophage repolarisation by MSC. TNFα stimulates MSC to produce TSG-6 and COX-2 which inhibit inflammatory macrophages and promote polarisation to M2 type through increased IL-10 and inhibition of TNFα. Adapted from [103]

Other studies have demonstrated this effect in other models of inflammation such as cornea chemical injury [104]. Notably, TSG-6 was also a key marker of efficacy as opposed to MSC tri differentiation potential which bore no correlation to in vivo efficacy [104].

Mechanistically, TSG-6 binds to CD44 receptor on macrophages. Upon binding, TLR2 activation of NF-κB and subsequent release of pro inflammatory cytokines such as TNFα is blocked [105]. This inhibits the negative feedback loop by reducing the stimulation of surrounding cells of proinflammatory cytokines and subsequent further recruitment of neutrophils and macrophages.

1.2.5. Source of MSC

Currently, one of the major questions in the field of MSC therapy for tissue repair is the role of MSC source. For the majority of these wound healing studies BM MSC have been utilised. However, from a clinical prospective BM isolated MSC have several drawbacks. Isolation of BM is quite an invasive and painful procedure. Generally, a large 4 mm pin is inserted through the skin, which forcefully punctures the iliac crest. The inner mandrel is removed and the BM is aspirated. Using this method a total of 10 ml of BM aspirate can be obtained without diluting it with peripheral blood [106]. To obtain adequate amounts of cells multiple punctures and aspirates must be performed. In cases of severe trauma or burns, BM depletion can to occur [107, 108] inhibiting bone marrow harvest.

MSC reside in multiple niches in the connective tissue and in a perivascular locations and adipose tissue is another potential source of MSC. With over 400,000 liposuctions performed in the United States each year, adipose tissue presents a readily available source of MSC [109]. The tissue is first digested using collagenases and then centrifuged at high speed to separate the cells from the fat. After centrifugation, the floating lipid rich tissue is removed and the pelleted stromal vascular fraction (SVF) can be observed. This can then be used directly as SVF or else is further cultured and characterised before application. From 1g of tissue, 40-80 x10^6 MSC can be isolated making it a much more efficient process than BM isolation.

1.2.6. ASC vs MSC Comparative studies

As adipose derived MSC (AD-MSC) are a much more clinically translatable source of MSC, much research is now being conducted using AD-MSC. Several studies have corroborated their efficacy in pre-clinical models of wound healing [110-113]. However, there is still a paucity of equivalency studies that have examined the efficacy and mechanism of action. Recent studies suggest that AD-MSC are more immune suppressive than BM-MSC taken from aged matched donors [114]. In vitro studies showed no difference in differentiation capacity and expression of MSC markers barring CD34 (AD-MSC had a significantly higher expression). Co culture of MSC with PBMC demonstrated a greater ability of AD-MSC to inhibit PBMC proliferation, increasing IL-10 in stimulated PBMC MSC co-cultures. Differences were also observed in IL-12 and TGF-β1 in unstimulated MSC cytokine secretion [114].

In a pig model of cutaneous wound healing of excised skin both AD-MSC and BM-MSC enhanced wound repair, there was no statistical difference between the groups however, sample size was small n=2 per time point and the study was limited in terms of mechanistic insights [115]. Larger studies are required to determine the role of cell source in terms of efficacy using matched donors in clinically relevant models.

1.3. The role of CCL-2 in MSC mediated inflammation resolution within the wound

Chemokines are small proteins used to signal extracellularly throughout the body, primarily for the purpose of cell recruitment. Chemokines are vital in orchestrating the wound healing process and are required for the biological processes of angiogenesis and tissue remodelling, but they also have detrimental roles such as in fibrosis. Monocyte chemoattractant protein 1 (CCL-2), renamed under the CC ligand (CCL) nomenclature, belongs to a family of chemokines called CC chemokines, due to similarities in structure based on the positioning of two highly conserved cysteine residues at the N terminus. All chemokines have a similar 3-dimensional structure, however their amino acid sequence may differ as much as 90% [116, 117]. CCL-2 consists of three distinct domains; a highly flexible N-terminal domain attached to two disulphide bonds, followed by a long loop leading into three anti-parallel β pleated sheets over which the C terminal α helix domain extends.

The chemokine CCL-2 first discovered in mouse fibroblasts stimulated with Platelet-derived growth factor (PDGF) [118] was later determined to be the same gene product as CCL-2 in humans. Subsequently, several other members of CCL family have been identified including; CCL8 (or its old naming convention MCP-2) CCL7 (MCP-3) CCL13 (MCP-4) CCL12 (MCP-5) [119]. CCL-2 is a 15 kDa heparin binding protein [120] thought to be involved in many pathologies and biological processes including Inflammation, bone re-modelling, angiogenesis, atherosclerosis and tumour development. Accordingly, a variety of cells produce and secrete CCL-2 such as MSC, monocytes, macrophages, endothelial cells, epithelial cells, fibroblasts and some types of tumour cells [58, 118, 120-123].

1.3.1. CCL-2 induced Monocyte, macrophage chemotaxis

Induced chemotaxis CCL-2 is initiated upon CCR-2 binding and detection of CCL-2 gradient. Polarisation of the cell in the direction of the stimuli allows for the formation of the leading edge pseudopod through activation of G-protein coupled receptor via Gi alpha sub unit protein whereas $G_{12/13}$ activation is required for uropod formation at the rear. This binding of CCL-2 drives a cascade of signalling events, which alter cellular structures and drive cell migration.

Upon protrusion of lamellipodia, integrin activation occurs further stabilising the protrusion. Integrin activation is mediated through Protein kinase C (PKC), Rap1 and Phosphatidylinositol-4,5-bisphosphate 3-kinase (PI-3K) signalling pathways leading to integrin clustering and recruitment of structural proteins to focal adhesion sites to drive motility [124]. In the rear of the cell, adhesion sites are

disassembled and retracted. Several signalling pathways mediate this process including myosin II, sarcoma (Src)/ Focal adhesion kinase (FAK)/extracellular signal–regulated kinases (ERK) and Rho [125].

1.3.2. CCL-2 in wound healing

The chemokine CCL-2 has a pivotal function in the progression of normal wound healing. Mice deficient for CCL-2 had poor revascularisation in a skin flap injury model and at day (d) 10 had significantly reduced monocyte/macrophage recruitment as well as a reduced angiogenic response [126]. CCL-2 peaked in mouse excisional wounds at 24 h, significantly reducing by d-3 and disappearing after d-7 [127]. Treatment of wounds with anti CCL-2 reduced macrophage recruitment into the wounds by 46% on d-3. Topical application of recombinant CCL-2 (5ng) increased macrophage recruitment by nearly 24%. Re-epithelialisation however, was only marginally improved with a slight increase in wound strength [127].

Recruitment of Ly6C hi monocyte/macrophages (M1) is CCL-2 dependent, when anti-CCL-2 was administered in spinal cord injury, M1 recruitment was diminished. However, this did not affect recruitment of Ly6C low CCR-2 negative monocytes from which, it is believed, the M2 population is derived [128]. Depletion of CCR-2+ monocytes also inhibited recovery from spinal cord injury indicating that the CCL-2/CCR-2 axis plays a fundamental role in orchestrating the recruitment of various cell populations, which are crucial for the orderly transition through the phases of wound healing [129].

1.3.3. The role of CCL-2 in MSC paracrine function

One of the first (and widely cited) papers to describe paracrine function of MSC in wound healing [130] demonstrated that MSCs secrete a wide variety of cytokines including CCL-2. However, its role has never been defined or robustly investigated. MSC CM induces monocyte and keratinocyte migration in a dose dependent manner [58] and also induces endothelial cell migration and proliferation [58]. Blocking of VEGF and fibroblast growth factor (FGF) in CM with neutralising antibodies only partially reduced endothelial cell proliferation [130]. In vivo, MSC CM also accelerated wound closure in sutured punch wound mouse model [58]. Chen et al demonstrated increased presence of F4/80, CD68+ macrophages and CD31, c-kit+ endothelial cell infiltration into the treated wounds [58]. This makes biological sense, as classically, CCL-2 is known as a potent chemotactic factor for monocytes/macrophages.

Under unstimulated conditions, MSC secrete significant quantities of CCL-2 (about 0.2-2 ng/ml) [20, 131]. When stimulated with TNFα, MSC secrete up to 10 fold more CCL-2 and were found to recruit Ly6C hi CD11b monocytes, F4/80 macrophages and CD11b+Ly6G+ neutrophils in a CCR-2 dependent manner in vivo [132]. When cultured with macrophage CM, MSC displayed an altered gene expression with a fourfold increase in CCL-2 expression. MSC CM enhanced monocyte migration and this could be attenuated with magnetic bead CCL-2 depletion of MSC CM [133].

MSC are efficacious in cutaneous wound healing and have an immune modulatory effect on both the innate and adaptive immune systems. MSC can induce an M2 like phenotype when co-cultured in vitro, giving rise to increased

CD206 expression, increased IL-10, IL-6 secretion, reduced TNFα and decreased ability to induce Th-17 cell expansion [20]. It is important to highlight that while CCL-2 is classically associated with the innate immune system, there is a significant lack of research investigating the role of CCL-2 in MSC modulation of the innate immune system. However, its modulation of the adaptive immune system has been well described in the literature.

1.3.4. Complexity and redundancy in CCL-2 signal transduction

Despite a wealth of literature demonstrating CCL-2 as a potent inducer of the recruitment of monocytes/macrophages, its role in MSC modulation of wound healing is still not clear due in part to the complexity and redundancy of downstream signalling cascades, posttranslational modifications and decoy receptors involved in CC signalling [134-136]. Its role remains an important question to be answered for further development of this therapy.

1.4. Thesis outline

The role of cell source in clinically relevant animal model of burn wound healing

As outlined in section 1.2.3 there is a substantial amount of pre-clinical and clinical studies that have demonstrated BM-MSC accelerate wound healing. However, as a clinical source of cells, BM is not ideal. AD-MSC are isolated from

adipose tissue and this represents a very large and easily obtainable source of these cells [109]. There is growing evidence that AD-MSC also have a therapeutic effect in both cutaneous wound healing and other applications [109, 111, 113, 137]. However, there is a little research exploring the role of cell source in a clinically relevant model of cutaneous wound healing or burn wound healing. In this study, we compare the efficaciousness of allogeneic AD-MSC and BM-MSC derived from donor matched animals in a clinically relevant large animal model of burn wound healing.

Improving efficacy of MSC through pre-stimulation with inflammatory cytokine TNFα

MSC both promote and reduce inflammatory responses under certain circumstances (**section 1.2.4**). In certain models, MSC activation with pro-inflammatory cytokines was necessary to induce its immune modulatory properties. MSC pre-treated with either or both TNF and IFNγ have demonstrated enhanced reduction in TNFα and increased M2 polarisation. While this method of MSC pre-stimulation has shown promise, it has not been attempted in a cutaneous injury model. We performed pre-stimulation of MSC with TNFα to determine if this pre-treatment would enhance the efficacy of these cells in a clinically relevant large animal model of burn wound healing and also in a mouse model of excisional wound healing.

The role of CCL-2 CCR-2 axis in MSC mediated cutaneous wound healing

In cutaneous wound healing, monocyte/macrophages are the dominant leukocyte effector cell secreting greater quantities of both pro and anti-inflammatory cytokines compared to other leukocyte subsets [138] and while CCL-2/CCR-2 axis is classically associated with the innate immune system, to date the role of MSC secreted CCL-2 in cutaneous wound healing has not been addressed. Furthermore, TNFα pre-treatment has shown promise in enhancing
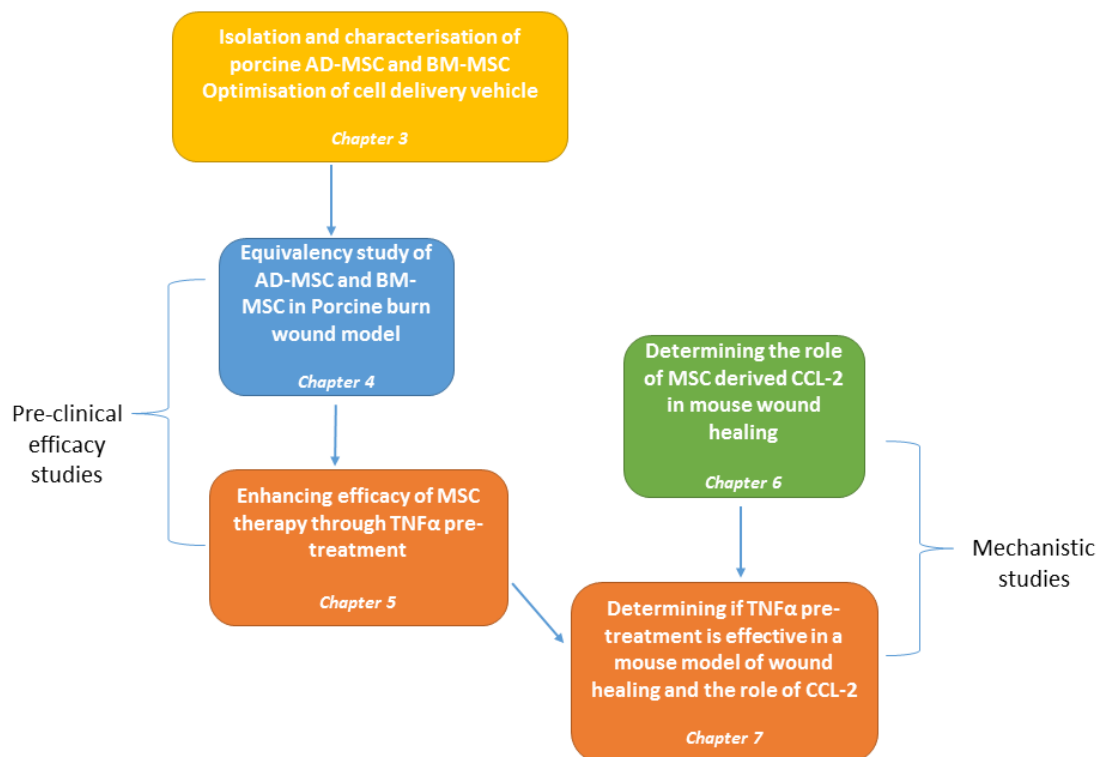
Figure 1.7 Thesis outline
In this work, efficacy studies of MSC therapy in a clinically relevant porcine model of burn wound healing were performed. To explore the mechanism in detail, in particular the role of CCL-2, a murine model of wound healing was used.

the immune-modulatory properties of MSC and is (as outlined in **section 1.3.3**) a significant inducer of CCL-2 secretion in MSC. The apparent redundancy of chemokine signalling poses some challenging and complex questions as to the nature and roles of those individual chemokines. If we wish to further refine our understanding of its mechanism and enhance its efficacy, it is necessary to unravel the complexities of chemokine promiscuity and apparent redundancy. To this end, we used CCL-2 deficient MSC to determine the role of CCL-2 signalling in MSC treated wounds with and without TNFα pre-treatment.

2. General materials and methods

In this chapter general methods and materials are described that are common to several chapters. Specific methods used in each study are detailed in each corresponding chapter.

2.1. Cell culture

All the cell lines were cultured in a class II biohazard safety cabinet at 37°C under 5% CO_2 atmosphere. Cells unless otherwise stated were maintained in Dulbecco's Modified Eagle Medium alpha modification (α-MEM) media (Sigma Aldrich, Ireland) supplemented with 10% foetal bovine serum (FBS, Life technologies) and antibiotic antimycotic solution (Sigma Aldrich, Ireland) containing penicillin (100 units/ml) streptomycin (0.1 mg/ml) and amphotericin B (0.25 μg/ml). For passaging (p), cells were washed once with phosphate buffer saline (PBS, Sigma Aldrich, Ireland) and detached from the tissue culture flask by incubating at 37°C in 0.25% trypsin/ Ethylenediaminetetraacetic acid (EDTA) solution (Life technologies) until cells had detached. Trypsinisation was followed by, neutralisation of trypsin with equal volume of serum supplemented media. Cells were then recovered by centrifugation at 500 g for 5 min, followed by re-suspension in appropriate volume of cell growth specific medium.

2.1.1. Macrophage cell culture

Murine macrophages were obtained from American type culture collection (ATCC). RAW 264.7 macrophage cell line was established from a tumour induced by Abelson murine leukemia virus on Balb/c mice. RAW cells are cultured in Dulbecco's Modified Eagle Medium (DMEM, Sigma Aldrich, Ireland) supplemented with 10% FBS and 1x antibiotic antimycotic.

2.2.   Flow cytometry analysis of cell surface antigens

Flow cytometry was used to analyse the level of MSC associated surface markers present to characterise isolated MSC populations. Expression of associated MSC markers was evaluated to ensure pure population of stromal cells. Cultured cells at P2-3 were washed once with PBS and detached from the tissue culture flask by incubating at 37°C in 0.25% trypsin/EDTA solution until cells had detached. Trypsinisation was followed by, neutralisation of trypsin with equal volume of serum supplemented medium (10% FBS). Cells were then recovered by centrifugation at 500 g for 5 min, followed by re-suspension in PBS and aliquoted out into several tubes containing $1x10^5$ cells for primary antibody staining. Cells were centrifuged and re-suspended in 100 μl of diluted antibody in Fluorescence-activated cell sorting (FACS) buffer (PBS containing 1% FBS and 0.1% EDTA) and incubated for 1h at 4°C cells were then washed in PBS centrifuged and re-suspended in 100 μl of secondary antibody solution for 30 min in the dark at room temperature (rt). Cells were then re-suspended in 100 μl FACS buffer and analysed on flow cytometer (BD FACSARIA II running BD FACSDIVA flow

cytometry software v6.1). Cell populations were gated to remove debris and dead cells from analysis and control isotypes were used to determine positive cell populations.

2.3. Animal experimental models

All animal experiments performed were approved by University College Cork Animal Experimentation Ethics Committee (AEEC) and project authorisation was granted by the Health Product Regulatory Authority (HPRA), the governmental regulatory body for experimental animal studies in Ireland. Animal experiments are detailed in chapter specific methodology (porcine burn induction, section 4.2.1 and murine excisional wounding, section 6.2.8)

2.4. CCL-2 deficient mice

Three breeding pairs of CCL-2 knockout mice (CCL-2tm1Rol) were obtained from JAX laboratories (Unites States). CCL2 -/- mice were created by introduction of a small deletion and an in frame stop codon created in exon 1 [139]. A PGK-neomycin resistance cassette was also inserted into exon 2 and the construct was electroporated into 129S4/SvJae derived J1 embryonic stem cells [139]. Correctly targeted embryonic stem cells were injected into C57BL/6 blastocysts. The resulting chimeric animals were crossed to C57BL/6 mice, and then backcrossed to C57BL/6 for ten generations. Mice that are homozygous for the

targeted mutation are viable, fertile, normal in size and do not display any gross physical or behavioural abnormalities [139].

2.5.   Wound healing image analysis

Wounds were imaged with a graduated ruler, using a Canon DSLR camera, at various time points. Images were imported into ImageJ image analysis software (National institute of health, USA) (v1.48g) where wound area was calculated and expressed as a percentage of original wound area at d-0. Using the following formula: [(total section length – unepithelialised length)/total section length]x100 [140].

2.6.   Immunostaining of wound tissue sections

Tissue samples were rinsed with chilled PBS, followed by immediate fixing with 4% paraformaldehyde (PFA, Sigma Aldrich, Ireland) for 1 h (or overnight (o/n) for thicker porcine tissues) at 4°C. Tissue samples were then rinsed in PBS and stored o/n at 4°C in 15% sucrose followed by 30% sucrose o/n to dehydrate tissues and reduce ice crystal artefacts. Samples were then embedded into the optimal temperature cutting compound (OCT, Cellpath, UK), and frozen immediately at -80°C. Embedded tissue samples were cut at 10 µm slices onto Superfrost plus glass slides (Thermo Fisher Scientific, UK). Slides were stored at -80°C until ready to be stained.

Slides were removed from the freezer and allowed to come to room temperature for 30 min. Sections were then rehydrated in PBS for 10 min followed by blocking

for 1 h in 10% normal goat serum and PBS + 0.1% Tween 20 (Thermo Fisher Scientific, UK) (PBST). Primary antibodies were diluted at various concentrations (see chapter specific methods) in 1% bovine serum albumin (BSA, Sigma Aldrich, Ireland) in PBST and 100 µl of antibody solution was applied to each section. Slides were incubated o/n at 4°C in a humidified chamber. Slides were then washed 3x in PBST 0.1% for 5 min followed by application of secondary antibody. Secondary antibodies were diluted in 1% BSA in PBST and 100 µl was applied to each tissue section. Slides were incubated at rt for 1 h in the dark humidified chamber. Slides were washed 3x in PBST for 5 min and stained with 4',6-diamidino-2-phenylindole (DAPI, Sigma Aldrich, Ireland) at final concentration of 1ug/ml for 10 min. Slides were again washed 3x in PBS for 5 min and mounted with coverslip using immunomount (Thermo Fisher Scientific, UK).

2.7.   Histology

Harvested tissue samples were fixed overnight in 4% PFA at 4°C. Next day, samples were then processed in automatic benchtop tissue processor (Histokinette, Leica, Germany) overnight and embedded in paraffin blocks. Sections 10 µm in thickness were cut from the paraffin blocks and plated on charged glass slides. These slides were then heated overnight at 60°C to remove excess paraffin and then deparaffinised by 2x washes in xylene for 3 min, followed by 3 min in 1:1 xylene/ethanol solution. Slides were cleared in series of graded alcohol changes. Slides were washed 2x for 3 min in 100% ethanol, 1x 3 min in 95% ethanol and 1x 3 min in 75% ethanol followed by a 3 min in 50% ethanol. Slides were then placed under running tap water for 10 min prior to

further staining using Hematoxylin & Eosin (Sigma Aldrich, Ireland)or Tri-chrome staining (Abcam, UK).

2.7.1. Hematoxylin and Eosin staining

Deparaffinised slides stained with Mayer's Hematoxylin (Sigma Aldrich, Ireland) stain for 15 min followed by 15 min rinsing in cold tap water. Slides were then immersed in eosin (Sigma Aldrich, Ireland) for 30 s, dehydrated through series of alcohol changes, then cleared in xylene prior to mounting with distyrene, plasticiser, and xylene (DPX, Thermo Fisher Scientific, UK) and cover slipped.

2.7.2. Trichrome staining

Slides were first deparaffinised and Trichrome staining was performed using a kit purchased from Abcam (UK). The slides were heated in Bouin's solution for 15 min at 56 °C. Slides were then rinsed and nuclei stained with Hematoxylin for 5 min. Cytoplasmic and muscle tissues were then stained with scarlet acid Fucshin followed by counter staining of collagens with Aniline Blue before rinsing with acetic acid, dehydrating in ethanol, clearing in xylene and mounting with DPX and coverslip.

2.8.   Quantitative Reverse-Transcription PCR

RNA was isolated from wound samples using rotar stator (IKA, Germany) in a solution of phenol, guanidine isothiocyanate (Qiazol, Qiagen, UK) for 1 min. RNA

purification was then performed using RNAeasy universal kit (Qiagen, UK) as per manufactures instructions.

Purity (A_{260}/A_{280}) and concentration of isolated RNA was measured using Nanodrop spectrophotometer (Thermo Fisher Scientific, UK). Integrity of RNA was assessed using denaturing agarose gel electrophoresis and ethidium bromide staining. Only high purity (A_{260}/A_{280} >1.8) RNA samples that had sharp bands of 28s and 18s ribosomal RNA (rRNA) and apparent 2:1 ratio were used.

RNA (1 µg) was reverse transcribed into cDNA using Qiagen RT^2 First Strand Kit (UK). This was then used for each qRT-PCR (Real-Time Quantitative Reverse Transcription PCR) reaction with RT^2 SYBR Green Mastermix containing Hotstart DNA Taq polymerase (Qiagen, UK). This was added to RT^2 profiler array (Qiagen, UK) Data was analysed using the $\Delta\Delta$ CT method, quantification was calculated in relation to 18s expression in each sample calculated before 35 cycles. Both positive, negative and genomic DNA contamination controls were included in the assays. The minimum information for publication of quantitative real-time PCR experiments (MIQE) guidelines were followed as described by Bustin et al [141].

2.9. Statistical analysis

All data are represented as mean ± standard error mean (SEM). Difference between groups was analysed by unpaired Student t-test or when more than two groups by analysis of variance (ANOVA) followed either Mann-Whitney or Tukey's post-hoc testing. All statistics were carried out using Graphpad Prism v7.03 (Graphpad software, USA)

3. Isolation and characterisation of porcine adipose and bone marrow derived MSC

3.1.   Introduction

Pre-clinical research allows us to translate basic science into clinical practice. Using clinically relevant animal models, we can further optimise and develop a greater understanding of how these new therapies may work.

Rodents have been used to model various diseases and are an invaluable tool for mechanistic studies and for preliminary evaluation of therapies. However, in some cases their findings do not translate well into clinical studies [142, 143]. Often large animal models provide more realistic scenarios and have more clinically relevant and scalable findings [144, 145].

While much research has been conducted into MSC therapy for burn wound healing in rodents, they are not ideal as they have loose skin structure and a well-developed panniculus carnosus, which allows them to heal primarily through wound contraction whereas humans have a fixed skin structure which adheres tightly to sub dermal structures and heals primarily through re- epithelialisation. For pre-clinical evaluation of efficacy, the porcine burn model is quite advantageous. Histologically porcine skin is quite analogous to human skin, containing similar epithelial and dermal layers and similar sub dermal fat

deposits [146] (rodents have a sub dermal layer, which is not present in either human or porcine skin) and contains a similar number and distribution of sebaceous glands and hair follicles [146]. Pigs are relatively hairless compared to rodents, and as re-epithelialisation of partial thickness wounds is driven to a large extent by the epithelial cells lining hair follicles, the density and pattern of hair growth of the surrounding hair can influence wound healing dynamics. As porcine skin is also rigidly attached to the underlying facia, it heals primarily through re-epithelialisation. Anatomically, pigs are also quite similar, their large size allows for topical application of treatment (without systemic effects) and importantly, they have immune systems comparable to humans [146, 147].

As well as establishing the efficacy of MSC therapy in a large animal model of burn wound healing, the role of cell source will also be addressed. MSC can be isolated from many locations in the body and not just the bone marrow. In the field of plastic surgery, adipose tissue provides an easy and abundant source from which to harvest MSC. However, it is not well established if adipose derived MSC have equivalent efficacy to that of bone marrow MSC.

3.1.1. Chapter aims

This chapter lays the groundwork for subsequent in vivo chapters, which evaluate the efficacy, the ideal cell source and explore potential ways to increase the efficacy of this therapy.

- In order to evaluate these therapies, a reproducible porcine MSC cell culture must first be established for both AD-MSC and BM-MSC and to demonstrate that these cells can be repeatedly isolated, expanded and meet the minimum criteria for defining MSC as set out by the ISCT [30].

- To validate that MSC can be delivered viably to the wound and survive for a sufficient period

3.2. Materials and methods

3.2.1. Isolation of porcine BM-MSC

Aspirates of BM were taken from approx. 3-month-old female landrace pigs during terminal procedures. Pigs were anesthetised by intramuscular (IM) injection of ketamine (10 mg/kg) (Vetoquinol, UK) and xylazine (2 mg/kg) (Vetoquinol, UK). While anesthetised, an area above the iliac crest was disinfected with povidone-iodine. The aspiration needle (11 gauge 6") was advanced through the skin until it contacted bone. To penetrate into the bone cavity, the needle was rotated while applying steady pressure. Once the needle was in the marrow, the stylet of the aspiration needle was removed and a heparinised luer-lock syringe was attached. 15-30 ml of bone marrow aspirate was removed and transferred into 9 ml vacuum tubes (Greiner-bio-one, Austria) containers. Under a sterile laminar flow hood, cells were washed by diluting (1:10) in in PBS and then centrifuging for 10 min at 900 g. To quantify cell

number a diluted BM suspension (1:5) was added to 4% (v/v) acetic acid (Sigma Aldrich, Ireland) solution (1:2) and allowed to sit for approximately 1 min to allow for sufficient lysing of erythrocytes. Cell numbers were then counted using a hemocytometer. The cells were re-suspended in αMEM supplemented with 10% FBS and 1x antibiotic antimycotic solution and plated at a density of 2.2×10^5 cells/cm^2 in a T-175 flask (Sarstedt, Germany). On d-3, 15 ml additional fresh media was added to each flask. Cells were then washed in PBS and non-adherent cells were removed on d-5. Fresh complete media was also added. After 1 wk, the formation of discrete colonies was observed. Colonies were grown until quite confluent and then were passaged and further expanded prior to characterisation.

3.2.2. Isolation of porcine AD-MSC

Adipose tissue was isolated from matched BM donor pigs. During anaesthesia, an area on the gluteal region was sterilised by application of povidone-iodine. An incision was then made and the cutaneous layer was peeled back to reveal subcutaneous white adipose deposits. These were then removed by scalpel, taking care not to include muscle tissue. Approx. 10-20 g of adipose tissue was isolated from each donor pig and put into a tube containing αMEM and 2x penicillin, streptomycin and amphotericin. Working under a laminar flow hood in sterile conditions the tissue was then finely minced using a sharp sterile scissors. The minced tissue was incubated in a shaker for 2 h in αMEM containing 2 mg/ml collagenase II (Sigma Aldrich, Ireland) at 36°C to breakdown the tissue and release the cells. To isolate the SVF, the digested tissue was centrifuged at

1200 g for 10 min. The supernatant and floating lipid deposits was removed while the pelleted cells were then re-suspended and filtered prior to counting. Cells were then plated at a density of $1x10^5/cm^2$ in a T-175 flask. After 24 h non adherent cells were removed and fresh media was added. Cells were grown to confluency prior to passaging for characterisation and further expansion.

3.2.3. Flow cytometry analysis of cell surface antigens

Flow cytometry was used to analyse the level of MSC associated surface markers present to characterise isolated BM and AD cell populations. Expression of associated MSC markers CD29, CD90 and CD105 along with absence of CD45 (common leukocyte antigen) was evaluated to ensure pure population of stromal cells. Cultured cells at P2-3 were washed once with PBS and detached from the tissue culture flask by incubating at 37°C in 0.25% trypsin/EDTA solution until cells had detached. Trypsin was neutralised with equal volume of serum supplemented medium. Cells were then recovered by centrifugation at 500 g for 5 min, followed by re-suspension in PBS and aliquoted out into several tubes contain $1x10^5$ cells for primary antibody staining. Cells were centrifuged and re-suspended in 100 μl of diluted antibody (see table below) in FACS buffer (PBS containing 1% FBS and 0.1% EDTA) and incubated for 1 h at 4°C cells were then washed in PBS centrifuged and re-suspended in 100 μl of secondary antibody solution for 30 min in the dark at rt. Cells were then re-suspended in 100 μl FACS buffer and analysed on flow cytometer. Control isotypes were used to determine positive cell populations.

Table 3-1 Antibodies used in flow cytometry characterisation of porcine MSC

Primary antibody	Clone	Manufacture	Final Concentration	Isotype
CD29	NaM160-1A3	BD Pharmingen	1 µg/ml	Mouse IgG$_1$
CD45	N-19	Santa Cruz	2 µg/ml	Goat polyclonal IgG
CD90	5E10	BD Pharmingen	5 µg/ml	Mouse IgG$_1$
CD105	MEM-229	Acris	1 µg/ml	Mouse IgG$_{2a}$
Isotype control Mouse IgG$_1$	MOPC-31C	BD Bioscience	Adjusted to primary ab concentration	Mouse
Isotype control Mouse IgG$_{2a}$	NA	Santa Cruz	Adjusted to primary ab concentration	Mouse

Secondary antibody	Clonality	Manufacturer	Concentration	Host
488 αMouse IgG H+L	polyclonal	Abcam, UK	2 µg/ml	Goat

3.2.4. Lineage differentiation assays

MSC phenotype was validated by subjecting BM-MSC and AD-MSC to in vitro differentiation assays to confirm their potential to differentiate into adipocytes, chondrocytes and osteocytes. Tri-differentiation potential was verified using well established previously published protocols [25, 148].

Briefly, for adipogenic differentiation, cells in culture were subjected to 3 cycles of adipogenic induction media for 3 d followed by adipogenic maintenance media for 1 d. Adipogenic induction media consisted of DMEM with dexamethasone 1 mM, insulin 1 mg/ml (Sigma Aldrich, Ireland), indomethacin 100 mM (Sigma Aldrich, Ireland) and 500 mM MIX (Sigma Aldrich, Ireland), the adipogenic

maintenance media contained insulin 1 mg/ml in DMEM. Adipogenic differentiation was confirmed with Oil red O (Sigma Aldrich, Ireland) staining.

The cells were fixed in 10% formalin (Sigma Aldrich, Ireland) for 10 min. Oil Red O stock solution contains 0.3 mg Oil Red O in 100 ml of isopropanol (99%) (Sigma Aldrich, Ireland). To make Oil Red O working solution, 6 parts of stock Oil Red O was mixed with 4 parts of distilled water and allowed to stand for 10 minutes. The solution was filtered using Whatman no. 1 filter paper. Cells were stained with oil red o working solution for 5 min, rinsed with tap water and counterstained with H&E. Oil red o stains lipid vacuoles present within the cells red.

For osteogenic differentiation, cells were cultured in osteogenic differentiation media, DMEM containing β glycerol phosphate (Sigma Aldrich, Ireland) 1 M and ascorbic acid (Sigma Aldrich, Ireland) 2-P 10 mM for 21 d. Osteogenic differentiation was confirmed by Alizarin Red staining. Cells were washed in PBS and then fixed in 10% formalin for 10 min at room temperature. Cells were washed and 1 ml of Alizarin Red solution was added to the fixed cells and allowed to stain for 20min. Excess stain was removed and the cells were washed with dH2O. Finally, 1ml of dH2O was added to each well and cells were examined under the microscope for red deposits indicating the presence of calcium deposits associated with osteocyte differentiation.

For chondrogenic differentiation, pelleted cells were cultured for 21 d in chondrogenic differentiation media, DMEM containing 10 ng/ml TGF-β3 (Sigma Aldrich, Ireland). After 21 d, pellets were incubated in 4% PFA overnight (o/n).

Pellets were then removed from PFA and carefully placed on wattman paper, folded over and placed in paraffin embedding cassettes. Pellets were embedded in paraffin and 10 μm thin sections were cut and adhered to glass slides. Slides were then deparaffinised (as described in **section 4.2.3**) and chondrogenic differentiation was confirmed by positive staining with toluidine blue (Sigma Aldrich, Ireland).

3.2.5. Formulation of fibrin gel

To make fibrin gels 100 μl fibrinogen and 100 μl thrombin were quickly mixed. A range of concentrations were evaluated to assess gel capacity to support cell viability. Fibrinogen was reconstituted in PBS to stock concentration of 100 mg/ml. Thrombin was reconstituted in diH$_2$0 to 25 U/ml.

3.3. Results

3.3.1. Isolation and expansion of porcine AD-MSC and BM-MSC

To determine if either cell source was more efficacious, AD-MSC and BM-MSC were isolated from matched female landrace pigs of 3-4 months of age. Isolation of adipose tissue and BM was performed on eight pigs. Adipose tissue was isolated from the gluteal region (as shown in **Figure 3.1**) The adipose tissue was washed in PBS and then digested in collagenases before centrifugation to isolate the SVF (as detailed in **section 3.2.2**) On average about 10-15 g of tissue was excised and from this, about 20×10^6 cells were isolated. The cells quickly adhered to plastic and formed large colonies of rapidly growing cells. These cells were then expanded for 2-3 wk prior to characterisation. To isolate BM-MSC, 10-15 ml bone marrow was extracted from iliac crest using puncture technique (**Figure 3.1**). From this, approximately $5-10 \times 10^6$ cells were retrieved. After 1 wk, plastic adherent cells began to form colonies, which subsequently became confluent. These cells were expanded through several population doublings until approximately 50×10^6 cells were obtained, enough to provide sufficient cells for in vivo study and characterisation.

3.3.2. Porcine MSC characterisation

Culture expanded MSC were then further characterised using flow cytometry to assess cell surface receptor expression (representative plots shown in **Figure 3.2**, n=6). As no single unique marker exists for MSC, a profile of expression

associated with MSC was used to characterise this cell population. Flow cytometry indicated both populations were positive for CD29, CD90 and CD105 and negative for the leukocyte common antigen CD45 [30]. After flow cytometry, multipotency of the cells was determined (representative images shown in **Figure 3.3** n=6). Samples from both cell populations were cultured in various differentiating conditions using well established protocols (as previously described [149, 150]). Adipogenic differentiation was confirmed in both cell types by the presence of lipid vacuoles stained with oil red O (**Figure 3.3 A**). Strong Alizarin red staining indicated the presence of calcium deposits associated with osteoblast formation (**Figure 3.3 B**). Chondrogenic differentiation was confirmed using toluidine blue staining of pellet cultures. Both BM-MSC and AD-MSC pellets had deep purple staining indicative of the presence of sulfated glycosaminoglycans (**Figure 3.3 C**)

3.3.3. Fibrin gel optimisation

Cells were to be delivered topically to the wounds in a fibrin gel. Fibrin is composed of fibrinogen that is polymerised with thrombin. To validate that sufficient viable cells could be delivered topically various concentrations were tested to determine optimal formulation. **Figure 3.4 A** shows cell viability assay using a cell permeable peptide substrate (fluorescein diacetatecetate) which when cleaved by enzymatic processes within live cells will fluoresce green under a blue light. Three concentrations of fibrinogen were formulated (3 mg/ml, 6.25 mg/ml and 12.5 mg/ml) based on previous studies [50, 151] and polymerised using thrombin at a final enzymatic activity of 12.5 U. After 24 h there was a small reduction in viable cells in the two higher concentration fibrin groups (3 mg/ml

group; 98.4% ± 0.34, vs 6.25 mg/ml group; 80.24% ± 0.05, vs 12.5 mg/ml group 72.0% ± 0.01, Control vs. 3mg/ml p=0.931, Control vs. 6.25mg/ml, p<0.001, Control vs. 12.5mg/ml, p<0.001, ANOVA, n=3), however, cell viability normalised between groups to some degree after 48 h (3 mg/ml group; 90.02% ± 0.02, vs 6.25 mg/ml group; 83.09% ± 0.002, vs 12.5 mg/ml group 83.15% ±0.02, Control vs. 3mg/ml p<0.001, Control vs. 6.25mg/ml, p<0.001, Control vs. 12.5mg/ml, p<0.001, ANOVA n=3) (**Figure 3.4 A**).

In terms of usability, the lowest concentration fibrin gel was very slow to polymerise and unpolymerised liquid remained. This was not suitable for application onto wounds, as unpolymerised liquid containing cells was likely to run off the wound. The 6.25 mg/ml concentration was found to be optimal, polymerising quickly but not resulting in an overly rigid gel. This gel formulation was easily degraded by the cells with approximately 50% reduction in gel size observed after 7 d in culture (**Figure 3.4 B**). This formulation was selected based on its usability and propensity for maintaining cell viability.

Following on from this, long-term viability was assessed in–vitro using propidium iodide staining (**Figure 3.4 B**). After 1 wk in culture, the gel was digested using trypsin and non-viable cells were assessed by flow cytometry using propidium iodide. No significant difference was observed (Control; 8.93% ± 0.72, Fibrin; 11.03% ± 0.24, p= 0.057, Mann-Whitney test, n=3) suggesting fibrin gel did not have a deleterious effect on cell viability.

3.3.4. Porcine burn model

The pig burn model is a previously established model in the Centre for Research in Vascular Biology lab. A deep partial thickness burn is induced in anaesthetised pigs using a solid metal bar preheated in water bath to 80°C (specific methodology is detailed n section 4.2.1). Pressure is applied using the weight of the metal bar for 20 s, this produces consistent, deep partial thickness burns (**Figure 3.5 A**). Images taken two hours after the induction of partial thickness burn show the formation of a leathery white eschar and surrounding erythema (**Figure 3.5 A**). Mass cell death and denaturation of tissue proteins initiate large inflammatory response that increases local vascular permeability [152]. Histological sections, taken at 2 h post burning and stained with Hematoxylin and eosin (H&E) show loss of epidermal layer, coagulation and tissue necrosis (**Figure 3.5 B**).

Figure 3.1

A)

Adipose tissue isolation

B)

Bone marrow isolation

Figure 3.1 Isolation of adipose tissue and bone marrow aspirates from the pig
A) *AD-MSC were isolated from subcutaneous adipose tissue that was harvested from the gluteal region. Adipose tissue was stored in PBS until digestion and isolation of SVF. **B)** BM-MSC were isolated from bone marrow aspirates obtained from the iliac crest. The bone marrow was stored in heparinised tubes prior to further processing. Adipose tissue and bone marrow aspirates were harvested from the same donor. Cells from six different donors were used in this study.*
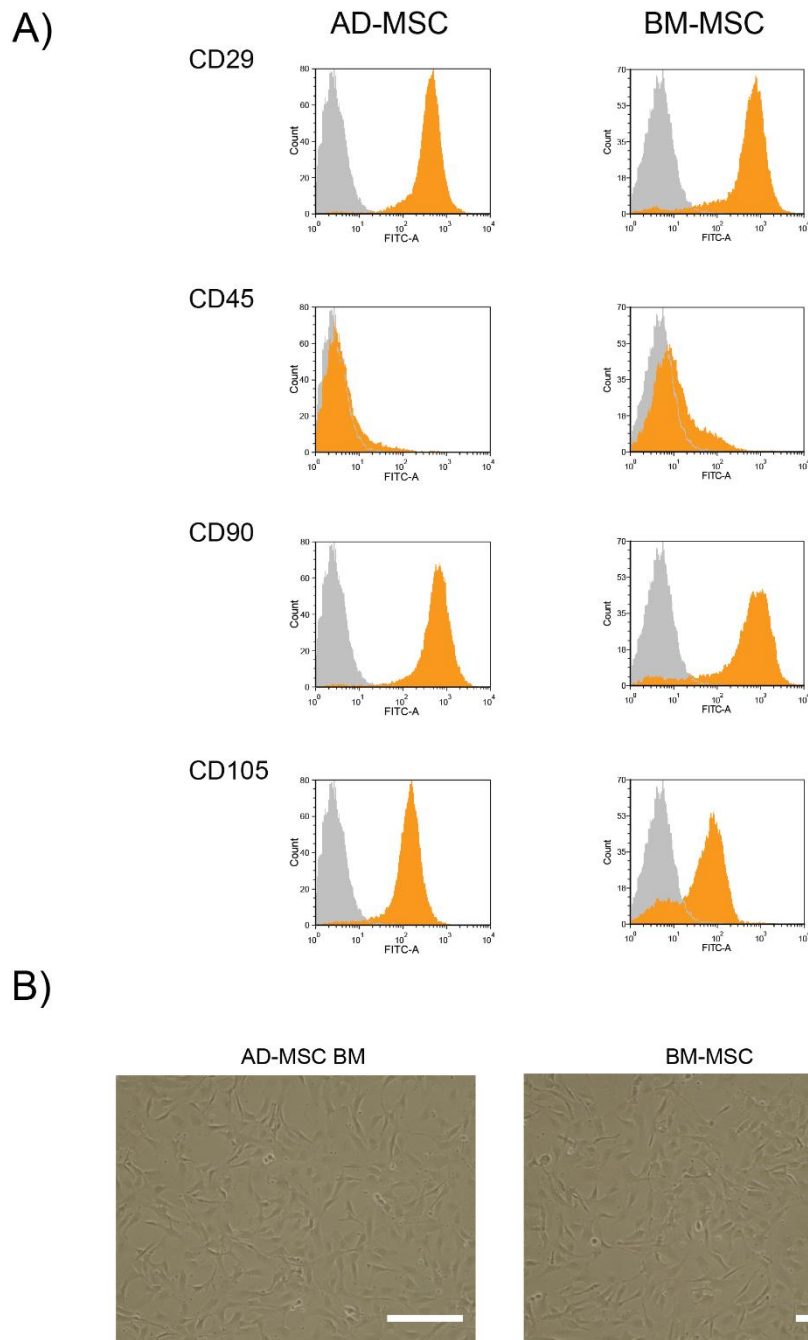
Figure 3.2 MSC cell surface receptor profiling by flow cytometry
Isolated BM-MSC and AD-MSC were characterised for expression of cell surface markers. A) Representative plots, both cell types were positive for mesenchymal markers CD29, CD90 and CD105 whilst negative for common leukocyte antigen CD45 (shown in orange histograms, control IgG are shown in grey histograms). B) In culture both AD-MSC and BM-MSC show large fibroblast spindle like appearance. Scale bar represents 100 μm (n=6).
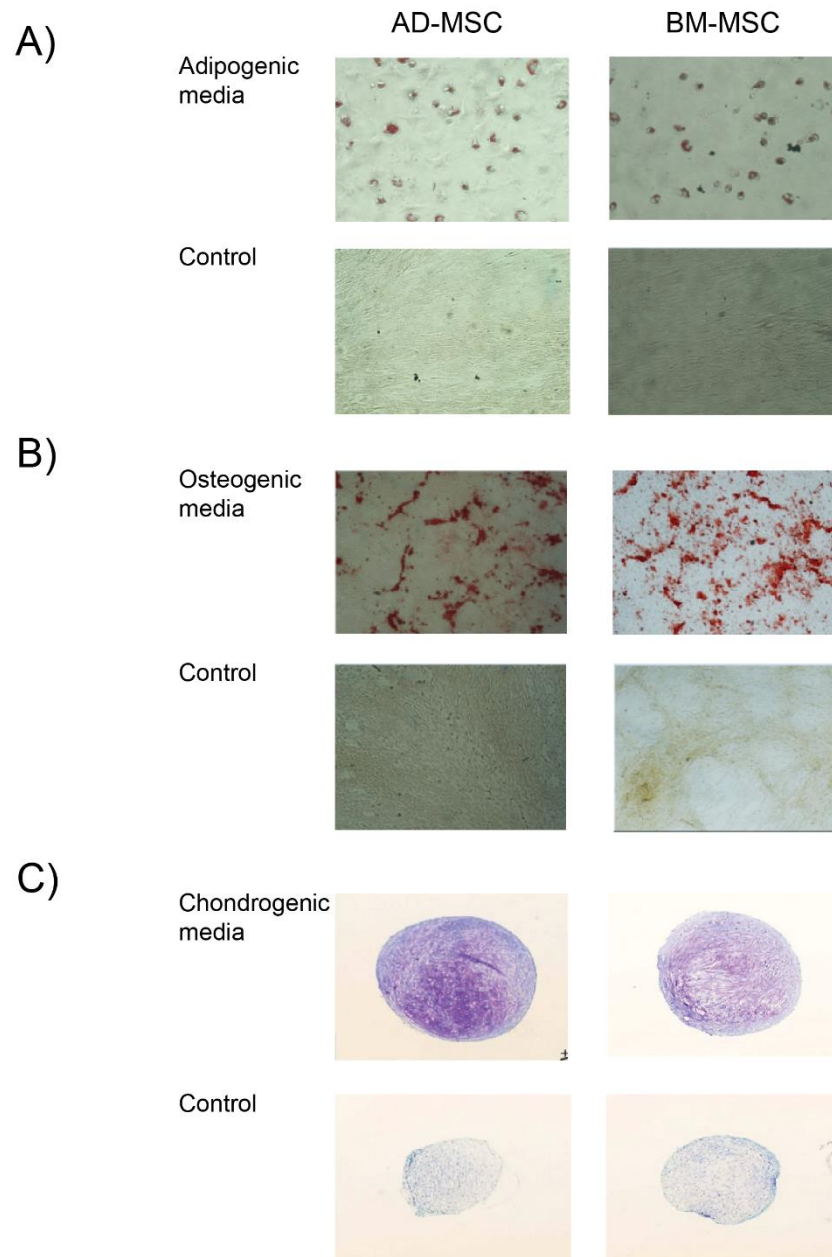
Figure 3.3

Figure 3.3 Tri-lineage differentiation of isolated MSC

*AD-MSC and BM-MSC were exposed to various differentiating media and subsequently differentiated into **A)** adipocytes (verified with Oil red o) **B)** osteocytes (alizarin red stain) and **C)** chondrocytes (toluidine blue stain). Both cell populations were readily able to differentiate into these lineages, while cells cultured in control media did not differentiate. Representative images of differentiation potential. (n=6)*
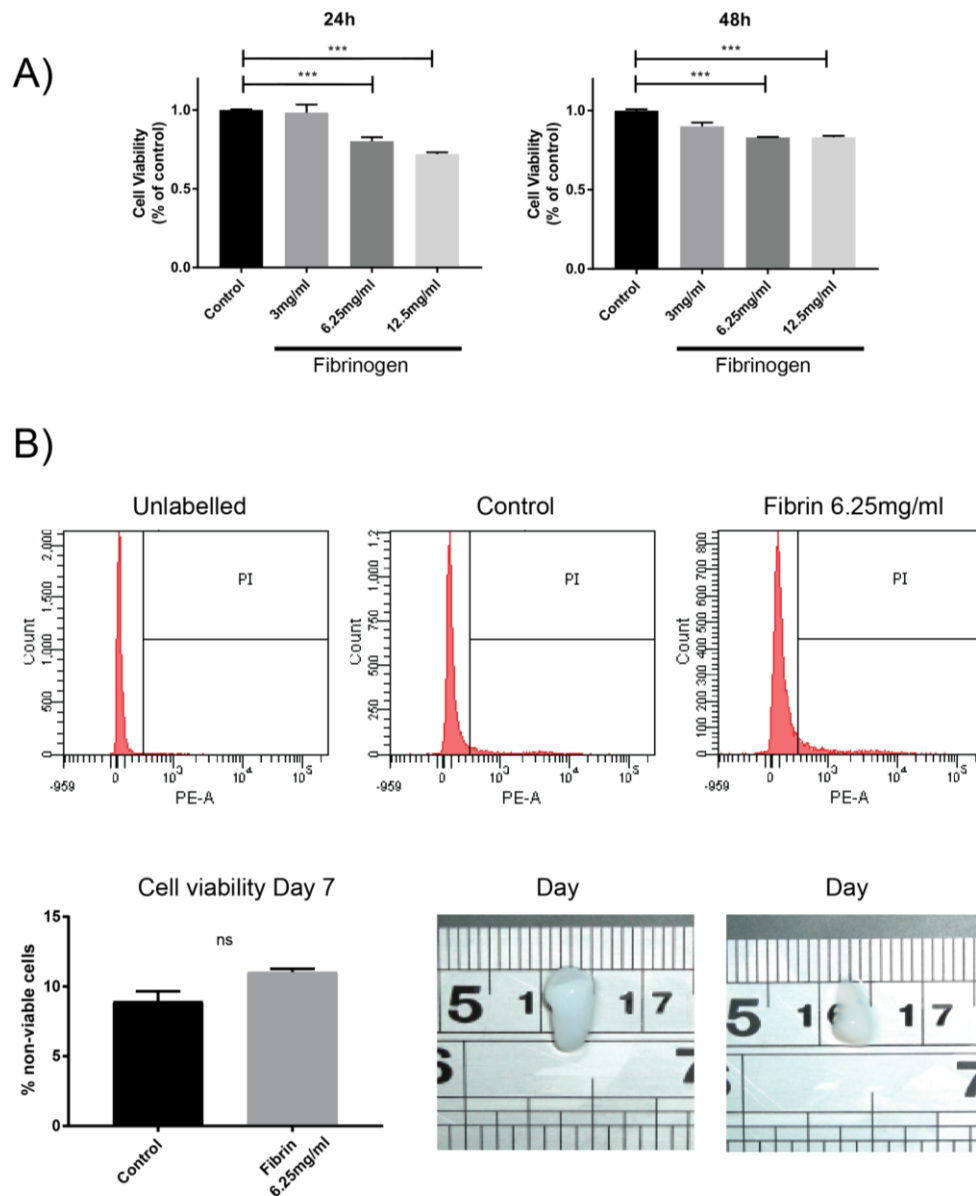
Figure 3.4 MSC viability in fibrin gels of various composition

*A) Cell viability was assessed at 24h and 48h using cell permeable cell substrate in fibrin gels of various compositions. A reduction in viability was observed at 24 h in high fibrinogen concentration gels however, this recovered somewhat after 48 h (n=3 *** P<0.001). **B)** Upper panel, 6.25 mg/ml concentration of fibrinogen was selected based on usability and long-term cell viability was assessed by propidium iodide (PI) uptake as determined by flow cytometry, Increased fluorescence, as represented by red histogram, compared to unlabelled control indicates PI uptake and cell apoptosis. **B)** Lower panel left, graphical representation of cell viability quantification. **B)** Lower panel right, fibrin gel containing MSC at d-7 show significant size reduction as approximated by graduations on ruler indicating MSC are able to digest and breakdown fibrin*

Figure 3.5

A)

B)

Figure 3.5 Induction of burns in porcine pig model
*A) Experimental setup demonstrating induction of deep partial thickness burns to dorsum of pig using a preheated solid brass rod. Photographic images taken 2 h post wounding show erythema and leathery white appearance of skin, consistent with partial thickness burns [149]. **B)** Left, Histological sections of burns stained with H&E show detachment and loss of epidermal layer (indicated with black arrows), tissue coagulation and necrosis. B) Right normal skin shows intact epidermis (indicated with arrows) and healthy dermis. Scale bar represents 50 μm*

3.4.   Discussion

In this chapter, robust and reproducible protocols were established to isolate both AD-MSC and BM-MSC from pigs. These cells were then characterised and identified as MSC as set out by ISCT criteria [30]. Namely, it was confirmed that MSC expressed cell surface markers associated with MSC (CD29+, CD90+ CD105+ and were negative for Leukocyte markers such as CD45) and have multipotent differentiation potential. Here it was demonstrated that both of these cell populations could differentiate towards adipo- chondro- and osteo- lineages.

3.4.1. Identification of MSC

As no MSC specific marker exists, a minimum criterion was previously defined by the ISCT, which involves several conditions a cell population must meet [30]. This requires positive and negative expression of a broad range of surface antigens which define the population as mesenchymal and not of leukocyte origin. These cells are also required to be plastic adherent and capable of multipotency, which usually involves the ability to differentiate towards adipo, chondro and osteo linages. Unfortunately, this still leaves a broad and heterogeneous population of cells that can increase experimental variability and lead to conflicting results as illustrated by prolonged debate in the literature [28]. The term bestowed on this cell population has also added further confusion, with some researchers referring to them as stromal cells while others using the term stem cells. Variations in isolation and non-standardisation of culture conditions also add to

the complexity of interpreting the data across studies. Clearly, the field could benefit from a unique marker however to date none have been discovered. While a unique marker may be helpful, industry and some research groups are attempting to further characterise these cells based on the expression of multiple receptors to build a unique fingerprint of MSC. The field has readily adopted the basic ISCT criteria and could benefit from an updated and expanded criteria to better define these cells for experimental studies.

3.4.2. ASC as a source for MSC

BM-MSC have shown much promise in cell therapy [50, 153], however invasive and painful isolation procedures limit its future widespread use [154] leading to evaluation of alternative tissue sources of MSC for therapeutic use. MSC can be isolated from multiple tissues within the body such as synovial membrane [155], skin [156], skeletal muscle [157], umbilical cord [158] and adipose tissue [159].

Over 400,000 liposuction procedures are performed in the United States annually yielding between 0.1-3 L of aspirate, the majority of which is discarded [109]. Adipose tissue is derived from the mesodermal layer during embryonic development [109]. It is a highly complex tissue composed mainly of lobules of adipocytes. Within this is the stromal vascular fraction which contains; pericytes, pre-adipocytes, fibroblasts, vascular SMCs, endothelial cells and AD-MSC [109].

 Adipose tissue can be broken down in two types, white adipose tissue (energy storage) and brown adipose tissue (heat generation). Anatomically, adipose tissue can be found in sub cutaneous depots, as visceral fat around organs, in the

bone marrow, in muscle and in the mammary gland, each with distinct functions [109]. AD-MSC are frequently isolated from white subcutaneous fat deposits which offer the greatest yields, plasticity and ease of access [160], but AD-MSC can also be isolated from brown adipose tissue [161].

The primary benefit of AD-MSC is that adipose tissue is the largest reservoir of stem cells in the body. AD-MSC are routinely isolated at concentrations of approximately $30x10^6$ per 100 ml lipo-aspirate [162] which equates to 5,000 fibroblast colony forming units (CFU-F) per gram of adipose tissue, significantly higher than the estimates of 100-1000 CFU-F per ml of bone marrow [163]. Bone marrow isolation can result in donor site morbidity and this significantly limits amount of bone marrow that can be aspirated, this then extends the amount of culture time to generate a therapeutic dose. From this perspective AD-MSC may be superior to BM-MSC in terms of expansion potential and density but, it remains to be determined which one is therapeutically superior, this will be addressed in greater detail in chapter 4.

3.4.3. Fibrin as a delivery vehicle

The choice of delivery vehicle for cells onto the wounds is an important consideration. Fibrin is an ideal substrate for delivery of cells for wound healing. Its biological effects have been well characterised [164-166] and it has been utilised as a delivery system in many tissue-engineering applications [50, 167, 168]. Fibrin hydrogels have a very high water content mimicking that of soft tissues and also provide efficient cell seeding, ensuring even distribution and

immobilisation. Fibrin has been used extensively for delivery of many cell types such as keratinocytes [168], fibroblasts [169] and MSC [50]. A variety of cell types are able to proliferate, remodel and migrate out of fibrin gels [151, 170]. Fibrin is formed from the cross linking of fibrinogen fibres by thrombin. This polymerisation can be controlled by the concentration of each factor. A range of concentrations were evaluated to achieve a gel that would quickly polymerise but not too rapidly so as the cells can be dispersed in the gel and be uniformly delivered onto the wound. Both thrombin and fibrinogen concentrations will alter polymerisation kinetics; therefore, thrombin was kept constant at 12.5 U/ml (higher thrombin concentrations in fibrin gels can induce apoptosis in some cell types [171]). Increased concentrations of fibrinogen provided more substrate for cross linking, resulting in a more rigid gel which increased time taken for embedded cells to migrate out of the gel [151, 172]. Fibrin gels with concentration 6.25 mg/ml were found to have the most suitable polymerisation time, taking about 1-2 min to set, which allowed time for even distribution of cells and application to the wound. This reduced reaction time and allows time for greater self-organisation and gel homogeneity.

Initial cell viability was assessed and while some reduction was observed at 24 h by 48 h this had mostly recovered. This may be due to an initial culture shock, loss of cell-cell contact or reduction in nutrient supply. MSC secrete various fibrinolytic enzymes that break down the fibrin fibres allowing the re-establishment of cell-cell contact with other cells and formation of characteristic fibroblast morphology [151]. Subsequent analysis demonstrated that gels at this concentration were able to support MSC viability for at least 7 d and the gel was

easily degraded by the cells, allowing for migration into the wound. This is in agreement with several other studies which have assessed viability of human BM-MSC in fibrin gels of similar concentrations [151, 173].

Generally, cell proliferation is greatest in low fibrinogen concentrations and medium to low thrombin concentrations [174, 175]. However, where proliferation was slow initially, it increases rapidly after several days [174]. Increasing fibrinogen concentrations can decrease MSC proliferation and alter cell morphology [175]. Human MSC in low concentration fibrinogen gels, at 5 mg/ml, are elongated and stretched while at higher concentrations MSC appear rounded [175]. Lower fibrinogen concentrations yield fibrin clots with a more open pore ultra-structure and greater structural homogeneity, this observed level of structural homogeneity is due to a reduced reaction time because of the low thrombin concentration [175]. Increased pore quantity and distribution throughout the gel is important because it allows the cells to form a network throughout these pores.

In this study, the optimal concentration of fibrinogen and thrombin in terms of usability and acceptable cell viability was found to be 6.25 mg/ml fibrinogen and 12.5 U/ml thrombin, other studies have also reported using similar concentrations [50, 176, 177]. In a seminal paper by Falanga et al, they use MSC to treat cutaneous wounds on humans and mice which were topically applied in a fibrin spray at a concentration of 5 mg/ml fibrinogen and 25 U/ml thrombin. Fibrin has also been used to deliver keratinocytes in a porcine wound healing model [178]. Autologous fibrinogen was extracted from plasma and used to deliver autologous keratinocytes at a final concentration of approx. 10 mg/ml

fibrinogen, endogenous prothrombin on surface of wound initiates coagulation cascade [178]. Several formulations of fibrinogen and thrombin were examined in a rabbit model of wound healing, and the investigators found increased granulation in gels with a reduced fibrinogen concentration (17 mg/ml fibrinogen vs 50 mg/ml) when delivered with fibroblasts [176]. No difference was observed when fibrin was used without cells, suggesting that fibrinogen concentration alters outward migration of encapsulated cells [176].

In summary, AD-MSC have the potential to be a very useful source of MSC in the context of plastic surgery and wound healing. Both AD-MSC and BM-MSC can be isolated and fulfil the minimum criteria as set out for MSC by the ISCT. Fibrin gel can be used to deliver these cells topically to the wound and can support their viability for at least 7 d. In the next chapter, the efficacy of these cells in a porcine burn model will be examined.

4. AD-MSC and BM-MSC are therapeutically equivalent in porcine burn model

4.1.   Introduction

Burn injuries are the fourth most common trauma worldwide. While significant advances have been made in reduction in mortality, through better management of sepsis and fluid loss, scarring and wound closure remain problematic [6]. It has been well established that MSC therapy can improve wound healing and this has been validated in several animal models including; radiation [179], excisional [50] and burn wounds [180]. As detailed in **section 1.2.4,** central to this process are the secretion of paracrine factors that influence immune response and promote angiogenesis and granulation tissue formation [29].

 Currently, there are only a handful of human clinical studies on the efficacy of MSC, mostly in chronic wound healing (summarised in **Table 4-1**). A major clinical trial investigating the efficacy of MSC in burn wounds is on-going [181] and another trial has been completed, but no results have been reported (NCT 02394873). In general, MSC therapy is efficacious in treating both chronic and acute wounds [51, 182].

Many phase I and phase II clinical trials have been conducted to assess safety and efficacy of MSC in other pathologies such as; GVHD and non-union bone fractures

[183-185].To the best of the author's knowledge, these clinical trials have demonstrated little if any adverse events associated with the safety of MSC therapy. However, due in part to heterogeneity present in the human population (compared to laboratory animals), the rigorous design of clinical trials and inter species variation, the effectiveness of MSC therapy has declined somewhat compared to pre-clinical studies [186]. More robust pre-clinical studies are required to determine optimal parameters of MSC therapy before entering into further clinical trials. This will allow for the better design and optimisation of clinical trials to evaluate these potential therapies.

Table 4-1 Clinical studies of MSC therapy used in cutaneous wounds

Wound type	Cell type + delivery method	Sample size (n)	Ref	Outcome
Chronic wounds	BM-Mononuclear cells (MNC) (ID) + BM-MSC (topical) Approx. $0.25x10^6$/cm^2	3	[51]	Non healing wounds (1yr +) wounds healed after various treatments. Increased granulation and re-epithelisation
Acute + Chronic wounds	BM-MSC (topical fibrin spray) $1x10^6$/cm^2	Acute =5 Chronic =8	[50]	Reduction in wound size
Chronic wounds	Auto BM-MSC vs	24 Randomised controlled study	[47]	Reduced wound size increased pain free walking distance
Foot ulcer, CLI	$9.3x10^8$ Auto BM-MSC vs BM-MNC (IM)	41 a double-blind, randomised, controlled trial	[187]	Accelerated healing rate compared to BM-MNC. Increased limb perfusion
Extensive full thickness burns	Allogeneic (Allo)BM-MSC $3x10^4$/cm^2 topical application	1	[53]	Increased angiogenesis and wound healing

Cell source of MSC is one parameter that has not been well established, MSC from a variety of sources have been utilised in pre-clinical studies including BM-MSC, AD-MSC, umbilical cord and Wharton's jelly [188-191]. However, few equivalency studies have examined the efficacy of these cells, and it remains to be determined which cell source is therapeutically superior.

AD-MSC as a potential source

As discussed in **section 3.4.2**, adipose tissue is an advantageous candidate source as it is a readily available tissue for plastic surgeons, easily harvested under routinely performed procedures, has less donor site morbidity compared to BM isolation and provides a much greater yield of stromal cells [192]. AD-MSC have superior growth characteristics and a significantly lower population doubling time when in logarithmic growth phase [193, 194]. Although BM-MSC are a more widely studied cell type, BM isolation is a more invasive and painful procedure and may be more beneficial if reserved for hematopoietic stem cell transplantations [192].

AD-MSC are thought to be biologically equivalent to BM-MSC, express similar immuno-phenotypic profiles and have comparable multipotency [159]. However, some notable differences have been reported, that suggest that these different cell types may not be therapeutically similar [195]. For example, a certain population of AD-MSC express CD34 when freshly isolated, which BM-MSC lack, expression then begins to decline and is subsequently lost during cell culture [195, 196]. Several other immuno-phenotypic differences have been reported with some estimates of up to 10% difference in expression profile [159]. However, as such profiles are largely influenced by culture and isolation

conditions, not to mention differential binding of various antibody clones, there is much disparity in these studies [195]. Other global proteomic studies suggest that 23% of proteins are specifically expressed in one cell type and not the other and differential expression of over 30 other proteins was noted (such as VEGF, VCAM-1 and angiopoietin, all increased in AD-MSC), further suggesting innate difference in these cell types [196].

Furthermore, AD-MSC and BM-MSC employ distinct molecular mechanisms by which they induce angiogenesis, a key component of MSC therapy. The formation of new blood vessels involves the recruitment of endothelial cells, degradation of the basement membrane in surrounding vessels, endothelial cell proliferation, vessel maturation and subsequent pruning of vessels [197]. Proteases are crucial mediators of this process and are required for the remodelling of fibrin matrices in the wound clot, either through plasmin dependent serine proteases or plasmin independent MMPs [197]. AD-MSC mediated vessel morphogenesis primarily occurs through plasmin family of proteases (and to a lesser degree MMPs) which are required for endothelial cell invasion and elongation similar to fibroblasts whereas BM-MSC rely solely on MMPs [197]. Analysis of secreted soluble factors that promote angiogenic response suggest AD-MSC secrete larger quantities of VEGF-D; however, no differences were observed in secretion of VEGF-A and FGF-2 [198]. Conversely, in another study, analysis of messenger RNA (mRNA) expression suggests an increased expression in BM-MSC [193]. Similarly, other studies have observed differential secretion of angiogenic factors FGF-2, stromal derived factor-1 (SDF-1) and HGF (increased in BM-MSC) under normal culture conditions [194]. Co-culture of MSC with HUVECs resulted in significant

induction in HGF in AD-MSC but not BM-MSC co-cultures [197]. The expression of various soluble factors alters in response to time in culture and growth conditions, and may account for some of the observed discrepancies [193].

One of the other primary mechanisms of MSC therapy is through their immune-regulatory function, and again key difference have been observed between these cell types suggesting they may have different therapeutic responses in vivo [199]. Both BM-MSC and AD-MSC can reduce NK cell proliferation to a similar extent [199] and in co-culture with activated T-cells both cell types are able to inhibit T-cell proliferation associated with reduced TNFα and increased secretion of IL-10 [199, 200]. However, in vitro co-culture experiments suggest human AD-MSC are more potent in suppressing peripheral blood mononuclear cell (PBMNC) proliferation [114]. Similarly, AD-MSC are more potent inhibitors of DC differentiation [114, 201]. Taken together these data suggests AD-MSC may be more efficacious in resolving inflammatory responses and accelerating wound healing.

Comparative Wound healing studies

At the outset of this PhD study, there were no comparative analysis studies of AD-MSC and BM-MSC in cutaneous wound healing described in the literature, and to the best of the author's knowledge, only three such studies have since been published (summarised in **Table 4-2**), none of which involve burn wounds.

The fact that three separate studies have been published since the beginning of this PhD, validates that this is a pertinent and relevant research question to be

addressed. However, distinct differences exist between excisional wounds and burn wounds which add further complexity in interpreting results and therefore require separate studies to validate therapeutic efficacy in pre-clinical burn wound models.

In a recently published study, of a porcine model of excisional wound healing treated with either donor matched AD-MSC or BM-MSC, MSC therapy reduced scar index as assessed using the Vancouver scale, no difference was observed between cell groups [115]. Epidermal thickness measured at d-7, 10, 14 and 21, and was significantly increased in both MSC therapy groups compared to saline on d-21 only, again, no difference was observed between cell groups [115]. It should be noted that this study is not ideal, as the sample number is small (n=2 per time point) and characterisation of wound healing is limited, as no assessment of re-epithelialisation was conducted. In addition, the Vancouver scar scale which assesses scar qualities like pliability, height and pigmentation is a subjective measurement designed for clinical evaluation of burn scars [202] and is not appropriate measurement in an animal model of excisional wounding after 21 days.

In a rabbit model of excisional wound healing using rabbit allogenic MSC, AD-MSC were superior, promoting granulation tissue formation compared to BM-MSC and dermal fibroblast [203].

Table 4-2 Comparative pre-clinical studies in cutaneous wound healing

Wound type	Treatment	Delivery	Species	Ref	Outcome
Excisional, partial thickness 4cm^2	Allo donor matched AD-MSC, BM-MSC, 1x10^6	ID injection with autograft	Pig	[115]	Accelerated re-epithelialisation no significant difference between cell types
Excisional wound, 0.785 cm^2	Human AD-MSC , BM-MSC, 1x10^6	ID injection	Mouse	[204]	AD-MSC was significantly accelerated wound closure compared to BM-MSC, in vitro increased VEGF, FGF-7
Excisional full thickness ear 0.38cm^2	Allo AD-MSC vs BM-MSC vs dermal fibroblast	Topical 7 µl PBS	Rabbit	[203]	increased granulation tissue in AD-MSC treated wounds. No significant increase in re-epithelialisation

Similarly, in a xenogeneic mouse model of wound healing treated with human MSC, AD-MSC significantly accelerated wound closure compared to BM-MSC at all time points. In vitro analysis demonstrated increased VEGF, TGF-β, FGF-2 and FGF-7 (factors associated with increased angiogenesis and wound healing) secretion from AD-MSC compared to BM-MSC and also greater dermal fibroblast recruitment [204].

It is apparent from the literature that there are some conflicting results and it has not been well established which cell type is therapeutically superior. Furthermore, while several studies have been conducted using BM-MSC in burn wound healing (summarised in Appendix I), only four studies could be identified that investigated the efficacy of cultured AD-MSC in burn wound healing (Appendix II). To the best of the author's knowledge, no equivalency studies have been performed to determine optimal cell source in the context of burn wound healing. Previous studies suggest that AD-MSC may be therapeutically superior, or at least a more abundant and scalable source of cells. The knowledge gained

from this study will allow us to determine if indeed adipose tissue is the optimal source and if so large scale dosage escalation studies can be conducted to further optimise this therapy. Thus, to address this knowledge deficiency, the role of cell source in MSC efficacy in a large animal model of burn wound healing was investigated.

4.1.1. Chapter aims

- Measure efficacy of MSC cell therapy in porcine burn wound model
- Determine if either cell type is therapeutically superior

4.2.   Materials and methods

In this study the therapeutic efficacy of allogenic MSC derived from either BM or adipose tissue was investigated. The study consisted of two experimental treatments; AD-MSC, BM-MSC and a control treatment of fibrin only. Each animal received all three treatments thus providing intra animal controls. Allogenic AD-MSC and BM-MSC isolated from the same donor pig were characterised, as described in **section 3.3.2**, prior to use in following burn experiments.

Cells were harvested prior to the procedure by trypsinisation, viable cells counted and aliquoted into separate tubes for each wound (4.5×10^6 cells). The

tubes were centrifuged and then re-suspended in fibrinogen at a concentration of 12.5 mg/ml and stored on ice until application onto burn wounds.

4.2.1. Burn Induction

Eight female landrace pigs (25-30 kg) were used in this study. Animals were housed in the animal facility for one week prior to experiments to acclimatise. Pigs were anaesthetised with IM injection of xylazine (2.0 mg/kg), ketamine (15 mg/kg) and glycopyrollate (0.01 mg/kg). An IV cannula was placed into the ear veins for administration of IV fluids and drugs. Propofol (3 mg/kg i.v.) was administered and the pig was then intubated and maintained on 2% Isofluorane administered by inhalation. The animal was placed on its side and the area to be burned was shaved with an electric clippers. The area was then treated with a povidone-iodine solution. A template was then used to mark the area to induce burns so that all burns were over the ribcage and spaced 5 cm apart.

Burn wounds were induced as described by Brans et al [152]. A solid brass rod with a surface area of 4.5 cm^2 was preheated in a water bath at 80°C for 30 min prior use, (three sections of brass pipe were used to facilitate timely induction of multiple burns) and then blotted dry before direct application onto the animal's skin. The rod was balanced on the animal's skin and the rods own weight (570 g) used to apply pressure. The brass rod was applied for 20 s, inducing a deep partial thickness burn. 12 burns, 6 on each side (4 wounds for each experimental and control group) were induced in each pig, approximately 5% total body surface area. The burn wounds were then debrided of the burn eschar to reveal

a wound bed with fresh punctate bleeding. Prior to treatment, the wounds were randomised, to proximal, medial and distal dorsal regions.
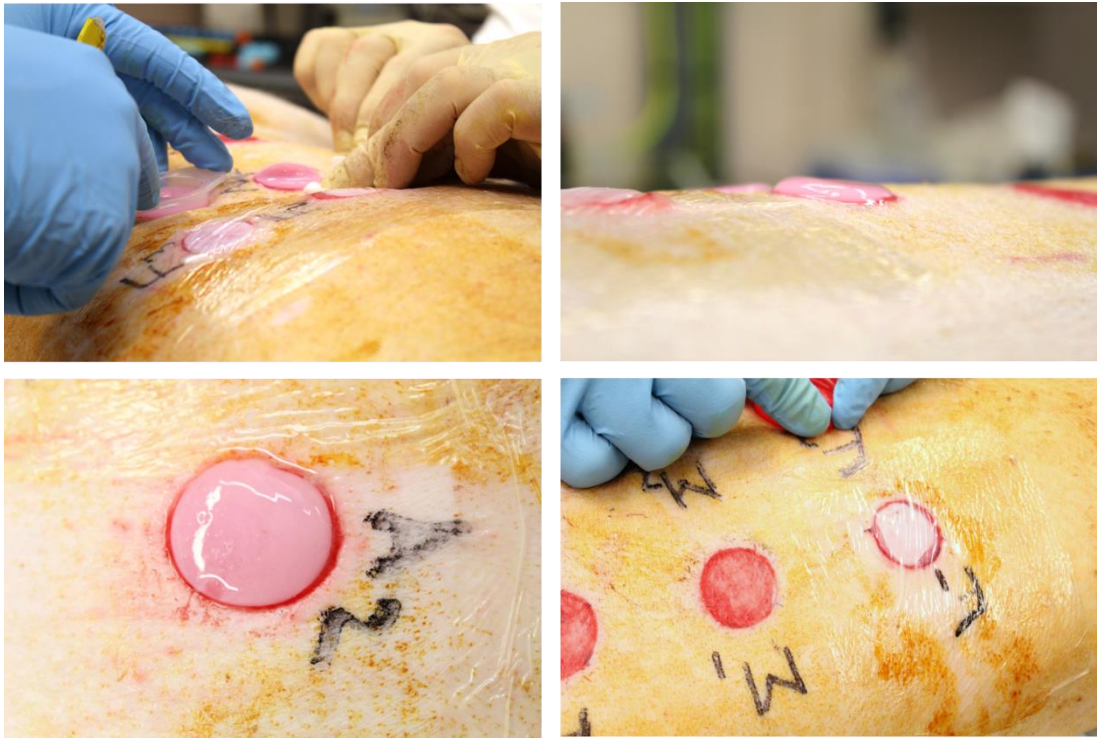
Figure 4.1 Application of Fibrin gel containing MSC
Fibrinogen was mixed with thrombin and allowed to polymerise forming a gel which was then covered using Tegaderm occlusive dressings.

The cells, either AD-MSC or BM-MSC were (4.5×10^6) suspended in 500 μl fibrinogen were mixed with 500 μl thrombin (25 U/ml) to give a fibrin gel of final concentration 6.25 mg/ml fibrinogen 12.5 U/ml thrombin. This polymerised within 1-2 min and was applied to the wound as it polymerised and contained to the wound using a mould (as shown in **Figure 4.1** top left) As a control, fibrin without any cells was applied to the wounds.

The wounds were then dressed with an occlusive adhesive dressing (Tegaderm™, 3M Healthcare, Belgium), followed by a layered non slip dressing composed of

gauze and melonin (Smith and Nephew, UK) secured with an adhesive tape and then covered with a double tubigrip and secured with further taping. Dressings were changed on d-4, d-7, and d-10 at which time wounds assessed for healing and imaged using DLSR camera (Canon, Japan).

4.2.2. Wound image analysis

Wound area was calculated using ImageJ software (NIH.gov). Area was measured at d-0 and again at d-14. To measure percentage wound closure the following formula was used: [(area of wound d-0 – area of wound d-14) /area of wound d-0] x 100 as previously described [205]. Wound closure image analysis was conducted by a blinded observer.

4.2.3. Histology

After the animal was euthanised (IV injection Pentababitone, 50mg/kg) a 4 cm^2 sample of both wound and wound margin was excised. Tissue samples were fixed overnight in 4% PFA at 4°C. The next day, samples were processed in histokinette overnight and embedded in paraffin blocks. 10 μm sections were cut from the paraffin blocks and plated on charged glass slides. Sections were then heated overnight at 60°C to remove excess paraffin and then deparaffinised by several changes of xylenes and cleared by several graded changes of ethanol (detailed in section 2.7.).

Re-epithelialisation

To determine re-epithelialisation, wound sections were stained with H&E (as detailed in **section 2.7.1**). Several over lapping images were taken of the entire wound section at 4x magnification. These images were then spliced together and the percentage of section epithelialised was calculated by blinded observers using following equation [(total section length – unepithelialised length)/total section length]x 100 [140].

Collagen formation

Early formation of granulation tissue of wounds is predicative good wound healing out comes [206]. To evaluate this response, histological sections were stained with Masson's tri-chrome as detailed in **section 2.7.2**, which stains all collagen fibres blue and cell cytoplasm red. Nuclei were counter stained with Hematoxylin. Percentage area of blue staining present on each wound section is an indicator of collagen and thus, granulation tissue. Quantitative analysis by blinded observer was performed at five randomly sampled points across the wound section and percentage blue staining of each section was quantified using NIS elements software (Nikon).

4.2.4. Immunofluorescent staining

Wound samples were stored in 4% PFA overnight at 4°C, dehydrated in graded sucrose solution and then embed in OCT (as detailed in **section 2.6**). Sections were cut at 10 μm thickness in cryostat and stored at -80°C until required. Prior to staining, slides were removed and left to defrost for 30 min at rt.

Slides were rehydrated in PBS (10 min) and then blocked for 1 h in 10% normal goat serum in PBS-Tween (0.5%) solution. Sections were then incubated o/n at 4°C with primary antibody diluted in antibody buffer (1% BSA PBST). The next day, sections were washed x3 in PBST and slides were incubated with secondary antibody solution in antibody buffer for 2 h at rt, followed by 3x washes in PBST. Nuclei were stained with DAPI (1 μg/ml) for 10 min followed by 3x washes in PBS prior to mounting in immunomount and cover slipped.

Table 4-3 Immunohistochemistry antibodies used in porcine wound sections

Primary antibody	Clone	Manufacture	Final Concentration	Isotype
CD163	2A10/11	BioRad (USA)	10 μg/ml	Mouse IgG$_1$
αSMA	1A4	Dako (Agilent USA)	10 μg/ml	Mouse IgG$_{2a}$
Isotype control Mouse IgG$_1$	MOPC-31C	BD Bioscience (UK)	Adjusted to primary ab concentration	Mouse
Isotype control Mouse IgG$_{2a}$	na	Santa Cruz (USA)	Adjusted to primary ab concentration	Mouse

Secondary antibody	Clonality	Manufacturer	Concentration	Host
488 αMouse IgG (H+L)	polyclonal	Abcam, UK	2 μg/ml	Goat

4.2.4.1. CD163 quantification

To determine the inflammatory response M2 macrophage (CD163+) populations within the wound were quantified. CD163 is a member of the scavenger receptor cysteine rich family and is expressed specifically on cells of the myeloid lineage, on macrophages it is expressed primarily on M2 type macrophages [207, 208]. It is strongly upregulated on monocytes differentiated with M-CSF and also in response to IL-10, whereas it is greatly suppressed by TNFα and LPS [207].

Sections were imaged at five random points within the wound bed and CD163+ cells were quantified by blinded observer; three sections were analysed per animal.

4.2.4.2.   Smooth muscle actin alpha quantification

To assess angiogenic response, wound sections from d-14 were probed with alpha smooth muscle actin (αSMA). This protein is expressed in vascular SMCs and pericytes that line arterioles and capillaries [209]. Sections were imaged at five random points within the wound bed and vessel density was calculated (by blinded observer) based on αSMA+ vessels; three sections were analysed per animal.

4.2.5. RNA extraction and qRT-PCR

A 4 cm^2 template was used to excise wounds which contained both healed wound margin and wound. This was bisected and 1 quarter was snap frozen in liquid nitrogen. Samples were kept at -80°C until required. To extract RNA, samples were crushed using pestle and mortar in liquid nitrogen. Samples were then homogenised using rotar stator in a solution of phenol, guanidine isothiocyanate for 1 min. RNA purification was then performed using RNAeasy universal kit as per manufactures instructions.

Purity (A_{260}/A_{280}) and concentration of isolated RNA was measured using Nanodrop spectrophotometer. Integrity of RNA was assessed using denaturing agarose gel electrophoresis and ethidium bromide staining. Only high purity

(A_{260}/A_{280} >1.8) RNA samples that had sharp bands of 28s and 18s rRNA and apparent 2:1 ratio were used.

Two wound samples from each treatment group per pig were used for RT^2 profiler array (n=6). RNA (1 µg) was reverse transcribed into cDNA using RT^2 First Strand Kit. This was then used for each qRT-PCR reaction with RT^2 SYBR Green Mastermix containing Hotstart DNA Taq polymerase. This was added to RT^2 profiler array containing 10 pre coated validated primer assays for TNFα, IL-10, IL-6, IL-8, VEGF, MMP-2, Col1, Col3, CD206 and TGF-β. Data was analysed using the ΔΔ CT method, quantification was calculated in relation to 18s expression in each sample calculated before 35 cycles. Both positive, negative and genomic DNA contamination controls were included in the assays.

4.2.6. Statistical analysis

The sample size for each animal experiment calculated based on power analysis to detect a minimum of 10% difference between means in experimental and control groups with standard deviation less than 8 based on our own previous studies and results reported in the literature. The power of the test was set at 0.80. The Type I error probability associated with the test was set at 0.05.

Each animal received all treatments including control which reduces the effects of inter animal variability and allows the use of paired wound measurements. Difference between groups was analysed by repeated measures analysis of variance (rmANOVA) followed by Tukey's post-hoc testing. Results are reported as means ± SEM. All statistics were carried out using Graphpad Prism v7.03.

4.3.   Results

4.3.1. MSC treatment of burn wounds increased rate of wound closure

The wounds were first debrided and imaged (**Figure 4.2 A**). Wounds with a combined mean area of 5.3 cm^2 ± 0.1 were consistently produced and no significant differences were observed between the groups (**Figure 4.2 B**). Wound closure at d-14 was quantified as shown in **Figure 4.2 B**. Application of either BM-MSC or AD-MSC induced a modest, but significant enhancement in wound closure (Fibrin; 18.39% ± 1.9 vs AD-MSC; 13.95% ± 1.7 vs BM-MSC; 14.48% ± 2.1, Fibrin v AD-MSC p=0.26, Fibrin v BM-MSC p=0.3 n=7), no significant difference was observed between AD-MSC and BM-MSC (p=0.8). Eight animals were used for these experiments, however, one animal was excluded from wound image analysis as significant eschar was still present at d-14. In this case, the calculated percentage wound open was significantly deviated from the mean and was not suitable for inclusion in wound image analysis. These outliers are shown in Appendix III.

4.3.2. Neither AD-MSC or BM-MSC significantly accelerated re-epithelisation

Re-epithelialisation of wounds is a primary determinant of wound healing. By d-14, all wounds had re-epithelialised to some degree, with all wounds at least

over 50% re-epithelialised (Fibrin; 69.77% ± 3.6, AD-MSC; 80.32 ± 4.3, BM-MSC; 77.7% ± 4.1, Fibrin v AD-MSC p=0.27, Fibrin v BM-MSC p=0.34, n=8). There was improved re-epithelialisation in both AD-MSC and BM-MSC treated wounds however this was not significant when compared to control group (**Figure 4.3 B**).

4.3.3. MSC therapy was associated with increased wound maturity

As the wound matures more collagen is deposited giving the tissue greater strength. Initially collagen type III is deposited which is later replaced with stronger collagen type I. The quantification of collagen within the wound is an indicator of wound maturity. To evaluate this response, histological sections were stained with Masson's tri-chrome (as described in **section 4.2.3**), which stains all collagen fibres blue and cell cytoplasm red (**Figure 4.4 A**). Nuclei were counter stained with Hematoxylin. Percentage of blue staining present on each wound section is a semi-quantitative indicator of collagen content and thus, wound maturity. Quantitative analysis of staining (randomly sampled at five points across the wound section) suggests significantly increased collagen content in both cell treated groups (Fibrin; 40.9% ± 2.1, v AD-MSC; 65.1% ± 3.1, v BM-MSC; 60.6% ± 3.3, Fibrin vs AD-MSC p<0.001, Fibrin vs BM-MSC p=0.002, AD-MSC vs BM-MSC p=0.13, n=8). Additionally, fibrin only treated wounds had markedly more cellular infiltrates within the wound bed, associated with ongoing inflammatory response.

The maturation of granulation tissue is driven by collagen formation but also by MMPs, which remodel and breakdown denatured proteins from the burn, and the TGF family of growth factors, which control fibrotic responses but also drive re-epithelialisation [210]. Analysis of mRNA expression indicated neither collagen type I (COL1) (Fibrin; 1.05 ± 0.09 vs AD-MSC; 0.88 ± 0.06 vs BM-MSC; 1.08 ± 0.14) collagen type III (COL3) (Fibrin; 1.07 ± 0.11 vs AD-MSC; 0.88 ± 0.09 vs BM-MSC; 1.12 ± 0.14) MMP2 (Fibrin;1.05 ± 0.09 vs AD-MSC; 0.88 ± 0.08 vs BM-MSC; 1.08 ± 0.10) or TGF-β (Fibrin;1.04 ± 0.09 vs AD-MSC; 0.87 ± 0.09 vs BM-MSC; 1.16 ± 0.15, n=8)   were significantly different in either MSC versus control group (**Figure 4.4 B**). For mRNA extraction, samples contained both healed wound margin and wound itself, which may have resulted in skewed qRT-PCR readouts.

4.3.4. BM-MSC increased M2 macrophage population within wound

To characterise the ability of MSC therapy to modulate inflammatory environment the M2 population within the wound bed was quantified using the M2 marker CD163. An increased number of CD163+ cells per high power field (HPF) was detected in BM-MSC treated wounds compared to fibrin treated wounds (Fibrin; 12.1 ± 4 v BM-MSC; 20.74 ± 6, AD-MSC; 20.49 ± 7.8, Fibrin vs BM-MSC p=0.02, Fibrin vs AD-MSC p=0.16, AD-MSC vs BM-MSC p=0.99, n=8). Thus while AD-MSC treated wounds had a similar mean of CD163+ cells it was not statistically different as it had a greater variability.

The expression of several inflammatory cytokines at d-14 was analysed by qRT-PCR, however, in all cases no significant differences were observed (**Figure 4.5 B**). Cytokines assayed were IL-10 (Fibrin; 1.05 ± 0.23 vs AD-MSC; 0.91 ± 0.11 vs BM-MSC; 1.31 ± 0.44), TNFα (Fibrin; 1.20 ± 0.28 vs AD-MSC; 1.66 ± 0.63 vs BM-MSC; 0.98 ± 0.2), IL-6 (Fibrin; 2.01 ± 0.82 vs AD-MSC; 1.30 ± 0.42 vs BM-MSC; 4.34 ± 1.88) and IL-8 (Fibrin; 2.38 ± 0.86 vs AD-MSC; 2.33 ± 0.77 vs BM-MSC; 1.73 ± 0.66, n=8).

4.3.5. Both AD-MSC and BM-MSC increased vessel density within the wound

Immuno-histological staining demonstrated a modest but significant increase in vessel density per HPF in MSC treated wounds as determined by quantification of αSMA+ vessels (Fibrin; 4.1 ± 0.8, v AD-MSC; 6.2 ± 0.9, v BM-MSC; 7.2 ± 1.3, Fibrin vs AD-MSC p=0.006, Fibrin vs BM-MSC p=0.04, AD-MSC vs BM-MSC p=0.29, n=8) (**Figure 4.6 A**). Increased αSMA vessel density is indicative of increased angiogenesis formation of stable vasculature and wound progression. Analysis of RNA expression of VEGF across wound and wound margin at d-14 show no significant difference between groups (Fibrin 1.07 ± 0.12 vs BM-MSC; 1.107 ± 0.14, vs AD-MSC; 1.109 ± 0.15, n=8) (**Figure 4.6 B**).

Figure 4.2

A)

B)
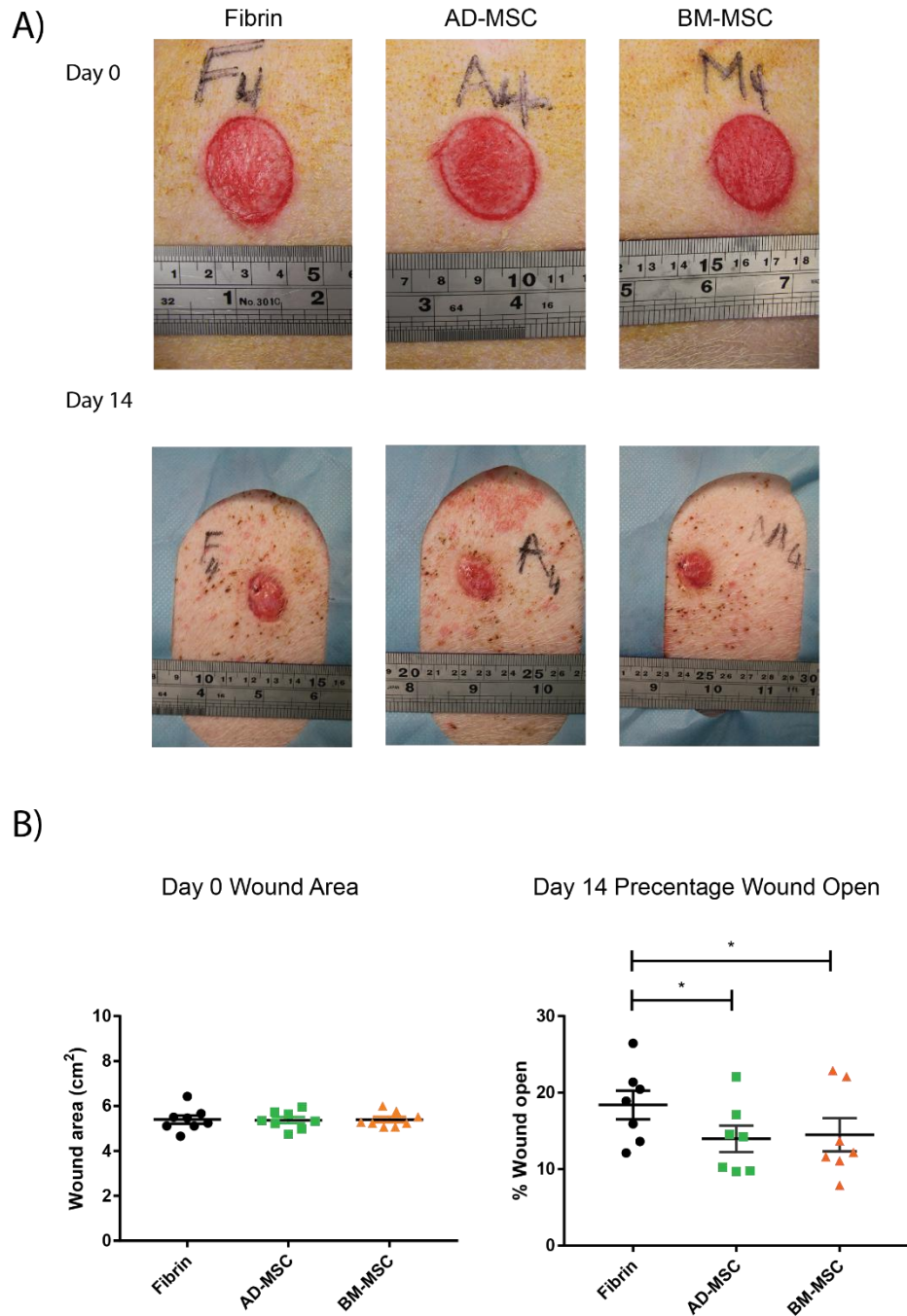
Figure 4.2 Application of MSC in porcine burn wounds increases wound closure at d-14
*A) Burn wounds were induced on dorsum of pigs and imaged on d-0 after debridement, prior to application of cells. **Lower panel A)** wounds were imaged on d-14 post wounding, blue drape in-situ. **B) Left** - Quantification of wound area at d-0, no significant difference was observed. **B) Right** - Percentage wound open was calculated by dividing wound area at d-14 by original wound area. Treatment of wounds with either AD-MSC or BM-MSC improved wound closure, no significant difference was observed between AD-MSC and BM-MSC. (n=7 * p<0.05).*

Figure 4.3

A)

Day 14 Re-epithelialisation

Fibrin

AD-MSC

BM-MSC

B)
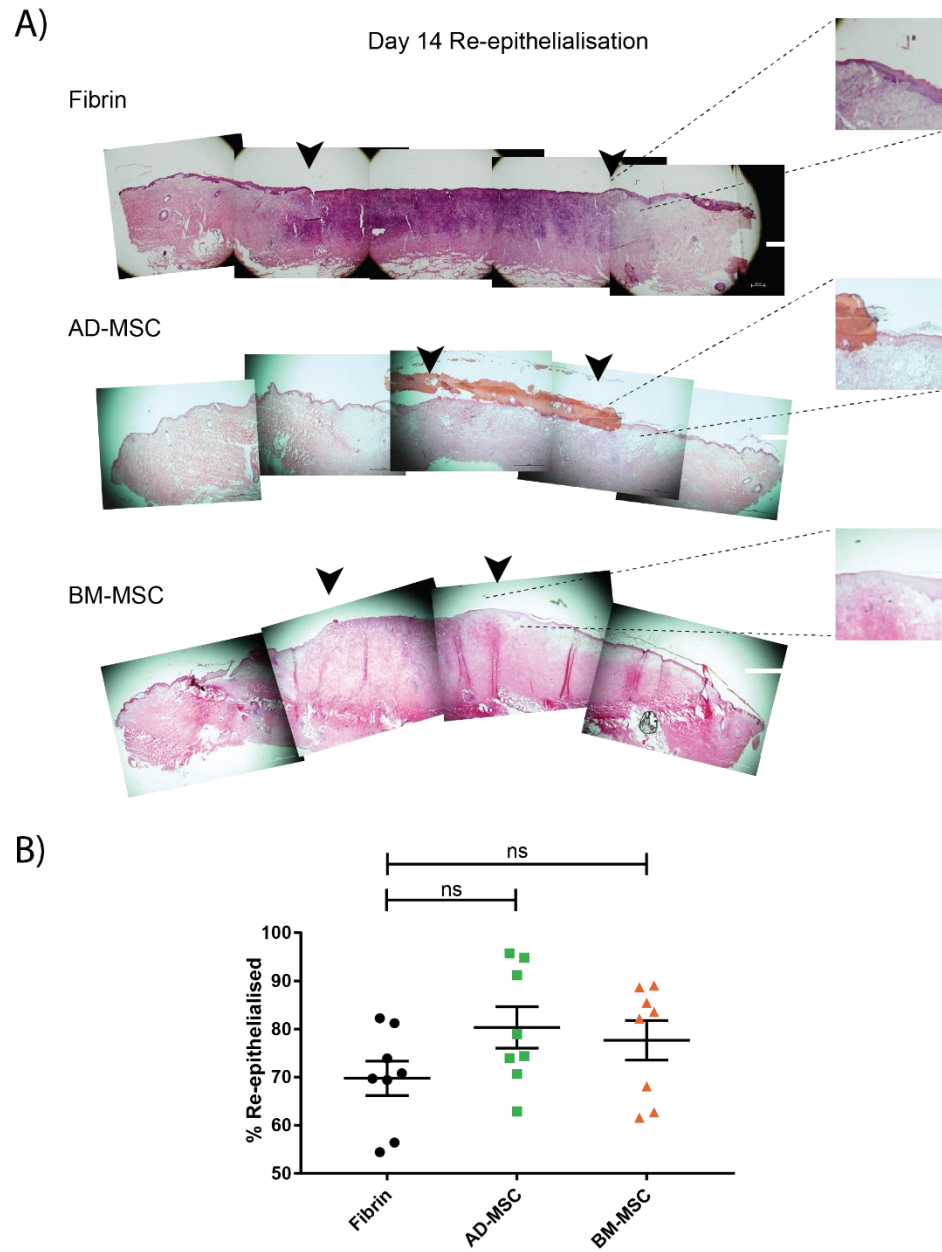
Figure 4.3 MSC therapy did not increase re-epithelisation of burn wounds at d-14
A) Histological samples of wounds taken at d-14 were stained with H&E to assess re-epithelialisation. Several overlapping Images were taken at 4x and composite image formed of the entire section. Green arrows indicate epithelial front. Scale bar 500 μm. B) Percentage re-epithelialisation was determined as epithelial gap divided by section length as measured using ImageJ. (n=8 ns, not significant).

Figure 4.4
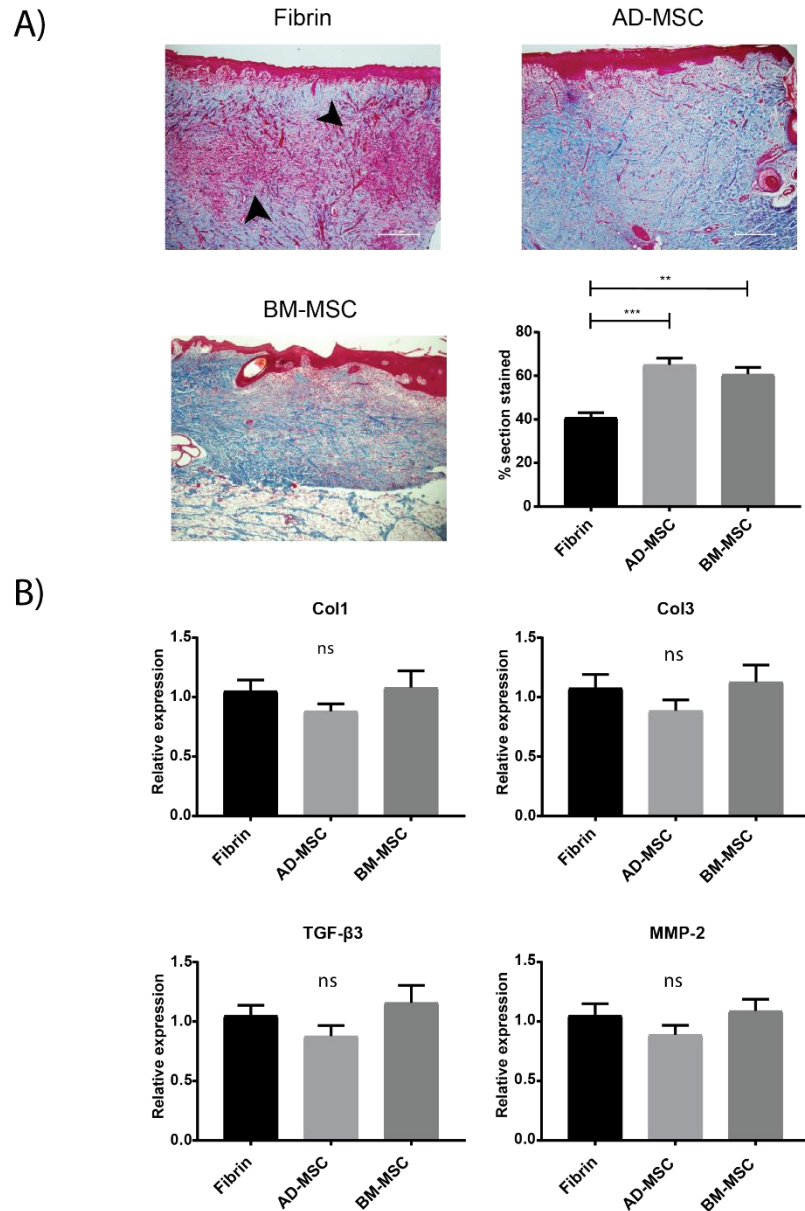
Figure 4.4 Application of MSC increased collagen deposition in porcine burn wound
A) Histological samples of d-14 were stained with Masson's tri-chrome as a semi quantitative measurement of collagen within the wound bed, scale bar = 100 μm. Percentage blue staining (indicative of collagen fibres) was quantified using NIS elements software. Increased collagen is associated with increased wound maturity (n=8, **p<0.05, *** p<0.001); presence of red staining (indicated with black arrows) suggests persistent inflammatory cellular infiltrate. B) qRT-PCR was performed on d-14 wound samples to evaluate the expression of collagen type 1(Col1), collagen type 3 (Col3), MMP-2 and TGF-β3. No significant differences were observed between the groups (n=8, ns, not significant)

Figure 4.5
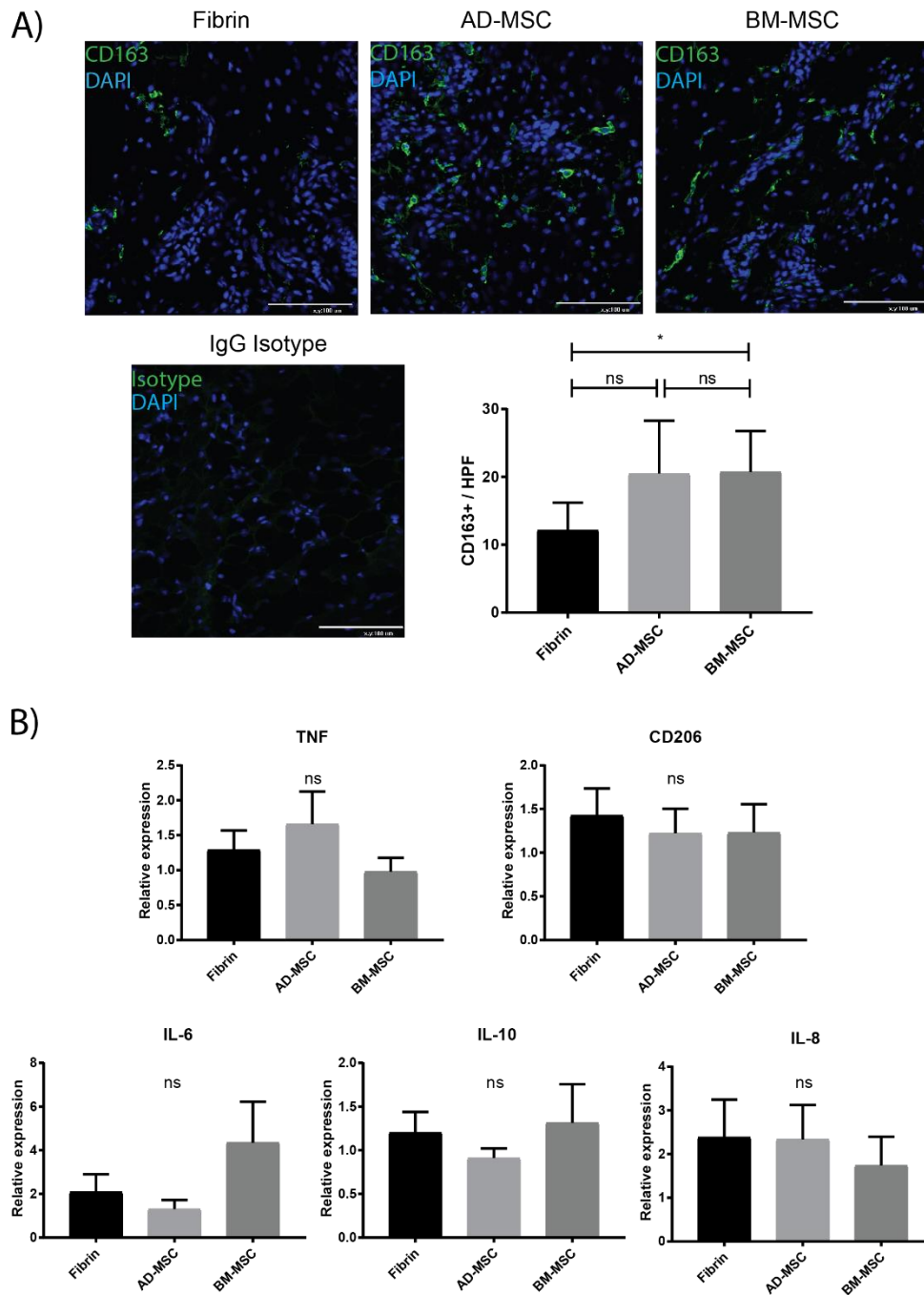
Figure 4.5 BM-MSC increased M2 macrophage population within the wound at d-14
*A) Wound sections from d-14 were probed with CD163 antibody (green) and nuclei stained with DAPI (blue) indicating increased M2 population in MSC treated wounds. However, only BM-MSC treated wounds had a statistically increase in CD163+ cells (n=8, ns, not significant, * p<0.05). B) Analysis of mRNA expression of several inflammatory cytokines across the wound and healed wound margin by qRT-PCR. No statistically significant differences were observed between any of the groups (n=8, ns, not significant)*

Figure 4.6
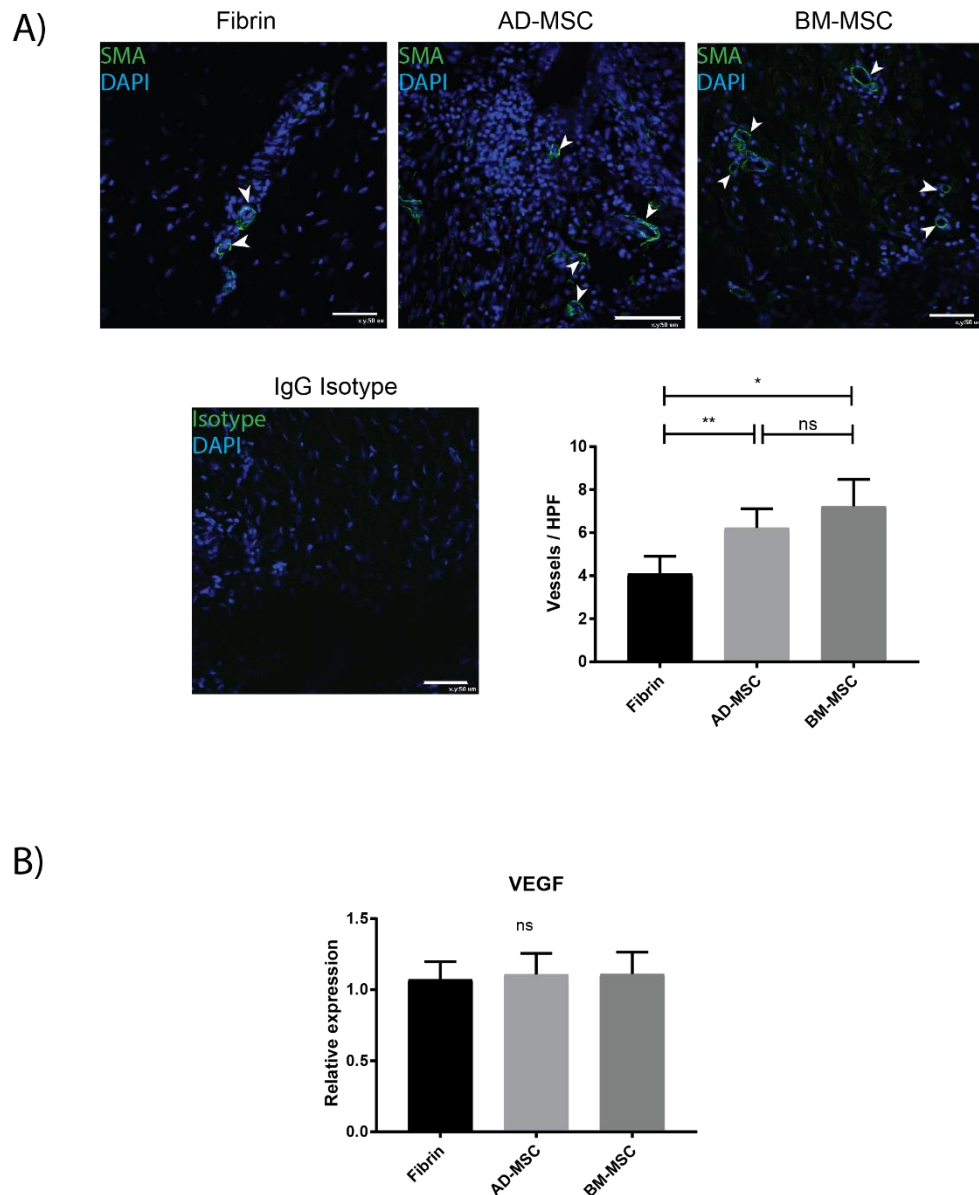
Figure 4.6 MSC therapy induced angiogenic response within the wound
*A) wound sections at d-14 were probed with SMA antibody (green) and nuclei stained with DAPI (blue). SMA+ vessels were quantified (intact vessel lumen highlighted with white arrows) within the wound bed. Both AD-MSC and BM-MSC treated wounds had increased vessel density per HPF (n=8, ns, not significant * p<0.05, ** p<0.01). B) Analysis of VEGF expression by qRT-PCR across the wound and wound margin showed no statistically significant difference between groups (n=8, ns, not significant)*

4.4. Discussion

The aim of this chapter was to determine the optimal cell source of MSC used for treating burn wounds. AD-MSC has many benefits in terms of availability, ease of isolation and expansion potential. In vitro analysis of immune regulatory and angiogenic responses suggest that AD-MSC may also be more beneficial [114, 201]. However, preclinical animal studies of AD-MSC in burn wound healing are lacking and to the best of the author's knowledge, there are no published equivalency studies of AD-MSC and BM-MSC in burn wound healing. Pre-clinical studies in large animal models are required to validate and optimise potential therapies prior to clinical trials. The porcine burn model is beneficial as porcine skin is quite histologically similar to humans and is a good predictor of human response [211]. Pigs, like humans have a fixed skin, heal primarily through re-epithelisation and do not have a panniculus carnosus, a subdermal muscle layer, which is present in rodents [211].

4.4.1. Equivalency studies of AD-MSC and BM-MSC in wound healing models

Donor matched MSC isolated from both adipose tissue and BM were used to treat deep partial thickness burns. The primary endpoints for the assessment of the rate of wound healing were wound size, as measured by image analysis; and re-epithelisation, as measured by histology. Treatment of burns with either cell type significantly improved wound closure. Whilst this is the first equivalency study,

other studies have reported similar findings independently for each cell type. Previously, this lab has established a porcine burn model and published a pilot study (n=3) comparing efficacy of allogenic BM-MSC in fibrin vs cultured autologous PBMNC in fibrin vs fibrin only vs dressings only [149]. In that study allogeneic MSC were the most efficacious treatment, increasing wound closure and granulation tissue [149]. There was no significant difference between fibrin only and dressing only groups [149]. Only three other studies using a pig burn model could be identified in a review of the literature (Appendix I). In one study by Mansilla et al (2010), a large 300 cm^2 full thickness burn was induced on the pig [212]. The burnt tissue was immediately excised and a combination of two treatments of BM-MSC ($2x10^6$/cm^2) delivered in fibrin and one treatment of a dermal matrix coated with CD44 antibodies was applied [212]. Mansilla et al report outstanding regeneration of both bone, muscle and dermal structures along with minimal scarring and regrowth of hair follicles [212]. However, this study is very limited as it does not have a control group and these findings are only from one pig. Despite such a positive outcome it is disappointing that no larger follow up studies have ever been performed.

In a more comparable study, Liu et al induced deep partial thickness burns (19.6 cm^2, 100°C for 20 s) on the dorsum of anesthetised pigs and applied collagen scaffolds seeded with allogenic BM-MSC ($1x10^5$/cm^2) to the wounds [180]. Similar to the findings reported here, MSC increased wound healing, reduced wound contraction at 4 weeks and improved histological appearance compared to control and scaffold only treated wounds [180]. However, Liu et al did not investigate any immune or angiogenic responses to the treatment.

Another study performed in pigs used autologous BM-MSC (ID injection of $0.8x10^6/cm^2$) to treat deep partial thickness burns (100°C, 15 s under defined pressure of 0.5 kg/ cm^2, wound area 2.5 cm^2) [188]. Histological examination of wounds indicated a trend towards increased granulation tissue on d-14 and d-21, increased capillary sprouting was observed in BM-MSC group but was not significantly different to control. No significant difference was observed in re-epithelisation but, as seen in the current study, a trend towards increased re-epithelialisation was noted [188].

As stated above, there is a lack of studies investigating MSC in porcine burn models; however, AD-MSC and BM-MSC have been studied in a porcine excisional wound healing model [115]. Excisional wounds (4 cm^2) were induced and treated with an ID injection of either AD-MSC or BM-MSC ($1x10^6$) [115]. Cosmetic appearance was improved with MSC treatment as assessed by Vancouver scar scale and importantly, no significant difference was observed between AD-MSC and BM-MSC groups [115]. In agreement to results presented here, no significant increase in re-epithelisation was observed between treated and non-treated groups [115]. However, an increase in epidermal thickness was noted at d-21 in MSC treated wounds compared to saline controls. Taken together our current results suggest that application of either cell type induces a biological response associated with improved wound healing and that neither cell type is more efficacious.

Similar to Lui et al, the study by Hanson et al was limited in scope by assessing only histological features. The limited availability of antibodies and assays available made mechanistic insights of these therapies in porcine models

difficult, but valuable. In this study a modest increase in wound closure (and a trend towards increased re-epithelialisation) was observed in wounds treated with either BM-MSC or AD-MSC. This was associated with increased angiogenic and immune response. Several studies of burn wound healing in rat models support this finding as detailed in Appendix I and Appendix II [213-215].

In this study wound closure was calculated from images taken of the wound at d-0 and d-14 and areas calculated from image analysis software. Wound closure is composed of both wound contraction and re-epithelisation components [216]. In full thickness excisional models wound contraction is the dominant component, as underlying dermis is removed, stimulating myofibroblast proliferation and subsequent activation of contractile proteins leading to wound contraction [211, 217]. In this model the wound was not excised and underlying dermis was not disrupted which prevents major contraction. While image analysis of wounds is a good macro indicator of wound progression it is not ideal for assessing the contribution of contraction to wound closure. To better determine its contribution permeant marking of original wound outline using tattooing could be utilised. As wound contraction was not expected to be a major component in this model, we used histological analysis of re-epithelialisation as a primary endpoint of wound healing, which gives much greater resolution to detect differences in wound closure.

4.4.2. Mechanism of MSC accelerated wound healing

Previously, it has been established that MSC can repolarise macrophage population towards a reparative M2 phenotype to elicit improved wound healing [20]. To characterise this response, sections were interrogated with a CD163 (M2 marker) antibody. A greater amount of CD163+ cells were detected in wound beds of MSC treated wounds but this was only significant in BM-MSC treated wounds shown in **Figure 4.5 A**, AD-MSC displayed a trend toward increased CD163+ infiltration but increased variation between animals in this treatment group limited statistical significance. No significant difference between groups could be detected in the expression of several inflammatory cytokines by qRT-PCR analysis (**Figure 4.5 B**). However, wound samples used for qRT-PCR analysis consisted of the whole wound plus outer healed wound margin which may have normalised the results. Although d-14 is not an ideal time point to capture some of the dynamics in expression of these cytokines, the fact that no significant difference was observed in any of the several cytokines and growth factors assayed is unexpected. The RNA used was validated as high purity and was not degraded, in addition the custom assay obtained from Qiagen contained both positive, negative and genomic DNA contamination controls, all of which were satisfactory. This possible sampling bias is apparent in all of the qRT-PCR results (no significant differences were detected in any of the assays). Immunofluorescent imaging was performed in the wound bed and may be more representative of the wound microenvironment. The immuno-staining results obtained here are in better agreement with previous findings in the literature. Similar findings of increased M2 population in MSC treated wounds have been

shown in MSC treated burn wounds of rats, mice and also in excisional wound healing [20, 191, 213].

Treatment of wounds with either cell type resulted in increased vessel density (**Figure 4.6 A**). Normally CD31 would be used as a marker for endothelial cells and vascular density, however two different CD31 antibodies were tested unsuccessfully on these porcine wound sections. An antibody for αSMA was successful however in detecting antigens in these wound sections and this was used to quantify vessel density. αSMA is a contractile protein expressed in pericytes that line capillaries and other larger vessels. During early phase of wound healing, VEGF stimulates the sprouting of endothelial tubes; after several days the new vasculature is stabilised by pericytes and VEGF is no longer required to maintain endothelial sprouts [209]. This may also account for The lack of difference in VEGF expression between experimental groups as detected by qRT-PCR on day 14. Many studies corroborate the finding of increased vascular density in response to MSC treatment in burn wounds [214, 215, 218, 219]. While several in vitro studies suggest that AD-MSC may be more angiogenic [197, 198], no significant difference was observed in vessel density in the wound sections between BM-MSC or AD-MSC treated wounds in this study. A good blood supply is crucial for the formation of granulation tissue (and subsequent re-epithelialisation) and for survival of cells, and this appears to be one of the primary drivers of the therapeutic effect observed in MSC [29].

In conclusion, the findings of this study suggest that both AD-MSC and BM-MSC have a biological response associated with improved wound healing. However, application of either cell type did not improve re-epithelisation, one of the primary endpoints. While a positive biological response was observed, it was quite modest. In an effort to improve the efficacy of this therapy and to determine if either cell type has a differential response, cells were pre-stimulated with the inflammatory cytokine TNFα prior to administration.

5. TNF alpha pre-treatment of MSC enhances efficacy in porcine burn model

5.1. Introduction

MSC treatment in humans has been demonstrated to be safe; however, results from clinical trials indicate mixed and somewhat disappointing therapeutic results across a range of pathologies. Based on the modest therapeutic effect observed in chapter 4, a means of enhancing MSC efficacy was investigated.

Recent studies emanating from our current mechanistic understanding of MSC therapy have attempted to promote or over-drive certain aspects of it, in order to increase the therapeutic effect. For instance, MSC are known to elicit a potent angiogenic response and are beneficial in ischemic limb studies [220]. One of the primary mechanisms of this is through VEGF. MSC engineered to over express VEGF, using a lenti-viral vector, had a fourfold increase in VEGF secretion [220]. Injection (IM) of MSC/VEGF significantly increased blood flow (at 6-11 weeks) as assessed by Doppler in a mouse model of hind-limb ischemia [220]. One of the primary deficiencies of MSC is their low engraftment and survival after transplantation, and thus several studies have investigated strategies overexpressing pro-survival factors including B-cell lymphoma 2 (BCL-2) [221]

or AKT [222] which enhanced their persistence within the tissue following transplantation.

Lentiviral overexpression of SDF-1 in MSC enhanced cardiomyocyte survival in a mouse model of MI; through C-X-C motif chemokine receptor 4 (CXCR4) activation in cardiomyocytes within the border zone [223]. This approach was beneficial in terms of MSC retention and homing to sites of injury and was combined with over-expression of VEGF to further enhance efficacy [224].

Other non-viral strategies to improve MSC functionality included preconditioning MSC in various culture conditions, such as under hypoxia; the rationale being that in vivo MSC usually exist in hypoxic conditions and culturing under such, may enhance their regenerative potential. Hypoxic conditioning (HC) increased MSC motility and responsiveness to HGF [225]. Significantly, HC-MSC induced revascularisation of mouse model in a hind limb ischemia at earlier time points than MSC cultured under normoxic conditions [225].

Recent studies have elucidated idiosyncrasies in MSC immunomodulation [226]. Unstimulated MSC injected prior to induction of dextran sulphate sodium induced colitis had no therapeutic effect [226]. This observation led to the concept of MSC licensing or activation, which is a multi-step process defined as the functional maturation of MSC in response to inflammatory micro environmental cues [227]. Under resting conditions MSC can take on either anti-inflammatory or antigen presenting and pro-inflammatory functions [227]. Activation or licensing of MSC in response to inflammatory cytokines such as TNFα, IL-β and IFNγ stimulate MSC to alter their secretome and to release

increased amounts of immunomodulatory factors such as TSG-6 PGE2, IDO and IL-4 [227].

Previous studies indicate that pre-treatment of MSC with inflammatory cytokines may improve their therapeutic potential [79]. Pre-treatment of MSC with IFNγ prior to application to a model of colitis improved therapeutic efficacy through increased immunosuppressive capacity of transplanted MSC [228]. In a rat model of MI, TNFα activated (10 ng/ml 24 h) MSC increased expression of several factors including IL-6, BMP-2 and CCL-2 [229]. Pre-treated MSC were superior to untreated MSC in reduction of myocardial fibrosis and significantly improved recovery of ejection fraction post MI [229]. Similarly, TNFα activated MSC increased localisation of MSC in ischemic limbs, mediated in part through increased expression of ICAM-1 [230]. Other studies using MSC CM have shown beneficial results when pre-treated with TNFα [80]. Activation of MSC with a combination of TNFα, IL-1β and NO was beneficial improving radiation induced intestinal injury in rats [231]. In a mouse model of ischemic limb TNFα stimulated MSC CM significantly attenuated limb loss compared to non-stimulated MSC CM [75]. In cutaneous wound healing studies in mice, TNFα pre-treated MSC CM accelerated wound healing compared to saline control [80]. Normal MSC CM did not significantly increase wound closure. In TNFα MSC CM treated group, wound closure was significantly increased on d-6 and d-9, while epithelialisation was also improved [80]. Histological analysis demonstrated increased angiogenesis and significant recruitment of CD68+ macrophages on d-3 and d-6, in a IL-6 and IL-8 dependent manner [80].

Pre-treatment of MSC with TNFα is a potentially advantageous way to improve efficacy as it is a simple addition to culture medium and potentially improves several key aspects of MSC therapy, through increased angiogenesis [75], immunomodulatory capacity [79] and engraftment or persistence [229], all of which are particularly relevant to burn wounds.

However, to the best of the author's knowledge no studies have investigated the effect of TNFα in a burn wound model, nor in a porcine animal model. Moreover, several studies report MSC isolated from different tissues exhibit differential responses to inflammatory cytokines [83, 232, 233].

To test the hypothesis that TNFα pre-treatment of MSC would increase therapeutic response and to determine if either cell type responded more favourably, both AD-MSC and BM-MSC were pre-treated with TNFα prior to wound application and wound healing was evaluated.

5.1.1. Chapter aims

- To determine if TNFα pre-treatment of MSC will enhance therapeutic efficacy in porcine burn wound model
- To establish if there is a differential response of MSC isolated from either BM or adipose tissue and to determine if any type is therapeutically superior

5.2.   Materials and methods

5.2.1. TNFα pre-treatment of porcine MSC

In this study, the therapeutic efficacy of allogenic MSC derived from either BM or adipose tissue pre-treated with recombinant porcine TNFα was investigated. The study consisted of two experimental treatments; TNFα pre-treated AD-MSC, TNFα pre-treated BM-MSC and a control treatment of fibrin only. A total of six animals were used in this study and each animal received all three treatments (12 wounds in total, 4 wounds per group) providing intra animal controls. Allogenic AD-MSC and BM-MSC isolated from the same donor pig were characterised, as described in **section 3.2**, prior to use in the following burn experiments. Cells isolated from six different donor pigs were used in the following experiments.

Both AD-MSC and BM-MSC were pre-treated with 10 ng/ml of recombinant porcine TNFα (R&D systems) in complete culture media for 24 h prior to harvesting and administration in burn wound.

Burn protocol and subsequent analysis was performed as detailed in **section 4.2.**

5.3. Results

5.3.1. MSC treatment of burn wounds increase rate of wound closure

After induction of wounds and debridement, wounds were imaged (**Figure 5.1 A** upper panel), wound area was similar for all groups, combined mean was 4.8 cm^2 ± 0.08. After 14 d, wounds were imaged (lower panel **Figure 5.1 A**) and wound closure calculated as shown in **Figure 5.1 B**. Treatment of wounds with either cell type significantly increased wound closure on d-14 (Fibrin; 15.54% ± 2.0 vs AD-MSC; 8.5% ± 1.9 vs BM-MSC; 7.7% ± 2.1, Fibrin v AD-MSC p=0.003, Fibrin v BM-MSC p<0.001, AD-MSC vs BM-MSC p=0.72, n=6). No significant difference was observed between AD-MSC and BM-MSC. Wound closure was superior in TNFα pre-treated MSC to untreated MSC (**Figure 4.2 B**)

5.3.2. TNFα pre-treated MSC significantly increase re-epithelisation

One of the primary evaluations of wound healing is re-epithelialisation. This was determined from histological sections of the wound taken from d-14 and stained with H&E (**Figure 5.2**). At d-14 re-epithelialisation was significantly improved in both AD-MSC and BM-MSC groups (Fibrin 62.9% ± 5.9, vs AD-MSC 88.8% ± 3.6, vs BM-MSC 96.7% ± 2.0, Fibrin v AD-MSC p=0.003, Fibrin v BM-MSC p=0.014, AD-MSC vs BM-MSC p=0.264, n=5). This is significantly greater re-epithelialisation

than observed in MSC without TNFα pre-treatment (**Figure 4.3 B**). Importantly, no significant difference was observed between AD-MSC and BM-MSC. Due to a paraffin embedding tissue processing error, samples from one animal could not be used for histological analysis (hence n=5) but samples from this animal were suitable for immunostaining and RNA extraction.

5.3.3. MSC therapy is associated with increased wound maturity

Collagen deposition was assessed using Masson's trichrome staining. Histological sections from the wound were imaged at five random sections within the wound bed (data shown in **Figure 5.3 A**). Increased percentage of blue staining (semi quantitative indictor of collagen content) was observed in both MSC treated wounds in comparison to Fibrin alone (Fibrin, 34.9% ± 3.9, vs AD-MSC 75.32% ± 4.3, vs BM-MSC, 74.2% ± 3.8, Fibrin v AD-MSC $p<0.001$, Fibrin v BM-MSC $p<0.001$, AD-MSC vs BM-MSC $p=0.982$, n=5), suggestive of more collagen content, a marker for wound maturity. Fibrin only treated wounds displayed more red staining, (cytoplasm stains red) indicative of cellular infiltrate still present within the wound, which was not observed in MSC treated groups. TNFα pre-treated MSC had greater percentage blue staining compared to untreated MSC (**Figure 4.4 A**) Analysis of mRNA expression at d-14 did not reveal any difference in expression of either COL1 (Fibrin; 1.32 ± 0.17 AD-MSC; 1.33 ± 0.14 BM-MSC; 1.15 ± 0.13) COL3 (Fibrin; 1.33 ± 0.16 AD-MSC; 1.28 ± 0.08 BM-MSC; 1.25 ± 0.1), TGF-β3 (Fibrin; 1.25 ± 0.1 AD-MSC; 1.2 ± 0.07 BM-MSC; 1.06 ± 0.08) or MMP-2 (Fibrin;

1.01 ± 0.12,vs AD-MSC; 0.94.33 ± 0.09, vs BM-MSC; 0.81 ± 0.08) in samples containing both wound and healed wound margins (data shown in **Figure 5.3 B**).

5.3.4. Pre-treated MSC significantly induce M2 population within the wound

In the previous chapter (**Figure 4.5 A**), quantification of immunostaining indicated that application of BM-MSC induced a modest but statistically significant increase in M2 macrophages within the wound as demonstrated by increased CD163+ cells. Treatment of burn wounds with TNFα pre-treated MSC markedly increased CD163+ cells within the wound bed in contrast to findings from chapter 4 (**section 4.3.4)** and this was significant for both AD-MSC and BM-MSC (Fibrin; 17.5 ± 2.7 vs AD-MSC; 35.2 ± 2.0, vs BM-MSC; 40.4 ± 3.0, Fibrin v AD-MSC p=0.006, Fibrin v BM-MSC p=0.001, AD-MSC vs BM-MSC p=0.182, n=6) as shown in **Figure 5.4 A**., suggestive of an increased inflammatory resolution response and wound progression. Notably, no significant difference was observed between AD-MSC and BM-MSC groups.

Analysis of RNA expression (**Figure 5.4 B**) at d-14 of several inflammatory cytokines across the wound and the wound margin by qRT-PCR did not demonstrate any significant differences between control and treatment groups for TNFα (Fibrin; 1.27 ± 0.15, vs AD-MSC; 1.74 ± 0.24, vs BM-MSC; 1.79 ± 0.26, Fibrin vs AD-MSC p=0.347, Fibrin vs BM-MSC p=0.375 AD-MSC vs BM-MSC p=0.988, n=6), IL-6 (Fibrin; 2.32 ± 1.49 AD-MSC; 0.69 ± 0.21 BM-MSC; 0.65 ± 0.25 Fibrin vs AD-MSC p=0.55, Fibrin vs BM-MSC p=0.541 AD-MSC vs BM-MSC

p=0.942,) IL-8 (Fibrin; 1.75 ± 0.77 AD-MSC; 0.47 ± 0.14 BM-MSC; 0.64 ± 0.21, Fibrin vs AD-MSC p=0.902, Fibrin vs BM-MSC p=0.388 AD-MSC vs BM-MSC p=0.374, n=6) or IL-10 (Fibrin; 0.67 ± 0.07 vs AD-MSC; 0.65 ± 0.1 vs BM-MSC; 0.62 ± 0.1, Fibrin vs AD-MSC p=0.981, Fibrin vs BM-MSC p=0.906 AD-MSC vs BM-MSC p=0.968, n=6).

5.3.5. TNFα pre-treated MSC significantly increase vessel density within the wound

On d-14, both AD-MSC and BM-MSC treated wounds had significantly increased vessel density per HPF (Fibrin; 4.4 ± 0.4, vs AD-MSC; 12.2 ± 2.0, vs BM-MSC; 10.2 ± 0.5, Fibrin v AD-MSC p=0.031, Fibrin v BM-MSC p=0.001, AD-MSC vs BM-MSC p=0.569, n=6) as shown in **Figure 5.5 A**. Analysis of VEGF expression (in **Figure 5.5 B**) by qRT-PCR across the wound and wound margin showed no significant difference between groups (Fibrin; 0.94 ± 0.09 AD-MSC; 0.86 ± 0.08 BM-MSC; 0.87 ± 0.04, Fibrin v AD-MSC p=0.655, Fibrin v BM-MSC p=0.831, AD-MSC vs BM-MSC p=0.979, n=6).

Figure 5.1

A)

B)
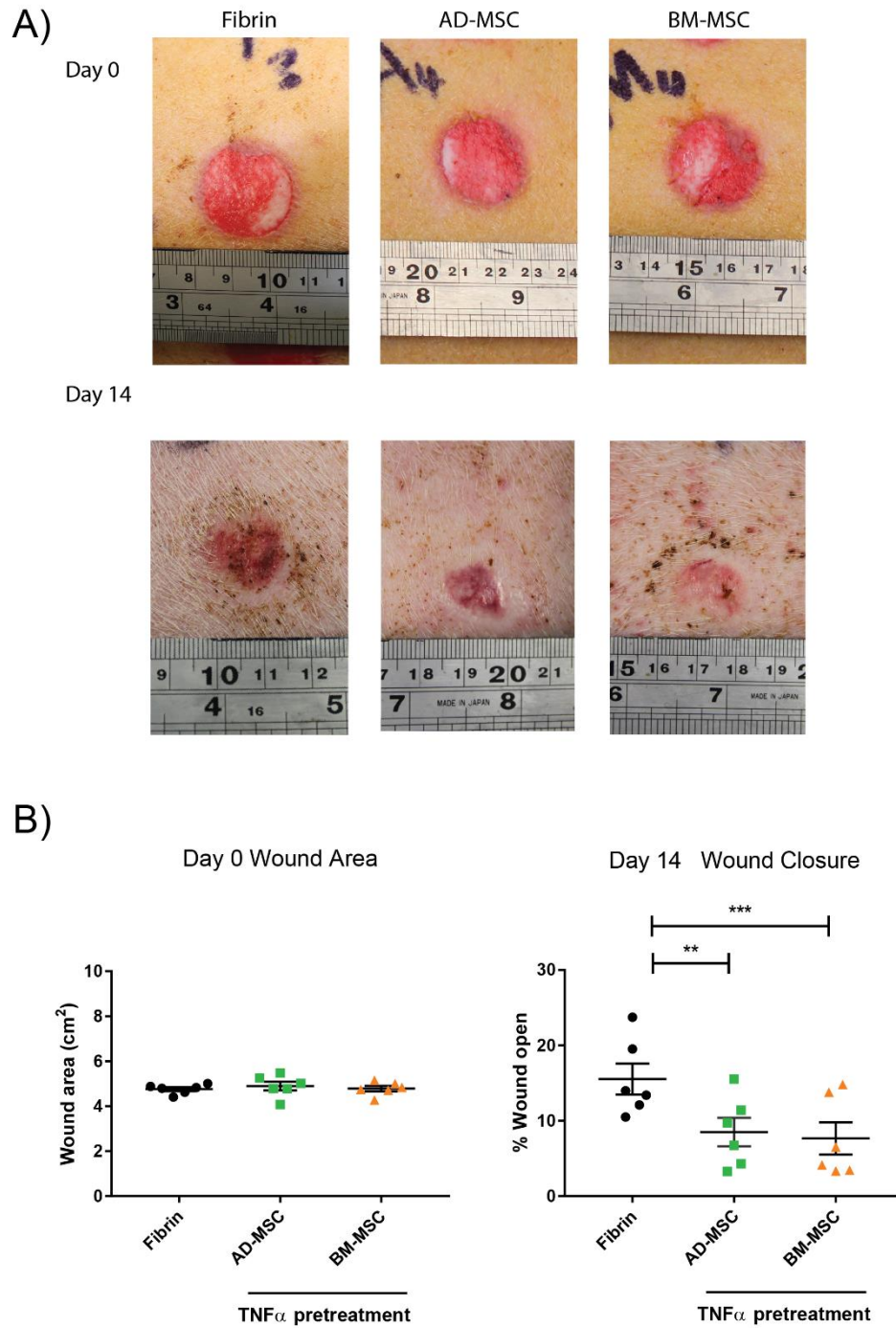
Figure 5.1 TNFα pre-treatment of MSC increased wound closure at day 14
*A) Burn wounds were induced on dorsum of pigs and imaged on d-0 after debridement, prior to application of cells. **A) Lower panel -** Wounds were imaged on d-14 post wounding. **B) Left -** Quantification of wound area at d-0. No significant difference was observed between wound areas at d-0. **B) Right -** Treatment of wounds with MSC significantly increased wound closure on d-14 (n=6 **p<0.01, *** p<0.001). No significant difference observed between AD-MSC and BM-MSC.*

Figure 5.2

A)

Day 14 Re-epithelialisation

Fibrin

AD-MSC

BM-MSC

B)

Day 14 Re-epitheliasation
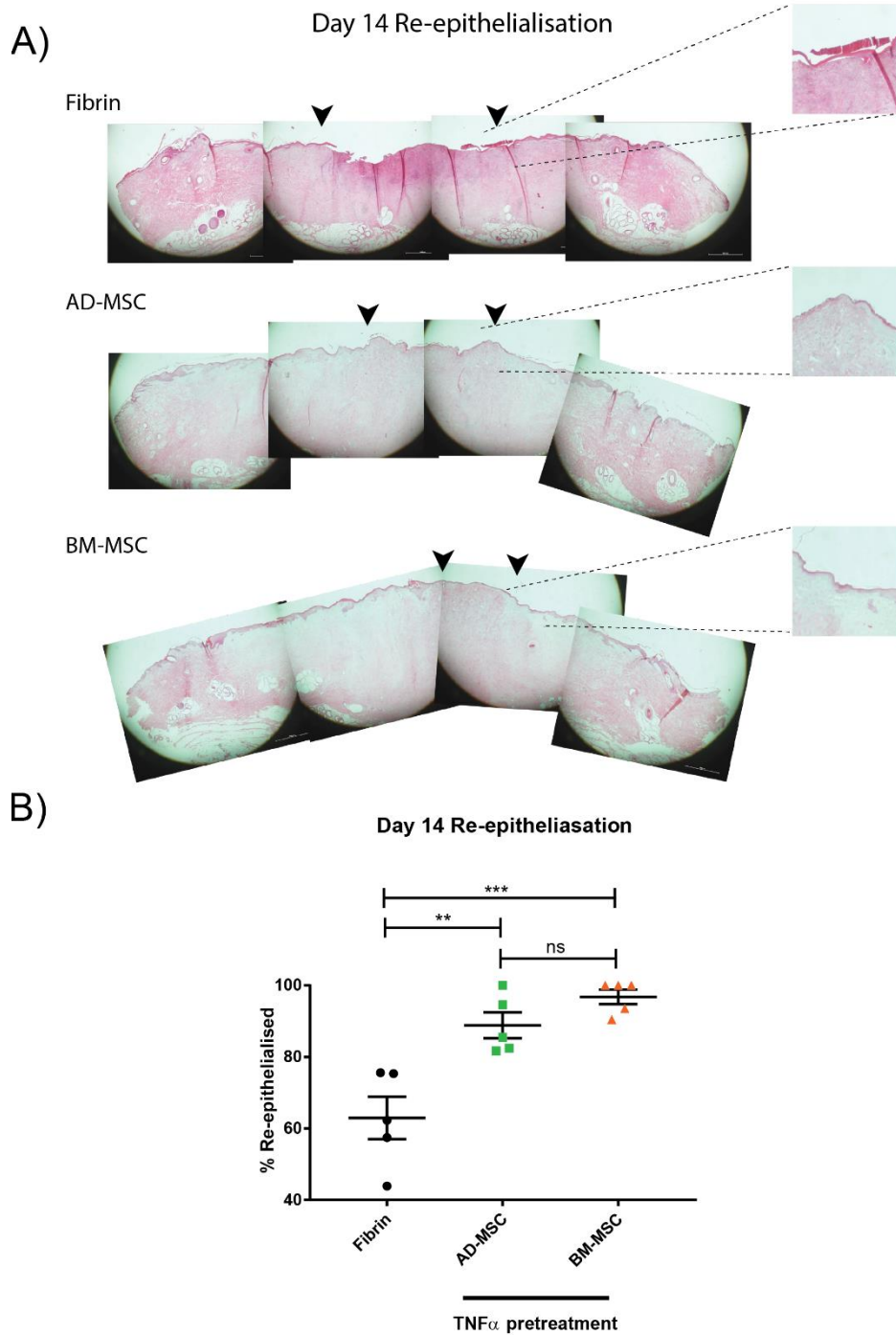
Figure 5.2 TNFα pre-treatment of MSC increased re-epithelialisation of burn wounds at d-14
A) Histological samples of wounds taken at d-14 were stained with H&E to assess re-epithelialisation. Several overlapping Images were taken at 4x and composite image formed of the entire section. Black arrows indicate epithelial front, inset shows magnified image of migrating front. Scale bar 500 μm. B) Percentage re-epithelialisation was measured using ImageJ software. MSC therapy primed with TNFα significantly increased re-epithelisation of wounds (n=5 ns, not significant, **p<0.01, *** p<0.001). No statistical difference was observed between AD-MSC and BM-MSC groups.

Figure 5.3

A)

Fibrin

AD-MSC

BM-MSC

B)
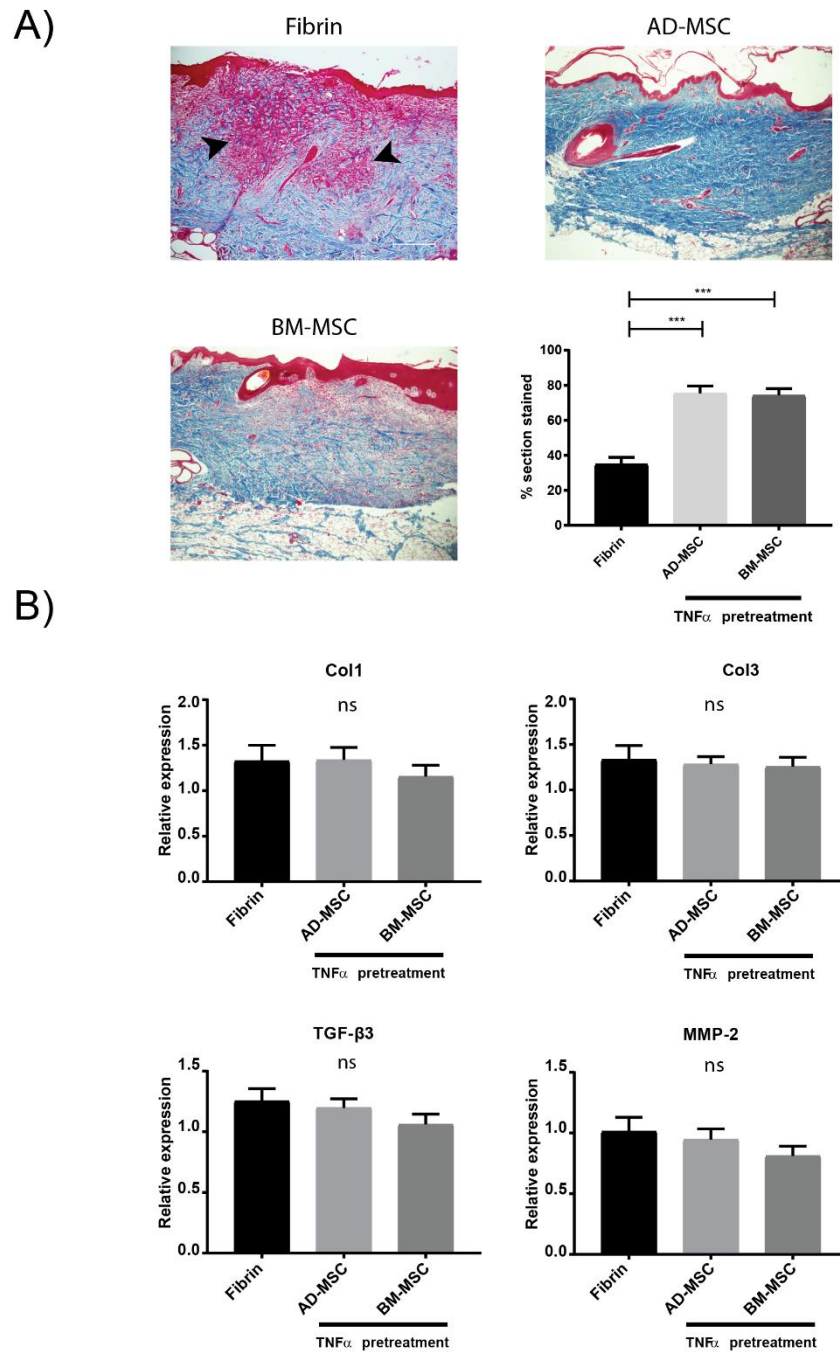
Figure 5.3 TNFα pre-treated MSC increased wound maturity

A) Histological samples of d-14 were stained with Masson's tri-chrome. Scale bar 100 μm. Percentage blue staining (indicative of collagen fibres) was quantified using NIS elements software (n=5 *** p<0.001). B) qRT-PCR was performed on d-14 wound samples containing both the wound and wound margins to evaluate the expression of collagen type 1(Col1), collagen type 3 (Col3), MMP-2 and TGF-β3. No statistically significant differences were observed between the groups (n=6, ns, not significant)

Figure 5.4

A)
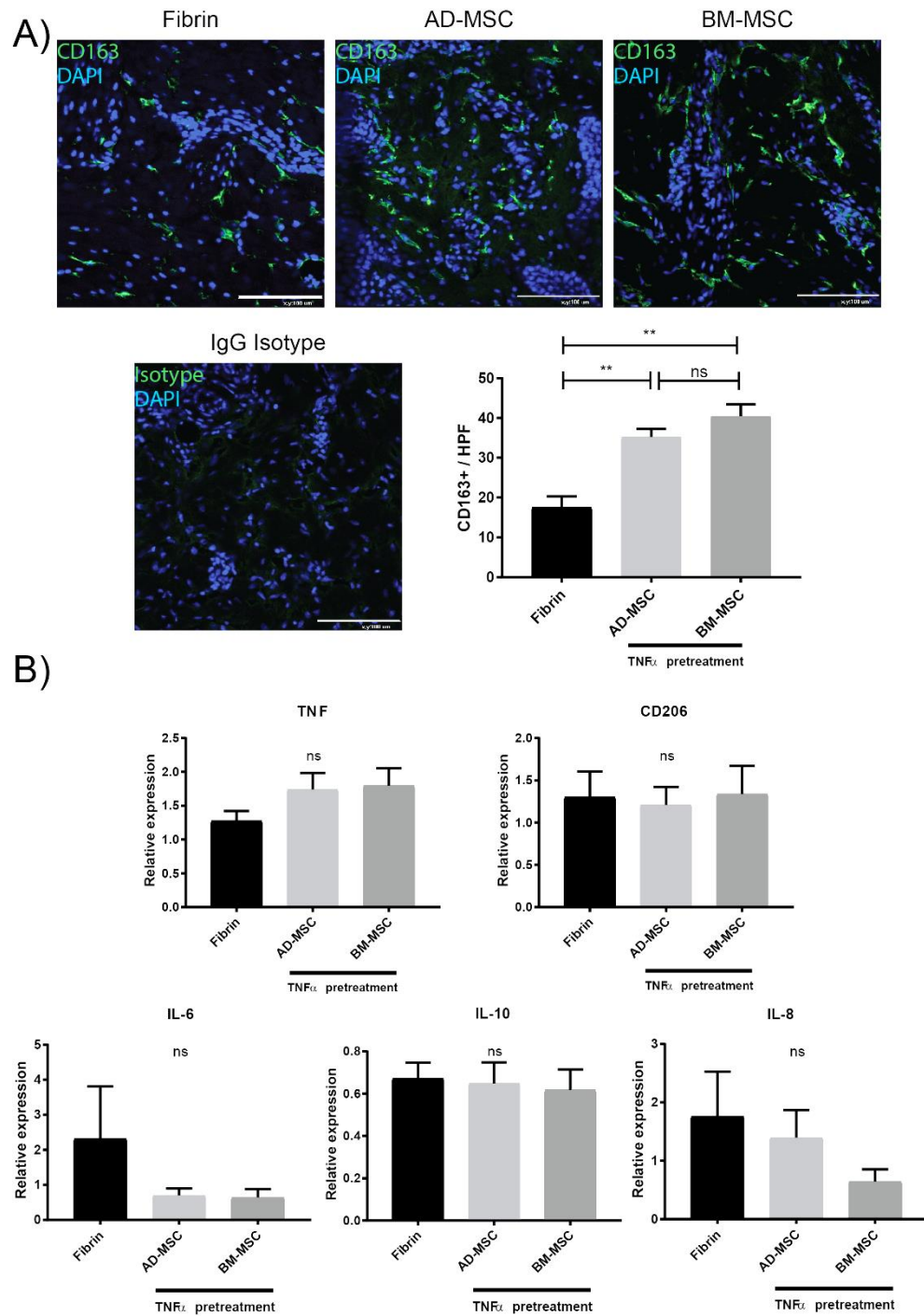
Figure 5.4 TNFα pre-treated MSC increased CD163+ population within the wound
*A) Wound sections from d-14 probed with CD163 antibody (green), nuclei stained with DAPI (blue), indicate significantly increased M2 macrophage population within the wound bed of both AD-MSC and BM-MSC treated wounds (n=6, ns, not significant ** p<0.01) No significant difference was observed between AD-MSC and BM-MSC groups. B) Analysis of RNA expression of several inflammatory cytokines across the wound and the wound margin by qRT-PCR. No significant differences were observed between any of the groups (n=6, ns, not significant).*

Figure 5.5
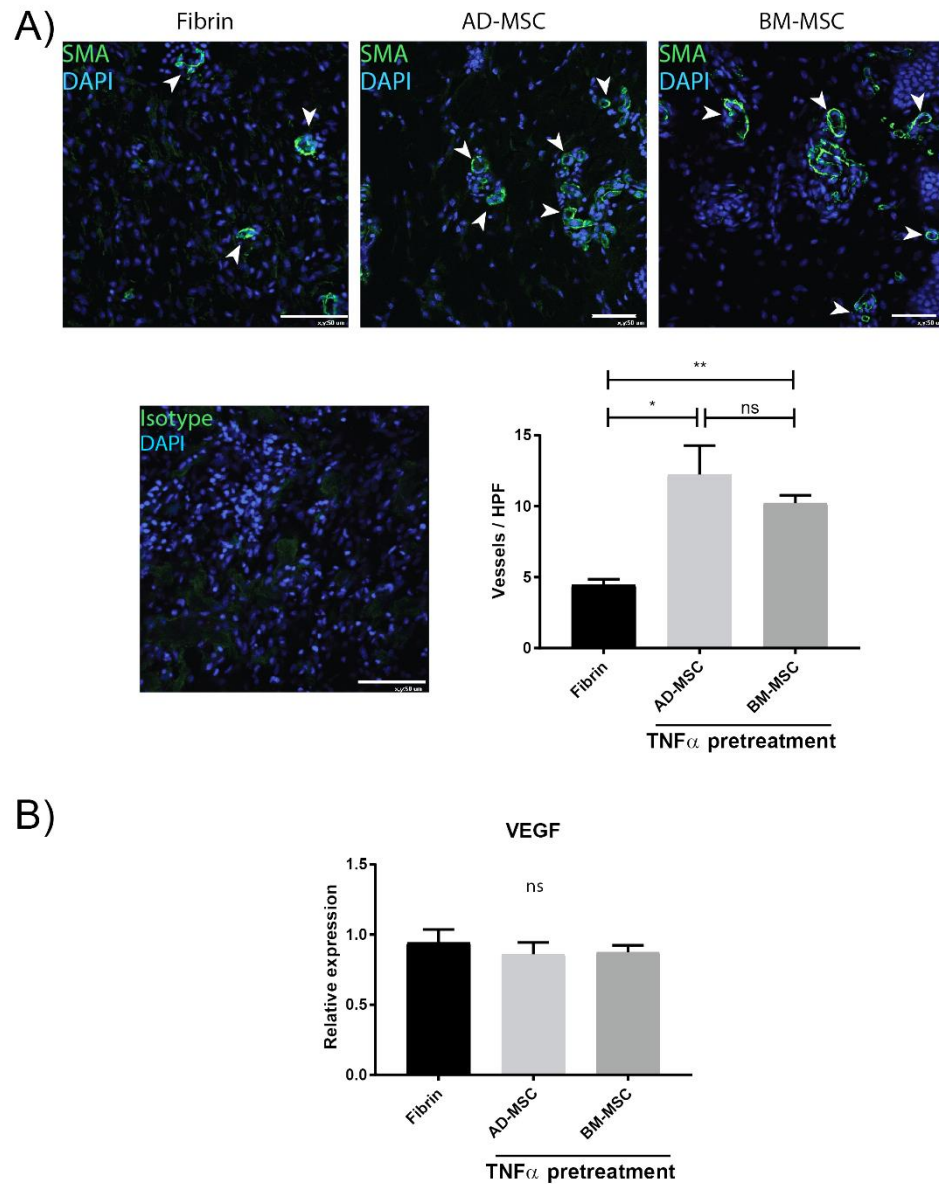
Figure 5.5 TNFα pre-treated BM-MSC induced angiogenic response within the wound
A) wound sections d-14 were probed with SMA antibody(green), nuclei stained with DAPI (blue). SMA+ vessels were quantified within the wound bed; white arrows highlight intact vessel lumens. Both AD-MSC and BM-MSC treated wounds had increased vessel density per HPF (n=6, ns, not significant * p<0.05, ** p<0.01). *B)* Analysis of VEGF expression by qRT-PCR across the wound and wound margin showed no significant difference between groups (n=6 ns, not significant).

5.4.   Discussion

In chapter 4, MSC were used to treat deep partial thickness burns in a pig model. Application of either AD-MSC or BM-MSC improved wound closure, however the effect was modest and no significant increase in re-epithelialisation, a primary determinate of wound healing, was observed in either group. Pre-stimulating MSC with inflammatory cytokines has been established to be beneficial in improving immunomodulatory and angiogenic functions of MSC therapy [75, 80]. However, this has not been explored in a burn wound model. In this study, the effectiveness of TNFα pre-treatment of MSC was investigated in a porcine burn wound model.

Porcine MSC were incubated for 24 h in culture media containing 10ng/ml recombinant porcine TNFα. The cells were harvested and the porcine burn model was performed as described in **section 4.2.1**. Measurement of wound closure demonstrated an accelerated rate of wound healing. Crucially, TNFα pre-treated MSC significantly increased re-epithelisation, a primary determinant of wound healing. TNFα pre-treatment of MSC was superior to untreated MSC as neither AD-MSC or BM-MSC significantly increased re-epithelisation in as shown in **Figure 4.3**, chapter 4 (despite a trend towards increase). These results are in agreement with a previous study by Heo et al, who used MSC CM to treat rat excisional wounds [80]. Application of TNF MSC CM significantly enhanced wound closure and re-epithelialisation [80]. This latter finding would support a paracrine effect. Depletion of CM with IL-6 or IL-10 reduced re-epithelisation and

wound closure [80]. In an in vitro wound healing study using bronchial epithelial cells, treatment with TNFα and IL-1β pre-treated MSC CM resulted in enhanced wound closure compared normal MSC CM mediated through EGF receptor activation and downstream ERK signalling [234]. Stimulation of MSC with TNFα revealed increased expression of several factors including IL-6, EGF, FGF-2, VEGF [234]. TNFα also increased PGE2, HGF and TGF-β1 [79] along with TSG-6 [235] BMP-2, CCL-2 and VEGF [229].

In this study, quantification of αSMA positive vessels indicated an increased stable vascular density in burn wounds treated with TNF pre-treated MSC, suggestive of increased wound healing progression. In line with results for re-epithelialisation and wound closure, no significant difference was observed between AD-MSC and BM-MSC treated wounds. Increased vessel density was also noted compared to untreated MSC (**Figure 4.6**). Application of MSC therapy in burn wounds has been previously shown to induce an angiogenic response in mice [214], rats [191] and in pigs [180]. TNFα pre-treated MSC provide a potent angiogenic stimulus driven through secretion of a factors such as CCL-2, VEGF and HGF [72, 236]. In conjunction, increased VCAM-1 expression in MSC in response to TNFα may also augment endothelial cell interaction [237]. In this study, qRT-PCR analysis of treated wounds did not show any increased expression of VEGF. This discrepancy may be accounted for the timing of VEGF measurement. VEGF released from MSC may occur at an earlier time point and by d-14 MSC expressing VEGF are likely absent from the wound. The quantified αSMA+ vessel density accounts for stable non leaky vasculature that have pericyte covering and therefore do not require VEGF to sustain. TNFα stimulated

MSC CM increased αSMA+ vessel density and limb salvage in a mouse model of hind limb ischemia, partially mediated through IL-6 and IL-8 [75]. Increased endothelial cell migration was observed in response to TNFα MSC CM compared to control CM and this could be attenuated by IL-6 and IL-8 blocking antibodies [75].

In addition to increased vessel density, a significant increase in CD163+ cells was observed. CD163 is a marker for M2 macrophages and this increase in M2 population within the wound suggests a shift from inflammatory to reparative phenotype of the wound environment in line with other studies [191, 208, 216]. The induction of M2 macrophages was far superior in TNFα pre-treated MSC compared to untreated MSC **Figure 4.5 A**). qRT-PCR analysis of several pro/anti-inflammatory cytokines did not detect a difference in expression between treated and untreated wounds. As discussed in **section 4.4.2** the sample used contained both healed wound margin and unhealed wound and therefore may have skewed the result. It should also be noted that this study was not designed to capture these shifts in inflammatory phenotype of the wound. The primary endpoint of this study was to detect a difference in wound healing outcomes specifically, wound closure and re-epithelialisation. Analysis of d-3 or d-5 may be a more appropriate time point to capture these inflammatory cell dynamics within the wound.

Macrophage repolarisation, a key feature of MSC therapy, has been reported in several other studies [20, 102, 191] and is associated with fibroblast proliferation and angiogenesis. This is in agreement with findings presented here, which show increased vessel density and increased collagen content within the wound (as

assessed by Masson's trichrome staining). Taken together these studies support the concept that a reduced inflammatory response coupled with increased granulation tissue which in-turn is supported by increased vascularisation may be promoting accelerated re-epithelialisation and wound closure as observed in this study.

Low or transient engraftment of MSC in many interventions and trials remains an issue that is seen to limit the therapeutic capacity of MSC [238]. TNFα stimulation of MSC can induce expression of ICAM-1 and VCAM-1, adhesion molecules involved in cell interactions and may also play a role in increased engraftment of MSC. In a rat model of MI, MSC were pre-treated with (10ng/ml) TNFα and stained with DAPI prior to IV injection [229]. Two weeks later heart tissue was collected and increased amounts of DAPI labelled TNFα pre-treated MSC were located in infarct boarder zone compared to untreated MSC. Functionally, TNFα pre-treated MSC were therapeutically superior, enhancing ejection fraction and reducing fibrosis of the left ventricle [229]. Previous studies in our lab have established that few MSC persist in wounds after two weeks [149] and it would be interesting to see if TNFα pre-treatment increased engraftment of MSC within the burn wounds and if this was indeed mediated through VCAM-1 or ICAM-1 expression and if this was correlated with increased efficacy. Further studies will be required to validate the engraftment potential of TNFα pre-treatment.

5.4.1. TNFα induced immunomodulation in MSC

Compared to the findings from chapter 4 an increased M2 population is observed within the wound at d-14. This increased presence of M2 macrophages is suggestive of increased immune regulatory capacity of MSC driven by TNFα pre-treatment and several studies support this finding [79, 80, 105, 132]. In vitro stimulation of MSC with TNFα increases secretion of key immunomodulatory factors such as TSG-6 [105], CCL-2 [132] and COX-2 [79] which is metabolised to give PGE2 [79]. To further characterise total macrophage numbers within the wound, frozen sections were stained with several porcine specific antibodies (including SWC8-BioRad, CD68-BioRad, CD45-Abcam, UK) however these commercial antibodies were unable to successfully detect frozen tissue antigens, this is an acknowledged disadvantage of the porcine model in that limited tissue specific antibodies are available. It would be useful to determine if increased macrophage recruitment was occurring or if increased repolarisation was driving this process. It is plausible that both of these processes are contributing to increased M2 population in a synergistic way. A study by Ren et al elegantly demonstrated CCR-2 dependent recruitment of macrophages by tumour associated MSC is driven by the chemokine CCL-2 [132]. CCL-2 is a potent chemotactic factor for inflammatory macrophages. Polarisation of macrophages towards a M2 type was driven by tumour associated MSC and assisted tumour growth [132]. Analysis of tumour associated MSC showed that they secrete increased amount of CCL-2, and inhibition of CCL-2 prevented tumour growth [132]. Stimulation of normal MSC with TNFα increased CCL-2 and enhanced tumour growth, mimicking tumour associated MSC. Ren et al showed that MSC

are stimulated by the tumour through TNFα, this induces them to secrete increased amounts of CCL-2. This in turn recruits CCR-2+ macrophages to the tumour site [132]. They proposed that this interaction with macrophages and MSC drove inflammatory macrophages towards an M2 type (via PGE2 and other mechanisms) and facilitated growth of the tumour [132]. One could speculate that a similar mechanism is at play in the burn wounds treated with TNFα stimulated MSC. This may account for increased CD163+ cells and improved wound healing. Similarly, this same mechanism could also account for increased angiogenesis observed in the wounds which has been shown to be driven by a small population of CCR-2+ macrophages [239].

The results herein suggest that TNFα may promote increased wound healing through CCL-2 mediated interaction with macrophages. This is an interesting hypothesis that requires further investigation. However, while the pig is excellent for pre-clinical efficacy studies, it is not well suited for such mechanistic studies. To explore the role of CCL-2 would require knockdown or inhibition of CCL-2 in MSC. This would be challenging in a larger model as genetically modified pigs are not available and the production of a therapeutic numbers of CCL-2 deficient porcine MSC (via lentivirus or SiRNA knockdown) would be impractical (based on the amount of reagents required). In this context the mouse is more suitable, inducing a partial thickness burn in mice is technically challenging and highly variable due to its thin skin (50 µm thick) and small size [217]. A simpler, more practical and reproducible model is the mouse excisional wound healing model. While important differences exist between excisional wounds and burn wounds (such as increased necrosis, eschar and vascular permeability), this model allow

us to explore the role of MSC derived CCL-2 and gives us a basis for interrogation of the mechanism behind TNFα mediated increased efficacy demonstrated in this section. Therefore, in the next chapter the role of CCL-2 is investigated in a mouse model of excisional wound healing.

In conclusion, pre-treatment of either AD-MSC or BM-MSC significantly accelerated wound closure and wound re-epithelialisation. This was associated with increased M2 population within the wounds at d-14 and increased angiogenesis. TNFα pre-treatment is an easy and less problematic method (then genetic modification) to increase the efficacy of MSC therapy for cutaneous wound healing. Co-stimulation with other inflammatory cytokines such as IFNγ may further increase efficacy. Neither AD-MSC or BM-MSC were therapeutically superior. Therefore, based on findings from this study, AD-MSC would be the optimal cell source as it is therapeutically equivalent to BM-MSC but has more scalable potential and ease of isolation.

6. MSC secreted CCL-2 has a non redundant role in accelerated wound healing in mouse model

6.1. Introduction

Macrophages are pivotal in controlling the progression of wound repair phases [138, 240, 241] In cutaneous wound healing, macrophages are the principal producer of cytokines and chemokines involved in stimulating angiogenesis, collagen formation and re-epithelialisation [138]. Conceptually, macrophages can be broadly divided into two phenotypically distinct groups, M1 (inflammatory) and M2 (reparative); however, in reality they exist in a continuum and alter their phenotype in response to cues from the local micro environment. In the early stages of wound healing M1 macrophages predominate and are associated with increased TNFα and NO. As the wound progresses, M2 macrophages become more abundant and begin to dominate cytokine production, TNFα declines and IL-10 significantly increases. Experimental depletion of either cell type can significantly hinder wound healing and several studies have demonstrated that dysregulation of this M1-M2 progression can lead to chronic non-healing wounds [205, 240-243].

Several studies have corroborated findings that MSC therapy accelerates wound healing, which is mediated through soluble factors and cell contact mechanisms

leading to increased angiogenesis, granulation tissue formation and re-epithelialisation [20, 50, 58]. Previous studies have also established that MSC have immuno-modulatory properties and can skew M1 macrophages towards and an M2 phenotype, thereby accelerating wound healing progression [20]. This mechanism is cell contact dependent and involves PGE2, among others [96, 244].

The chemokine CCL-2 has many biological functions (as outlined in section 1.3.3), in both the normal recruitment of monocytes and macrophages to inflamed tissues [122, 127], as a driver of angiogenesis [126] and in bone reabsorption [245]. CCL-2 is required for normal progression of wound healing phases, in a mouse model of excisional wound healing CCL-2 KO mice had reduced re-epithelialisation and reduced angiogenic activity and collagen deposition associated with reduced macrophage infiltration of wounds [127, 246]. The concentration of CCL-2 within wounds peaks at d-1 and is associated with neutrophil driven monocyte recruitment to the wound [127].

Several cell types including MSC, secrete CCL-2 and MSC derived CCL-2 has been suggested to be involved in recruitment of M1 macrophages in cutaneous wound healing [58], thereby allowing for polarisation towards an M2 phenotype. However, this has not been experimentally demonstrated.

While there is much evidence for a role of CCL-2 in recruiting macrophages, the role of CCL-2 in MSC modulation of wound healing is not clear, due to the complexity and redundancy of downstream signalling cascades and post-translational modifications in CC signalling, some of which are outlined below.

CCL-2 predominantly binds to a G coupled protein receptor named CCR-2. Once bound, CCL-2 initiates a cascade of signalling pathways. Chemokine receptors are categorised according to which chemokine family they belong to and annotated with R. For chemokines CCL1-10 the receptor is termed CCR1-10 and so on for the other respective sub families [247]. Chemokine receptors are notoriously promiscuous, binding several different chemokine ligands such as CCR-1 which reportedly binds CCL-2, CCL-3, CCL-4, CCL-5, CCL-13, CCL-14 as well as CCL-23 [247]. CCL-2 can bind its primary ligand CCR-2 and will also bind scavenging receptors Atypical Chemokine Receptor 1 (ACKR-1) and ACKR-2 (previously referred to as D6) [248]. ACKR-1 also binds CCL-5, CCL-3and CCL-4. However, each receptor has varying degrees of affinity for each chemokine and will act with different extents of agonism. To complicate matters further, interspecies variations also exist, such as CCL8, which is also a ligand of CCR-2 in humans. In mice however, it only specifically binds CCR8 [249]. Similarly, CCL-1 is the primary ligand of CCR-8 while CCL-8 is also an agonist of CCR-8.

CCL-2 stimulation of CCR-2 induces swift phosphorylation of ERK associated with integrin activation and chemotaxis [250-252]. The biological response of this signalling is associated with chemotaxis and superoxidase release [253]. Importantly, these signal transduction cascades are quite similar for a variety of CC chemokines and other G protein-couple receptors (GPCR) that seem to converge on common pathways suggesting functional redundancy.

While GPCR signalling of CC chemokines seem to converge on common pathways, they can also have varying biological effects. How these subtle differences can have differing systemic effects yet maintain a level of redundancy remains to be

elucidated and begs the question whether one single CC cytokine like CCL-2 may have non-redundant roles?

To determine if CCL-2 plays a non-redundant role in MSC accelerated wound healing, CCL-2 deficient MSC were isolated from CCL-2 KO mice and used in splinted excisional wound healing experiments on wild type (WT) mice and compared to WT MSC for efficacy.

6.1.1. Chapter aims

- Isolate BM-MSC from CCL-2 KO mice and demonstrate they can be identified as MSC

- Determine ability of CCL-2 KO MSC to recruit macrophages in vitro

- Determine if CCL-2 is required for accelerated wound healing in a mouse excisional wound healing model

6.2.   Materials and methods

6.2.1. Isolation of murine MSC

Primary MSC were isolated from C57 mice (8 wk old) as per protocol published by Soleimani *et al* [254]. Mice were first euthanised by cervical dislocation. The body was then disinfected by dipping twice in 70% ethanol. An incision was made on the limb and the skin was peeled back to expose underlying muscle. The hind limbs were then removed from the body. Working under sterile conditions, the hind limbs were further trimmed and outer skin removed. The muscle surrounding the femur and tibia was then removed and the ends of the bones were cut. The bone marrow was then flushed out of the femur and tibia and collected in a 15 ml centrifuge tube.

The cell suspension was then filtered and plated at a density of 25×10^6 cells/ml in α-MEM media, supplemented with 10% FBS and 1x antibiotic/antimycotic. After two weeks, colonies formed and became confluent. Cells were then passaged and further expanded up to P5 prior to characterisation and subsequent experimental use.

6.2.2. Isolation of murine CCL-2 KO MSC

Using the same protocol as outlined in **section 6.2.1**, BM-MSC were isolated from 8wk old CCL-2 deficient mice (referred to as MSC-KO). CCL-2 deficiency was validated by enzyme-linked immunosorbent assay (ELISA) as detailed in **section 6.2.7.**

6.2.3. Flow cytometry analysis of cell surface antigens

Expression of associated MSC markers CD44, CD90 and Sca-1 along with CD45 were evaluated to ensure pure population of MSC. Cultured cells at P5 were washed once with PBS and detached from the tissue culture flask by trypsinisation followed by neutralisation with equal volume of serum supplemented medium. Cells were then recovered by centrifugation at 500g for 5 minutes, followed by re-suspension in PBS aliquoted out into several tubes contain 1×10^5 cells for primary antibody staining. Cells were centrifuged and re-suspended in 100 µl of diluted antibody (see **Table 6-1**) in FACS buffer (described in **section 2.2**) and incubated for 1 h at 4°C. Cells were then washed in PBS centrifuged and re-suspended in 100 µl of secondary antibody solution for 30mins in the dark at room temperature (rt). Cells were then re-suspended in 100 µl FACS buffer and analysed on flow cytometer. Control isotypes were used to determine positive cell populations.

Table 6-1 Antibodies used in flow cytometry characterisation of murine MSC

Conjugated antibody	Clone	Manufacturer	Final Concentration
CD90-APC-Cy7	53-2.1	BD Pharmingen	2 µg/ml
CD44-PE	IM7	eBioscience	2 µg/ml
SCA-1-PE-Cy7	D7	BD Pharmingen	2 µg/ml
CD45-PerCP-Cy5.5	104	BD Pharmingen	2 µg/ml
Isotype Control- APC-Cy7	R35-95	BD Pharmingen	Matched to primary ab
Isotype Control- PE	eB149/10H5	eBioscience	Matched to primary ab
Isotype Control- PE-Cy7	R35-95	BD Pharmingen	Matched to primary ab
Isotype Control- PerCP-Cy5.5	G155-178	BD Pharmingen	Matched to primary ab

6.2.4. Lineage Differentiation assays

MSC phenotype was validated by subjecting BM-MSC isolated from both WT and CCL-2 KO mice to in vitro differentiation assays to confirm their potential to differentiate into adipocytes, chondrocytes and osteocytes. Tri-differentiation potential was verified using well established previously published protocols [25, 148].

Briefly, for adipogenic differentiation, cells in culture were subjected to 3 cycles of adipogenic induction media for 3 d followed by adipogenic maintenance media for 1 d. Adipogenic induction media contained dexamethasone 1 mM, insulin 1 mg/ml (Sigma Aldrich, Ireland), indomethacin 100 mM (Sigma Aldrich, Ireland) and 500 mM MIX (Sigma Aldrich, Ireland), the adipogenic maintenance media contained insulin 1 mg/ml. Adipogenic differentiation was confirmed with oil red O (Sigma Aldrich, Ireland) staining.

For osteogenic differentiation, cells were cultured in osteogenic differentiation media containing β glycerol phosphate (Sigma Aldrich, Ireland) 1 M and ascorbic acid (Sigma Aldrich, Ireland) 2-P 10 mM for 21 d. Osteogenic differentiation was confirmed by Alizarin Red staining.

For chondrogenic differentiation, pelleted cells were cultured for 21 d in chondrogenic differentiation media containing 10 ng/ml TGF-β3 (Sigma Aldrich, Ireland). Chondrogenic differentiation was confirmed by mounting the pellets in OCT, sectioning them at 10 μm, and staining with toluidine blue (Sigma Aldrich, Ireland).

6.2.5. Transswell migration assay

To determine the migratory response of macrophages towards WT and MSC-KO, with and without TNFα, MSC were plated in bottom chamber at a density of 2.5×10^4 and grown overnight. RAW 264.7 macrophage cell-line were then plated in the top chamber of 8 μm transwell insert (Corning). Growth media was replaced with serum free media and incubated for 12 h. Transwell inserts were then removed and rinsed in PBS. A cotton bud was used to remove un-migrated cells from upper side of membrane. Membranes were further rinsed, then stained with Hoechst (Thermo Fisher Scientific, UK) live cell nuclear stain for 15 min and then imaged using a microscope (Nikon eclipse TE2000-E, Japan) at five random locations and the amount of migrated cells quantified (Nis Elements v3.0, Nikon, Japan). All experiments were performed in triplicate and repeated three times.

6.2.6. Macrophage MSC co-culture

To determine the immunomodulatory capacity of WT MSC vs MSC-KO to polarise stimulated macrophages towards M2 phenotype. Macrophages were co-cultured in direct contact with MSC and culture supernatants were assayed for concentrations of TNFα and IL-10 (as previously described [255]). MSC (P5) were plated in 24 well plate at a concentration of 1×10^5. On the next day, 1×10^5 macrophages (RAW 264.7) were plated with MSC. After 24 h culture, macrophages were stimulated with LPS (30 ng/ml). Culture supernatants were collected after 48 h. and centrifuged at 2000g to remove any cell debris before storing at -20°C prior to use in ELISAs. Experiments were performed in triplicate and repeated three times.

6.2.7. ELISAs

To determine concentrations of IL-10, TNFα and CCL-2, ELISAs were performed on culture supernatants using kits provided by R&D systems (USA). Following manufacturer protocols 96 well clear plastic plates were coated overnight at room temperature with capture antibody (0.2 µg/ml) (R&D systems). 100 µl of diluted culture supernatants was added to the plate for 2 h at room temperature. The plate was washed and detection antibody (50 ng/ml) (R&D systems) applied for 2 h. After washes, streptavidin conjugated horseradish peroxidase (R&D systems) was incubated for 20 min on the plate followed by substrate colour solution (hydrogen peroxide and tetramethylbenzidine) (R&D systems). The reaction was then stopped after 20 min by addition of 100 µl of 2N sulphuric acid (Sigma Aldrich, Ireland). The optical density was measured using microplate reader (Molecular Devices, Spectra Max, UK) and sample concentration was calculated from a generated standard curve (Soft Max pro v5.4.3, UK). Each standards and sample was measured in duplicate and experiments had multiple replicates.

6.2.8. Excisional sutured wound induction

This protocol was adapted from a published protocol by Wang et al [256]. The day before surgery following anaesthesia by an IP injection of Ketamine (90 mg/kg) and Xylazine (10 mg/kg), the dorsum of the mouse was shaved using clippers and hair depilated using hair cream remover.

On the day of wounding, mice were anaesthetised and skin was sterilised with 70% (vol/vol) ethanol swab. To induce the punch wounds, the loose dorsal skin

was gently pulled away from the back, and placed on a hard flat surface. Once the skin was extended far enough, the punch biopsy was firmly pushed down through the skin creating two 5 mm punch wounds. Images of the wounds were taken using canon DLSR camera.

Wounds were injected at four points in the dermis at the edge of the wound with a total of 1×10^6 MSC in 100 µl PBS. A silicone splint was used to prevent contraction of the wound, allowing it to heal in a similar fashion to human wounds. The silicone ring was attached with an adhesive and then sutured into place. The wounds were covered with a non-occlusive dressing (Tegadem) and then covered with a self-adhering elastic bandage (Optitape) and care was taken not to impede movement or breathing of mice with the bandage.

Dressings were changed and wounds imaged on d-3, d-5, d-7, and d-10. On d-10, the mice were euthanised by CO_2 administration and wounds were harvested for further analysis.

Several animals had to be excluded from all groups as the sutured ring came off at an early time point. In the control group two animals were excluded (n=9), in WT MSC group three animals was excluded (n=9), while in CCL-2 KO group one animal were excluded (n=8).

6.2.8.1. Re-epithelialisation

Wounds were excised, and trimmed to 1 cm². This was bisected and one half was stored in 4% PFA o/n. To determine re-epithelialisation, wound sections were stained with H&E (as detailed in **section 2.7.1**). The wound section was imaged

at 4x magnification. Unepithelialised length (or wound gap) was measured using ImageJ software by blinded observers

6.2.8.2. Granulation tissue area

The area of granulation tissue was assessed from previously stained H&E sections (as described in **section 2.7.1**. Area was quantified form 4x images using ImageJ software, by a blinded observer.

6.2.9. Immunofluorescent staining

Wounds were excised, and trimmed to 1 cm² containing both wound and healed wound margins. This was bisected and one half was stored in 4% PFA for 1 h at 4°C, then dehydrated in graded sucrose solution and then embed in OCT (as detailed in **section 2.6**). Frozen sections were cut at 10 μm thickness in cryostat and stored at -80°C until required. Prior to staining, slides were removed and left to defrost for 30 min at rt.

Slides were rehydrated in PBS (10 min) and then blocked for 1 h in 10% normal goat serum in PBS-Tween (0.5%) solution. Sections were then incubated o/n at 4°C with primary antibody diluted in antibody buffer (1% BSA PBST). The next day, sections were washed x3 in PBST and slides were incubated with secondary antibody solution in antibody buffer for 2 h at rt, followed by 3x washes in PBST. Nuclei were stained with DAPI (1 μg/ml) for 10 min followed by 3x washes in PBS prior to mounting in immunomount and cover slipping.

Table 6-2 Immunohistochemistry antibodies used in murine wound sections

Primary antibody	Clone	Manufacture	Final Concentration	Isotype
Ly6G	RB6-8C5	Abcam, UK	5 µg/ml	Rat IgG$_{2b}$
CD3	SP7	Abcam, UK	1:100	Rabbit IgG
CD31	NA	Abcam, UK	1:100	Rabbit IgG
CD206	NA	Abcam, UK	10 µg/ml	Rabbit IgG
F4/80	CI:A3-1	Abcam, UK	10 µg/ml	Rat IgG$_{2b}$
Isotype control Rabbit polyclonal IgG	NA	Abcam, UK	Adjusted to primary ab concentration	Rabbit
Isotype control Rat IgG$_{2b}$	NA	Santa Cruz	Adjusted to primary ab concentration	Rat

Secondary antibody	Clonality	Manufacturer	Concentration	Host
488 αRabbit IgG (H+L)	polyclonal	Thermo Fisher Scientific	2 µg/ml	Goat
546 αRat IgG (H+L)	polyclonal	Thermo Fisher Scientific	2 µg/ml	Goat

6.2.9.1. Neutrophil infiltration quantification

Neutrophils are the most abundant cell type of the innate immune system and are the first immune cell to infiltrate the wound, beginning to accumulate within minutes after injury [257]. Neutrophils are relatively short lived and usually begin to decline in the wound after 48-72 h post injury [258]. The neutrophil marker Ly6G is a 25 kDa glycosylphosphatidylinositol linked differentiation antigen that is predominantly expressed by neutrophils and transiently expressed on some monocytes in the bone marrow. It is a well-established marker of neutrophils [259]. Neutrophils were quantified as follows; wound sections were imaged at five random points within the wound bed and Ly6G+ cells were quantified by blinded observer; three sections were analysed per animal.

6.2.9.2. T-lymphocyte quantification

MSC induced response of T-lymphocyte wound infiltration was quantified by probing tissue sections with the pan T-cell marker CD3 as previously established [61, 260] . Sections were imaged at five random points within the wound bed and CD3+ cells were quantified by blinded observer; three sections were analysed per animal.

6.2.9.3. M2 macrophage response

Overall determination of macrophage population was assessed by staining with pan macrophage marker F4/80 [242, 261]. To determine the polarisation of macrophages to reparative M2 phenotype, co-staining of F4/80 and the M2 marker CD206 was performed. The mannose receptor (CD206) is highly associated with macrophage M2 phenotype; it is significantly upregulated on IL-4 treated macrophages and is widely used to quantify M2 macrophages [20, 257, 262]. Sections were imaged at five random points within the wound bed and CD206+ cells were quantified by blinded observer; three sections were analysed per animal.

6.2.9.4. Angiogenic response

To assess angiogenic response, wound sections from d-10 were probed with endothelial cell marker CD31. Platelet endothelial cell adhesion molecule-1 or CD31 is an adhesion molecule expressed on endothelial cells that line capillaries and other blood vessels and is widely used to quantify angiogenesis [263]. Sections were imaged at five random points within the wound bed and vessel density was calculated (by blinded observer) based on CD31+ vessels (as determined by intact open lumen); three sections were analysed per animal.

6.2.10.   RNA extraction and qRT-PCR

Wounds were excised, and trimmed to 1 cm^2 containing both wound and healed wound margins. This was bisected and 1 half was snap frozen in liquid nitrogen. Samples were kept at -80°C until required. To extract RNA, samples were crushed in using pestle and mortar in liquid nitrogen. Samples were then homogenised using rotor stator homogeniser in a solution of phenol, guanidine isothiocyanate (Qiazol) for 1 min. RNA purification was then performed using RNAeasy universal kit (Qiagen, UK) as per manufactures instructions.

Purity (A_{260}/A_{280}) and concentration of isolated RNA was measured using Nanodrop spectrophotometer. Integrity of RNA was assessed using denaturing agarose gel electrophoresis and ethidium bromide staining. Only high purity (A_{260}/A_{280} >1.8) RNA samples that had sharp bands of 28s and 18s rRNA and apparent 2:1 ratio were used. Degraded RNA was apparent in several samples, in addition some samples we not of sufficient purity and were excluded, this left n=5 in all groups.

Five samples were used from each treatment group for RT^2 profiler array. RNA (1 µg) was reverse transcribed into cDNA using Qiagen RT^2 First Strand Kit. This was then used for each qRT-PCR reaction with RT^2 SYBR Green Mastermix containing Hotstart DNA Taq polymerase (Qiagen, UK). This was added to RT^2 profiler array (Qiagen, UK) containing 10 pre coated validated primer assays for IL-10, IL-6, CCL-2, VEGFa, and CD31. Data was analysed using the ΔΔ CT method, quantification was calculated in relation to 18s expression in each sample

calculated before 35 cycles. Both positive, negative and genomic DNA contamination controls were included in the assays.

6.2.11. Statistical analysis

Difference between multiple groups was analysed by analysis of variance (ANOVA) followed by Tukey's post-hoc testing. Results are expressed as mean ± SEM. All statistics were carried out using Graphpad Prism v7.03.

6.3. Results

6.3.1. Isolation and characterisation of MSC from WT and CCL-2 deficient mice

MSC were expanded to p5 and samples were taken for flow cytometry and for tri-lineage differentiation assays (as described in **section 6.2.4**). Samples from both cell populations were cultured in various differentiating conditions using well established protocols (as previously described [149, 150]). Adipogenic differentiation was confirmed in both cell types by the presence of lipid vacuoles stained with oil red O (**Figure 6.1 A**). Positive Alizarin red staining indicated the presence of calcium deposits associated with osteoblast formation (**Figure 6.1**

B). Chondrogenic differentiation was confirmed using toluidine blue staining of pellet cultures (**Figure 6.1 C**).

Cell surface antigen expression was determined using flow cytometry. Both MSC-WT and MSC-KO were positive for CD44, CD90 and SCA-1, while also negative for CD45

6.3.2. WT MSC express CCL-2 and stimulate macrophage migration in vitro

Unstimulated MSC-WT secreted 0.3ng/ml ± 0.04 CCL-2 (n=3) **Figure 6.3 A**. No signal was detected from MSC-KO. Transwell experiments were used to determine migratory response of macrophages towards MSC in response to CCL-2 (**Figure 6.3 B**). MSC-WT group had significantly more migrated macrophages (MSC; 42 ± 5.9 vs Control; 9 ± 1.65 vs CCL-2 KO; 20 ± 4.94) compared to control and to MSC-KO group (Control vs MSC-WT, $p<0.001$, Control vs MSC-KO $p=0.112$, MSC-WT vs MSC-KO, $p=0.01$, n=3).

6.3.3. CCL-2 deficient MSC have reduced therapeutic efficacy in excisional mouse model

Excisional wounding of mice was carried out (as described in **section 6.2.8.**) and image analysis was performed to calculate the wound size at d-0. No significant differences in wound area were observed at d-0 (**Figure 6.4 B left**).

Application of WT MSC accelerated wound closure at all time points compared to Control (**Figure 6.4 B right**). On d-3, MSC-WT treated wounds had a wound size of 72.35% ± 4.1 (MSC-WT vs Control, p=0.053, n≥8) compared to control; 87.48% ± 4.2 while MSC-KO had a mean wound size of 88.74% ± 4.1 (MSC-WT vs MSC-KO p=0.034, n≥8) By d-5, MSC-WT treated group had a wound size of 54.23% ± 2.7 vs Control 71.24% ± 3.9 vs CCL-2 KO; 72.39% ± 2.5. (Control vs MSC-WT p<0.001, Control vs MSC-KO p=0.945, MSC-WT vs MSC-KO p<0.001, n≥8). On d-7, MSC-WT treated group was 37.05% ± 3.12 vs Control; 56.67% ± 4.46 vs CCL-2 KO; 59.59% ± 3.04 (Control vs MSC p<0.001, Control vs MSC-KO p=0.828, MSC-WT vs MSC-KO p<0.001, n≥8). Finally, on d-10, MSC-WT wounds were 8.26% ± 1.05 vs Control wounds; 13.58% ± 3.89 vs CCL-2 KO group; 19.01% ± 3.5 (Control vs MSC-WT p=0.390, Control vs MSC-KO p=0.425, MSC-WT vs MSC-KO p=0.032, n≥8). MSC-KO did not accelerate wound closure and there was no statistical difference between this group and the control group at any time point.

6.3.4. MSC-KO do not enhance re-epithelialisation of excisional wounds

Injection of MSC into the wounds accelerated re-epithelialisation as measured on d-10 (Control; 2290 μm ± 668 vs MSC; 272.1 μm ± 136 and CCL-2 KO 1198 μm ± 199, Control vs MSC-WT p=0.002, Control vs MSC-KO p=0.11, MSC-WT vs MSC-KO p=0.165, n≥8). Several MSC-WT treated wounds were fully re-epithelialised at the time of analysis. Epithelial gap was reduced in MSC-KO group but, this was not statistically different to Control.

Using ImageJ, granulation area was also measured and found to be largest in the control group (Control; 22583 μm^2 ± 2268 vs MSC-WT; 13273 μm^2 ± 2021 vs MSC-KO; 19615 μm^2 ± 2162, Control vs MSC-WT p=0.011, Control vs MSC-KO p=0.606, MSC-WT vs MSC-KO p=0.097, n≥8). MSC-WT treated wounds had statistically significantly smaller granulation area indicating resolution of inflammatory response and wound maturation.

6.3.5. MSC derived CCL-2 is required for angiogenic effect

To determine if MSC derived CCL-2 was important for induction of an angiogenic response to cell therapy, wound sections were stained for CD31 (green) and blood vessel density within the wound bed was calculated (**Figure 6.6 A**).

Vessel density was significantly improved with application of MSC-WT to the wounds compared to Control (Control; 7.5 ± 1.6 vs MSC-WT; 25.4 ± 3.2 vs MSC-KO; 10.7 ± 2.8, Control vs MSC-WT p<0.001, Control vs MSC-KO p=0.632, MSC-WT vs MSC-KO p=0.003, n≥8). In contrast, CCL-2 deficient MSC did not significantly increase vessel density compared to control.

CD31 mRNA expression was also quantified by qRT-PCR in wounds samples taken from 5 animals per group (**Figure 6.6 B**). No significant difference was found between the groups. VEGFa expression was also quantified and found to be marginally higher in both MSC-WT and MSC-KO groups however, no significant differences were observed between the groups (Control; 1 ± 0.02 vs MSC-WT; 1.15 ± 0.1 vs MSC-KO; 1.07 ± 0.06, Control vs MSC-WT p=0.364, Control vs MSC-KO p=0.717, MSC-WT vs MSC-KO, p=0.721, n=5).

6.3.6. MSC derived CCL-2 is required for reduced inflammatory response and accumulation of CD206+ macrophages

To characterise neutrophil response, d-10 wound sections were stained for the neutrophil marker Ly6G (**Figure 6.7 A**). Wounds treated with MSC-WT showed a significant reduction in Ly6G+ neutrophil infiltration compared to PBS treated controls (Control; 29.87 ± 4.83, vs MSC-WT; 11.27 ± 1.82, vs MSC-KO; 25.13 ± 4.83, Control vs MSC-WT, $p<0.001$, Control vs MSC-KO, $p=0.435$, MSC-WT vs MSC-KO, $p=0.009$, n≥8). while MSC-KO have a significant amount Ly6G+ positive cells remaining within the wound similar to control wounds. Sustained neutrophil presence or late re-entry of neutrophils can indicate ongoing inflammatory response, possibly due to lack of epithelium.

Whilst the adaptive system does not play a major role in normal cutaneous wound healing, the pan T-Cell markers was used to evaluate T-cell presence within the wound (**Figure 6.7 B**). As expected T-cell numbers are low at d-10, however there is a trend towards more CD3+ T-cells in both MSC-WT and MSC-KO groups compared to the control group (Control; 3.6 ± 1.33, vs MSC-WT; 9.62 ± 1.86, vs CCL2 KO MSC; 8.2 ± 2.33, Control vs MSC-WT, $p=0.1$, Control vs MSC-KO, $p=0.246$, MSC-WT vs MSC-KO, $p=0.857$, n≥8). While this was not statistically significant, it may indicate that T-cell infiltration is driven by MSC but is not CCL-2 dependent.

CCL-2 is classically associated with monocyte and macrophage recruitment, to investigate the response towards MSC derived CCL-2, immunohistochemistry was performed on tissues sections for pan macrophage marker F4/80 (red)

(**Figure 6.8 A**). To determine the polarisation of macrophages towards reparative M2 phenotype, sections were co-stained with CD206 (green). Quantification was performed of positive cells within the wound bed. No significant difference in macrophages numbers was observed within the wound between treatment groups (Control; 67.9 ± 6.0, vs MSC-WT; 63.7 ± 5.6, vs CCL2 KO MSC; 65.2 ± 2.6, Control vs MSC-WT p=0.826, Control vs MSC-KO p=0.92, MSC-WT vs MSC-KO p=0.98, n≥8) (**Figure 6.8 B Left**). However, the frequency of CD206+ macrophages was greatly increased in MSC-WT treated group (Control; 10.5% ± 1.7, vs MSC-WT; 29.0% ± 2.5, vs MSC-KO; 14.8% ± 1.5, Control vs MSC p<0.001, Control vs MSC-KO p=0.277, MSC-WT vs MSC-KO p<0.001, n≥8). MSC-KO treated wounds had significantly less CD206+ macrophages compared to MSC-WT group. There was no significant difference between MSC-KO and control groups.

Polarisation of macrophages from inflammatory to reparative phenotype is believed to exist on a continuum and is associated with increased expression of CD206, increased IL-10 and reduced TNFα cytokine levels within the wound. To further characterise the inflammatory cytokine profile of the wound, qRT-PCR was performed on wound samples from d-10 (**Figure 6.9**). Significantly, there was a dramatic increase with IL-10 expression with MSC-WT treated wounds compared to both control and MSC-KO treated wounds (Control; 1.04 ± 0.13 vs MSC; 2.13 ± 0.39 vs MSC-KO; 1.07 ± 0.21, Control vs MSC-WT p=0.037, Control vs MSC-KO p=0.998, MSC-WT vs MSC-KO p=0.02, n=5). There was no significant difference between MSC-KO and control, groups.

The expression of IL-6 was also evaluated and while it was not statistically significant, there was a trend towards increased expression that was observable in both MSC treated groups compared to controls (Control; 1.12 ± 0.26 vs MSC-WT; 2.11 ± 0.68 vs MSC-KO; 1.85 ± 0.6, Control vs MSC-WT p=0.517, Control vs MSC-KO p=0.634, MSC-WT vs MSC-KO p=0.944, n=5). Conversely, CCL-2 expression was increased in MSC-WT treated wounds compared to MSC-KO and control groups (Control; 1.03 ± 0.11 vs MSC-WT; 2.03 ± 0.38 vs MSC-KO; 1.33 ± 0.27, Control vs MSC-WT p=0.09, Control vs MSC-KO p=0.746, MSC-WT vs MSC-KO p=0.208, n=5). This could be as a result of MSC transplantation, but as it is not statistically different could be due to biological variation. Similarly, no significant difference was observed between groups for TNFα, which may have resolved by d-10 (Control; 1.02 ± 0.07 vs MSC-WT; 1.46 ± 0.28 vs MSC-KO; 1.01 ± 0.13, Control vs MSC-WT p=0.234, Control vs MSC-KO p>0.999, MSC vs MSC-KO p=0.161, n=5).

6.3.7. CCL-2 deficient MSC have reduced immunomodulatory capacity

To verify in vivo results that CCL-2 is required for efficient M2 polarisation, MSC-WT and MSC-KO were co-cultured with LPS stimulated macrophages and supernatant concentrations of TNFα and IL-10 were assessed (as described in **section 6.2.6**).

In response to LPS stimulation of macrophages significantly increased TNFα secretion associated with activated M1 macrophage phenotype (**Mφ + LPS**; 1601

pg/ml ± 61.8 vs **Mφ**; 106.7 pg/ml ± 13.3, p<0.001 n=3). Co-culture of MSC-WT significantly reduced TNFα to baseline secretion consistent with increased M2 polarisation and this was only observed when cultured with stimulated macrophages (**MSC-WT + Mφ + LPS**; 285.8 pg/ml ± 22.31, vs **Mφ + LPS**; 1601 pg/ml ± 61.8, p< 0.001, n=3).

MSC-KO were not as efficient as MSC-WT in reducing TNFα and associated M2 polarisation as significantly greater concentrations of TNFα were detected in this group (**MSC-KO + Mφ + LPS**; 682.3pg/ml ± 23.28**,** vs **MSC-WT + Mφ + LPS**; 285.8 pg/ml ± 22.31, p<0.001, n=3). MSC-KO were, however, able to induce a statistically significant reduction in TNFα, albeit smaller (**Mφ + LPS** vs **MSC-KO + Mφ + LPS**, p<0.001, n=3).

Detection of IL-10 in supernatants demonstrated both MSC-WT and MSC-KO were capable of increasing IL-10 in response to stimulated macrophages (**Mφ + LPS**; 94.96 pg/ml ± 9.9 vs **MSC-WT + Mφ + LPS**; 470.6 pg/ml ± 13.4 vs **MSC-KO + Mφ + LPS**; 522.1 pg/ml ± 19.3, **Mφ + LPS** vs **MSC-WT + Mφ + LPS** p<0.001, **Mφ + LPS** vs **MSC-KO + Mφ + LPS** p<0.001, n=3)

Figure 6.1
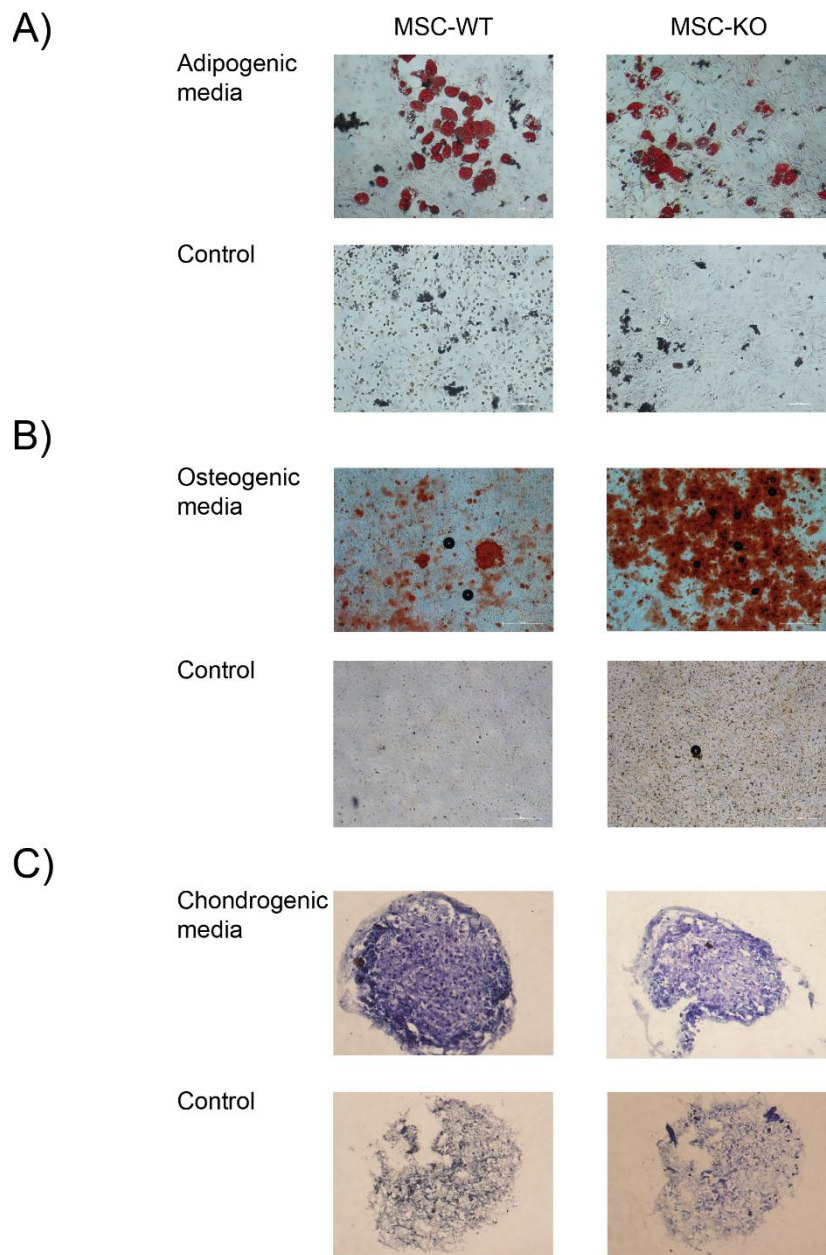
Figure 6.1 Both MSC and MSC-KO have tri differentiation potential

*WT MSC and MSC-KO were exposed to various differentiating media and subsequently differentiated into **A)** adipocytes (verified with Oil red o) **B)** osteocytes (alizarin red stain) and **C)** chondrocytes (toluidine blue stain). Both cell populations were readily able to differentiate into these lineages, while cells cultured in control media did not differentiate. Representative images of differentiation potential (n=3).*

Figure 6.2
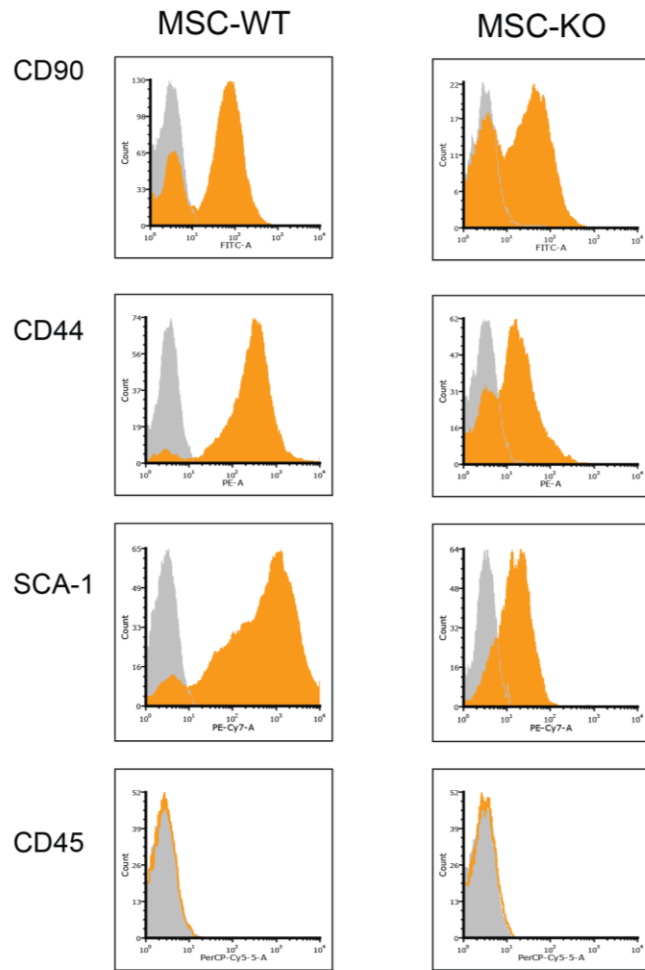
Figure 6.2 Cell surface antigen expression of MSC

Isolated MSC were characterised for expression of cell surface markers using FACS. Both MSC-WT and MSC-KO were found to express common MSC cell surface antigens CD90, SCA-1 and CD29 (as indicated by orange histograms). MSC were negative for CD45. Control isotype represented in grey histograms. Representative plots (n=3).

Figure 6.3

A)
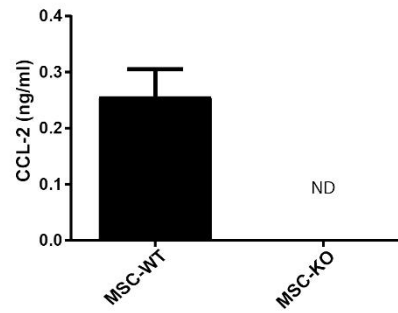
B)
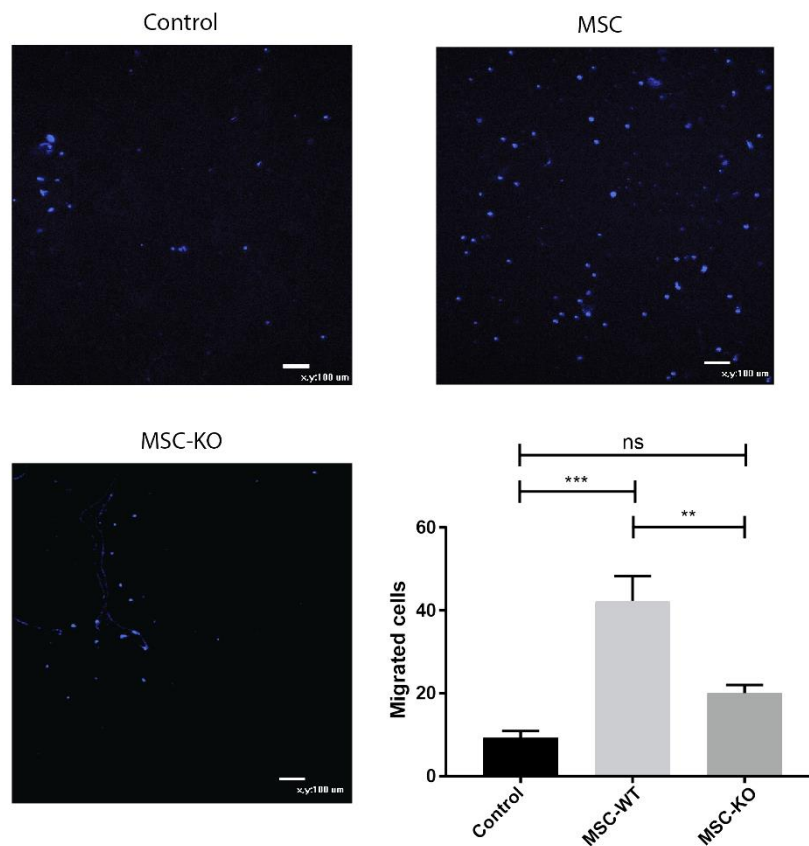
Figure 6.3 MSC secreted CCL-2 and stimulated migration of macrophages in vitro

A) Cells culture supernatants collected at 24h from both MSC-WT and MSC-KO were assayed for CCL-2 secretion using ELISA. Under unstimulated conditions MSC secrete CCL-2 (0.25ng/ml), no CCL-2 was detected in MSC-KO supernatants (n=3). B) Transwell migration assay, Images of migrated macrophages (stained with Hoechst live stain, blue) demonstrate significantly reduced migration towards MSC-KO compared to WT (n=3 ** p<0.01, *** p<0.001).

Figure 6.4

A)
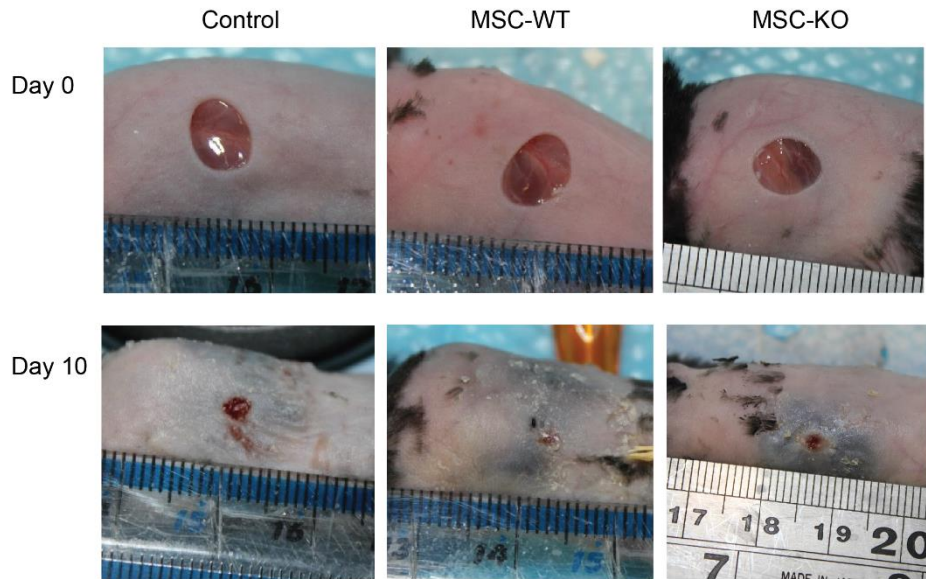
B)
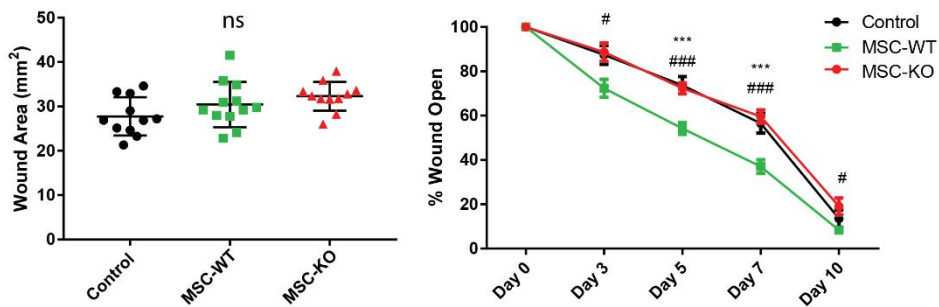
Figure 6.4 CCL-2 deficiency reduces therapeutic efficacy of MSC
*A) Images of mouse excisional wounds at d-0 and at d-10. Two 5 mm punch wounds were created on the dorsum of each mouse. B) Left - Wound area was quantified at d-0 and no significant differences were observed between any of the groups (n≥ 11, ns, not significant). Time course of wound closure from image analysis demonstrated accelerated wound closure in MSC-WT treated wounds (n≥8, * = MSC-WT vs Control, *** p<0.001). MSC-KO completely abrogated this therapeutic effect and were not statistically different to control treated wounds, but were statistically different to MSC-WT treated wounds at all time points (n≥8, # = MSC-WT vs MSC-KO, # p<0.05, ## p<0.001).*

Figure 6.5

A)

B)
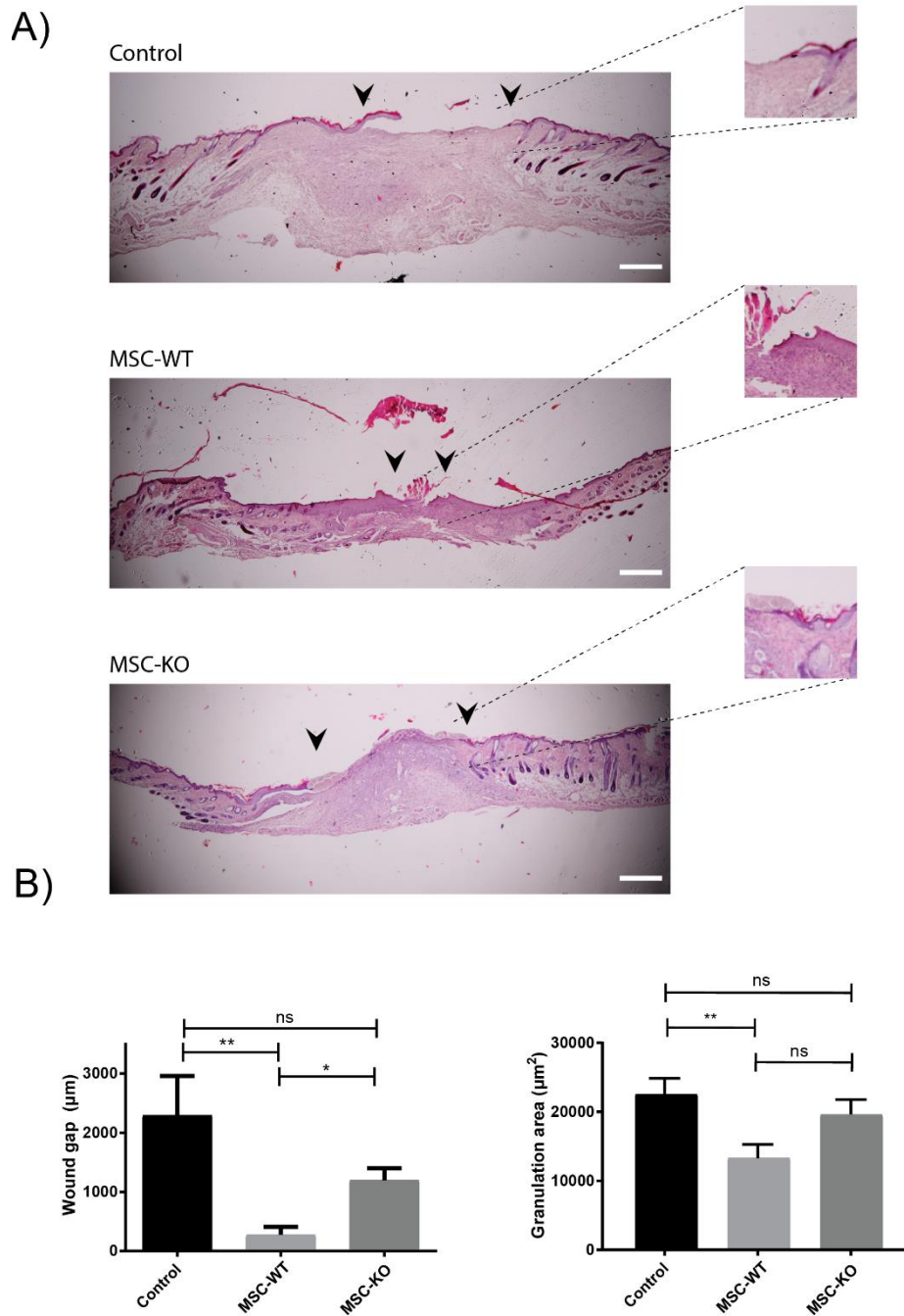
Figure 6.5 CCL-2 deficiency delayed wound re-epithelialisation compared to WT MSC
*A) Histological samples taken at d-10 post wounding were stained with H&E. Images of stained tissue sections were taken at 4x. Black arrows indicate migrating front of Keratinocytes; insets show magnified image of migrating front. Scale bar, 100 μm. B) Left- Quantification of unepithelialised gap demonstrated significantly reduced unepithelialised wound in MSC-WT treated wounds compared to both control and MSC-KO (n≥8 ns, not significant * p<0.05, ** p<0.01). B) Right - Granulation area was measured using ImageJ software indicated significantly reduced area in MSC-WT treated wounds compared to control suggestive of reduced inflammatory response and increased wound maturity (n≥8 ns, not significant, ** p<0.01).*

Figure 6.6

A)

B)
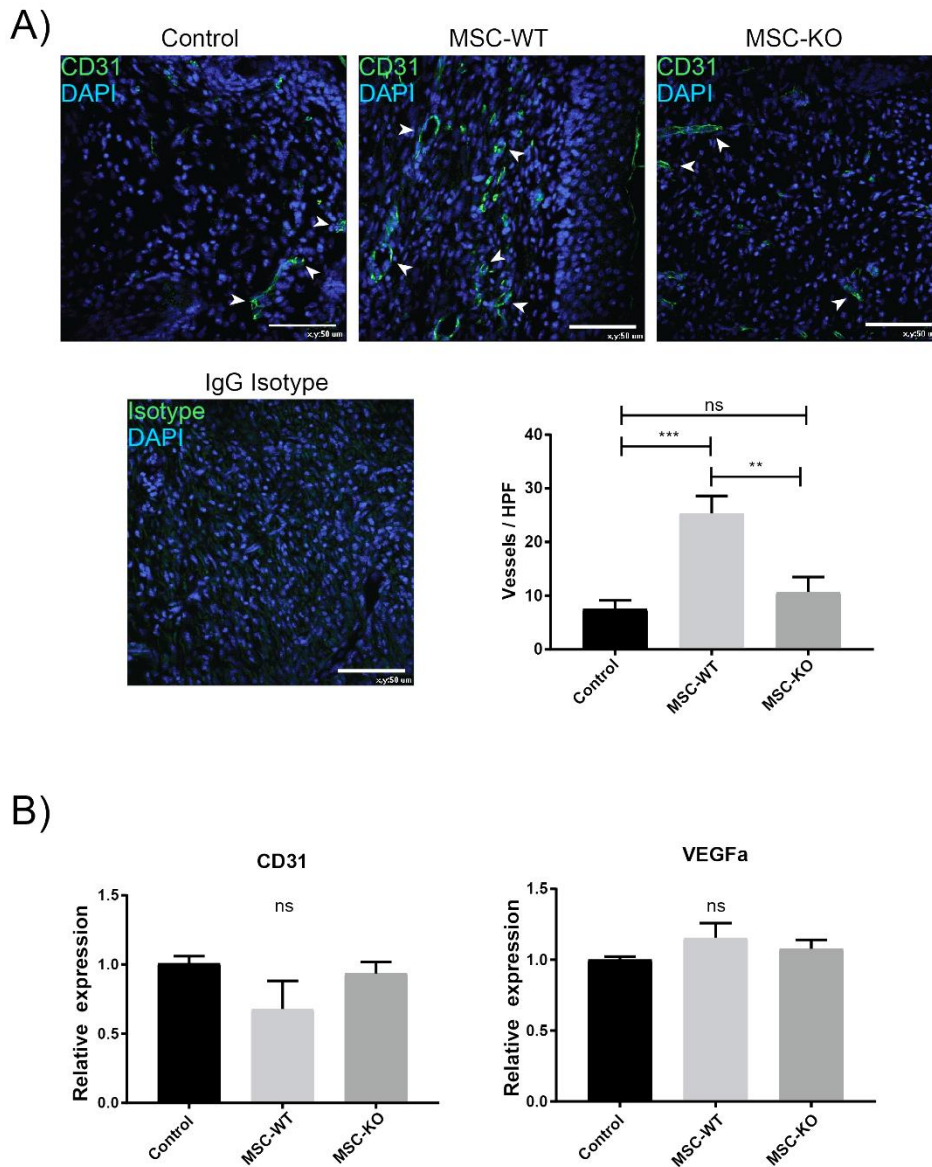
Figure 6.6 Application of WT MSC increased vascularity of wounds

*A) Representative images of wound sections at d-10 post wounding, probed with CD31 antibody (green) and nuclei counter stained with DAPI (blue) scale bar, 50 μm. Vessels per high power field were quantified within the wound bed, white arrows indicate intact vessel lumens. MSC treated wounds had increased vessel density compared to both control and MSC-KO treated wounds (n≥8 ns, not significant * p<0.05, ** p<0.01, *** p<0.001). B) qRT-PCR expression of CD31 and VEGFa was assessed from wound samples containing both wound and healed wound margin, no significant difference in expression was detected (n=5 ns, not significant).*

Figure 6.7
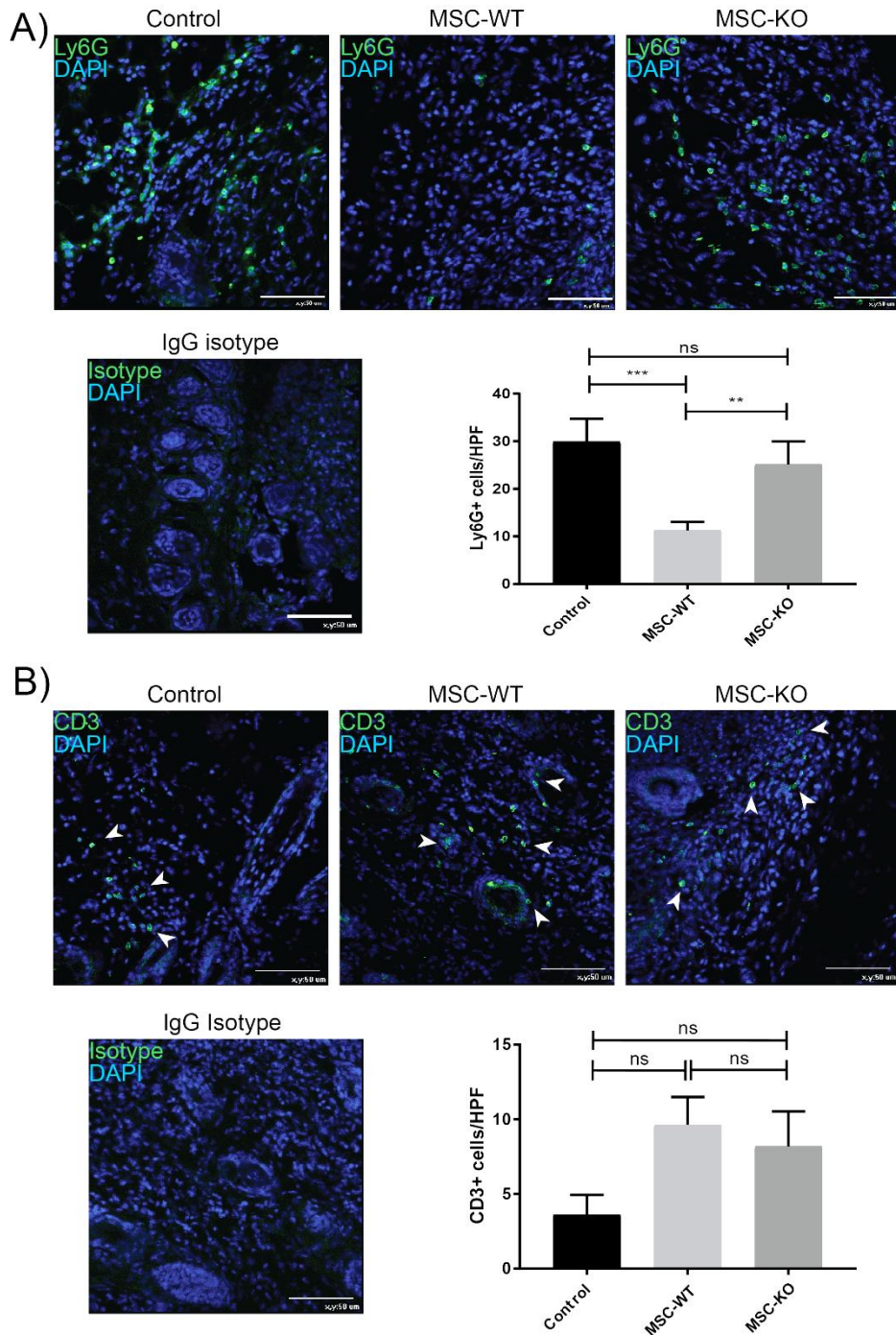
Figure 6.7 MSC altered immune response in CCL-2 dependent mechanism
A) *Representative images of wound sections d-10 post wounding, stained for neutrophil marker Ly6G (green), cell nuclei were counter stained with DAPI (blue) scale bar, 50 μm. MSC-WT treated wounds had significantly reduced neutrophil infiltration at d-10 compared to control and MSC–KO treated wounds (n≥8, ns, not significant ** p<0.01, *** p<0.001).* **B)** *Representative images of wound sections d-10 post wounding, stained for T-cell marker CD3 (green), cell nuclei stained with DAPI (blue) scale bar, 50 μm. Both MSC-WT and MSC-KO treated wounds had a trend towards increased CD3+ T-cells within the wound bed at d-10 however this was not statistically different to controls (n≥8, ns, not significant).*

Figure 6.8
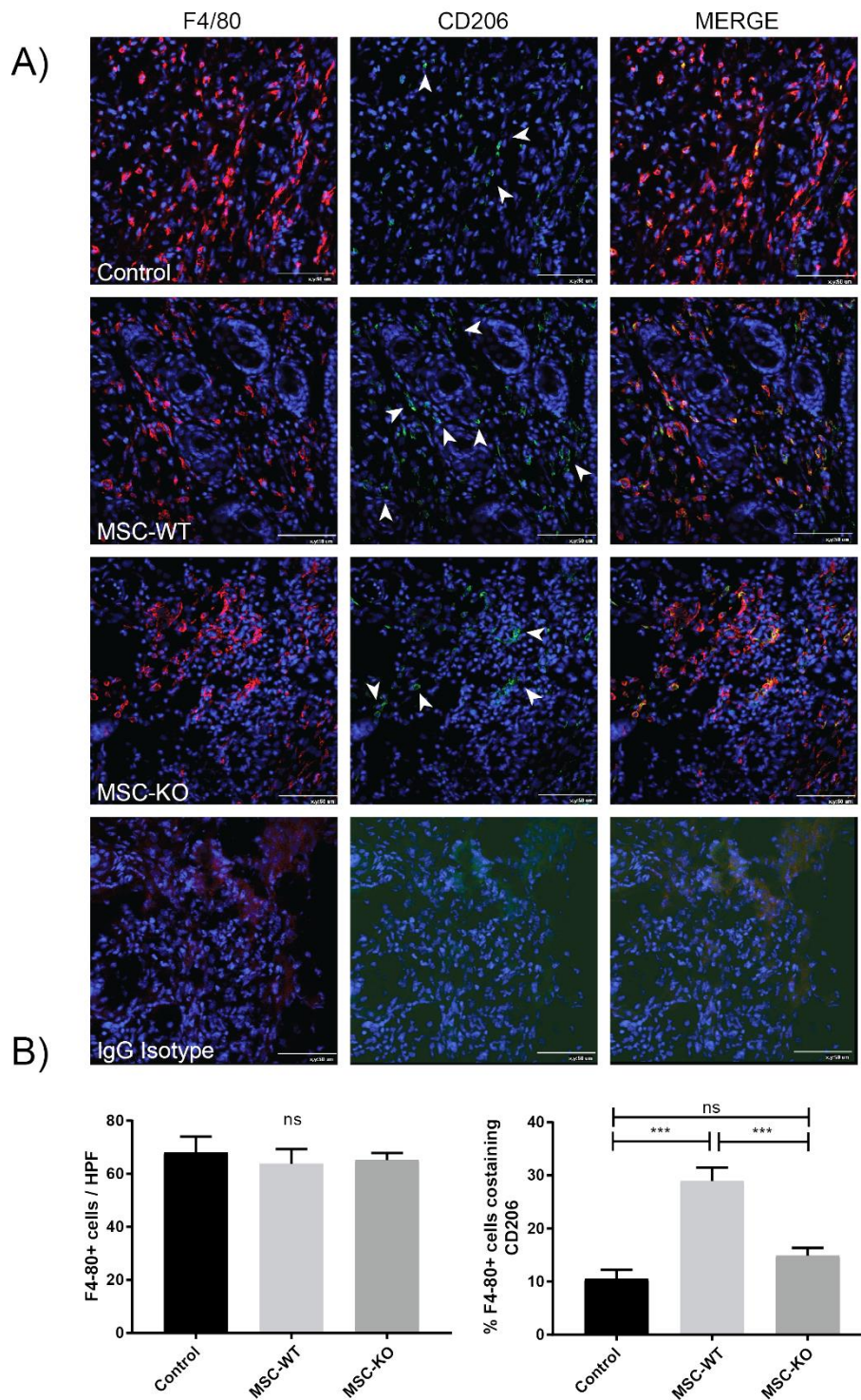
Figure 6.8 MSC derived CCL-2 is required for alteration of macrophage phenotype
A) *Representative images of wound sections d-10, stained for pan macrophage marker F4/80 (red) and M2 marker CD206 (green), cell nuclei were counter stained with DAPI (blue), for clarity arrowheads indicate CD206+ cells, scale bar, 50 µm.* **B) Left-** *total macrophage within the wound bed, no difference between any of the groups was detected at d-10 (n≥8 ns, not significant).* **B) Right-** *percentage macrophages co-expressing CD206 was significantly increased in MSC-WT treated wounds compared to both control and MSC-KO treated wounds. (n≥8 ns, not significant *** p<0.001).*

Figure 6.9
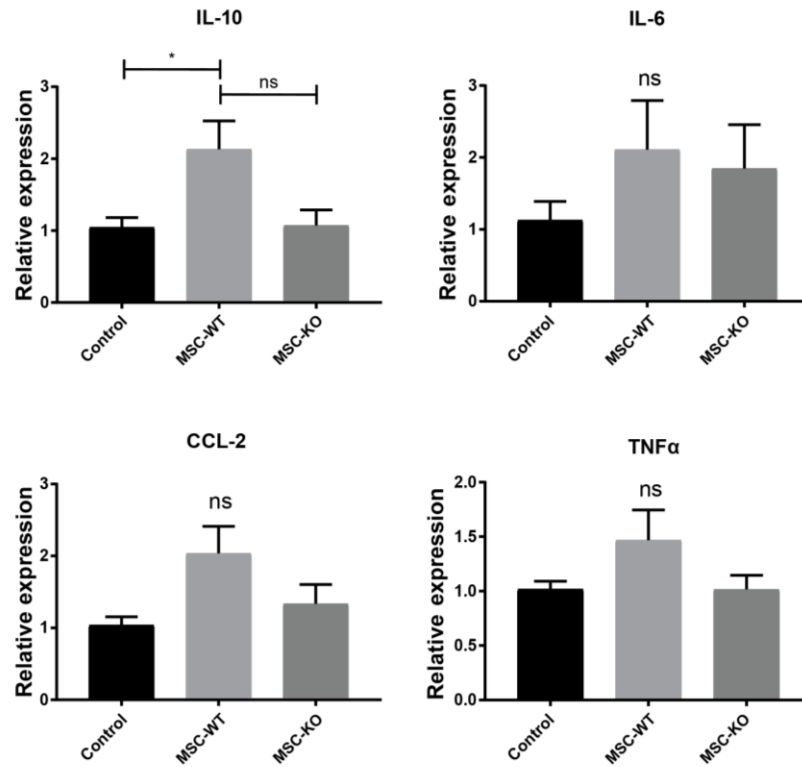
Figure 6.9 MSC alter expression of wound cytokines

*Analysis of cytokine expression (qRT-PCR) from samples containing both wound and healed wound margin at d-10. Application of MSC significantly increased IL-10 associated with macrophage M2 transition, which was abrogated with MSC-KO (n=5, ns, not significant * p<0.05). No difference in either IL-6, CCL-2 or TNFα was detected. (n=5, ns, not significant * p<0.05).*

Figure 6.10

A)
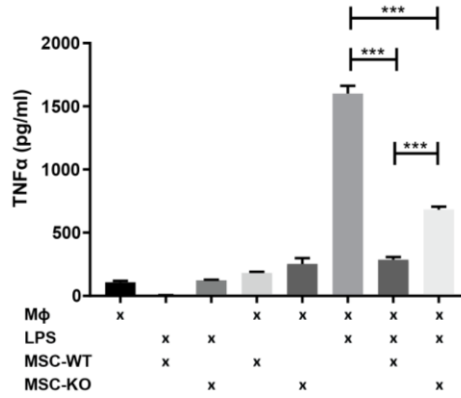
B)
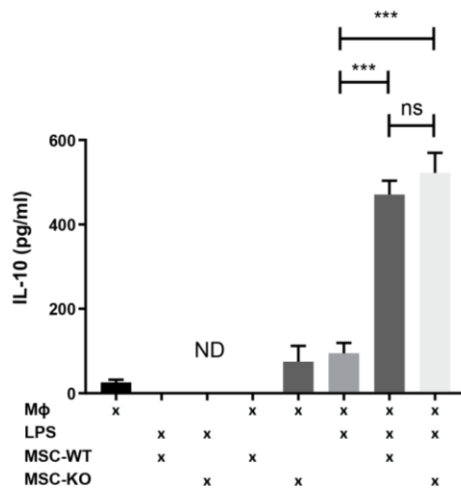
Figure 6.10 CCL-2 deficiency reduced MSC immunomodulatory capacity
A) *Co-culture of MSC-WT in direct cell contact with stimulated macrophages (LPS 30ng/ml) significantly reduced TNFα as detected by ELISA in culture supernatants at 48h. MSC-KO were also able to reduce TNFα however, not to the same extent as MSC-WT (n=3 *** p<0.001). B) Detection of IL-10 in supernatants demonstrate both MSC-WT and MSC-KO were capable of significantly increasing IL-10, (n=3, ND - not detected, ns - not significant, *** p<0.001)*

6.4.   Discussion

In the introduction of this thesis a strong rationale was presented for a role of CCL-2 in MSC therapy in cutaneous wound healing. Briefly, CCL-2 is a potent chemotactic cytokine which is well known recruiter of monocytes and macrophage [127, 250, 264]. Wound healing is a complex process involving several different cell types and includes phases of pathogen clearance, proliferation, re-epithelisation and remodelling. Cells of the myeloid lineage are one of the main effector cells in wound repair and secrete the largest amounts of cytokines which control the progression of wound healing phases [138, 240, 241]. Therefore, it is quite plausible to assume CCL-2 may play a role in MSC therapy.

However, several reasons were cited for why the role of MSC derived CCL-2 may not be so clear (in **section 6.1**.) due in part to chemokine redundancy, decoy receptors and post translational modifications to the chemokine. Clearly, what is evident form this study is that CCL-2 has a profound effect on many aspects of MSC therapy in a mouse model of excisional wound healing.

Several studies have corroborated the therapeutic effect of MSC therapy in cutaneous wound healing [20, 50, 58, 61, 102, 265], the effects of which, have been observed in mouse [41], rabbit [266], rat [110], pig [115] and human [47]. The molecular mechanisms behind this accelerated wound healing are still being delineated, however, certain aspects are now well established. As outlined in section 1.2.4, MSC therapy accelerates wound closure, involving earlier granulation tissue formation [110] and increased re-epithelialisation [56]. This

is driven by a potent angiogenic effect which has been observed both in vivo and in vitro, and is mediated primarily through VEGF secretion [56, 267]. Finally, MSC are potent immune-modulators of both adaptive and innate immune systems, and several chemokines have been identified (TSG-6 [102], IDO or inducible NOS [98] and PGE2 [88] as responsible for altering the inflammatory environment.

In the context of cutaneous wounds, macrophages and neutrophils are key drivers and inhibitors of wound progression. MSC are involved in a phenotypic switch of inflammatory macrophages towards a reparative type phenotype (M2) associated with reduced TNFα and increased IL-10 production [244]. To understand how CCL-2 may play a role in MSC accelerated wound healing it is useful to look at each of these parameters and see how they are connected.

Re-epithelisation is a major milestone in wound healing and is influenced by several factors, including proliferation, migration and differentiation of keratinocytes at the wound edges. One of the key therapeutic benefits of MSC therapy, as observed in this study, is accelerated re-epithelialisation [56]. CCR-2 has recently been found to be expressed by normal keratinocytes, although these cells are not responsive to CCL-2 treatment [268]. MSC secrete many cytokines such as FGF-7, IGF and EGF [58] and MSC CM has been shown to accelerate keratinocyte migration in vitro [269]. To what extent this drives re-epithelialisation in vivo is unknown. CCL-2 is not involved in the secretion of these cytokines, so it is unlikely that MSC-KO would have an abnormal cytokine profile. A more plausible explanation is through the early formation of granulation tissue. In excisional wound healing, the dermal layer is removed and therefore keratinocytes have no substrate to migrate on. In mice, wound closure

is driven by wound contraction, however in this study, a sutured ring prevented this from occurring. Lack of contraction required granulation tissue to be formed to allow re-epithelisation and wound closure to progress. MSC therapy accelerates the formation of granulation tissue [110, 270] and CCL-2 may be involved in this respect. Granulation tissue is a vascular dense connective tissue consisting of a provisional extra cellular matrix of fibronectin, fibrin and other components and is required substrate for keratinocytes to migrate on. Increased angiogenesis in MSC treated wounds accelerate the process of granulation tissue formation, thereby, providing a substrate for keratinocytes to migrate across, leading to augmented re-epithelialisation that was observed in this study.

6.4.1. CCL-2 and angiogenesis

In this study a significantly increased angiogenic response in MSC treated wounds was manifested in increased vascular density in the wound bed. This phenomenon has been reported by several other studies and is believed to be a major contributor to accelerated wound closure [56, 74, 76, 110, 265]. CCL-2 plays a pivotal role in angiogenesis and importantly, no significant increase in vascularisation was observed in MSC-KO treated wounds. While a significant increase in CD31 immunostaining was observed, no difference in mRNA expression of VEGF or CD31 was found. One possible explanation for this aberrant finding is that CD31 immunostaining staining was quantified in the wound bed, whereas, the sample used for qRT-PCR analysis contained both the wound and the healed wound margins which may have skewed the results. By

d-10, VEGF may also have normalised between the groups. Early sprouting of endothelial cells is dependent on presence of VEGF however as the vessels mature, VEGF is no longer required.

The role of angiogenesis during wound repair is well established and involves the migration and proliferation of vascular cells. CCL-2 induces downstream effects on SMCs and endothelial cells [271]. Vascular SMC (VSMC) express CCR-2 and when treated with CCL-2 induces significant proliferative response, primarily through NF-κB and activator protein 1 [271].

In addition, endothelial cells express CCR-2 and migrate in response to CCL-2 [272]. In a Chick CAM assay, administration of CCL-2 was as potent an inducer of angiogenesis as VEGF, and could also be inhibited through VEGF inhibition [273]. Similarly, Matrigel plugs and aortic rings seeded with CCL-2 induced significant angiogenesis in a leukocyte independent and CCR-2 dependent manner [272]. Treatment of human endothelial cells with CCL-2 induces hypoxia inducible factor 1 (HIF-1) gene expression this in turn induces VEGF A_{165} in the aortic wall [273]. The activation of CCR-2 by binding of CCL-2 also induces a transcription factor called monocyte chemotactic protein induced protein (MCPIP) [274]. Over-expression of MCPIP in human umbilical vein endothelial cells (HUVECs) induced an angiogenic response [275]. Treatment with CCL-2 induced MCPIP and capillary like tube formation [275]. Cadherins 12 and 19, trans-membrane proteins involved in cell adhesion, induced upon CCL-2 stimulation, were required for tube formation and were MCPIP dependent [275].

MSC CM can induce an angiogenic response in endothelial cells and may have a protective effect under hypoxic conditions which is CCL-2 dependent [74]. Endothelial cells cultured under hypoxia for 24h displayed a 16% reduction in caspase 3 activation when cultured in MSC CM and only recombinant CCL-2 alone was able to replicate this [74].

In this study MSC-KO had a reduced angiogenic response and it is reasonable to suggest, as outlined above, that this may be mediated through a CCL-2 dependent reduction in both endogenous VEGF, reduced SMC and endothelial cell proliferative/survival responses. However, further in vitro studies are needed to fully characterise this reduced angiogenic response.

6.4.2. CCL-2 and it role in MSC immune-modulation

Another aspect of MSC therapy is the ability to regulate immune responses. MSC can modulate both adaptive an innate immune responses based on the micro environmental cues. MSC inhibit the proliferation and activity of B-cells [276], T-cells [277] and NK cells though a range of cytokines such as TSG-6 and COX-2 activity leading to downstream PGE2 release. One of the major attributes of MSC therapy in cutaneous wound healing is the ability to polarise macrophage phenotype towards reparative M2 type [20, 96, 97]. This is characterised with increased CD206+ macrophages within the wound, reduced inflammatory cytokine TNFα and increased IL-10, as was established in vitro in this study. This results in an accelerated progression of wound healing. As the inflammatory phase resolves, M2 macrophages increase fibroblast proliferation, allowing

formation of granulation tissue and vascularisation to occur. This study replicates earlier findings that MSC application in a mouse excisional wound healing model accelerates wound closure. Similarly, this study corroborates the finding that MSC application increases CD206+ macrophages within the wound and increases IL-10 expression associated with a reduced inflammatory response. Significantly, this work demonstrates a non-redundant role of MSC derived CCL-2 in this M1-M2 polarising mechanism. CCL-2 deficient MSC were unable to expand the M2 macrophage population within the wound as observed with MSC-WT and there was no significant increase in IL-10 compared to controls. Significantly, in vitro studies confirmed the CCL-2 deficient MSC had a reduced capacity to modulate TNFα secretion by stimulated macrophages. To the best of the author's knowledge this finding has not been established before. MSC derived CCL-2 could perhaps be inducing increased recruitment of monocytes into the wound as it is a potent chemotactic factor for monocytes and as transwell experiments indicate. However, at d-10 no difference was observed in total macrophage (F4/80+) numbers between the groups. There are several possible reasons that may account for this discrepancy. One possible explanation is that at d-10 macrophage numbers have levelled out between the groups and there may have indeed been differences at a much earlier time point. While this study clearly demonstrates that CCL-2 does play a significant role, these events underlying this mechanism occur during early stages of wound healing and are not fully captured in this study. It would be interesting to look at the evolution of macrophage populations at early time points, such as d-5. However, several other

studies have examined this area (as outlined below) and this may give some insight.

In a study of diabetic murine wound healing, early macrophage infiltration was significantly inhibited compared to WT controls. Application of recombinant CCL-2 significantly increased macrophages numbers in the wounds and accelerated wound healing [278].

Previous work by Jackman et al demonstrate that CCL-2 is quickly expressed in normal excisional wounds within the mouse [246]. Reaching a peak within 6 h after wounding and gradually declining therein, consistent with macrophage recruitment into the wound [279]. In this context, addition of MSC expressing CCL-2 may not function in recruiting monocytes to the wound per se, as the amount of CCL-2 globally, within the wound will already be quite high. It may, however, facilitate short range homing and cell contact between recruited monocytes/macrophages and MSC within the wound.

Nemeth et al elegantly elucidated the mechanisms of M2 polarisation, in a series of co-culture experiments they demonstrate that a significant increase in IL-10 only occurs when stimulated macrophages are co-cultured with MSC [96]. If cultured in a transwell system, no significant increase in IL-10 is observed, demonstrating the requirement of cell contact to initiate polarisation [96]. Conversely, TNFα was only significantly reduced with direct co-culture of MSC and stimulated macrophages [96]. Other studies have reported similar results [100, 280]. In this study, these findings were exactly replicated with WT MSC. However, MSC-KO were not as efficient in repolarising stimulated macrophages

and reducing TNFα, establishing a possible causative mechanism for the reduced efficacy of MSC-KO observed in-vivo.

Using a series of inhibitors, Nemeth et al explored the signalling pathways involved and demonstrated that cell contact induces iNOS signalling (IDO in human MSC [98]) which elevates COX-2, simultaneously TNFα from macrophage binds TNNFR-1 and also up-regulates NF-κB further inducing downstream COX. Increased COX leads to the synthesis of PGE2 which then binds to EP-4 and EP-2 on the macrophage increases IL-10 release. In this study in vitro co-culture of WT MSC was able to significantly increase IL-10 in stimulated macrophages. Conversely to previous findings with TNFα, MSC-KO were also capable of inducing IL-10, this could potentially be happing in an IL-6 dependent manner [281]. The time point of 48 h used in these experiments may also not capture possible early induction of IL-10 by MSC-WT. While no difference in IL-10 was observed in-vitro, it should be noted that IL-10 was significantly increased in WT MSC treated wounds and not MSC-KO treated wounds. In-vitro co-cultures may also not entirely reflect the complex multi cellular environment present in-vivo.

The in vivo data presented here in conjunction with reduced in vitro macrophage recruitment and reduced capacity to inhibit TNFα, suggests that CCL-2 is required for local contact of MSC and macrophages which facilitates increased M2 polarisation.

MSC derived CCL-2 may also directly influence macrophage polarisation [282]. M1 polarised macrophages isolated from CCR-2 -/- deficient mice show reduced

IL-10 expression compared to wild type, while normal M1 when stimulated with CCL-2 increased IL-10 secretion [282].

MSC may also have secondary inhibitory effects based on IL-10, increased IL-10 from other immune cells, such as macrophages, can inhibit rolling, adhesion and trans-epithelial migration of neutrophils [95] and may prevent their re-entry into the wound cutting off the negative feedback loop in response to macrophage stimulation. This is consistent with observations in this study, where MSC treated wounds had increased expression of IL-10 and significantly less Ly6G+ neutrophils present compared to MSC-KO and control treated wounds at d-10.

In Conclusion, in this chapter a role for MSC derived CCL-2 was established in M2 polarisation. MSC alter their secretome in response to environmental cues which skews M2 polarisation accelerating wound closure. As outlined in this discussion one of the major environmental cues driving this is TNFα. In chapter 5 a therapeutic benefit was demonstrated from pre-stimulation of MSC with TNFα in a porcine burn model. The next chapter will examine if this can be applied to excisional wound healing in a mouse model, and using the MSC-KO, determine if CCL-2 is involved.

7. Assessment of TNFα pre-treatment of MSC in a murine excisional wound model

7.1.   Introduction

The application of MSC for excisional wound healing is beneficial as several studies, including results presented in Chapter 6, have confirmed [20, 50, 56, 102]. This therapeutic response is driven in part through attenuation of the body's inflammatory response and promotion of innate reparative responses [20, 102]. This immune modulatory function is mediated by several key factors including PGE2, TSG-6, IL-6 and IL-8 [85, 96, 255].

MSC respond to micro-environmental cues in their proximity them which under particular circumstances can be either anti-inflammatory or pro-inflammatory mediators [283]. This has led to the concept of MSC licensing, whereby MSC are stimulated with pro inflammatory cytokines to prime them before therapeutic application [228, 229]. Several studies have reported beneficial effects when MSC were primed or pre-treated with various inflammatory cytokines such as TNFα, IL-1β and IFNγ [229, 231, 234]. In Chapter 5, TNFα was used to pre-treat porcine MSC prior to application in a partial thickness burn wound. Pre-treatment significantly increased the therapeutic response, augmented re-epithelisation of the wounds and improved the immunomodulatory response. In a mouse model of excisional wound healing human MSC CM taken from TNFα pre-treated MSC

was also found to be beneficial [80]. MSC CM was generated by culturing AD-MSC in 10ng/ml of TNFα for 48h. Wounds (8mm punch) were treated daily with 20 µl topical application of CM [80]. Application of CM accelerated wound closure compared to MSC CM without pre-treatment, and this was mediated in part through IL-6 and IL-8 both of which were significantly increased in MSC CM after TNFα stimulation [80]. However, these experiments were performed in an unsplinted wound model, which may not accurately reflect human wound healing, as it is driven primarily through wound contraction [284, 285].

Several studies have established that TNFα stimulation of MSC induces the secretion of a wide variety of factors including VEGF, HGF, TSG-6, PGE2 and CCL-2 [72, 79, 105, 286]. In Chapter 6, it was established that CCL-2 is required for MSC induced therapeutic effect in an excisional mouse model. Previous studies have implicated TNFα in a similar process in tumour development [132]. In a study by Ren et al, MSC were found in the developing tumour stroma and secreted large amounts of CCL-2 [132]. This in turn recruited macrophages to the tumour stroma allowing them to interact with MSC where they are polarised towards an M2 type phenotype (known as tumour associated macrophages) in a CCR2 dependent process [132]. This reduced the inflammatory response and promoted tissue repair, similar to application of MSC and formation of granulation tissue in a cutaneous wound. At the heart of this process is a MSC/macrophage interaction driven through TNFα/CCL-2. Taken together, these studies suggest that TNFα pre-treatment may enhance the therapeutic efficacy of MSC in an excisional wound model and this process could be driven through a TNFα/CCL2 axis involving MSC and macrophages.

Therefore, the experiments described in this chapter were designed to answer two questions, 1) does TNFα pre-treatment enhance MSC therapeutic response in a mouse excisional wound healing model (as established in the pig in chapter 5) and 2) If TNFα pre-treatment does enhance MSC efficacy, is this process driven through MSC derived CCL-2?

7.1.1. Chapter aims

- To determine if TNFα pre-treatment of MSC is beneficial in a mouse model of excisional wound healing

- To evaluate if CCL-2 is required for enhanced therapeutic response using previously established CCL-2 deficient MSC

7.2.   Materials and methods

The response of MSC to TNFα pre-treatment was evaluated in mouse excisional wound healing model as described in **section 6.2.** This study was performed in batches in tandem with previous study outlined in chapter 6 using the same control group. For clarity the results of the combined study have been broken into separate chapters; Chapter 6 (which deals with the role of MSC derived CCL-2 in accelerated wound healing) and Chapter 7 (which investigates the effect of TNFα pre-treatment on MSC efficacy and the role of CCL-2). Several animals had to be excluded from all groups as the sutured ring came off at an early time point. In the control group two animals were excluded (n=9), in MSC-WT group one animal was excluded as sutured ring came off (n=8), while in MSC-KO group two animals were excluded for the same reason (n=8).

7.2.1. Evaluation of CCL-2 cytokine secretion in response to TNFα in murine MSC

CCL-2 cytokine secretion in murine MSC was evaluated in response to TNFα. The cells were first plated in 6 well plate and grown until confluent. The cells were then stimulated with either 5, 10, or 50ng/ml of TNFα (R&D systems) in complete media. Normal complete media without TNFα was used as a control and CCL-2 KO MSC were also used as a negative control.

7.2.2. TNFα pre-treatment of Murine MSC

After cells had been isolated and characterised (as described in **sections 6.2.1-6.2.3**) MSC-WT and MSC-KO were grown to confluency and stimulated with 50 ng/ml murine recombinant TNFα (R&D systems) in complete culture media for 24 h prior to administration to the wounds (as described in **section 6.2.8**). TNFα pre-treated MSC-WT are designated MSC-WT$_T$ and TNFα pre-treated MSC-KO are designated MSC-KO$_T$.

7.3.   Results

7.3.1. TNFα increased MSC derived CCL-2 secretion in a dose dependent manner

Detection of CCL-2 in MSC-WT supernatants demonstrated a significant increase in CCL-2 in a dose dependent manner in response to TNFα stimulation (**Control**; 0.5 ng/ml ± 0.12, vs **TNFα 5 ng/ml**; 1.9 ng/ml ± 0.51, vs **TNFα 10ng/ml**; 2.61 ng/ml ± 0.63 vs **TNFα 50ng/ml**; 6.5 ng/ml ± 1.6) (Control vs TNFα 5 ng/ml p=0.056, Control vs TNFα 10 ng/ml p= 0.03, Control vs TNFα 50ng/ml p=0.02, n=3)(**Figure 7.1. A**)   As 50 ng/ml TNFα stimulation induced the greatest CCL-2 response, it was decided to use this concentration for further experiments. Migratory response of macrophages towards MSC-WT$_T$ and MSC-KO$_T$ was investigated as shown in **Figure 7.1 B.** Macrophage migration was significantly

increased in response to MSC-WT$_T$ compared to pre-treated MSC-KO$_T$ or control (**Control**; 9.28 ± 1.6, vs **MSC TNF**; 122.6 ± 2, vs **CCL-2 KO TNF**; 58.8 ± 18.5. Control vs MSC-WT$_T$ TNF $p<0.001$, Control vs MSC-KO$_T$; $p=0.03$, MSC-WT$_T$ vs MSC-KO$_T$ $p=0.004$, n=3).

7.3.2. TNFα pre-treatment of CCL-2 deficient MSC increased therapeutic efficacy in excisional mouse model

TNFα pre-treatment of MSC-WT marginally increased wound closure compared to MSC-WT as presented in **section 6.3.3** (combined wound healing rates shown in **Appendix V**). MSC-WT$_T$ significantly increased wound closure at all time points compared to control group (**Figure 7.2**). TNFα pre-treatment of CCL-2 deficient MSC improved wound closure, which became statistically significant on d-7 compared to control (**Figure 7.2**) (Control; 59.7% ± 3.5 vs MSC-WT$_T$; 27.6% ± 3.9 vs MSC-KO$_T$; 40.9% ±4.6, (Control; vs MSC-WT$_T$ $p<0.001$, Control vs MSC-KO$_T$ $p=0.011$, MSC-WT$_T$ vs MSC-KO$_T$ $p=0.079$, n≥8). By d-10 no significant difference was observed between MSC-KO$_T$ and control group (Control; 15.3 ±4.0 vs MSC-WT$_T$; 3.7% ± 0.7 vs MSC-KO$_T$; 12.1% ± 1.5, (Control; vs MSC-WT$_T$ $p<0.005$, Control vs MSC-KO$_T$ $p=0.638$, MSC-WT$_T$ vs MSC-KO$_T$ $p=0.042$, n≥8).

7.3.3. TNFα pre-treatment of WT MSC enhanced re-epithelialisation of excisional wounds

To determine re-epithelialisation of wounds, histological sections were stained with H&E (as described in **section 2.7.1**) and unepithelialised length quantified (described in **section 6.2.8**). MSC-WT$_T$ treated wounds demonstrated statistically significant increase in re-epithelisation compared to control group (Control; 2292 μm ± 668, vs MSC-WT$_T$; 0 μm vs MSC-KO$_T$; 1861 μm ±370, Control vs MSC-WT$_T$ p=0.001, MSC-WT$_T$ vs MSC-KO$_T$ p=0.009, n≥8) **Figure 7.2**. In all cases MSC-WT$_T$ treated wounds exhibited complete re-epithelisation. MSC-KO$_T$ treated wounds had a marginally smaller wound gap than controls; however, this was not statistically significant (Control vs MSC-KO$_T$, p=0.75 n≥8). Measurement of granulation area demonstrates a statistically significant reduction in MSC-WT$_T$ wounds compared to control treated wounds (Control; 22583 μm^2 ± 2268, vs MSC-WT$_T$; 13499 μm^2± 1973 vs MSC-KO$_T$; 19884 μm^2 ±1796) (Control vs MSC-WT$_T$ p=0.021, Control vs MSC-KO$_T$ p=0.58, MSC-WT$_T$ vs MSC-KO$_T$ p= 0.12 n≥8) **Figure 7.3 B.**

7.3.4. MSC derived CCL-2 was required for enhanced angiogenesis

To measure angiogenic stimulus of MSC-WT$_T$ or MSC-KO$_T$ wound sections were stained with CD31 and vessel density quantified (as described in **section 6.2**). Application of MSC-WT$_T$ significantly increased vessel density compared to control measured at d-10 within the wound bed, a statistically significant

difference was also observed between MSC-WT$_T$ and MSC-KO$_T$ (Control; 7.5 ± 1.6, vs MSC-WT$_T$; 26.4 ± 2.9, vs MSC-KO$_T$; 11.03 ± 0.9, (Control vs MSC-WT$_T$ p<0.001, Control vs MSC-KO$_T$ p=0.33, MSC-WT$_T$ vs MSC-KO$_T$ p<0.001, n≥8). Pre-treatment of cells with TNFα had no significant effect compared to untreated cells as presented in **section 6.3.5.** No significant differences were detected by qRT-PCR analysis for CD31 in either group (Control; 1.09 ± 0.05, vs MSC-WT$_T$; 0.04 ± 2.9, vs CCL2 KO MSC$_T$; 0.81 ± 0.1, Control vs MSC-WT$_T$ p=0.33, Control vs MSC-KO$_T$ p=0.17, MSC-WT$_T$ vs MSC-KO$_T$ p=0.87, n=5). Similarly, qRT-PCR analysis of VEGF expression across the wound and wound margin demonstrated no statistically significant differences (Control; 1.0 ± 0.2, vs MSC-WT$_T$; 0.79 ± 0.03, vs MSC KO$_T$; 0.87 ± 0.07, Control vs MSC-WT$_T$ p=0.2, Control vs MSC-KO$_T$ p=0.69, MSC-WT$_T$ vs MSC-KO$_T$ p=0.91, n=5).

7.3.5. MSC derived CCL-2 was required for reduced inflammatory response and accumulation of CD206+ macrophages

To examine the neutrophil response at d-10, wound sections were probed with Ly6G primary antibody and subsequently detected using a secondary 488 fluorochrome antibody. As shown in **Figure 7.5**, MSC-WT$_T$ treatment of wounds significantly reduced neutrophil invasion into the wound (Control; 29.9 ± 4.8, vs MSC-WT$_T$; 10.6 ± 1.7, vs MSC-KO$_T$; 16.0 ± 2.2, Control vs MSC-WT$_T$ p<0.001, Control vs MSC-KO$_T$ p=0.009, MSC-WT$_T$ vs MSC-KO$_T$ p=0.435, n≥8). MSC-KO$_T$

treated wounds also contained fewer neutrophils compared to control treated wounds at d-10.

To evaluate if MSC treatment altered T-cell response, total T-cell numbers were measured using pan T-cell marker CD3. While both MSC-WT$_T$ and MSC-KO$_T$ groups had a trend towards increased CD3+ T-cells, no statistical differences were observed between the groups (Control; 3.6 ± 1.3, vs MSC-WT$_T$; 11.6 ± 2.9, vs MSC-KO$_T$; 7.2 ± 3.4, n≥8, Control vs MSC-WT$_T$ p=0.11 Control v MSC-KO$_T$ p=0.55, MSC-WT$_T$ vs MSC-KO$_T$ p=0.57).

7.3.6. Inflammatory cytokine analysis at d-10

Wound samples which included both wound and healed wound margins were used for isolation of mRNA to detect expression of several inflammatory cytokines such as IL-10, IL-6, CCL-2 and TNFα (**Figure 7.7**.) No significant differences were observed in any of the groups for either IL-10 (Control; 1.04 ± 1.3, vs MSC-WT$_T$; 1.47 ± 0.25, vs MSC-KO$_T$; 1.12 ± 0.24, n=5, Control vs MSC-WT$_T$ p=0.35, Control vs MSC-KO$_T$ p=0.96, MSC-WT$_T$ vs MSC-KO$_T$ p=0.54) IL-6 (Control; 1.12 ± 0.26, vs MSC-WT$_T$; 1.21 ± 0.27, vs MSC-KO$_T$; 13.23 ± 37.52, n=5, Control vs MSC-WT$_T$ p=0.99 Control v MSC-KO$_T$ p=0.19, MSC-WT$_T$ vs MSC-KO$_T$ p=0.15).

Similarly, no differences were observed in CCL-2 (Control; 1.17 ± 0.07, vs MSC-WT$_T$; 0.92 ± 0.16, vs MSC-KO$_T$; 0.62 ± 0.08, n=5, Control vs MSC-WT$_T$ p=0.79 Control v MSC-KO$_T$ p=0.79, MSC-WT$_T$ vs MSC-KO$_T$ p=0.37) or TNFα (Control; 1.04 ± 0.11, vs MSC-WT$_T$; 0.82 ± 0.14, vs MSC-KO$_T$; 1.26 ± 0.36, n=5, Control vs MSC-WT$_T$ p=0.869 Control v MSC-KO$_T$ p=0.114, MSC-WT$_T$ vs MSC-KO$_T$ p=0.207).

Figure 7.1

A)

B)
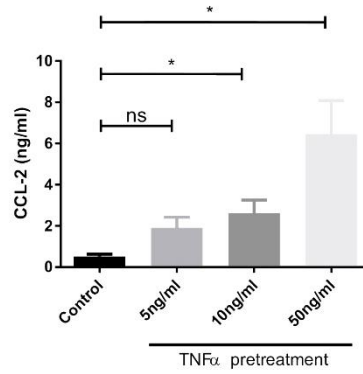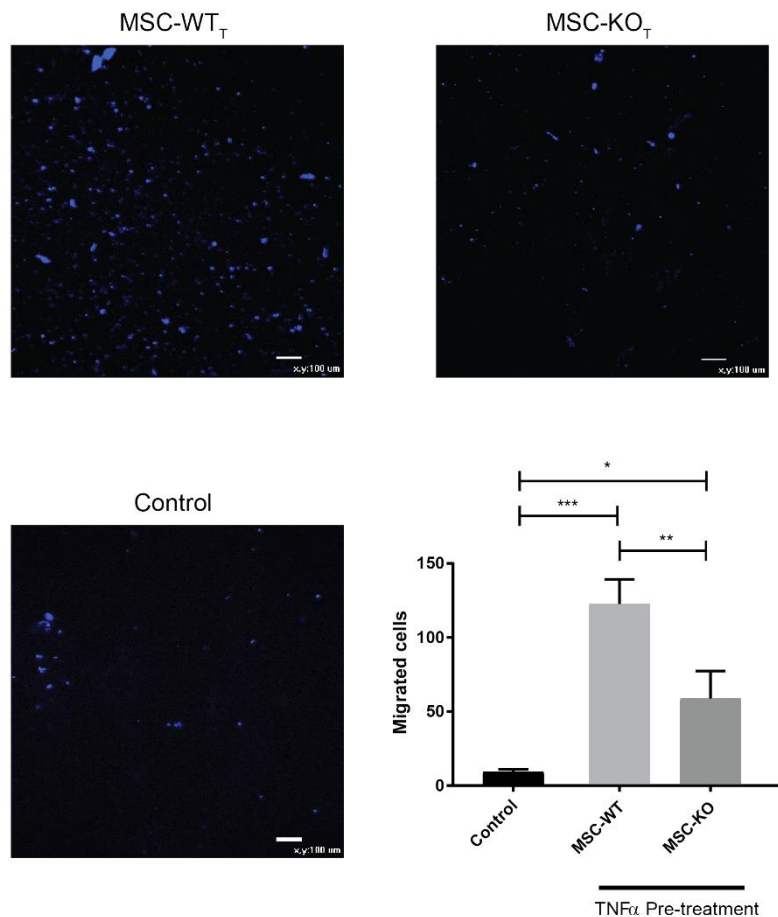
Figure 7.1 TNFα increased MSC derived CCL-2 secretion in a dose dependent manner
*A) Cells culture supernatants collected from MSC-WT stimulated with increasing concentration of TNFα for 24h. Supernatants were assayed for CCL-2 using ELISA.TNFα stimulation of MSC-WT increased CCL-2 secretion in a dose dependent manner. (n=3, ns, not significant * p<0.05). B) Transwell migration assay demonstrated reduced macrophage migration (stained blue with Hoescht live stain) towards MSC-KO compared to MSC-WT (n=3, * p<0.05, ** p<0.01, *** p<0.001).*

Figure 7.2

A)
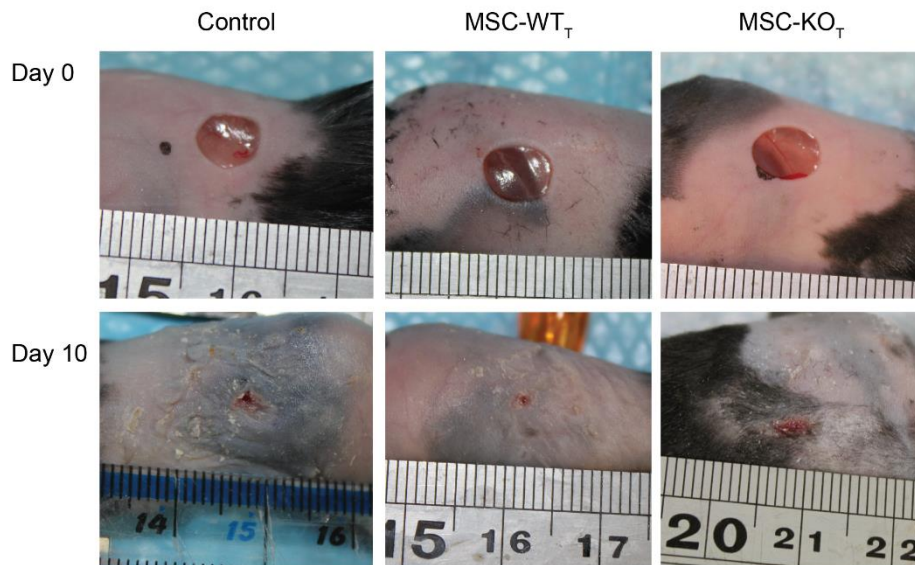
B)
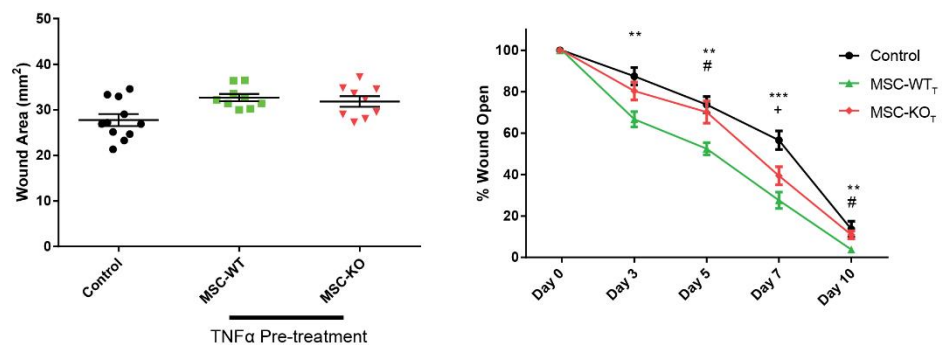
Figure 7.2 CCL-2 deficient MSC responded to TNFα pre-treatment

*A) Images of mouse excisional wounds at d-0 and at d-10. Two 5 mm punch wounds were created on the dorsum of each mouse. **B) Left -** Wound area was quantified at d-0, no significant differences were observed between the groups. **B) Right -** Time course of wound closure from image analysis demonstrated accelerated wound closure in MSC-WT$_T$ treated wounds. This was statistically different from controls at all time points. MSC-KO$_T$ had reduced efficacy and were only statistically different from control treated wounds on day 7. (n≥8, * = MSC vs Control, + = MSC-KO vs Control, # = MSC vs MSC-KO ns not significant, ** p<0.01, *** p<0.001, # p<0.05, + p<0.05).*

Figure 7.3

A)

B)
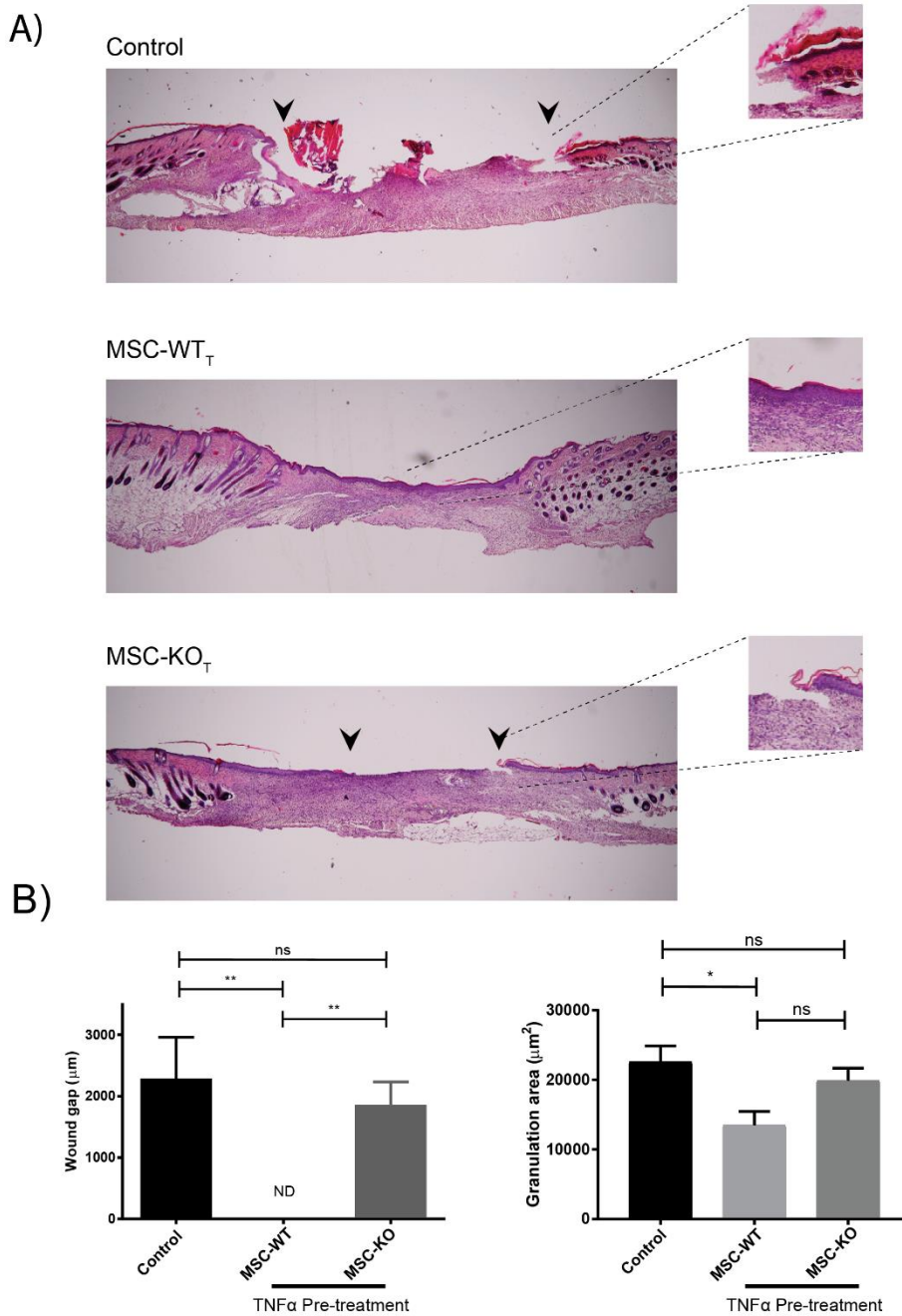
Figure 7.3 MSC-WT$_T$ enhanced re-epithelialisation

*A) Histological samples taken at d-10 were stained with H&E. Black arrows indicate migrating front of keratinocytes, insets show magnified image of migrating front. Images taken at 4x, Scale bar, 100 μm. B) Left - By d-10 MSC-WT$_T$ Treated wounds were all completely re-epithelialised, no statistical differences were observed between MSC-KO$_T$ and control groups (n≥8, ns, not significant, ** p<0.01). Granulation area was only significantly decreased in MSC-WT$_T$ treated wounds, suggestive of a reduced inflammatory response and increased wound maturity (n≥8, ns, not significant * p<0.05).*

Figure 7.4

A)

B)
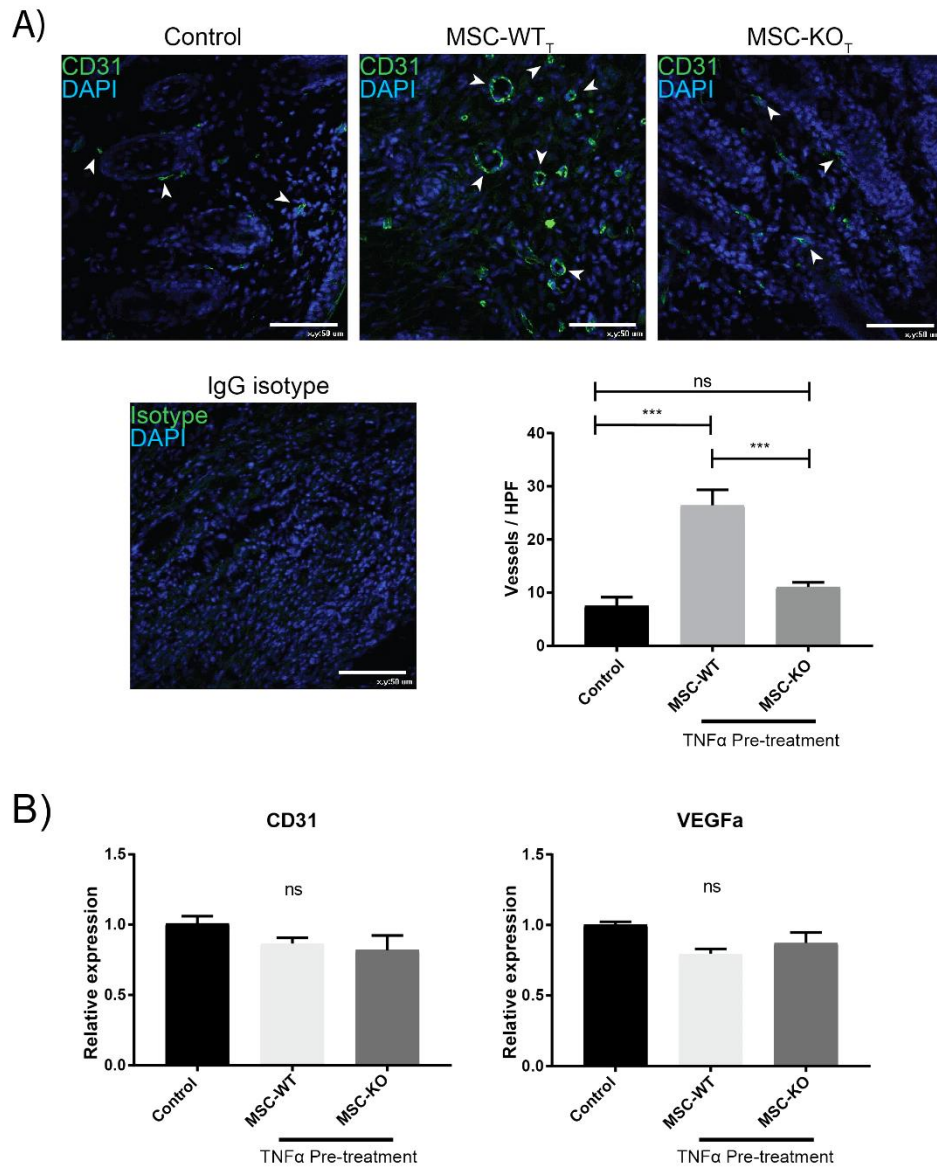
Figure 7.4 MSC derived CCL-2 was required for angiogenic effect

A) Representative images of wound sections d-10 post wounding, stained for CD31 (green) and nuclei counter stained with DAPI (blue) scale bar, 50 µm. Vessels per high power field were quantified within the wound bed (intact vessel lumens highlighted with arrowheads) and show statistically significantly increased vessel density in MSC-WT$_T$ treated wounds compared to control and MSC-KO$_T$ treated wounds (n≥8, ns, not significant, *** p<0.001). B) No statistically significant differences of CD31 or VEGFa expression were detected by analysis qRT-PCR of tissue samples from each group. (n≥5 ns, not significant).

Figure 7.5
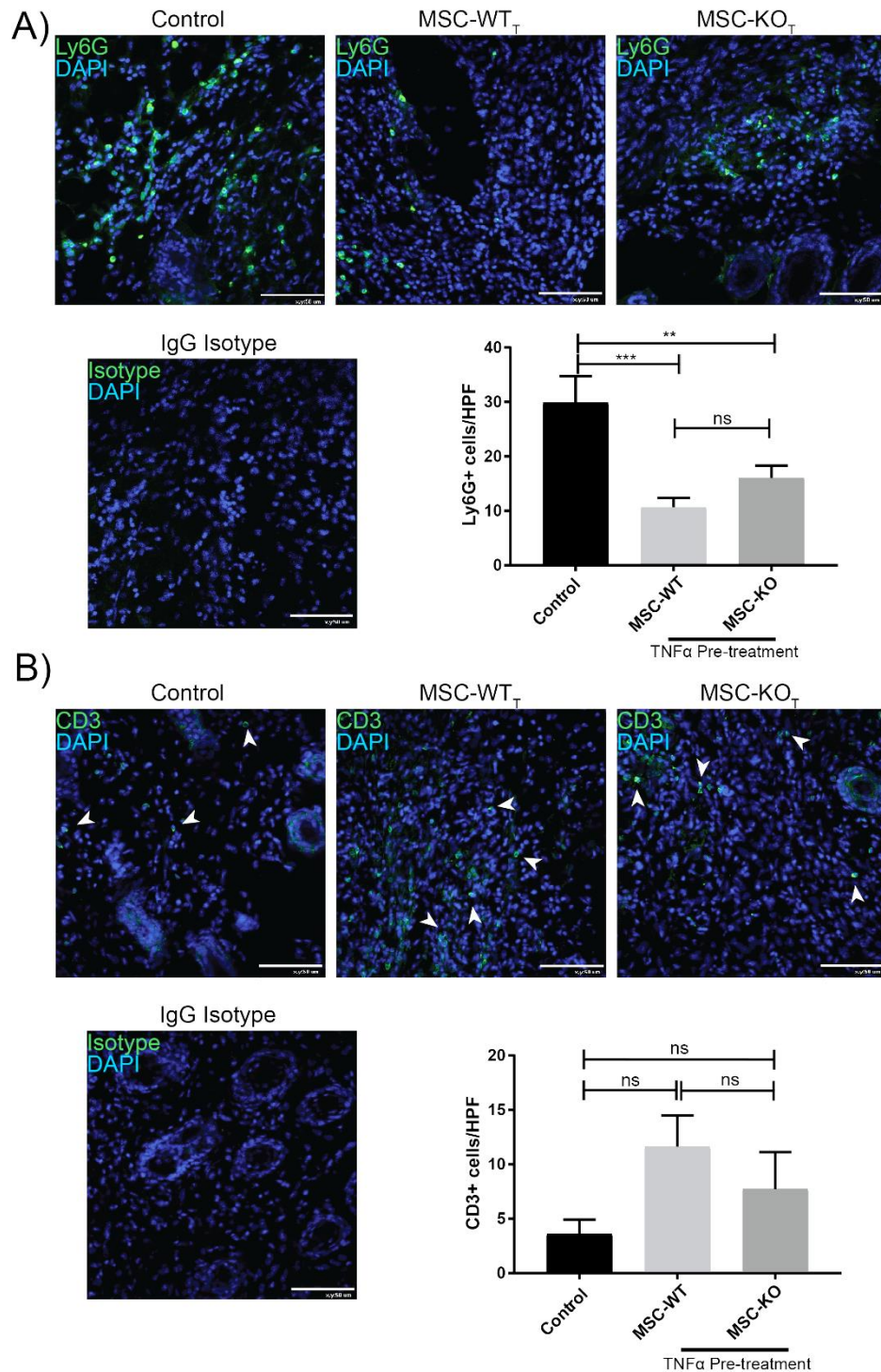
Figure 7.5 Neutrophil invasion was attenuated by both MSC-WT$_T$ and MSC-KO$_T$ treatment
A) *Representative images of wound sections d-10 post wounding, stained for neutrophil marker Ly6G (green), cell nuclei were counter stained with DAPI (blue) scale bar, 50 μm. Reductions in neutrophil numbers were observed in MSC-WT$_T$ and MSC-KO$_T$ compared to control groups (n>8, ** p<0.01, *** p<0.001). **B)** Representative images of wound sections d-10 post wounding, stained for T-cell marker CD3 (green, indicated with arrowheads for clarity), cell nuclei were counter stained with DAPI (blue), no significant difference was observed between any of the groups. Scale bar, 50 μm (n>8, ns, not significant).*

Figure 7.6
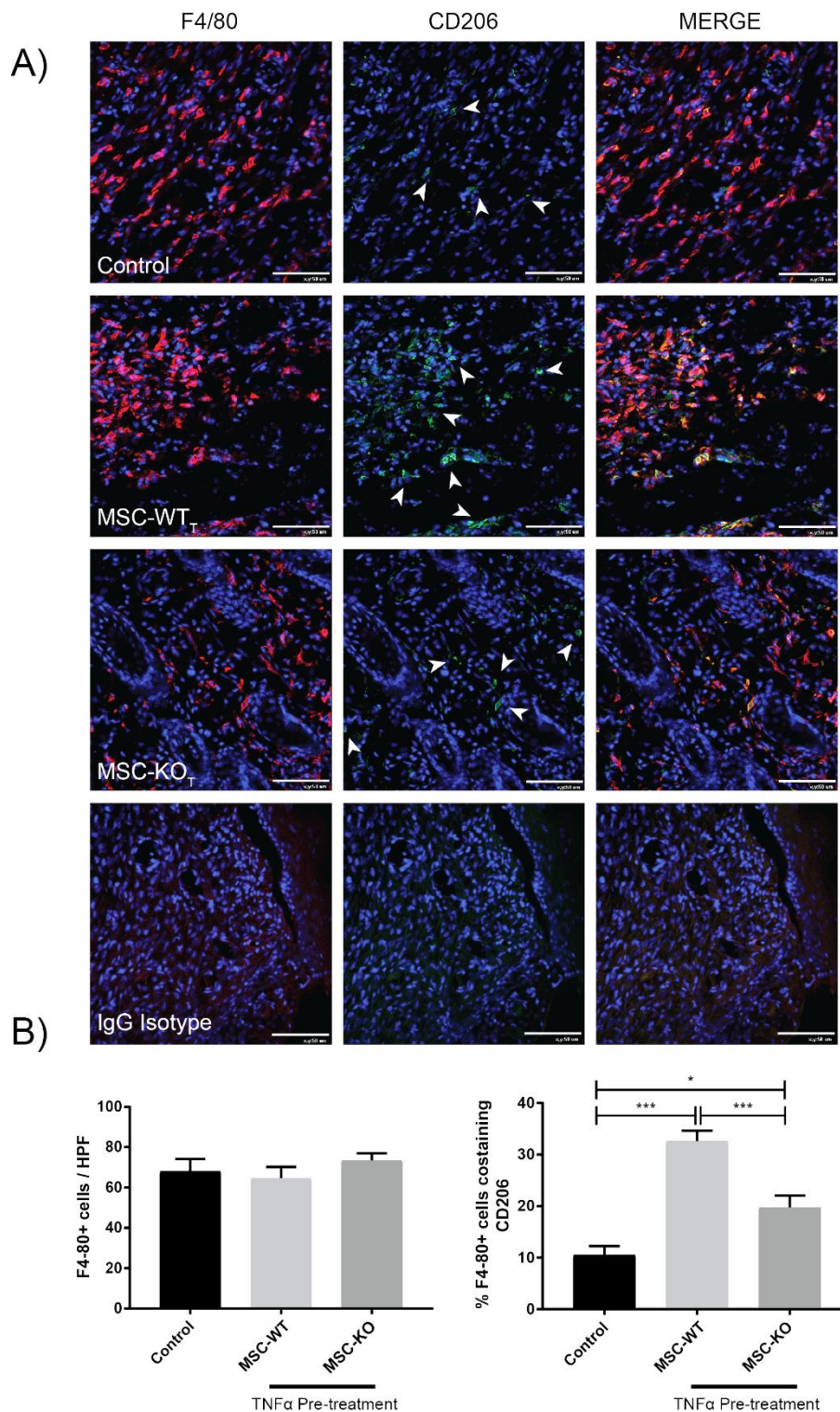
Figure 7.6 Both MSC$_T$ and MSC-KO$_T$ increased CD206+ macrophages within the wound
A) *Wound sections at d-10 post wounding stained for pan macrophage marker F4/80 (red) and M2 marker CD206 (green, indicated with arrow heads for clarity), cell nuclei were counter stained with DAPI (blue) scale bar, 50 µm.* **B) Left -** *Total macrophage quantification within the wound, no difference was observed between any of the groups* **B) Right -** *Percentage macrophages co-expressing CD206, significantly increased in MSC-WT$_T$ treated wounds compared to control and MSC-KO$_T$ treated groups (n≥8, * p<0.05, *** p<0.001).*

Figure 7.7
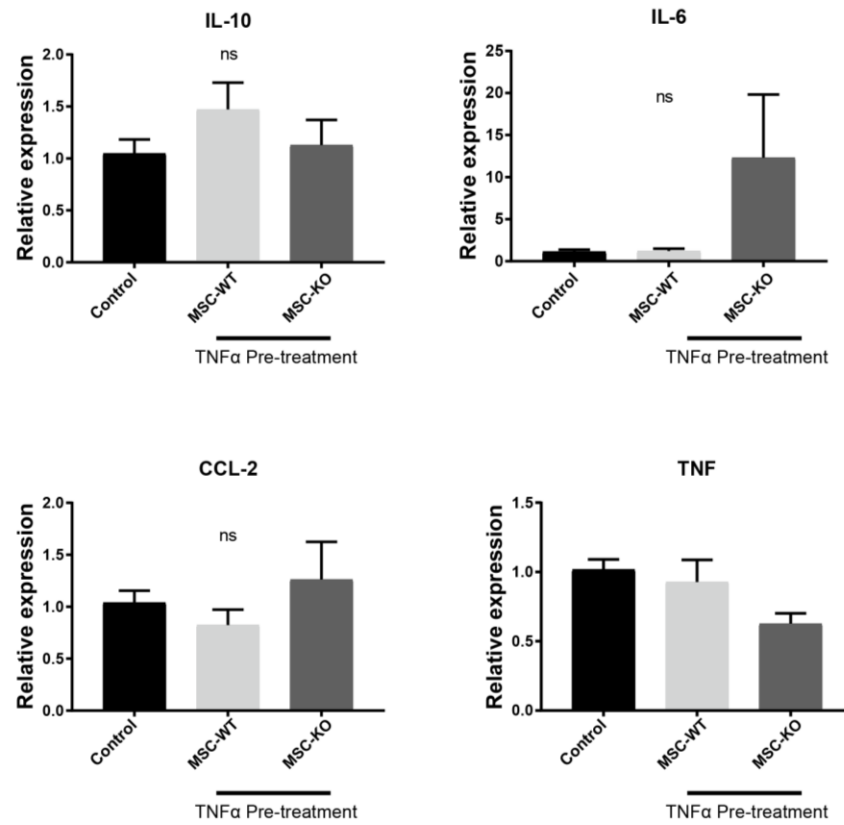
Figure 7.7 Neither MSC$_T$ and MSC-KO$_T$ altered wound expression of selected cytokines
qRT-PCR analysis of d-10 wound samples containing both wound and healed wound margin. No statistically significant differences were observed in any of the groups for either IL-10 IL-6, CCL-2 or TNFα (n=5, ns, not significant).

7.4.   Discussion

In this study, TNFα was used to pre-treat MSC prior to application in a mouse excisional wound model. This study was conducted to ascertain if TNFα pre-treatment was effective in improving MSC efficacy (as seen in pig burn model) and also to determine if CCL-2 was involved in this response.

A range of concentrations (10-50 ng/ml) of TNFα have been used to pre-treat MSC as reported in the literature [72, 79, 230]. In the pig model a concentration of 10 ng/ml was selected as it was the only practical concentration when stimulating large amounts of cells. The hypothesis was that TNFα was inducing CCL-2 secretion and that this may further enhance macrophage recruitment. Therefore, experiments were conducted to evaluate CCL-2 secretion in response to TNFα pre-treatment. A range of concentrations from 5-50 ng/ml were assessed. CCL-2 was found to be maximally secreted when stimulated with 50 ng/ml TNFα and induced significantly more macrophage migration compared to unstimulated MSC as presented in chapter 6. A significantly reduced migratory response was observed with MSC-KO$_T$.

Results from this study demonstrated that TNF pre-treatment of MSC significantly enhanced re-epithelialisation of wounds. By d-10, all wounds had completely re-epithelialised, as compared to findings from chapter 6. Wound closure, as measured by macroscopic image analysis, was also accelerated. Taken together these data are in broad agreement with several other studies, including results presented in chapter 5, that reported increased MSC efficacy when pre-treated with TNFα [75, 80, 229].

TNFα pre-treatment of CCL-2 deficient MSC was also found to induce an increased therapeutic response. While still largely inferior to WT MSC, a statistically significant increase compared to control was observed in wound closure on d-7. This suggests the benefits observed from TNFα pre-treatment my not be entirely dependent on CCL-2; however, CCL-2 deficiency still greatly attenuates the therapeutic response. These results are in agreement with previous published studies that suggest TNFα stimulates MSC to secrete a wide variety of factors not limited to CCL-2 [79, 236, 286].

Interestingly, no significant increase in angiogenic response was observed in wounds treated with MSC-WT$_T$. TNFα is known to stimulate MSC to secrete VEGF and CCL-2, both potent inducers of angiogenesis [132, 236]. Nevertheless, no increase in CD31 vessel density was observed in either MSC-WT$_T$ or MSC-KO$_T$. Studies using MSC CM generated from TNFα pre-treatment demonstrate increased angiogenesis and limb salvage in an ischemic limb model (MSC CM was generated by stimulating AD-MSC with TNFα (10ng/ml) for 48h) [75]. CM was injected (IM) three times a week for four weeks which resulted in increased blood flow with TNF MSC CM treatment and increased αSMA+ vessel density [75]. Blockade of either IL-6 or IL-8 significantly reduced vessel density and Doppler measured blood flow [75]. In a similar study the same investigators TNFα MSC CM significantly increased vessel density in cutaneous wounds compared to normal MSC CM [80]. Blockade of either IL-6 or IL-8 or both significantly reduced vessel densities [80]. Besides IL-6 and IL-8, TNFα stimulation of MSC increased several other angiogenic factors including CCL-2

[132]. In vitro TNFα pre-treatment (50 ng/ml) also increased VEGF secretion two-fold, suggesting that these pre-treated cells should be more angiogenic.

Expression of IL-6 was assessed in the wound samples at d-10 however no significant difference was observed. The results demonstrate expression of IL-6 across the entire wound including wound margin and does not reflect IL-6 expression of applied MSC which may be greater. The role of MSC-WT$_T$ induced IL-6/IL-8 was not addressed in this study but it may act to support the functions of CCL-2, primarily through recruiting macrophages and inhibiting TNFα through induction of TNFα antagonists [287].

CD3, a pan T-cell marker, was used to identify alterations in these populations as a result of MSC-WT$_T$ treatment. A small increase was observed in MSC-WT$_T$ but this was not statistically significant compared to control treated wounds. The time point of d-10 may be relevant here and it is not possible to rule out differences in these populations at earlier time points. In a previous study by English et al, TNFα pre-treated MSC were more effective in reducing alloantigen driven proliferation of splenocytes cells, this was driven primarily through increased PGE2 secretion from stimulated MSC [79]. To what extent MSC alter T-lymphocyte response within the wound is not known and deserves further analysis. However, within cutaneous wounds it is the innate immune system, particularly macrophages that orchestrate the progression of wound healing, so T-cell modulation may not be so impactful [138].

Analysis of macrophage populations within the wound indicate no significant difference between TNFα pre-treatment groups. Interestingly, there was a trend

towards increased F4/80+ macrophages within the wound at d-10 in MSC-KO$_T$ group. Most significantly however, was the percentage of CD206 macrophages in the MSC-KO$_T$ group. Compared to results presented in chapter 6, TNF pre-treatment significantly increased CD206+ macrophages compared to untreated MSC-KO. This increased M2 polarisation is occurred in a CCL-2 independent fashion, possibly through IL-6. Application of TNFα MSC CM in a cutaneous wound model also showed increased recruitment of CD68+ macrophages, which peaked at d-6, compared to control and MSC CM and was found to be IL-6 dependent [80]. IL-6 acts similarly to CCL-2, is a potent recruiter of macrophages, and can reduce TNFα through induced secretion of TNFα antagonists [287]. Therefore, it is plausible that increased MSC-KO$_T$ efficacy may be occurring through IL-6 mechanisms, similarly to previous results reported by Heo et al [80].

Treatment of wounds with MSC-WT$_T$ significantly reduced neutrophil infiltration on d-10 compared to control. Contrasting results from chapter 6, this effect indicates no significant difference between MSC and MSC$_T$ treated wounds and may have plateaued in the current experimental setting. Interestingly, application of MSC-KO$_T$ reduced Ly6G + cells present in the wounds, with statistical analysis indicating a significant difference between MSC-KO$_T$ and control. This taken together with increased wound closure on d-7 and significantly increased M2 macrophage population suggest CCL-2 independent factors reduced the inflammatory environment induced by TNFα pre-treatment. The most likely candidate responsible for CCL-2 independent effect is IL-6 which may be functioning in a similar manner to CCL-2. It is merely speculative, but IL-6 may be a redundant pathway for CCL-2 which is activated when cells are

exposed to highly inflammatory environment (such as TNFα at 50 ng/ml). It is also plausible that a lower inflammatory stimulus such as at (10 ng/ml as used in porcine study) may only initiate CCL-2 pathways. These are both interesting hypotheses that could be explored in future studies.

Increased re-epithelialisation was demonstrated in MSC-WT_T treated wounds, however this was not accounted for by any detected increase in angiogenic response or reduced inflammatory response. Similarly, no difference in granulation tissue area was observed between MSC-WT and MSC-WT_T treated wounds. Here again, IL-6 may be a possible candidate cytokine, while no direct evidence of this was obtained, previous in vitro studies have established that IL-6 induces keratinocyte migration through a fibroblast derived factor [288]. Similarly, wounds treated with TNFα stimulated MSC CM had increased wound closure and re-epithelialisation compared to normal MSC CM. Moreover, depletion of MSC CM with IL-6 antibodies attenuated this effect [80]. If IL-6 is a potent stimulator of keratinocyte migration through fibroblast activation, why then was there no increase in re-epithelisation observed in MSC-KO_T treated wounds? One possible explanation is that as seen in chapter 6, MSC derived CCL-2 is required for increased angiogenesis and increased resolution of inflammatory response. This increased M2 response is associated with fibroblast proliferation and the formation of granulation tissue and thereby, increased substrate for keratinocytes to migrate on.

A limitation of this study is that the inflammatory changes described herein are not well captured at d-10, and may be somewhat normalised at that stage. M1 to

M2 transitions occur around d-5 post wounding and future studies including these time points may be required to better capture this response.

Previous studies have demonstrated that TNFα stimulation of MSC increases expression of ICAM-1 and VCAM-1, which are adhesion molecules that allow MSC to interact with endothelial cells that line the vasculature and to home to sites of tissue damage. TNFα pre-treatment of MSC may also increase engraftment of MSC, possibly through this mechanism allowing the cells to remain within the wound for a greater period of time and therefore extend the therapeutic window.

This work affirms TNFα pre-treatment is beneficial for excisional wound healing in the mouse and is a simple and effective way to enhance efficacy of MSC therapy. It also has advantages over genetic modification of MSC, in that less processing and manipulation is required and it removes the requirement for viral vectors. This work also demonstrates that while beneficial effect of TNFα pre-treatment is not CCL-2 dependent, CCL-2 is required for proper function of MSC therapy, and lack of CCL-2 severely attenuates the therapeutic response. Fundamental understanding of how these interactions work will allow us to engineer better therapeutics into the future.

8. General Discussion

8.1.   Summary of work

The work outlined in the preceding chapters contributes significantly to the understanding of MSC derived CCL-2 in accelerated wound healing. In chapter 6, it was established that CCL-2 was required for MSC therapeutic benefit in excisional wound healing. Results showed that CCL-2 deficiency inhibited macrophage recruitment and may affect downstream local interactions, reducing MSC efficiency in repolarising macrophages towards an M2 phenotype.

This feature of M2 polarisation is a hallmark of MSC therapy in cutaneous wound healing and CCL-2 was first suggested to be implicated in this process by Chen et al who noted MSC secrete significant amounts of CCL-2 [58]. However, the functional significance of these observations has not been addressed until now.

Several elegant studies have elucidated the mechanism by which MSC exert an immunomodulatory effect and induce M2 polarisation [85, 96, 255]. This consists of several factors including PGE2, TSG-6 and IDO among others [85, 96, 102]. Activated inflammatory macrophages express TNFα which induces the expression of TSG-6, this binds to CD44 and activates NF-κB downstream signalling in macrophages to reduce TNFα secretion [105]. Concurrently, TNFα also induces COX-2 in MSC which is metabolised to PGE2 [85]. This binds to EP2

receptors on macrophages activating NF-κB and also downstream cAMP pathways, reducing TNFα and promoting expression of IL-10 [289]. Macrophages also secrete other factors that are involved in this crosstalk such as IL-1 and IFNγ [98]. Additionally, IDO induced in human MSC by IFNγ stimulates the catabolism of tryptophan to Kynurenic acid which has also been shown to inhibit LPS stimulated TNFα secretion [98, 290].

Proximity is vital in these interactions in that studies have shown that immunomodulatory factors like PGE2 and Gal-1 function locally [88, 96, 291](unlike TSG-6 which can act more systemically [235]) and in vitro modulation of both T-cell and macrophage inflammatory responses require cell-cell contact as opposed to transwell co-culture [88, 96, 255]. Further evidence of this local interaction is provided by immunostaining of wounds treated with MSC, which confirms co-localisation of MSC with CD11b+ macrophages and this co-localisation is concomitant with increased expression of CD206 and Arginase-1 (an enzyme associated with M2 phenotype) within the wound [20]. Moreover, other studies have observed these MSC/immune cell aggregates in a mouse model of colitis [292].

At the centre of this interaction is CCL-2. In this study, we show that CCL-2 deficient MSC are unable to increase wound closure and this is associated with reduced CD206+ macrophages and increased neutrophils present in the wound, indicative of ongoing inflammatory response. Crucially, in chapter 6 we established that CCL-2 deficient MSC are not as efficient in inhibiting TNFα from LPS stimulated macrophages as WT MSC, under in vitro co-cultures. These data support the hypothesis that CCL-2 acts locally, facilitating close cell contact

allowing for crosstalk between MSC and macrophages and subsequent repolarisation.

CCL-2 may also play a role in other aspects of this MSC/macrophage interaction. For example, recent studies have emerged describing some novel mechanisms for MSC mediated macrophage polarisation. MSC do not reside in great numbers in the wound for long (less than a week [61, 293]), yet still have a therapeutic effect [61, 149]. One mechanism may be a consequence of phagocytosis; macrophages that phagocytosed MSC expressed higher levels of IL-10 and TGF-β and had reduced levels of IL-6 compared to macrophages that did not phagocytose any MSC [294]. Liu et al, have also demonstrated that MSC secrete greater amounts of TSG-6 when undergoing apoptosis [295], so it is possible that phagocytosing macrophages may subsequently come in contact with TSG-6 which could account for the increased M2 polarisation. Phinney et al describe a novel process of mitophagy whereby the mitochondria of stressed MSC are shuttled across cell membrane and taken up by macrophages; simultaneously MSC secrete exosomes containing PGE2 which inhibit activation of macrophages [296]. It is conceivable that CCL-2 could also be facilitating these interactions. However, it is not known how pervasive these newly described mechanisms are and whether they extend to CCL-2.

CCL-2 may also benefit macrophage polarisation through other downstream mediators. The MCP-1 induced protein (MCPIP), was first found to be highly expressed after exposure to CCL-2 (then under the MCP-1 nomenclature), and recent studies have demonstrated that MCPIP is required for IL-4 induced M2 polarisation in vitro and genetically modified macrophages overexpressing

MCPIP display several M2 markers and have reduced TNFα levels when delivered in a peritoneal inflammatory model [297]. MCPIP mediated its action through inhibition of NF-κB and sequential induction of ROS production, ER stress and increased autophagy [297]. MSC derived CCL-2 may therefore act as a negative feedback loop, during its interactions. For instance, MSC are stimulated by inflammatory macrophages secreting TNFα, this induces CCL-2 (as demonstrated in chapter 5), among others, which is in turn secreted by MSC and subsequently binds to CCR-2 on inflammatory macrophages thus inducing the expression of MCPIP [274]. MCPIP may supress TNFα through NF-κB inhibition [297], dampening the inflammatory response. Induced MCPIP may also account for increased angiogenesis in this interaction [275].

MSC derived CCL-2 not only influences the innate immune system, but may be a key mediator in MSC therapy, involved in all aspects of MSC interactions with immune cells [276, 298]. BM MSC lacking the ligand FasL, have a reduced ability to lower number of CD3+ T-cells or induce apoptosis and also fail to elevate Foxp3 reg T-cells as normal MSC do [86]. Subsequent investigation established that these cells did not secrete CCL-2, although it was abundant in the cytoplasm. Interestingly, overexpression of Fas restored cytokine secretion, suggesting that Fas has an essential role in CCL-2 secretion. Correspondingly, MSC isolated from CCL-2 knockout mice were defective in reducing the number of CD3+ T-cells. Other studies have confirmed that in a two way mixed lymphocyte reaction, CCL-2 depletion of CM reduced MSC ability to modulate IFN-γ while both CCL-2 and MMP activity were required to dampen IL17 response in stimulated splenocytes [299].

MSC derived CCL-2 is also influential in modulating B-cell responses. MSC isolated from BM of Lupus (a systemic disease involving dysfunction of T-cell and polyclonal B cell activation) like mice have reduced CCL-2 expression and secretion [298]. When lupus MSC were applied to normal B cells, they were defective in reducing proliferation compared to normal MSC and treatment of normal MSC with anti-CCL-2 abrogated this effect. Treatment of B-cells with recombinant CCL-2 had little effect on proliferation; only proteolytic processing of CCL-2 by MMP-1 was able to recapitulate the MSC effect [298].

MSC CM also inhibits CD4+ T-cell activation through proteolytic processing of CCL-2 [299]. MSC driven matrix metalloproteinase processing of CCL-2 cleaves four N terminal amino acids to form an antagonist derivative. Administration of CCL-2 -/- knockout MSC were unable to reduce CD4+ T-cell infiltration into central nervous system and subsequent demyelination compared to wild type MSC [299].

Taken together, the work presented here and from previous studies demonstrates that CCL-2 is a central mediator in the interaction of MSC with various cells of both the innate and adaptive immune system. Dysfunction of MSC derived CCL-2 has profound effects on the efficacy of MSC therapy and may be something to consider in terms of characterisation of MSC for therapeutic use.

8.2. Aspects of MSC therapy in wound healing mimics biological processes in tumour growth

The parallels between wound healing and tumorigenesis have long been recognised [300]. In a seminal paper, Dvorak describes the striking similarities between the formulation of granulation tissue within the cutaneous wound and the development of tumour stroma, both consisting of a highly vascularised matrix of proliferative fibroblast cells intermixed with various immune cells [301]. Parallels in mechanism can also be drawn between the application of MSC therapy in cutaneous wounds and the development of tumour stroma [300, 301]. Several studies have described a mechanism whereby MSC recruit macrophages to the tumour site through CCL-2 [132, 133]. This interaction between MSC and macrophages induces an M2 type phenotype associated with immunosuppression [133] and angiogenesis [239], both of which support tumour growth in a CCL-2 dependent fashion [132]. Correspondingly, application of MSC into a cutaneous wound promotes the formation of granulation tissue through these same mechanisms of angiogenesis and immune suppression. This mechanism in tumorigenesis appears to mirror the mechanism of action of MSC therapy in cutaneous wounds and supports the findings of the work presented here. It should be noted that while the mechanisms appear similar and is something further insights can be garnered from, the author is not suggesting that application of MSC may induce tumour formation and to the best of the author's knowledge this has never been reported.

8.3.   TNFα pre-treatment of MSC

Another hallmark of cancer is a chronic inflammatory environment. Tumours secrete significant amounts of TNFα, and this further promotes the cycle as described above. Tumour associated MSC are more immunosuppressive and secrete greater amounts of CCL-2 [133]. Stimulation of normal BM-MSC with TNFα mimicked this effect [132]. As observed in the results presented here, TNFα pre-treated MSC significantly increased efficacy. However, this was shown to mostly occur in a CCL-2 independent fashion. Other candidates include IL-6, shown to enhance wound healing in TNF pre-treated MSC CM [80], which may act synergistically with CCL-2. In fact, a close association was established for these two cytokines. Stimulation monocytes with either IL-6 or CCL-2 was found to induce the other cytokine [262]. CCL-2 induced a four-fold expression of IL-6 in CD11b human monocytes. This was associated with increased phagocytic activity and increased expression of CD206, markers of M2 phenotype [262, 282].

In this work, TNFα pre-treatment enhanced the efficacy of MSC therapy in both animal models. In vitro studies demonstrate increased immunosuppressive properties when pre-treated with TNFα [79]. Recent findings suggest that stimulation of MSC with inflammatory cytokines may also reduce heterogeneity [302]. In a study by Szabo et al, they generated mouse BM-MSC clones and found that some clones displayed marked heterogeneity in terms of in vitro differentiation capability and immunosuppressive capacity in a mouse model delayed type hypersensitivity, this observed heterogeneity is a major impediment in the field of MSC research [303]. MSC were pre-treated with IFNγ (100 ng/ml) and TNFα (50 ng/ml) for 24 h which remarkably abolished

previously observed heterogeneity [302]. These recent findings need to be independently verified, but may be a promising avenue of research and hugely significant for the field as a whole, going forward. These findings could also account for some of the beneficial effects observed in inflammatory cytokine pre-treatment studies such as presented in chapters 5 and 7.

Pre-treatment of MSC with inflammatory cytokines such as TNFα may be an easy step to reduce heterogeneity and improve efficacy. Repeated TNFα stimulation can prolong and also increase secretion of CCL-2 and other immunomodulatory cytokines [132]. Allogenic AD-MSC are a readily available source of MSC that is amenable to further characterisation/enrichment (via section using a specific or expanded set of cell surface antigens) and pre-treatment with TNFα. Repeated TNFα stimulation is a process that could be easily incorporated into a manufacturing process, for an off the shelf allogenic cell therapy product.

8.4.   Future directions

MSC therapy holds much promise and research in this area has expanded immensely. Many lines of evidence now affirm that delivery of this therapy is safe. Several clinical trials and pre-clinical studies have shown promising results in certain pathologies. This work herein builds on the vast wealth of knowledge that has been gained and validates that AD-MSC are therapeutically equivalent to BM-MSC in a clinically relevant burn wound model. This will allow future studies to focus on optimising AD-MSC therapy. This work also demonstrates that TNFα pre-treatment is an effective way to enhance efficacy of MSC therapy. The broad

mechanisms of MSC therapy have been established; however, greater understanding of these mechanisms will lead to further insights to improve the efficacy of this treatment. In this regard, this work establishes for the first time, a pivotal role of MSC derived CCL-2 in accelerated wound healing.

In this study AD-MSC were validated as being therapeutically equivalent to BM-MSC at both baseline and in response to stimulation with inflammatory cytokine TNFα. One of the primary advantages of AD-MSC is the amount of cells that can be isolated. Many grams of tissue can be harvested from which vast quantities of MSC can be isolated using simple digestion protocols. Now that this cell source has been validated as therapeutically equivalent, dose escalation studies should be performed using this established burn model. The dosage used in this study was based on a previous pilot study [149] and the work of Falanga et al [50], who used concentrations of 1×10^6 cells/cm^2 and reported beneficial results. However, it has not been established if an increased concentration of cells would lead to better wound healing outcomes. In MI studies high doses of MSC had a negative effect, becoming entrapped in the vasculature and forming thrombus [150]. Further in-depth studies are required in the pig model to determine the optimal dosage. The pig model is ideal for dosing studies as it is more readily translatable to humans due to its similar anatomical size and skin structure. Scaling up from concentrations used in rodents based on dosage/weight can be problematic and may not a reliable indicator of dosage [304]. What may be most beneficial is multiple dosing strategies. Again, there is little research in this area; however, findings from several studies, including studies from this lab [61, 149], suggest that MSC do not survive long within the wound, with few surviving beyond a

week. Multiple dosing every 2-3 d could significantly bolster viable MSC to improve wound healing and these are additional hypotheses that could be explored.

Stimulation of MSC with TNFα induces upregulation of adhesion molecules ICAM-1 and VCAM-1 and may facilitate retention of MSC within the wound [91, 229] and increase homing of MSC to ischemic tissues [230]. TNFα pre-treatment of MSC increased persistence of MSC in infarcted myocardium of mice and was associated with improved cardiac function [229]. TNFα pre-treatment may improve the persistence of MSC in burn wounds and may account for increased efficacy observed in chapter 5. Further studies are required to characterise the effect of TNFα pre-treatment on MSC persistence in wounds. Pre-labelling of MSC with stable florescent dyes that are made cell impermeable upon cellular uptake would allow for accurate tracking of MSC persistence within the wound, which may be correlated with improved wound healing.

In this work, a role for CCL-2 was established in a mouse model of excisional wound healing, it was also hypothesised that a similar mechanism may be at hand in the pig model. However, this has not been experimentally established and interpreting between the mouse and pig is challenging. Moreover, important differences exist between burn and excisional wounds [6]. Burn wounds induce increased vascular permeability and have a stronger and ongoing inflammatory reactions due to the presence of denatured proteins which must be removed through MMP degradation [6]. However, for practical reasons it was not possible to explore a possible CCL-2 mechanism in the pig. No genetically modified pigs are available and amount of reagents required to produce therapeutic doses of

porcine CCL-2 knockdown MSC is currently impractical. To validate our mouse model findings, future work could focus on the development of a pig burn model with smaller wounds, which would require reduced cell quantities. Further optimisation of transfection efficiency may also make this experiment more feasible. As AD-MSC have been shown to be therapeutically equivalent to BM-MSC, future work should primarily focus on this cell source.

The mechanism described in the mouse model involving CCL-2/MSC and macrophage interactions are not fully captured here and by d-10 these population dynamics may have peaked or may have been in decline. This study was designed to evaluate if CCL-2 deficiency affected MSC efficacy as measured by primary endpoints of wound closure and re-epithelisation. Our findings suggest a more in-depth exploration of macrophage populations within the wound at an earlier time point (perhaps d-5) would give greater insight into how MSC derived CCL-2 is functioning. Multi-colour flow cytometry is a powerful tool and could be used to identify several cell populations within the wound at multiple time points. Well established digestion, labelling and gating protocols are available to characterise these cells [242].

MCPIP is induced by CCL-2 and could be a downstream mediator of the beneficial effects of MSC derived CCL-2 in terms of both angiogenesis and immunomodulation [275, 297]. It would be interesting to see if MCPIP is being expressed in MSC/macrophage interactions, and if so, it may be in part responsible for M2 polarisation. Further studies may be of interest to elucidate this mechanism.

The model established in this thesis demonstrates that MSC derived CCL-2 is involved in the local recruitment of CCR2+ macrophages, facilitating cell contact (or close proximity) and thus allowing for the repolarisation of macrophages towards an M2 phenotype, through factors that have been well described in the literature [96]. This results in reduced inflammatory response and increased wound healing. Conversely, this model implies that MSC deficient for CCL-2 would have reduced ability to facilitate MSC/macrophage contact. If this is true, then one would expect to find a greater number of WT MSC in close proximity with macrophages during the early stages of administration (d2-4) compared to CCL-2 deficient MSC. This could be confirmed by labelling MSC with a stable non-transferable cell fluorescent dyes and immunostaining wound sections for pan macrophage marker, like F4/80. Quantification of co-localisation may provide further corroborative proof of this proposed model.

In this study, MSC were isolated from CCL-2 KO mice. These mice are normal in size and do not display any gross physical or behavioural abnormalities [139]. Thioglycollate induced peritonitis results in impaired recruitment of monocytes and macrophages to peritoneal cavity in these mice consistent with CCL-2 deficiency [139]. As demonstrated in Chapter 6, isolated cells were classified as MSC under ISCT guidelines. However, one cannot rule out entirely, the possibility that CCL-2 KO may result in the isolation of a specific or different subpopulation of BM-MSC. To fully control for this, recovery of CCL-2, may be considered. This would require lenti-viral over-expression of CCL-2 in MSC-KO and the in-vivo experiments to be repeated. However, one could argue that MSC are heterogeneous by their nature and variation will exist from isolation to isolation,

based on what cells randomly adhere to flasks, in addition to donor variation and clonal heterogeneity present, that was recently demonstrated [302].

This thesis contributes to the field by deepening our understanding of the mechanism of action of MSC therapy and establishes AD-MSC as an optimal source that can be enhanced through TNFα pre-treatment. One of the major issues facing the MSC field is the characterisation of MSC and the heterogeneity present in these populations. This has resulted in mixed and conflicting reports of therapeutic efficacy. Research is ongoing in an attempt to define specific cell surface antigens or expand immunophenotypic profiles associated with these cells. Similarly, others are attempting to characterise these cells based on predicators of efficacy. In a recent study by Lee et al they describe TSG-6 expression in human MSC as a predictor of efficacy in corneal repair [104]. Lee et al also found that TSG-6 expression was strongly correlated with increased immunomodulatory capacity and corneal repair but was negatively correlated with osteogenic potential. The expression of TSG-6 was found to vary widely between donors [104]. Comparatively, this thesis finds that CCL-2 is required for MSC therapeutic functioning and may also be a useful addition in building a profile of paracrine factors that are required for MSC therapeutic effect allowing for further characterisation of these cells.

TNFα pre-treatment has recently been shown to reduce heterogeneity of clonal MSC and this thesis also demonstrated increased efficacy in response to TNFα pre-treatment. MSC response to TNFα could also be used as a possible way to further characterise these cells for therapeutic use. Other attempts to develop standardised immunomodulatory or potency assays such as suppression T-cell

proliferation [305] or corneal inflammatory model [104] may also be beneficial to determine potency [104, 306]. The validation that AD-MSC is therapeutically equivalent in this work supports the generation of large banks of AD-MSC which could be further characterised and enriched (using methods outlined above). These batches could be sorted based on potency or blended to achieve homogenous populations and reduce batch to batch variations.

In conclusion, MSC therapy provides an easy way to deliver a cocktail of factors to the appropriate cells at the most auspicious time. The use of CM or exosomes is also beneficial and may be more amenable to an off the shelf product. However, MSC have the ability to home to specific sites of injury and respond to the changing microenvironment through interactions with various cells. These interactions are extremely complex, yet through ongoing research these complexities can be unravelled. Ultimately we would like to achieve a level of sophistication to be able to deliver the right sequence of factors to specific target cells during a defined period to modulate wound healing without the necessity of delivering allogenic cells. However, this is some way off and for the moment, MSC are the most promising tool to accomplish this.

References

1. Peck, M.D., *Epidemiology of burns throughout the world. Part I: Distribution and risk factors.* Burns, 2011. **37**(7): p. 1087-100.
2. Association, A.B., *National Burn Repository*. 2015.
3. Johnson, R.M. and R. Richard, *Partial-Thickness Burns: Identification and Management.* Advances in Skin & Wound Care, 2003. **16**(4): p. 178-187.
4. University, R. *ANATOMY AND PHYSIOLOGY*. 2016 [cited 2016 22-10-2016]; Figure of skin structure]. Available from: https://opentextbc.ca/anatomyandphysiology/chapter/5-1-layers-of-the-skin/.
5. Jackson, D.M., *THE DIAGNOSIS OF THE DEPTH OF BURNING.* British Journal of Surgery, 1953. **40**(164): p. 588-596.
6. Keck, M., et al., *Pathophysiology of burns.* Wiener Medizinische Wochenschrift, 2009. **159**(13-14): p. 327-336.
7. Rawlins, J.M., *Management of burns.* Surgery (Oxford), 2011. **29**(10): p. 523-528.
8. Arturson, G. and L. Rammer, *Endogenous inhibition of fibrinolysis in patients with severe burns.* Acta Chirurgica Scandinavica, 1974. **140**(3): p. 181-184.
9. Rockwell, W.B. and H.P. Ehrlich, *Fibrinolysis inhibition in human burn blister fluid.* Journal of Burn Care and Rehabilitation, 1990. **11**(1): p. 1-6.
10. Arturson, G., *Pathophysiology of the burn wound and pharmacological treatment. The Rudi Hermans Lecture, 1995.* Burns, 1996. **22**(4): p. 255-274.
11. Sterling, J., Heimbach, DM., Gibran NS., *Management of the Burn Wound.* ACS Surgery, 2010: p. 1-13.
12. Phillips, A., *Management of burns.* 2005.
13. Groeber, F., et al., *Skin tissue engineering - In vivo and in vitro applications.* Advanced Drug Delivery Reviews, 2011. **63**(4): p. 352-366.
14. Klar, A.S., et al., *Tissue-engineered dermo-epidermal skin grafts prevascularized with adipose-derived cells.* Biomaterials, 2014. **35**(19): p. 5065-5078.
15. Falanga, V. and M. Sabolinski, *A bilayered living skin construct (APLIGRAF®) accelerates complete closure of hard-to-heal venous ulcers.* Wound Repair and Regeneration, 1999. **7**(4): p. 201-207.
16. van der Veen, V.C., et al., *Biological background of dermal substitutes.* Burns, 2010. **36**(3): p. 305-321.
17. Lenihan, C., et al., *The effect of isolation and culture methods on epithelial stem cell populations and their progeny-toward an improved cell expansion protocol for clinical application.* Cytotherapy, 2014. **16**(12): p. 1750-9.
18. Jubin, K., et al., *A fully autologous co-culture system utilising non-irradiated autologous fibroblasts to support the expansion of human keratinocytes for clinical use.* Cytotechnology, 2011. **63**(6): p. 655-62.
19. Rheinwald, J.G. and H. Green, *Serial cultivation of strains of human epidermal keratinocytes: the formation of keratinizing colonies from single cells.* Cell, 1975. **6**(3): p. 331-43.
20. Zhang, Q.Z., et al., *Human gingiva-derived mesenchymal stem cells elicit polarization of m2 macrophages and enhance cutaneous wound healing.* Stem Cells, 2010. **28**(10): p. 1856-68.
21. Kode, J.A., et al., *Mesenchymal stem cells: immunobiology and role in immunomodulation and tissue regeneration.* Cytotherapy, 2009. **11**(4): p. 377-91.

22. Friedenstein, A.J., R.K. Chailakhjan, and K.S. Lalykina, *THE DEVELOPMENT OF FIBROBLAST COLONIES IN MONOLAYER CULTURES OF GUINEA-PIG BONE MARROW AND SPLEEN CELLS.* Cell Proliferation, 1970. **3**(4): p. 393-403.

23. Caplan, A.I., *Mesenchymal stem cells.* J Orthop Res, 1991. **9**(5): p. 641-50.

24. Owen, M. and A.J. Friedenstein, *Stromal stem cells: marrow-derived osteogenic precursors.* Ciba Found Symp, 1988. **136**: p. 42-60.

25. Zuk, P.A., et al., *Multilineage cells from human adipose tissue: implications for cell-based therapies.* Tissue Eng, 2001. **7**(2): p. 211-28.

26. Gronthos, S., et al., *Postnatal human dental pulp stem cells (DPSCs) in vitro and in vivo.* Proceedings of the National Academy of Sciences, 2000. **97**(25): p. 13625-13630.

27. Williams, J.T., et al., *Cells isolated from adult human skeletal muscle capable of differentiating into multiple mesodermal phenotypes.* Am Surg, 1999. **65**(1): p. 22-6.

28. Bianco, P., et al., *The meaning, the sense and the significance: translating the science of mesenchymal stem cells into medicine.* Nat Med, 2013. **19**(1): p. 35-42.

29. Isakson, M., et al., *Mesenchymal Stem Cells and Cutaneous Wound Healing: Current Evidence and Future Potential.* Stem Cells Int, 2015. **2015**: p. 831095.

30. Dominici, M., et al., *Minimal criteria for defining multipotent mesenchymal stromal cells. The International Society for Cellular Therapy position statement.* Cytotherapy, 2006. **8**(4): p. 315-317.

31. Mendez-Ferrer, S., et al., *Mesenchymal and haematopoietic stem cells form a unique bone marrow niche.* Nature, 2010. **466**(7308): p. 829-834.

32. Mizoguchi, T., et al., *Osterix marks distinct waves of primitive and definitive stromal progenitors during bone marrow development.* Dev Cell, 2014. **29**(3): p. 340-9.

33. Aslan, H., et al., *Osteogenic differentiation of noncultured immunoisolated bone marrow-derived CD105+ cells.* Stem Cells, 2006. **24**(7): p. 1728-37.

34. Jones, E.A., et al., *Isolation and characterization of bone marrow multipotential mesenchymal progenitor cells.* Arthritis Rheum, 2002. **46**(12): p. 3349-60.

35. Tormin, A., et al., *CD146 expression on primary nonhematopoietic bone marrow stem cells is correlated with in situ localization.* Blood, 2011. **117**(19): p. 5067-77.

36. Shi, C., et al., *Bone marrow mesenchymal stem and progenitor cells induce monocyte emigration in response to circulating toll-like receptor ligands.* Immunity, 2011. **34**(4): p. 590-601.

37. Park, D., et al., *Endogenous Bone Marrow MSCs Are Dynamic, Fate-Restricted Participants in Bone Maintenance and Regeneration.* Cell Stem Cell, 2012. **10**(3): p. 259-272.

38. Opalenik, S.R. and J.M. Davidson, *Fibroblast differentiation of bone marrow-derived cells during wound repair.* Faseb j, 2005. **19**(11): p. 1561-3.

39. Higashiyama, R., et al., *Differential contribution of dermal resident and bone marrow-derived cells to collagen production during wound healing and fibrogenesis in mice.* J Invest Dermatol, 2011. **131**(2): p. 529-36.

40. Dickhut, A., et al., *Mesenchymal stem cells obtained after bone marrow transplantation or peripheral blood stem cell transplantation originate from host tissue.* Ann Hematol, 2005. **84**(11): p. 722-7.

41. Barisic-Dujmovic, T., I. Boban, and S.H. Clark, *Fibroblasts/myofibroblasts that participate in cutaneous wound healing are not derived from circulating progenitor cells.* J Cell Physiol, 2010. **222**(3): p. 703-12.

42. Mansilla, E., et al., *Bloodstream cells phenotypically identical to human mesenchymal bone marrow stem cells circulate in large amounts under the influence of acute large skin damage: New evidence for their use in regenerative medicine.* Transplantation Proceedings, 2006. **38**(3): p. 967-969.

43. Hong, H.S., et al., *A new role of substance P as an injury-inducible messenger for mobilization of CD29(+) stromal-like cells.* Nat Med, 2009. **15**(4): p. 425-35.

44. ClincalTrial.Gov. *Completed clincial trials involving Mesenchymal stem cells*. 2016 [cited 2016 10-07-2016]; Available from: https://clinicaltrials.gov/ct2/results?term=mesenchymal+stem+cells&no_unk=Y.

45. Ren, G., et al., *Concise review: mesenchymal stem cells and translational medicine: emerging issues.* Stem Cells Transl Med, 2012. **1**(1): p. 51-8.

46. Kebriaei, P., et al., *Phase II Trial of ProchymalTM (Ex-Vivo Cultured Adult Human Mesenchymal Stem Cells) and Corticosteroids as Primary Treatment for Acute Graft-Vs-Host Disease (aGVHD).* ASH Annual Meeting Abstracts, 2006. **108**(11): p. 3231-.

47. Dash, N.R., et al., *Targeting nonhealing ulcers of lower extremity in human through autologous bone marrow-derived mesenchymal stem cells.* Rejuvenation Res, 2009. **12**(5): p. 359-66.

48. Rosset, P., F. Deschaseaux, and P. Layrolle, *Cell therapy for bone repair.* Orthop Traumatol Surg Res, 2014. **100**(1 Suppl): p. S107-12.

49. Chen, S., et al., *Intracoronary transplantation of autologous bone marrow mesenchymal stem cells for ischemic cardiomyopathy due to isolated chronic occluded left anterior descending artery.* J Invasive Cardiol, 2006. **18**(11): p. 552-6.

50. Falanga, V., et al., *Autologous bone marrow-derived cultured mesenchymal stem cells delivered in a fibrin spray accelerate healing in murine and human cutaneous wounds.* Tissue Eng, 2007. **13**(6): p. 1299-312.

51. Badiavas, E.V. and V. Falanga, *Treatment of chronic wounds with bone marrow-derived cells.* Arch Dermatol, 2003. **139**(4): p. 510-6.

52. Yoshikawa, T., et al., *Wound therapy by marrow mesenchymal cell transplantation.* Plastic and Reconstructive Surgery, 2008. **121**(3): p. 860-877.

53. Rasulov, M.F., et al., *First experience of the use bone marrow mesenchymal stem cells for the treatment of a patient with deep skin burns.* Bull Exp Biol Med, 2005. **139**(1): p. 141-4.

54. Bey, E., et al., *Emerging therapy for improving wound repair of severe radiation burns using local bone marrow-derived stem cell administrations.* Wound Repair and Regeneration, 2010. **18**(1): p. 50-58.

55. Sasaki, M., et al., *Mesenchymal stem cells are recruited into wounded skin and contribute to wound repair by transdifferentiation into multiple skin cell type.* Journal of Immunology, 2008. **180**(4): p. 2581-2587.

56. Wu, Y., et al., *Mesenchymal stem cells enhance wound healing through differentiation and angiogenesis.* Stem Cells, 2007. **25**(10): p. 2648-2659.

57. Nygren, J.M., et al., *Bone marrow-derived hematopoietic cells generate cardiomyocytes at a low frequency through cell fusion, but not transdifferentiation.* Nat Med, 2004. **10**(5): p. 494-501.

58. Chen, L., et al., *Paracrine factors of mesenchymal stem cells recruit macrophages and endothelial lineage cells and enhance wound healing.* PLoS One, 2008. **3**(4): p. e1886.

59. Schrepfer, S., et al., *Stem cell transplantation: the lung barrier.* Transplant Proc, 2007. **39**(2): p. 573-6.

60. Park, C.W., et al., *Cytokine Secretion Profiling of Human Mesenchymal Stem Cells by Antibody Array.* International Journal of Stem Cells, 2009. **2**(1): p. 59-68.

61. Chen, L., et al., *Analysis of allogenicity of mesenchymal stem cells in engraftment and wound healing in mice.* PLoS One, 2009. **4**(9): p. e7119.

62. Zangi, L., et al., *Direct Imaging of Immune Rejection and Memory Induction by Allogeneic Mesenchymal Stromal Cells.* STEM CELLS, 2009. **27**(11): p. 2865-2874.

63. Toma, C., et al., *Fate Of Culture-Expanded Mesenchymal Stem Cells in The Microvasculature: In Vivo Observations of Cell Kinetics.* Circulation research, 2009. **104**(3): p. 398-402.

64. Risau, W., *Mechanisms of angiogenesis.* Nature, 1997. **386**(6626): p. 671-4.

65. Kajiguchi, M., et al., *Safety and efficacy of autologous progenitor cell transplantation for therapeutic angiogenesis in patients with critical limb ischemia.* Circ J, 2007. **71**(2): p. 196-201.

66. Kim, S.W., et al., *Successful stem cell therapy using umbilical cord blood-derived multipotent stem cells for Buerger's disease and ischemic limb disease animal model.* Stem Cells, 2006. **24**(6): p. 1620-6.

67. Strauer, B.E., et al., *Repair of Infarcted Myocardium by Autologous Intracoronary Mononuclear Bone Marrow Cell Transplantation in Humans.* Circulation, 2002. **106**(15): p. 1913-1918.

68. Moon, M.H., et al., *Human adipose tissue-derived mesenchymal stem cells improve postnatal neovascularization in a mouse model of hindlimb ischemia.* Cell Physiol Biochem, 2006. **17**(5-6): p. 279-90.

69. Nagaya, N., et al., *Intravenous administration of mesenchymal stem cells improves cardiac function in rats with acute myocardial infarction through angiogenesis and myogenesis.* Am J Physiol Heart Circ Physiol, 2004. **287**(6): p. H2670-6.

70. Zacharek, A., et al., *Angiopoietin1/Tie2 and VEGF/Flk1 induced by MSC treatment amplifies angiogenesis and vascular stabilization after stroke.* Journal of Cerebral Blood Flow and Metabolism, 2007. **27**(10): p. 1684-1691.

71. Lin, R.Z., et al., *Equal modulation of endothelial cell function by four distinct tissue-specific mesenchymal stem cells.* Angiogenesis, 2012. **15**(3): p. 443-55.

72. Crisostomo, P.R., et al., *Human mesenchymal stem cells stimulated by TNF-α, LPS, or hypoxia produce growth factors by an NFκB- but not JNK-dependent mechanism*. Vol. 294. 2008. C675-C682.

73. Zhang, B., et al., *Co-culture of mesenchymal stem cells with umbilical vein endothelial cells under hypoxic condition.* J Huazhong Univ Sci Technolog Med Sci, 2012. **32**(2): p. 173-80.

74. Boomsma, R.A. and D.L. Geenen, *Mesenchymal stem cells secrete multiple cytokines that promote angiogenesis and have contrasting effects on chemotaxis and apoptosis.* PLoS One, 2012. **7**(4): p. e35685.

75. Kwon, Y.W., et al., *Tumor necrosis factor-α-activated mesenchymal stem cells promote endothelial progenitor cell homing and angiogenesis.* Biochimica et Biophysica Acta (BBA) - Molecular Basis of Disease, 2013. **1832**(12): p. 2136-2144.

76. Carrion, B., et al., *Bone marrow-derived mesenchymal stem cells enhance angiogenesis via their α6β1 integrin receptor.* Experimental Cell Research, 2013. **319**(19): p. 2964-2976.

77. Chang, Y.S., et al., *Critical Role of Vascular Endothelial Growth Factor Secreted by Mesenchymal Stem Cells in Hyperoxic Lung Injury.* American Journal of Respiratory Cell and Molecular Biology, 2014. **51**(3): p. 391-399.

78. Tögel, F., et al., *VEGF is a mediator of the renoprotective effects of multipotent marrow stromal cells in acute kidney injury.* Journal of Cellular and Molecular Medicine, 2009. **13**(8b): p. 2109-2114.

79. English, K., et al., *IFN-γ and TNF-α differentially regulate immunomodulation by murine mesenchymal stem cells.* Immunology Letters, 2007. **110**(2): p. 91-100.

80. Heo, S.C., et al., *Tumor necrosis factor-α-activated human adipose tissue-derived mesenchymal stem cells accelerate cutaneous wound healing through paracrine mechanisms.* Journal of Investigative Dermatology, 2011. **131**(7): p. 1559-1567.

81. Di Nicola, M., et al., *Human bone marrow stromal cells suppress T-lymphocyte proliferation induced by cellular or nonspecific mitogenic stimuli.* Blood, 2002. **99**(10): p. 3838-43.

82. Bernardo, Maria E. and Willem E. Fibbe, *Mesenchymal Stromal Cells: Sensors and Switchers of Inflammation.* Cell Stem Cell. **13**(4): p. 392-402.

83. Najar, M., et al., *Mesenchymal stromal cells use PGE2 to modulate activation and proliferation of lymphocyte subsets: Combined comparison of adipose tissue, Wharton's Jelly and bone marrow sources.* Cell Immunol, 2010. **264**(2): p. 171-9.

84. Li, W., et al., *Mesenchymal stem cells: a double-edged sword in regulating immune responses.* Cell Death Differ, 2012. **19**(9): p. 1505-13.

85. English, K., *Mechanisms of mesenchymal stromal cell immunomodulation.* Immunol Cell Biol, 2013. **91**(1): p. 19-26.

86. Akiyama, K., et al., *Mesenchymal Stem Cell-Induced Immunoregulation Involves Fas Ligand/Fas-Mediated T Cell Apoptosis.* Cell Stem Cell, 2012. **10**(5): p. 544-555.

87. Bai, L., et al., *Human bone marrow-derived mesenchymal stem cells induce Th2-polarized immune response and promote endogenous repair in animal models of multiple sclerosis.* Glia, 2009. **57**(11): p. 1192-203.

88. Duffy, M.M., et al., *Mesenchymal stem cell inhibition of T-helper 17 cell-differentiation is triggered by cell-cell contact and mediated by prostaglandin E2 via the EP4 receptor.* Eur J Immunol, 2011. **41**(10): p. 2840-51.

89. English, K., F.P. Barry, and B.P. Mahon, *Murine mesenchymal stem cells suppress dendritic cell migration, maturation and antigen presentation.* Immunol Lett, 2008. **115**(1): p. 50-8.

90. Liu, X., et al., *Mesenchymal stem/stromal cells induce the generation of novel IL-10-dependent regulatory dendritic cells by SOCS3 activation.* J Immunol, 2012. **189**(3): p. 1182-92.

91. Ren, G., et al., *Inflammatory cytokine-induced intercellular adhesion molecule-1 and vascular cell adhesion molecule-1 in mesenchymal stem cells are critical for immunosuppression.* J Immunol, 2010. **184**(5): p. 2321-8.

92. Sotiropoulou, P.A., et al., *Interactions between human mesenchymal stem cells and natural killer cells.* Stem Cells, 2006. **24**(1): p. 74-85.

93. Xu, J., et al., *Mesenchymal stem cell-based angiopoietin-1 gene therapy for acute lung injury induced by lipopolysaccharide in mice.* J Pathol, 2008. **214**(4): p. 472-81.

94. Raffaghello, L., et al., *Human Mesenchymal Stem Cells Inhibit Neutrophil Apoptosis: A Model for Neutrophil Preservation in the Bone Marrow Niche.* STEM CELLS, 2008. **26**(1): p. 151-162.

95. Ajuebor, M.N., et al., *Role of resident peritoneal macrophages and mast cells in chemokine production and neutrophil migration in acute inflammation: evidence for an inhibitory loop involving endogenous IL-10.* J Immunol, 1999. **162**(3): p. 1685-91.

96. Nemeth, K., et al., *Bone marrow stromal cells attenuate sepsis via prostaglandin E(2)-dependent reprogramming of host macrophages to increase their interleukin-10 production.* Nat Med, 2009. **15**(1): p. 42-9.

97. Dayan, V., et al., *Mesenchymal stromal cells mediate a switch to alternatively activated monocytes/macrophages after acute myocardial infarction.* Basic Research in Cardiology, 2011. **106**(6): p. 1299-1310.

98. Francois, M., et al., *Human MSC suppression correlates with cytokine induction of indoleamine 2,3-dioxygenase and bystander M2 macrophage differentiation.* Mol Ther, 2012. **20**(1): p. 187-95.

99. Groh, M.E., et al., *Human mesenchymal stem cells require monocyte-mediated activation to suppress alloreactive T cells.* Experimental Hematology, 2005. **33**(8): p. 928-934.

100. Kim, J. and P. Hematti, *Mesenchymal stem cell-educated macrophages: a novel type of alternatively activated macrophages.* Experimental hematology, 2009. **37**(12): p. 1445-1453.

101. Milner, C.M., V.A. Higman, and A.J. Day, *TSG-6: a pluripotent inflammatory mediator?* Biochem Soc Trans, 2006. **34**(Pt 3): p. 446-50.

102. Qi, Y., et al., *TSG-6 released from intradermally injected mesenchymal stem cells accelerates wound healing and reduces tissue fibrosis in murine full-thickness skin wounds.* J Invest Dermatol, 2014. **134**(2): p. 526-37.

103. Le Blanc, K. and D. Mougiakakos, *Multipotent mesenchymal stromal cells and the innate immune system.* Nat Rev Immunol, 2012. **12**(5): p. 383-396.

104. Lee, R.H., et al., *TSG-6 as a biomarker to predict efficacy of human mesenchymal stem/progenitor cells (hMSCs) in modulating sterile inflammation in vivo.* Proceedings of the National Academy of Sciences, 2014. **111**(47): p. 16766-16771.

105. Choi, H., et al., *Anti-inflammatory protein TSG-6 secreted by activated MSCs attenuates zymosan-induced mouse peritonitis by decreasing TLR2/NF-κB signaling in resident macrophages.* Blood, 2011. **118**(2): p. 330-338.

106. Hernigou, P., et al., *Benefits of small volume and small syringe for bone marrow aspirations of mesenchymal stem cells.* Int Orthop, 2013. **37**(11): p. 2279-87.

107. Shoup, M., et al., *Mechanisms of neutropenia involving myeloid maturation arrest in burn sepsis.* Ann Surg, 1998. **228**(1): p. 112-22.

108. Gamelli, R.L., T.P. Paxton, and M. O'Reilly, *Bone marrow toxicity by silver sulfadiazine.* Surg Gynecol Obstet, 1993. **177**(2): p. 115-20.

109. Gimble, J.M., A.J. Katz, and B.A. Bunnell, *Adipose-derived stem cells for regenerative medicine.* Circ Res, 2007. **100**(9): p. 1249-60.

110. Nie, C., et al., *Locally administered adipose-derived stem cells accelerate wound healing through differentiation and vasculogenesis.* Cell Transplant, 2011. **20**(2): p. 205-16.

111. Alexaki, V.I., et al., *Adipose tissue-derived mesenchymal cells support skin reepithelialization through secretion of KGF-1 and PDGF-BB: Comparison with dermal fibroblasts.* Cell Transplantation, 2012. **21**(11): p. 2441-2454.

112. Blanton, M.W., et al., *Adipose Stromal Cells and Platelet-Rich Plasma Therapies Synergistically Increase Revascularization during Wound Healing.* Plastic and Reconstructive Surgery, 2009. **123**(2): p. 56S-64S.

113. Fu, X., et al., *Adipose tissue extract enhances skin wound healing.* Wound Repair Regen, 2007. **15**(4): p. 540-8.

114. Melief, S.M., et al., *Adipose tissue-derived multipotent stromal cells have a higher immunomodulatory capacity than their bone marrow-derived counterparts.* Stem Cells Transl Med, 2013. **2**(6): p. 455-63.

115. Hanson, S.E., et al., *Local delivery of allogeneic bone marrow and adipose tissue-derived mesenchymal stromal cells for cutaneous wound healing in a porcine model.* Journal of Tissue Engineering and Regenerative Medicine, 2016. **10**(2): p. E90-E100.

116. Clore, G.M. and A.M. Gronenborn, *Three-dimensional structures of alpha and beta chemokines.* FASEB J, 1995. **9**(1): p. 57-62.

117. Deshmane, S.L., et al., *Monocyte chemoattractant protein-1 (MCP-1): an overview.* J Interferon Cytokine Res, 2009. **29**(6): p. 313-26.

118. Cochran, B.H., A.C. Reffel, and C.D. Stiles, *Molecular cloning of gene sequences regulated by platelet-derived growth factor.* Cell, 1983. **33**(3): p. 939-947.

119. Yadav, A., V. Saini, and S. Arora, *MCP-1: Chemoattractant with a role beyond immunity: A review.* Clinica Chimica Acta, 2010. **411**(21–22): p. 1570-1579.

120. Matsushima, K., et al., *Purification and characterization of a novel monocyte chemotactic and activating factor produced by a human myelomonocytic cell line.* Journal of Experimental Medicine, 1989. **169**(4): p. 1485-1490.

121. Cushing, S.D., et al., *Minimally modified low density lipoprotein induces monocyte chemotactic protein 1 in human endothelial cells and smooth muscle cells.* Proceedings of the National Academy of Sciences, 1990. **87**(13): p. 5134-5138.

122. Brieland, J.K., et al., *Expression of monocyte chemoattractant protein-1 (MCP-1) by rat alveolar macrophages during chronic lung injury.* Am J Respir Cell Mol Biol, 1993. **9**(3): p. 300-5.

123. Jung, H.C., et al., *A distinct array of proinflammatory cytokines is expressed in human colon epithelial cells in response to bacterial invasion.* Journal of Clinical Investigation, 1995. **95**(1): p. 55-65.

124. Jones, G.E., *Cellular signaling in macrophage migration and chemotaxis.* J Leukoc Biol, 2000. **68**(5): p. 593-602.

125. Ridley, A.J., et al., *Cell migration: integrating signals from front to back.* Science, 2003. **302**(5651): p. 1704-9.

126. Khan, B., et al., *The role of monocyte subsets in myocutaneous revascularization.* J Surg Res, 2013. **183**(2): p. 963-75.

127. Dipietro, L.A., et al., *Modulation of macrophage recruitment into wounds by monocyte chemoattractant protein-1.* Wound Repair Regen, 2001. **9**(1): p. 28-33.

128. Shechter, R., et al., *Recruitment of Beneficial M2 Macrophages to Injured Spinal Cord Is Orchestrated by Remote Brain Choroid Plexus.* Immunity, 2013. **38**(3): p. 555-569.

129. Shechter, R., et al., *Infiltrating blood-derived macrophages are vital cells playing an anti-inflammatory role in recovery from spinal cord injury in mice.* PLoS Med, 2009. **6**(7): p. e1000113.

130. Kinnaird, T., et al., *Local Delivery of Marrow-Derived Stromal Cells Augments Collateral Perfusion Through Paracrine Mechanisms.* Circulation, 2004. **109**(12): p. 1543-1549.

131. Kinnaird, T., et al., *Local delivery of marrow-derived stromal cells augments collateral perfusion through paracrine mechanisms.* Circulation, 2004. **109**(12): p. 1543-9.

132. Ren, G., et al., *CCR2-dependent recruitment of macrophages by tumor-educated mesenchymal stromal cells promotes tumor development and is mimicked by TNFalpha.* Cell Stem Cell, 2012. **11**(6): p. 812-24.

133. Guilloton, F., et al., *Mesenchymal stromal cells orchestrate follicular lymphoma cell niche through the CCL2-dependent recruitment and polarization of monocytes.* Blood, 2012. **119**(11): p. 2556-67.

134. Denney, H., M.R. Clench, and M.N. Woodroofe, *Cleavage of chemokines CCL2 and CXCL10 by matrix metalloproteinases-2 and -9: implications for chemotaxis.* Biochem Biophys Res Commun, 2009. **382**(2): p. 341-7.

135. Charo, I.F., et al., *Molecular cloning and functional expression of two monocyte chemoattractant protein 1 receptors reveals alternative splicing of the carboxyl-terminal tails.* Proc Natl Acad Sci U S A, 1994. **91**(7): p. 2752-6.

136. Proost, P., et al., *Posttranslational modifications affect the activity of the human monocyte chemotactic proteins MCP-1 and MCP-2: identification of MCP-2(6-76) as a natural chemokine inhibitor.* J Immunol, 1998. **160**(8): p. 4034-41.

137. Garcia-Olmo, D., et al., *Expanded adipose-derived stem cells for the treatment of complex perianal fistula: a phase II clinical trial.* Dis Colon Rectum, 2009. **52**(1): p. 79-86.

138. Mirza, R.E. and T.J. Koh, *Contributions of cell subsets to cytokine production during normal and impaired wound healing.* Cytokine, 2015. **71**(2): p. 409-412.

139. JAX. *Mouse strain data sheet for CCL-2 KO mouse. The Jackson Labratory*. 30-01-2017]; Available from: https://www.jax.org/strain/004434.

140. Jeschke, M.G. and D.N. Herndon, *The combination of IGF-I and KGF cDNA improves dermal and epidermal regeneration by increased VEGF expression and neovascularization.* Gene Ther, 2007. **14**(16): p. 1235-42.

141. Bustin, S.A., et al., *The MIQE guidelines: minimum information for publication of quantitative real-time PCR experiments.* Clin Chem, 2009. **55**(4): p. 611-22.

142. Robson, M.C., et al., *Healing of chronic venous ulcers is not enhanced by the addition of topical repifermin (KGF-2) to standardized care.* Journal of Applied Research, 2004. **4**(2): p. 302-311.

143. Jimenez, P.A. and M.A. Rampy, *Keratinocyte growth factor-2 accelerates wound healing in incisional wounds.* J Surg Res, 1999. **81**(2): p. 238-42.

144. van der Spoel, T.I.G., et al., *Human relevance of pre-clinical studies in stem cell therapy: systematic review and meta-analysis of large animal models of ischaemic heart disease.* Cardiovascular Research, 2011. **91**(4): p. 649-658.

145. Harding, J., R.M. Roberts, and O. Mirochnitchenko, *Large animal models for stem cell therapy.* Stem Cell Research & Therapy, 2013. **4**(2): p. 23.

146. Summerfield, A., F. Meurens, and M.E. Ricklin, *The immunology of the porcine skin and its value as a model for human skin.* Molecular Immunology, 2015. **66**(1): p. 14-21.

147. Bailey, M., Z. Christoforidou, and M.C. Lewis, *The evolutionary basis for differences between the immune systems of man, mouse, pig and ruminants.* Veterinary Immunology and Immunopathology, 2013. **152**(1–2): p. 13-19.

148. Baksh, D., R. Yao, and R.S. Tuan, *Comparison of Proliferative and Multilineage Differentiation Potential of Human Mesenchymal Stem Cells Derived from Umbilical Cord and Bone Marrow.* STEM CELLS, 2007. **25**(6): p. 1384-1392.

149. Clover, A.J., et al., *Allogeneic mesenchymal stem cells, but not culture modified monocytes, improve burn wound healing.* Burns, 2014.

150. Gleeson, B.M., et al., *Bone marrow-derived mesenchymal stem cells have innate procoagulant activity and cause microvascular obstruction following intracoronary delivery: Amelioration by anti-thrombin therapy.* Stem Cells, 2015.

151. Bensaıd, W., et al., *A biodegradable fibrin scaffold for mesenchymal stem cell transplantation.* Biomaterials, 2003. **24**(14): p. 2497-2502.

152. Brans, T.A., et al., *Histopathological evaluation of scalds and contact burns in the pig model.* Burns, 1994. **20 Suppl 1**: p. S48-51.

153. Mansilla, E., et al., *Cadaveric bone marrow mesenchymal stem cells: first experience treating a patient with large severe burns.* Burns & Trauma, 2015. **3**: p. 17.

154. Schaffer, D., J.D. Bronzino, and D.R. Peterson, *Stem Cell Engineering: Principles and Practices*. 2012: CRC Press.

155. Harvanova, D., et al., *Isolation and characterization of synovial mesenchymal stem cells.* Folia Biol (Praha), 2011. **57**(3): p. 119-24.

156. Park, J.R., et al., *Isolation of human dermis derived mesenchymal stem cells using explants culture method: expansion and phenotypical characterization.* Cell Tissue Bank, 2015. **16**(2): p. 209-18.

157. Jackson, W.M., L.J. Nesti, and R.S. Tuan, *Potential therapeutic applications of muscle-derived mesenchymal stem and progenitor cells.* Expert opinion on biological therapy, 2010. **10**(4): p. 505-517.

158. Romanov, Y.A., V.A. Svintsitskaya, and V.N. Smirnov, *Searching for alternative sources of postnatal human mesenchymal stem cells: candidate MSC-like cells from umbilical cord.* Stem Cells, 2003. **21**(1): p. 105-10.

159. Zuk, P.A., et al., *Human Adipose Tissue Is a Source of Multipotent Stem Cells.* Molecular Biology of the Cell, 2002. **13**(12): p. 4279-4295.

160. Prunet-Marcassus, B., et al., *From heterogeneity to plasticity in adipose tissues: site-specific differences.* Exp Cell Res, 2006. **312**(6): p. 727-36.

161. Mizuno, H., M. Tobita, and A.C. Uysal, *Concise review: Adipose-derived stem cells as a novel tool for future regenerative medicine.* Stem Cells, 2012. **30**(5): p. 804-810.

162. Boquest, A.C., et al., *Isolation of stromal stem cells from human adipose tissue.* Methods in molecular biology (Clifton, N.J.), 2006. **325**: p. 35-46.

163. Strem, B.M., et al., *Multipotential differentiation of adipose tissue-derived stem cells.* Keio Journal of Medicine, 2005. **54**(3): p. 132-141.

164. Mana, M., et al., *Human U937 monocyte behavior and protein expression on various formulations of three-dimensional fibrin clots.* Wound Repair and Regeneration, 2006. **14**(1): p. 72-80.

165. Catelas, I., et al., *Human mesenchymal stem cell proliferation and osteogenic differentiation in fibrin gels in vitro.* Tissue Engineering, 2006. **12**(8): p. 2385-2396.

166. Kirilak, Y., et al., *Fibrin sealant promotes migration and proliferation of human articular chondrocytes: Possible involvement of thrombin and protease-activated receptors.* International Journal of Molecular Medicine, 2006. **17**(4): p. 551-558.

167. Bach, A.D., et al., *Fibrin glue as matrix for cultured autologous urothelial cells in urethral reconstruction.* Tissue Engineering, 2001. **7**(1): p. 45-53.

168. Gwak, S.J., et al., *Stable hepatocyte transplantation using fibrin matrix.* Biotechnology Letters, 2004. **26**(6): p. 505-508.

169. Idrus, R.B., et al., *Full-thickness skin wound healing using autologous keratinocytes and dermal fibroblasts with fibrin: bilayered versus single-layered substitute.* Adv Skin Wound Care, 2014. **27**(4): p. 171-80.

170. Tuan, T.L., et al., *In vitro fibroplasia: Matrix contraction, cell growth, and collagen production of fibroblasts cultured in fibrin gels.* Experimental Cell Research, 1996. **223**(1): p. 127-134.

171. Gugerell, A., et al., *High thrombin concentrations in fibrin sealants induce apoptosis in human keratinocytes.* Journal of Biomedical Materials Research - Part A, 2012. **100 A**(5): p. 1239-1247.

172. Hale, B.W., et al., *Effect of scaffold dilution on migration of mesenchymal stem cells from fibrin hydrogels.* American Journal of Veterinary Research, 2012. **73**(2): p. 313-318.

173. Peterbauer-Scherb, A., et al., *In vitro adipogenesis of adipose-derived stem cells in 3D fibrin matrix of low component concentration.* J Tissue Eng Regen Med, 2012. **6**(6): p. 434-42.

174. Cox, S., M. Cole, and B. Tawil, *Behavior of human dermal fibroblasts in three-dimensional fibrin clots: Dependence on fibrinogen and thrombin concentration.* Tissue Engineering, 2004. **10**(5-6): p. 942-954.

175. Ho, W., et al., *The behavior of human mesenchymal stem cells in 3D fibrin clots: Dependence on fibrinogen concentration and clot structure.* Tissue Engineering, 2006. **12**(6): p. 1587-1595.

176. Mogford, J.E., et al., *Fibrin sealant combined with fibroblasts and platelet-derived growth factor enhance wound healing in excisional wounds.* Wound Repair Regen, 2009. **17**(3): p. 405-10.

177. Geer, D.J., D.D. Swartz, and S.T. Andreadis, *Biomimetic delivery of keratinocyte growth factor upon cellular demand for accelerated wound healing in vitro and in vivo.* American Journal of Pathology, 2005. **167**(6): p. 1575-1586.

178. Grant, I., et al., *The co-application of sprayed cultured autologous keratinocytes and autologous fibrin sealant in a porcine wound model.* British Journal of Plastic Surgery, 2002. **55**(3): p. 219-227.

179. Bey, E., et al., *Emerging therapy for improving wound repair of severe radiation burns using local bone marrow-derived stem cell administrations.* Wound Repair Regen, 2010. **18**(1): p. 50-8.

180. Liu, P., et al., *Tissue-engineered skin containing mesenchymal stem cells improves burn wounds.* Artificial Organs, 2008. **32**(12): p. 925-931.

181. Mansilla, E., et al., *Time and regeneration in burns treatment: heading into the first worldwide clinical trial with cadaveric mesenchymal stem cells.* Burns, 2012. **38**(3): p. 450-2.

182. Falanga, V., *Stem cells in tissue repair and regeneration.* Journal of Investigative Dermatology, 2012. **132**(6): p. 1538-1541.

183. Le Blanc, K., et al., *Mesenchymal stem cells for treatment of steroid-resistant, severe, acute graft-versus-host disease: a phase II study.* Lancet, 2008. **371**(9624): p. 1579-86.

184. Gangji, V., et al., *Treatment of osteonecrosis of the femoral head with implantation of autologous bone-marrow cells. A pilot study.* J Bone Joint Surg Am, 2004. **86-a**(6): p. 1153-60.

185. Squillaro, T., G. Peluso, and U. Galderisi, *Clinical Trials With Mesenchymal Stem Cells: An Update.* Cell Transplant, 2016. **25**(5): p. 829-48.

186. Allison, M., *Genzyme backs Osiris, despite Prochymal flop.* Nat Biotech, 2009. **27**(11): p. 966-967.

187. Lu, D., et al., *Comparison of bone marrow mesenchymal stem cells with bone marrow-derived mononuclear cells for treatment of diabetic critical limb ischemia and foot ulcer: a double-blind, randomized, controlled trial.* Diabetes Res Clin Pract, 2011. **92**(1): p. 26-36.

188. Fu, X.B., et al., *Enhancing the repair quality of skin injury on porcine after autografting with the bone marrow mesenchymal stem cells.* Zhonghua yi xue za zhi, 2004. **84**(11): p. 920-924.

189. Doi, H., et al., *Potency of umbilical cord blood- and Wharton's jelly-derived mesenchymal stem cells for scarless wound healing.* Sci Rep, 2016. **6**: p. 18844.

190. Nan, W., et al., *Umbilical Cord Mesenchymal Stem Cells Combined With a Collagenfibrin Double-layered Membrane Accelerates Wound Healing.* Wounds, 2015. **27**(5): p. 134-40.

191. Chung, E., et al., *Fibrin-based stem cell containing scaffold improves the dynamics of burn wound healing.* Wound Repair Regen, 2016. **24**(5): p. 810-819.

192. De Ugarte, D.A., et al., *Comparison of multi-lineage cells from human adipose tissue and bone marrow.* Cells Tissues Organs, 2003. **174**(3): p. 101-9.

193. Peng, L., et al., *Comparative analysis of mesenchymal stem cells from bone marrow, cartilage, and adipose tissue.* Stem Cells Dev, 2008. **17**(4): p. 761-73.

194. Li, C.Y., et al., *Comparative analysis of human mesenchymal stem cells from bone marrow and adipose tissue under xeno-free conditions for cell therapy.* Stem Cell Res Ther, 2015. **6**: p. 55.

195. Strioga, M., et al., *Same or not the same? Comparison of adipose tissue-derived versus bone marrow-derived mesenchymal stem and stromal cells.* Stem Cells Dev, 2012. **21**(14): p. 2724-52.

196. Noel, D., et al., *Cell specific differences between human adipose-derived and mesenchymal-stromal cells despite similar differentiation potentials.* Exp Cell Res, 2008. **314**(7): p. 1575-84.

197.   Kachgal, S. and A.J. Putnam, *Mesenchymal stem cells from adipose and bone marrow promote angiogenesis via distinct cytokine and protease expression mechanisms.* Angiogenesis, 2011. **14**(1): p. 47-59.

198.   Hsiao, S.T.-F., et al., *Comparative Analysis of Paracrine Factor Expression in Human Adult Mesenchymal Stem Cells Derived from Bone Marrow, Adipose, and Dermal Tissue.* Stem Cells and Development, 2012. **21**(12): p. 2189-2203.

199.   Valencia, J., et al., *Comparative analysis of the immunomodulatory capacities of human bone marrow– and adipose tissue–derived mesenchymal stromal cells from the same donor.* Cytotherapy, 2016. **18**(10): p. 1297-1311.

200.   Puissant, B., et al., *Immunomodulatory effect of human adipose tissue-derived adult stem cells: comparison with bone marrow mesenchymal stem cells.* Br J Haematol, 2005. **129**(1): p. 118-29.

201.   Ivanova-Todorova, E., et al., *Adipose tissue-derived mesenchymal stem cells are more potent suppressors of dendritic cells differentiation compared to bone marrow-derived mesenchymal stem cells.* Immunol Lett, 2009. **126**(1-2): p. 37-42.

202.   Fearmonti, R., et al., *A Review of Scar Scales and Scar Measuring Devices.* Eplasty, 2010. **10**: p. e43.

203.   Hong, S.J., et al., *Topically Delivered Adipose Derived Stem Cells Show an Activated-Fibroblast Phenotype and Enhance Granulation Tissue Formation in Skin Wounds.* PLoS ONE, 2013. **8**(1).

204.   Liu, X., et al., *Direct comparison of the potency of human mesenchymal stem cells derived from amnion tissue, bone marrow and adipose tissue at inducing dermal fibroblast responses to cutaneous wounds.* International Journal of Molecular Medicine, 2013. **31**(2): p. 407-415.

205.   Clover, A.J., A.H. Kumar, and N.M. Caplice, *Deficiency of CX3CR1 delays burn wound healing and is associated with reduced myeloid cell recruitment and decreased sub-dermal angiogenesis.* Burns, 2011. **37**(8): p. 1386-93.

206.   Schultz, G.S., et al., *Wound bed preparation: a systematic approach to wound management.* Wound Repair Regen, 2003. **11 Suppl 1**: p. S1-28.

207.   Buechler, C., et al., *Regulation of scavenger receptor CD163 expression in human monocytes and macrophages by pro- and antiinflammatory stimuli.* J Leukoc Biol, 2000. **67**(1): p. 97-103.

208.   Lau, S.K., P.G. Chu, and L.M. Weiss, *CD163: a specific marker of macrophages in paraffin-embedded tissue samples.* Am J Clin Pathol, 2004. **122**(5): p. 794-801.

209.   Bergers, G. and S. Song, *The role of pericytes in blood-vessel formation and maintenance.* Neuro-Oncology, 2005. **7**(4): p. 452-464.

210.   Finnson, K.W., et al., *Dynamics of Transforming Growth Factor Beta Signaling in Wound Healing and Scarring.* Advances in Wound Care, 2013. **2**(5): p. 195-214.

211.   Sullivan, T.P., et al., *The pig as a model for human wound healing.* Wound Repair Regen, 2001. **9**(2): p. 66-76.

212.   Mansilla, E., et al., *Outstanding survival and regeneration process by the use of intelligent acellular dermal matrices and mesenchymal stem cells in a burn pig model.* Transplantation Proceedings, 2010. **42**(10): p. 4275-4278.

213.   Caliari-Oliveira, C., et al., *Xenogeneic Mesenchymal Stromal Cells Improve Wound Healing and Modulate the Immune Response in an Extensive Burn Model.* Cell Transplant, 2016. **25**(2): p. 201-15.

214.   Xue, L., et al., *Effects of human bone marrow mesenchymal stem cells on burn injury healing in a mouse model.* International Journal of Clinical and Experimental Pathology, 2013. **6**(7): p. 1327-1336.

215. Shumakov, V.I., et al., *Mesenchymal bone marrow stem cells more effectively stimulate regeneration of deep burn wounds than embryonic fibroblasts.* Bulletin of Experimental Biology and Medicine, 2003. **136**(2): p. 192-195.

216. Gurtner, G.C., et al., *Wound repair and regeneration.* Nature, 2008. **453**(7193): p. 314-321.

217. Seaton, M., A. Hocking, and N.S. Gibran, *Porcine models of cutaneous wound healing.* Ilar j, 2015. **56**(1): p. 127-38.

218. Atalay, S., A. Coruh, and K. Deniz, *Stromal vascular fraction improves deep partial thickness burn wound healing.* Burns, 2014. **40**(7): p. 1375-1383.

219. Bliley, J.M., et al., *Administration of adipose-derived stem cells enhances vascularity, induces collagen deposition, and dermal adipogenesis in burn wounds.* Burns, 2016. **42**(6): p. 1212-22.

220. Beegle, J.R., et al., *Preclinical evaluation of mesenchymal stem cells overexpressing VEGF to treat critical limb ischemia.* Molecular Therapy. Methods & Clinical Development, 2016. **3**: p. 16053.

221. Li, W., et al., *Bcl-2 engineered MSCs inhibited apoptosis and improved heart function.* Stem Cells, 2007. **25**(8): p. 2118-27.

222. Mangi, A.A., et al., *Mesenchymal stem cells modified with Akt prevent remodeling and restore performance of infarcted hearts.* Nat Med, 2003. **9**(9): p. 1195-201.

223. Zhang, M., et al., *SDF-1 expression by mesenchymal stem cells results in trophic support of cardiac myocytes after myocardial infarction.* The FASEB Journal, 2007. **21**(12): p. 3197-3207.

224. Tang, J.M., et al., *VEGF/SDF-1 promotes cardiac stem cell mobilization and myocardial repair in the infarcted heart.* Cardiovasc Res, 2011. **91**(3): p. 402-11.

225. Rosova, I., et al., *Hypoxic preconditioning results in increased motility and improved therapeutic potential of human mesenchymal stem cells.* Stem Cells, 2008. **26**(8): p. 2173-82.

226. Gonzalez-Rey, E., et al., *Human adult stem cells derived from adipose tissue protect against experimental colitis and sepsis.* Gut, 2009. **58**(7): p. 929-39.

227. Krampera, M., *Mesenchymal stromal cell licensing: A multistep process.* Leukemia, 2011. **25**(9): p. 1408-1414.

228. Duijvestein, M., et al., *Pretreatment with interferon-gamma enhances the therapeutic activity of mesenchymal stromal cells in animal models of colitis.* Stem Cells, 2011. **29**(10): p. 1549-58.

229. Kim, Y.S., et al., *TNF-alpha enhances engraftment of mesenchymal stem cells into infarcted myocardium.* Front Biosci (Landmark Ed), 2009. **14**: p. 2845-56.

230. Xiao, Q., et al., *TNF-alpha increases bone marrow mesenchymal stem cell migration to ischemic tissues.* Cell Biochem Biophys, 2012. **62**(3): p. 409-14.

231. Chen, H., et al., *Pre-activation of mesenchymal stem cells with TNF-alpha, IL-1beta and nitric oxide enhances its paracrine effects on radiation-induced intestinal injury.* Sci Rep, 2015. **5**: p. 8718.

232. Prasanna, S.J., et al., *Pro-Inflammatory Cytokines, IFNγ and TNFα, Influence Immune Properties of Human Bone Marrow and Wharton Jelly Mesenchymal Stem Cells Differentially.* PLOS ONE, 2010. **5**(2): p. e9016.

233. Raicevic, G., et al., *The source of human mesenchymal stromal cells influences their TLR profile as well as their functional properties.* Cellular Immunology, 2011. **270**(2): p. 207-216.

234. Broekman, W., et al., *TNF-α and IL-1β-activated human mesenchymal stromal cells increase airway epithelial wound healing in vitro via activation of the epidermal growth factor receptor.* Respiratory Research, 2016. **17**: p. 3.

235.   Lee, R.H., et al., *Intravenous hMSCs improve myocardial infarction in mice because cells embolized in lung are activated to secrete the anti-inflammatory protein TSG-6.* Cell Stem Cell, 2009. **5**(1): p. 54-63.

236.   Wang, M., et al., *Human progenitor cells from bone marrow or adipose tissue produce VEGF, HGF, and IGF-I in response to TNF by a p38 MAPK-dependent mechanism.* Am J Physiol Regul Integr Comp Physiol, 2006. **291**(4): p. R880-4.

237.   Fu, X., et al., *Migration of bone marrow-derived mesenchymal stem cells induced by tumor necrosis factor-alpha and its possible role in wound healing.* Wound Repair Regen, 2009. **17**(2): p. 185-91.

238.   Kean, T.J., et al., *MSCs: Delivery Routes and Engraftment, Cell-Targeting Strategies, and Immune Modulation.* Stem Cells Int, 2013. **2013**: p. 732742.

239.   Willenborg, S., et al., *CCR2 recruits an inflammatory macrophage subpopulation critical for angiogenesis in tissue repair.* Blood, 2012. **120**(3): p. 613-25.

240.   Mirza, R., L.A. DiPietro, and T.J. Koh, *Selective and Specific Macrophage Ablation Is Detrimental to Wound Healing in Mice.* The American Journal of Pathology, 2009. **175**(6): p. 2454-2462.

241.   Klinkert, K., et al., *Selective M2 Macrophage Depletion Leads to Prolonged Inflammation in Surgical Wounds.* Eur Surg Res, 2017. **58**(3-4): p. 109-120.

242.   Leblond, A.L., et al., *Systemic and Cardiac Depletion of M2 Macrophage through CSF-1R Signaling Inhibition Alters Cardiac Function Post Myocardial Infarction.* PLoS One, 2015. **10**(9): p. e0137515.

243.   van Amerongen, M.J., et al., *Macrophage Depletion Impairs Wound Healing and Increases Left Ventricular Remodeling after Myocardial Injury in Mice.* The American Journal of Pathology, 2007. **170**(3): p. 818-829.

244.   Zhang, Q., et al., *Mesenchymal stem cells derived from human gingiva are capable of immunomodulatory functions and ameliorate inflammation-related tissue destruction in experimental colitis.* J Immunol, 2009. **183**(12): p. 7787-98.

245.   Khan, U.A., et al., *CCL2 and CCR2 are Essential for the Formation of Osteoclasts and Foreign Body Giant Cells.* J Cell Biochem, 2016. **117**(2): p. 382-9.

246.   Low, Q.E., et al., *Wound healing in MIP-1alpha(-/-) and MCP-1(-/-) mice.* Am J Pathol, 2001. **159**(2): p. 457-63.

247.   New, D.C. and Y.H. Wong, *CC chemokine receptor-coupled signalling pathways.* Sheng Wu Hua Xue Yu Sheng Wu Wu Li Xue Bao (Shanghai), 2003. **35**(9): p. 779-88.

248.   Ford, L.B., et al., *Characterization of conventional and atypical receptors for the chemokine CCL2 on mouse leukocytes.* J Immunol, 2014. **193**(1): p. 400-11.

249.   Islam, S.A., et al., *Mouse CCL8, a CCR8 agonist, promotes atopic dermatitis by recruiting IL-5+ T(H)2 cells.* Nat Immunol, 2011. **12**(2): p. 167-77.

250.   Cambien, B., et al., *Signal transduction involved in MCP-1–mediated monocytic transendothelial migration.* Vol. 97. 2001. 359-366.

251.   Dubois, P.M., et al., *Early signal transduction by the receptor to the chemokine monocyte chemotactic protein-1 in a murine T cell hybrid.* J Immunol, 1996. **156**(4): p. 1356-61.

252.   Ashida, N., et al., *Distinct signaling pathways for MCP-1-dependent integrin activation and chemotaxis.* J Biol Chem, 2001. **276**(19): p. 16555-60.

253.   Turner, S.J., et al., *The CC chemokine monocyte chemotactic peptide-1 activates both the class I p85/p110 phosphatidylinositol 3-kinase and the class II PI3K-C2alpha.* J Biol Chem, 1998. **273**(40): p. 25987-95.

254.   Soleimani, M. and S. Nadri, *A protocol for isolation and culture of mesenchymal stem cells from mouse bone marrow.* Nat Protoc, 2009. **4**(1): p. 102-6.

255.   Maggini, J., et al., *Mouse bone marrow-derived mesenchymal stromal cells turn activated macrophages into a regulatory-like profile.* PLoS One, 2010. **5**(2): p. e9252.

256. Wang, X., et al., *The mouse excisional wound splinting model, including applications for stem cell transplantation.* Nat Protoc, 2013. **8**(2): p. 302-9.

257. Le Blanc, K. and L.C. Davies, *Mesenchymal stromal cells and the innate immune response.* Immunology Letters, 2015. **168**(2): p. 140-146.

258. Maxson, S., et al., *Concise Review: Role of Mesenchymal Stem Cells in Wound Repair.* Stem Cells Translational Medicine, 2012. **1**(2): p. 142-149.

259. Jiang, D., et al., *Suppression of Neutrophil-Mediated Tissue Damage—A Novel Skill of Mesenchymal Stem Cells.* Stem Cells, 2016. **34**(9): p. 2393-2406.

260. Poncelet, A.J., et al., *Intracardiac allogeneic mesenchymal stem cell transplantation elicits neo-angiogenesis in a fully immunocompetent ischaemic swine model.* Eur J Cardiothorac Surg, 2010. **38**(6): p. 781-7.

261. Gordon, S., A. Plüddemann, and F. Martinez Estrada, *Macrophage heterogeneity in tissues: phenotypic diversity and functions.* Immunological Reviews, 2014. **262**(1): p. 36-55.

262. Roca, H., et al., *CCL2 and interleukin-6 promote survival of human CD11b+ peripheral blood mononuclear cells and induce M2-type macrophage polarization.* J Biol Chem, 2009. **284**(49): p. 34342-54.

263. Wang, D., et al., *Immunohistochemistry in the evaluation of neovascularization in tumor xenografts.* Biotechnic & histochemistry : official publication of the Biological Stain Commission, 2008. **83**(0): p. 179-189.

264. Sozzani, S., et al., *Receptor-activated calcium influx in human monocytes exposed to monocyte chemotactic protein-1 and related cytokines.* J Immunol, 1993. **150**(4): p. 1544-53.

265. Hocking, A.M. and N.S. Gibran, *Mesenchymal stem cells: paracrine signaling and differentiation during cutaneous wound repair.* Exp Cell Res, 2010. **316**(14): p. 2213-9.

266. Borena, B.M., et al., *Evaluation of autologous bone marrow-derived nucleated cells for healing of full-thickness skin wounds in rabbits.* Int Wound J, 2010. **7**(4): p. 249-60.

267. Rustad, K.C., et al., *Enhancement of mesenchymal stem cell angiogenic capacity and stemness by a biomimetic hydrogel scaffold.* Biomaterials, 2012. **33**(1): p. 80-90.

268. Lee, W.J., et al., *The Effect of MCP-1/CCR2 on the Proliferation and Senescence of Epidermal Constituent Cells in Solar Lentigo.* International Journal of Molecular Sciences, 2016. **17**(6): p. 948.

269. Yoon, B.S., et al., *Secretory profiles and wound healing effects of human amniotic fluid-derived mesenchymal stem cells.* Stem Cells Dev, 2010. **19**(6): p. 887-902.

270. Kim, H., et al., *Enhanced wound healing effect of canine adipose-derived mesenchymal stem cells with low-level laser therapy in athymic mice.* Journal of Dermatological Science, 2012. **68**(3): p. 149-156.

271. Viedt, C., et al., *Monocyte chemoattractant protein-1 induces proliferation and interleukin-6 production in human smooth muscle cells by differential activation of nuclear factor-kappaB and activator protein-1.* Arterioscler Thromb Vasc Biol, 2002. **22**(6): p. 914-20.

272. Salcedo, R., et al., *Human endothelial cells express CCR2 and respond to MCP-1: direct role of MCP-1 in angiogenesis and tumor progression.* Vol. 96. 2000. 34-40.

273. Ryu, J.H., et al., *Implantation of bone marrow mononuclear cells using injectable fibrin matrix enhances neovascularization in infarcted myocardium.* Biomaterials, 2005. **26**(3): p. 319-326.

274. Zhou, L., et al., *Monocyte Chemoattractant Protein-1 Induces a Novel Transcription Factor That Causes Cardiac Myocyte Apoptosis and Ventricular Dysfunction.* Circulation Research, 2006. **98**(9): p. 1177-1185.

275. Niu, J., et al., *Monocyte chemotactic protein (MCP)-1 promotes angiogenesis via a novel transcription factor, MCP-1-induced protein (MCPIP).* J Biol Chem, 2008. **283**(21): p. 14542-51.

276. Rafei, M., et al., *Mesenchymal stromal cell-derived CCL2 suppresses plasma cell immunoglobulin production via STAT3 inactivation and PAX5 induction.* Blood, 2008. **112**(13): p. 4991-8.

277. Ren, G., et al., *Mesenchymal stem cell-mediated immunosuppression occurs via concerted action of chemokines and nitric oxide.* Cell Stem Cell, 2008. **2**(2): p. 141-50.

278. Wood, S., et al., *Pro-inflammatory chemokine CCL2 (MCP-1) promotes healing in diabetic wounds by restoring the macrophage response.* PLoS One, 2014. **9**(3): p. e91574.

279. Jackman, S.H., et al., *Differential expression of chemokines in a mouse model of wound healing.* Ann Clin Lab Sci, 2000. **30**(2): p. 201-7.

280. Adutler-Lieber, S., et al., *Human macrophage regulation via interaction with cardiac adipose tissue-derived mesenchymal stromal cells.* J Cardiovasc Pharmacol Ther, 2013. **18**(1): p. 78-86.

281. Mauer, J., et al., *Signaling by IL-6 promotes alternative activation of macrophages to limit endotoxemia and obesity-associated resistance to insulin.* Nat Immunol, 2014. **15**(5): p. 423-430.

282. Sierra-Filardi, E., et al., *CCL2 shapes macrophage polarization by GM-CSF and M-CSF: identification of CCL2/CCR2-dependent gene expression profile.* J Immunol, 2014. **192**(8): p. 3858-67.

283. Waterman, R.S., et al., *A New Mesenchymal Stem Cell (MSC) Paradigm: Polarization into a Pro-Inflammatory MSC1 or an Immunosuppressive MSC2 Phenotype.* PLOS ONE, 2010. **5**(4): p. e10088.

284. Davidson, J.M., F. Yu, and S.R. Opalenik, *Splinting Strategies to Overcome Confounding Wound Contraction in Experimental Animal Models.* Advances in Wound Care, 2013. **2**(4): p. 142-148.

285. Galiano, R.D., et al., *Quantitative and reproducible murine model of excisional wound healing.* Wound Repair Regen, 2004. **12**(4): p. 485-92.

286. Lee, M.J., et al., *Proteomic analysis of tumor necrosis factor-alpha-induced secretome of human adipose tissue-derived mesenchymal stem cells.* J Proteome Res, 2010. **9**(4): p. 1754-62.

287. Tilg, H., et al., *Interleukin-6 (IL-6) as an anti-inflammatory cytokine: induction of circulating IL-1 receptor antagonist and soluble tumor necrosis factor receptor p55.* Blood, 1994. **83**(1): p. 113-8.

288. Gallucci, R.M., et al., *Interleukin 6 Indirectly Induces Keratinocyte Migration.* Journal of Investigative Dermatology, 2004. **122**(3): p. 764-772.

289. MacKenzie, K.F., et al., *PGE(2) Induces Macrophage IL-10 Production and a Regulatory-like Phenotype via a Protein Kinase A–SIK–CRTC3 Pathway.* The Journal of Immunology Author Choice, 2013. **190**(2): p. 565-577.

290. Wang, J., et al., *Kynurenic acid as a ligand for orphan G protein-coupled receptor GPR35.* J Biol Chem, 2006. **281**(31): p. 22021-8.

291. Fajka-Boja, R., et al., *Galectin-1 is a local but not systemic immunomodulatory factor in mesenchymal stromal cells.* Cytotherapy, 2016. **18**(3): p. 360-370.

292. Sala, E., et al., *Mesenchymal Stem Cells Reduce Colitis in Mice via Release of TSG6, Independently of Their Localization to the Intestine.* Gastroenterology, 2015. **149**(1): p. 163-176.e20.

293. Eggenhofer, E., et al., *Mesenchymal stem cells are short-lived and do not migrate beyond the lungs after intravenous infusion.* Front Immunol, 2012. **3**: p. 297.

294. Braza, F., et al., *Mesenchymal Stem Cells Induce Suppressive Macrophages Through Phagocytosis in a Mouse Model of Asthma.* Stem Cells, 2016. **34**(7): p. 1836-45.

295. Liu, S., et al., *Mesenchymal Stem Cells Prevent Hypertrophic Scar Formation via Inflammatory Regulation when Undergoing Apoptosis.* J Invest Dermatol, 2014.

296. Phinney, D.G., et al., *Mesenchymal stem cells use extracellular vesicles to outsource mitophagy and shuttle microRNAs.* Nature Communications, 2015. **6**: p. 8472.

297. Kapoor, N., et al., *Transcription factors STAT6 and KLF4 implement macrophage polarization via the dual catalytic powers of MCPIP.* Journal of immunology (Baltimore, Md. : 1950), 2015. **194**(12): p. 6011-6023.

298. Che, N., et al., *Impaired B cell inhibition by lupus bone marrow mesenchymal stem cells is caused by reduced CCL2 expression.* J Immunol, 2014. **193**(10): p. 5306-14.

299. Rafei, M., et al., *Mesenchymal stromal cells ameliorate experimental autoimmune encephalomyelitis by inhibiting CD4 Th17 T cells in a CC chemokine ligand 2-dependent manner.* J Immunol, 2009. **182**(10): p. 5994-6002.

300. Dvorak, H.F., *Tumors: wounds that do not heal. Similarities between tumor stroma generation and wound healing.* N Engl J Med, 1986. **315**(26): p. 1650-9.

301. Schafer, M. and S. Werner, *Cancer as an overhealing wound: an old hypothesis revisited.* Nat Rev Mol Cell Biol, 2008. **9**(8): p. 628-38.

302. Szabo, E., et al., *Licensing by Inflammatory Cytokines Abolishes Heterogeneity of Immunosuppressive Function of Mesenchymal Stem Cell Population.* Stem Cells Dev, 2015. **24**(18): p. 2171-80.

303. Phinney, D.G., *Functional heterogeneity of mesenchymal stem cells: implications for cell therapy.* J Cell Biochem, 2012. **113**(9): p. 2806-12.

304. Sharma, V. and J.H. McNeill, *To scale or not to scale: the principles of dose extrapolation.* British Journal of Pharmacology, 2009. **157**(6): p. 907-921.

305. Bloom, D.D., et al., *A reproducible immunopotency assay to measure mesenchymal stromal cell–mediated T-cell suppression.* Cytotherapy, 2015. **17**(2): p. 140-151.

306. Jiao, J., et al., *A mesenchymal stem cell potency assay.* Methods Mol Biol, 2011. **677**: p. 221-31.

307. Shchegelskaya, E.A., et al., *Migration of labeled bone marrow MSCs and skin fibroblasts after systemic and local transplantation in rat burn wound model.* Biopolymers and Cell, 2015. **31**(5): p. 387-394.

308. Revilla, G., et al., *Effect of allogeneic bone marrow-mesenchymal stem cells (BM-MSCs) to accelerate burn healing of rat on the expression of collagen type i and integrin α2β1.* Pakistan Journal of Biological Sciences, 2016. **19**(8-9): p. 345-351.

309. Oksuz, S., et al., *The effect of subcutaneous mesenchymal stem cell injection on statis zone and apoptosis in an experimental burn model.* Plast Reconstr Surg, 2013. **131**(3): p. 463-71.

310. Yagi, H., et al., *Bone Marrow Mesenchymal Stromal Cells Attenuate Organ Injury Induced by LPS and Burn.* Cell Transplantation, 2010. **19**(6-7): p. 823-830.

311. Karimi, H., et al., *Burn wound healing with injection of adipose-derived stem cells: a mouse model study.* Annals of Burns and Fire Disasters, 2014. **27**(1): p. 44-49.

312. Loder, S., et al., *Wound Healing Immediately Post-Thermal Injury Is Improved by Fat and Adipose Derived Stem Cell Isografts.* Journal of burn care & research : official publication of the American Burn Association, 2015. **36**(1): p. 70-76.

313. Foubert, P., et al., *Uncultured adipose-derived regenerative cells (ADRCs) seeded in collagen scaffold improves dermal regeneration, enhancing early vascularization and structural organization following thermal burns.* Burns, 2015. **41**(7): p. 1504-1516.

314. Foubert, P., et al., *Adipose-Derived Regenerative Cell Therapy for Burn Wound Healing: A Comparison of Two Delivery Methods.* Advances in Wound Care, 2016. **5**(7): p. 288-298.

Appendices

Appendix I

Burn wound healing pre-clinical studies using BM-MSC

| Burn model	Wound size	Stem cell source	Dos-age	Route	Tim-ing	Ref	notes
Rat	12.57	Allo BM-MSC fibroblasts	0.4×10^6	IV injection Or fibrin	Once directly after	[307]	Tracking experiment IV MSC in kidney, topical MSC did not migrate to any organs. Topical application was better
Rat,	20mins, 100°C	Allo BM-MSC	2×10^6	SC	Once directly after	[308]	d-14 reduced healing time, increased col1
Rat severe burn	200°C 20s 11.25cm² x4	Mouse BM-MSC	5×10^6	SC	Once directly after	[213]	Increased survival, accelerated wound closure altered plasma cytokine
Mouse	90°C 3s 3-5% TBSA	Human BM-MSC	1×10^6	SC	Once directly after	[214]	Increase wound closure angiogenesis
Rat comb	100°C 20s 2cm² x 8	Allo BM-MSC	1×10^6 /wound	SC	Once, I h post	[309]	Higher apoptosis in control, Increased cell viability in stasis zone
Rat full thick-ness	100°C 10s, 30% TBSA	Human BM-MSC	2×10^6	IM	Once directly after	[310]	reduce infiltration of inflammatory cells in various target organs reducing cell death
Rats, deep burns	97°C, 8s + wet gauze	Allo	2×10^6	topical	D-2	[215]	Increased granulation tissue, neo vessels, reduction in cell infiltrate, better than embryonic fibroblast
Pig, Deep partial thick-ness	100°C, 20s 19.6cm² x6	Allo BM-MSC	2×10^6	Collagen./GAG scaffold	Once post injury	[180]	Increased wound closure re-epithelialisation angiogenesis, no quantification less wound contraction
Pig Full thick-ness	300cm² 1 pig	Rabbit BM-MSC	2×10^6/ml/cm²		D-7 D-14	[212]	Cd44 antibody PLGA matrix first applied, on d7,14 ~600×10^6 MSC applied. Significant regeneration, hair follicle etc.
Pig, deep partial thick-ness	80°C 20s 4cm²	Allo BM-MSC	1×10^6/cm²	Topical, Fibrin	Once directly after	[149]	Increased wound healing compared to auto PBMNC

Appendix II

Burn wound healing pre-clinical studies using AD-MSC

| Burn model	Wound size	Stem cell source	Dosage	Delivery	Timing	Ref	notes
Mouse, full thickness	2.25cm^2 96°C, 8s	Allo cultured AD-MSC	1x10^6/wound	ID	Directly after	[311]	Reduced wound area, increased macrophage count
Mouse, full thickness	0.78 cm^2, 70°C, 10s	Allo cultured AD-MSC	6.8x10^6/wound	Sub-eschar	24h post injury	[219]	Increased vascularity collagen deposition type I and III +increased ratio + adipogenesis
Mouse, partial thickness	60°C, 17s 30% TBSA	Allo cultured AD-MSC	1x10^6/wound	ID	Directly after	[312]	Reduced burn depth, inflammatory infiltrate d14, reduced apoptosis d5
Rat, full thickness	87°C, 10s	Allo cultured AD-MSC	2x10^6/wound	Topical, Fibrin gel	24 h post injury after wound excision	[191]	Increased vascularisation +cd206 cells increase monocyte recruitment and granulation tissue
Rat, deep partial thickness	7cm^2 70°C 30s, 2% TBSA	Allo, **uncultured SVF**	4x10^6 /wound	ID	Directly after	[218]	Increased VEGF, reduced inflammatory infiltrate
Pig, full thickness	10 cm^2, 180°C	Auto **uncultured SVF**	2.5 × 10^6 /wound	Topical spray, or ID	48 h post injury after wound excision	[313, 314]	Increased vascular density, re-epithelialisation, granulation tissue, collagen content. Reduced neutrophil infiltration d7 and d14

Appendix III

Excluded animal from wound closure image analysis from chapter 4
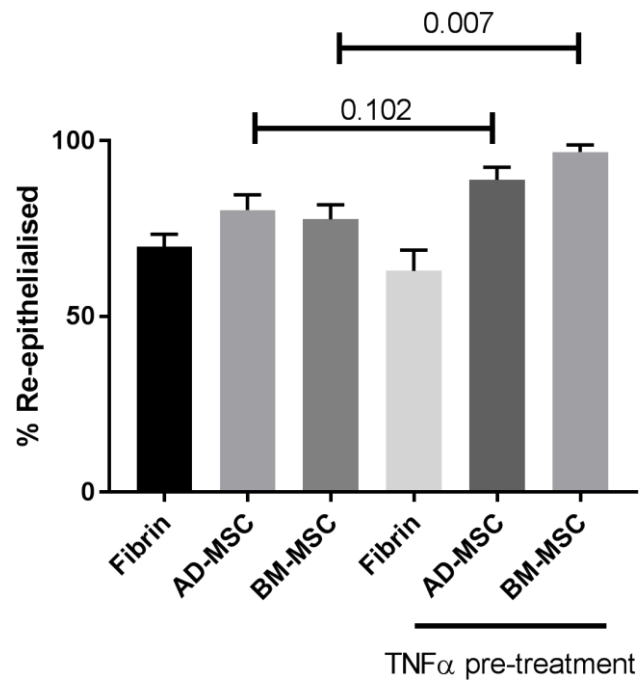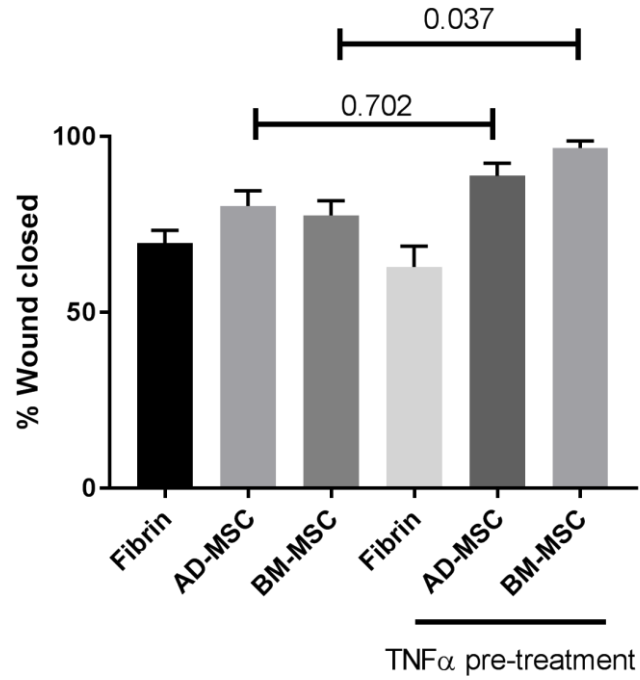

Day 14 wound closure
with excluded values
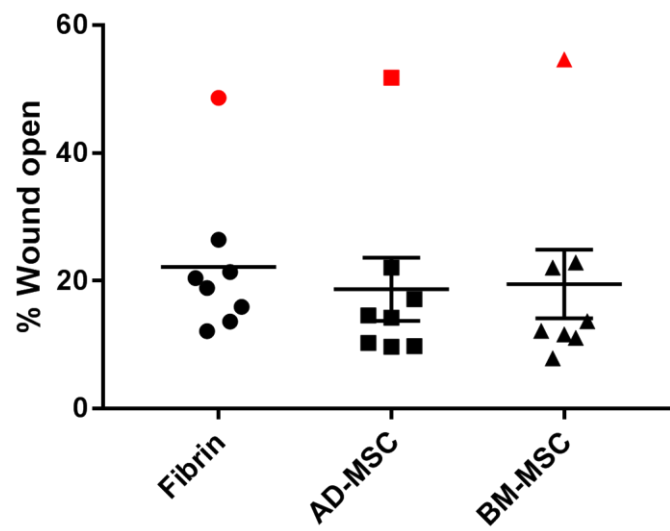
Appendix IV

Comparison of Fibrin only groups from animals used in chapter 4 and chapter 5, demonstrating no significant difference in rate of wound healing
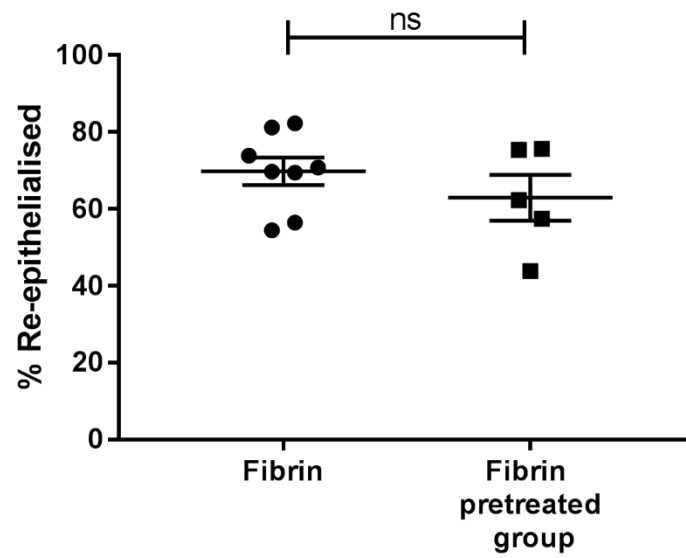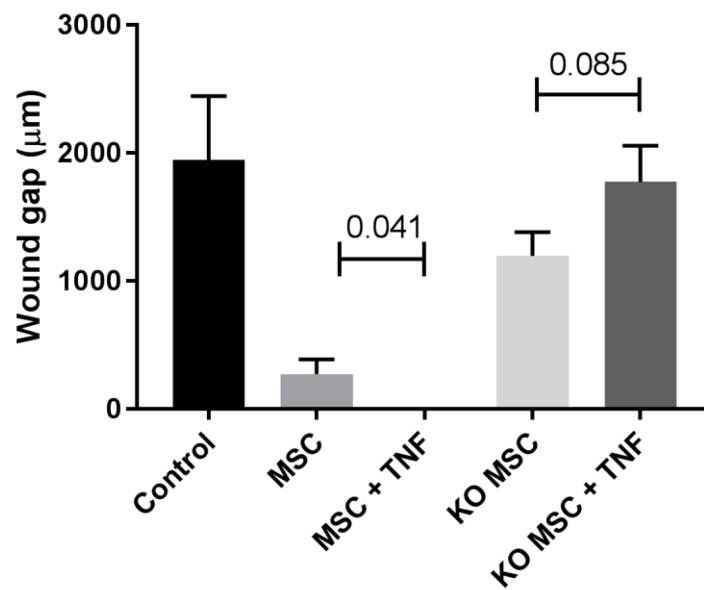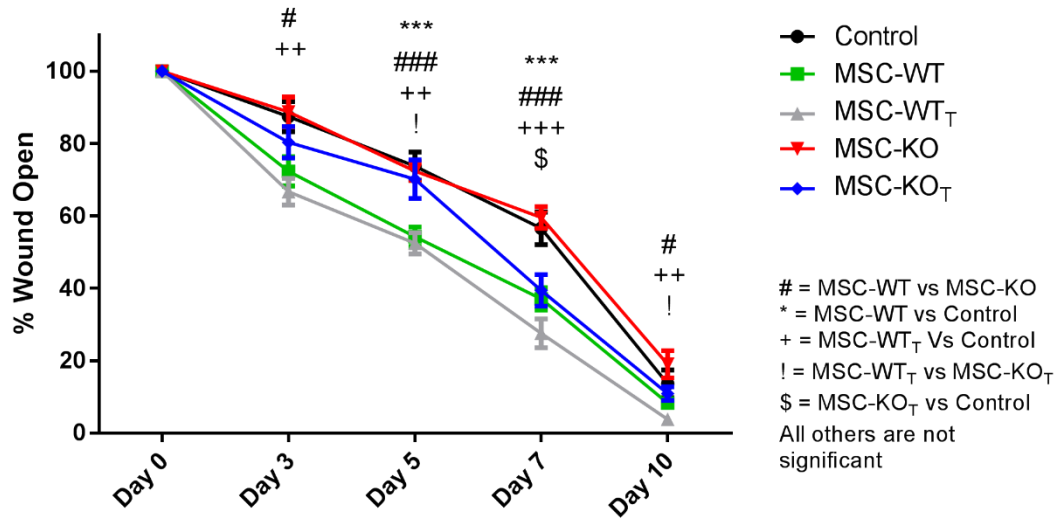
Appendix V

Comparison of wound closure and re-epithelialisation rates from results presented in chapter 4 and chapter 5

Appendix VI

Comparison of wound closure rates and re-epithelialisation from results presented in chapter 6 and chapter 7

Appendix VII

Comparison of qRT-PCR analysis from results presented in chapter 6 and Chapter 7